Engineering single domain antibodies into antivirals and vaccine delivery vehicles to combat infectious diseases

Ghent University – Faculty of Sciences
Deaprtment of Plant Biotechnology and Bioinformatics
VIB – Center for Plant Systems Biology

Academic year 2018-1019

Promoters:
Prof. Dr. Ann Depicker,
Prof. Dr. Xavier Saelens,
Dr. Bert Schepens

Shruti Bakshi

GHENT UNIVERSITY - FACULTY OF SCIENCES
DEPARTMENT OF PLANT BIOTECHNOLOGY AND BIOINFORMATICS
VIB CENTER FOR PLANT SYSTEMS BIOLOGY

Engineering single domain antibodies into antivirals and vaccine delivery vehicles to combat infectious diseases

Shruti Bakshi

Academic year 2018-2019

Promoters
Prof. Dr. Ann Depicker
Prof. Dr. Xavier Saelens
Dr. Bert Schepens

Thesis submitted as partial fulfillment of the requirements for obtaining the degree of Doctor of Philosophy (Ph.D.) in Sciences: Biochemistry and Biotechnology

EXAMINATION BOARD

Promoters

Prof. Dr. Ann Depicker — Ghent University – Faculty of Sciences – Department of Plant Biotechnology and Bioinformatics
VIB – Center for Plant Systems Biology

Prof. Dr. Xavier Saelens — Administrative promoter
Ghent University – Faculty of Sciences – Department of Biochemistry and Microbiology
VIB – Center for Medical Biotechnology

Dr. Bert Schepens — Ghent University – Faculty of Sciences – Department of Biomedical Molecular Biology
VIB – Center for Medical Biotechnology

Examination committee

Prof. Dr. Geert De Jaeger — **Chair**
Ghent University – Faculty of Sciences – Department of Plant Biotechnology and Bioinformatics
VIB – Center for Plant Systems Biology

Prof. Bart Devreese — **Secretary**
Ghent University – Department of Biochemistry and Microbiology

Dr. Bert Devriendt — Ghent University – Faculty of Veterinary medicine – Department of Virology, Parasitology and Immunology

Dr. Vikram Virdi — Ghent University – Department of Biochemistry and Microbiology
VIB – Center for Medical Biotechnology

Prof. Dr. Henri De Greve — Vrije Universiteit Brussel – Structural Biology Brussels
VIB – Structural Molecular Biology

Dr. Vicente Mas — Unidad de Biología Viral, Centro Nacional de Microbiología and CIBER de Enfermedades Respiratorias

Dr. Erik Depla — Orionis Biosciences, VIB Bioincubators

SUMMARY

Since their discovery in the late past century, single-domain antibodies (VHHs) attracted a lot of interest and have been studied intensively because they offer huge potential for several applications. For instance, VHHs fused with Fc domains of conventional antibodies offer added advantages such as increased half-life, avidity effect by bivalency, Fc-effector functions and purification on affinity ligands. We assessed several features of VHH-Fc fusions in this thesis for two applications: VHH-based targeted vaccination to combat enteric pathogens and VHH-based antivirals against respiratory syncytial virus (RSV).

The first aim of the project was to develop a mucosal-targeted vaccine delivery system against enteric pathogens. Thus, as a proof of concept, a model antigen was fused to an antibody against the aminopeptidase N (APN) receptor on the small intestine to enhance its uptake by intestinal epithelial cells, thereby increasing the immune response against the antigen. A monoclonal antibody IMM013 targeting APN has previously been shown to deliver antigens via β-glucan microparticles (Baert et al., 2015). Therefore, we first chose to make antigen-antibody fusion constructs with a single-chain variable fragment (scFv) derived from IMM013. However, because of their instability, fusion proteins containing scFv could not accumulate at high levels and further characterization could not be performed. Of note, replacing the scFv with an irrelevant VHH in several fusion constructs resulted in improved accumulation levels in the *Pichia pastoris* expression system. Therefore, we decided to concentrate on an alternative strategy using APN binding VHHs fused to an antigen. An anti-APN VHH library was generated by immunizing llamas with APN, followed by panning and screening on APN-expressing cells via flow cytometry. The APN-specific VHHs with strong APN-binding activity were fused to the Fc domain of murine IgG which could serve as a model antigen in piglets and which would convert the monovalent VHHs into bivalent molecules. The VHH-Fc fusions were sub-cloned in a yeast expression vector and produced to be further characterized for their binding capacity to APN in an ELISA, on APN-expressing cells and in intestinal tissues. Moreover, their uptake by APN-expressing cell lines and intestinal epithelium in gut-ligated loop experiments was also tested. The best performing VHH-Fcs were selected for further assessment of their potential to generate

a focused immune response against the murine Fc domain upon oral administration in piglets. A preliminary immunization experiment failed to demonstrate significant immunogenicity but remains to be validated further with controls. We then assessed the feasibility of formatting APN-specific VHH fusions with the Fc part of porcine IgGs and IgA into fusion constructs with the model antigen tetanus toxin C-fragment, as this would provide a better red-out of the targeted vaccine immunogenicity than the murine Fc part. We learned that, in contrast to scFv fusions, VHH-based tripartite fusions with an antigen and a dimerizing Fc part are feasible to make and can be produced in high quantities in *Pichia pastoris,* which will allow to characterize them in *in vitro* and *in vivo* experiment settings.

In the other part of my thesis, we aimed at evaluating the potential of VHH-Fc fusions as effective antivirals against RSV. We chose two previously isolated and described RSV-specific VHHs, one neutralizing (C4) and one non-neutralizing (E4) (Hultberg et al., 2011) and a non-RSV binding negative control. These three VHHs were fused to the Fc domain of murine IgG2a and produced by transient expression in *N. benthamiana*. The RSV-binding VHH-Fc fusions, and not the negative control, could efficiently bind to the RSV fusion protein (RSV F) and showed a far better *in vitro* neutralization activity than what was reported for their VHH monovalent counterparts. Remarkably, two of the three VHH-Fc fusions showed a very high thermostability and all three fusions were retained in lungs for an extended period compared to the VHHs alone. Of note, despite being non-neutralizing, VHH E4 also showed a reduced viral replication *in vivo*, suggesting an immunostimulatory role of Fc effector functions.

In parallel, we aimed to assess the merits of VHH-IgA fusions at the pulmonary mucosal surface and to compare them with our results obtained with the VHH-IgG fusions. However, the unavailability of an affinity ligand for murine IgA purification posed a major hurdle. We showed that a two-amino-acid mutation in the murine IgA Fc allowed purification of VHH-IgA fusions on the commercially available ligand staphylococcal superantigen-like protein 7 (SSL7). Moreover, the mutation in IgA Fc did not affect the binding activity to RSV F and the *in vitro* neutralizing potency of associated VHHs (Bakshi et al., 2019). Further validation of these mutant IgAs is required via *in vivo* settings to compare protection by VHH-IgA with VHH-IgG.

In conclusion, VHH-Fc fusions show a huge potential for targeted vaccination and for their use as antivirals. They can provide solutions to various limitations of VHH-based and conventional antibody-based therapeutics and need to be studied on a case-by-case basis.

SAMENVATTING

Sinds hun ontdekking aan het einde van de vorige eeuw, hebben single-domein-antilichamen (VHH's) veel belangstelling getrokken en zijn ze intensief bestudeerd omdat ze een enorm potentieel bieden voor verschillende toepassingen. VHH's gefuseerd met de Fc-domeinen van conventionele antilichamen bieden bijvoorbeeld toegevoegde voordelen zoals een verhoogde halfwaardetijd, een aviditeitseffect door bivalentie, Fc-effectorfuncties en zuivering op affiniteitsliganden. We hebben verschillende kenmerken van VHH-Fc-fusies in dit proefschrift beoordeeld voor twee toepassingen: op VHH-gebaseerde gerichte vaccinatie ter bestrijding van enterische pathogenen en op VHH-gebaseerde antivirale middelen tegen respiratoir syncytieel virus (RSV).

Het eerste doel van het project was om een mucosaal-gericht vaccin-afleveringssysteem tegen enterische pathogenen te ontwikkelen. Aldus werd als bewijs van het concept een modelantigeen gefuseerd aan een antilichaam tegen de aminopeptidase N (APN)-receptor van de dunne darm in biggen om de opname van dat antigen door darmepitheelcellen en de immuunrespons tegen het antigeen te verbeteren. Van een monoklonaal antilichaam IMM013 gericht tegen APN werd eerder aangetoond dat het antigenen afgeeft via β-glucaan microdeeltjes (Baert et al., 2015). Daarom kozen we eerst voor het maken van antigeen-antilichaam fusieconstructen met een enkele keten van de variabele fragmenten (scFv) afgeleid van IMM013. Vanwege hun instabiliteit konden fusie-eiwitten die scFv bevatten echter niet accumuleren tot hoge niveaus en verdere karakterisering kon niet worden uitgevoerd. Merk op dat het vervangen van de scFv door een irrelevant VHH in verschillende fusieconstructen resulteerde in verbeterde accumulatieniveaus in het *Pichia pastoris* expressiesysteem. Daarom hebben we besloten om in plaats van scFv's te gebruiken, ons te concentreren op de alternatieve strategie met APN bindende VHH-gebaseerde fusies. Een anti-APN VHH-bibliotheek werd gegenereerd door lama's te immuniseren met APN, gevolgd door panning en screening op APN-expresserende cellen via flowcytometrie. De APN-specifieke VHH's met een sterke APN-bindende activiteit werden gefuseerd aan het Fc-domein van muizen-IgG om aldus het Fc te gebruiken als model antigeen in

biggen en tegelijkertijd van de monovalente VHH's bivalente moleculen te bekomen. De VHH-muis Fc fusies werden gesubkloneerd in een gistexpressievector en geproduceerd om deze te karakteriseren voor hun bindingscapaciteit met APN in een ELISA, op APN-expresserende cellen en in darmweefsels. Bovendien werd hun opname door APN-expresserende cellijnen en darmepitheel in darmgeligeerde lus-experimenten ook getest. De best presterende VHH-Fcs werden geselecteerd voor een verdere analyse van hun potentieel voor het genereren van een gerichte immuunrespons tegen het muizen-Fc-domein na orale toediening aan biggen. Een voorlopig immunisatie-experiment kon geen significante immunogeniciteit aantonen, maar moet nog verder gevalideerd worden met meer gerichte controles. Vervolgens hebben we de haalbaarheid van het formatteren van APN-specifieke VHH's in tripartiete fusies met enerzijds het Fc domein van varkens IgG en IgA antilichamen en anderzijds het model antigeen tetanustoxine C-fragment onderzocht. We hebben geleerd, in tegenstelling tot scFv-fusies, dat op VHH-gebaseerde fusies met een Fc en met een antigeen haalbaar zijn en in grote hoeveelheden in *Pichia pastoris* kunnen worden geproduceerd om ze te karakteriseren via *in vitro*- en *in vivo*-experimenten.

In het andere deel van mijn proefschrift probeerden we het potentieel van VHH-Fc-fusies te evalueren als effectieve antivirale middelen tegen RSV. We kozen twee eerder geïsoleerde en beschreven RSV-specifieke VHH's, één neutraliserende (C4) en één niet-neutraliserende (E4) (Hultberg et al., 2011) en een niet-RSV bindende negatieve controle. Deze drie VHH's werden gefuseerd aan het Fc-domein van muizen-IgG2a en geproduceerd door transiënte expressie in *N. benthamiana*. De RSV-bindende VHH-Fc-fusies, en niet de negatieve controle, konden efficiënt binden aan het RSV-fusie-eiwit (RSV F) en vertoonden een veel betere *in vitro*-neutralisatieactiviteit dan wat werd gerapporteerd voor hun VHH-monovalente tegenhangers. Opmerkelijk was dat twee van de drie VHH-Fc-fusies een zeer hoge thermostabiliteit vertoonden en dat alle drie de fusies gedurende een langere tijd in de longen werden behouden vergeleken met alleen de VHH's. Hoewel VHH E4 niet-neutraliserend was, vertoonde het ook een verminderde virale replicatie *in vivo*, wat duidt op een immunostimulerende rol van Fc-effectorfuncties.

Parallel hiermee wilden we de voordelen van VHH-IgA-fusies op het pulmonaire mucosale oppervlak beoordelen en deze vergelijken met onze resultaten verkregen met de VHH-IgG-fusies. De niet-beschikbaarheid van een affiniteitsligand voor de zuivering van muizen-IgA vormde echter een belangrijke hindernis. We toonden aan dat een mutatie van twee aminozuren in het Fc-domein van muizen-IgA de zuivering mogelijk maakte van VHH-IgA-fusies op het in de handel verkrijgbare ligand stafylokokken-superantigeenachtig eiwit 7 (SSL7). Bovendien had de mutatie in IgA Fc geen invloed op de bindingsactiviteit met RSV F en de *in vitro*-neutraliserende potentie van geassocieerde VHH's (Bakshi et al., 2019). Verdere validatie van deze mutante IgA's is vereist via *in vivo*-experimenten om bescherming door VHH-IgA te vergelijken met VHH-IgG.

Als conclusie kunnen we stellen dat VHH-Fc-fusies een enorm potentieel tonen voor gerichte vaccinatie en voor hun gebruik als antivirale middelen. Ze kunnen oplossingen bieden voor verschillende beperkingen van op VHH- en conventionele antilichaam-gebaseerde therapieën en moeten geval tot geval worden onderzocht.

TABLE OF CONTENT

LIST OF ABBREVIATIONS

2S2	Signal peptide sequence of the 2S2 seed storage protein
35S	Cauliflower mosaic virus 35S promoter
Ab	Antibody
ADCC	Antibody-Dependent Cellular Cytotoxicity
ADCP	Antibody-Dependent Cellular Phagocytosis
Ag	Antigen
BGMY	Buffered glycerol-complex medium
BMMY	Buffered methanol-complex medium
BSA	Bovine serum albumin
CDC	Complement Dependent Cytotoxicity
CDSCO	Central Drugs Standard Control Organization
CDR	Complementary Determining Region
CFU	Colony forming units
CT	Cholera toxin
DPBS	Dulbecco's Modified Phosphate Buffered Saline
DTT	Dithiothreitol
ELISA	Enzyme-Linked Immuno Sorbent Assay
EMA	European Medicines Agency
ETEC	Enterotoxigenic *Escherichia coli*
Fc	Fragment crystallisable
FcRn	Neonatal Fc receptor
FcγR	Fc receptor for gamma globulins
FDA	Food and Drug administration
FW	Fresh weight of infiltrated leaves
GALT	Gut-associated lymphoid tissue
GBP	GFP binding VHH
GBP-MG	GBP fused to Fc domain of murine IgG3

GFP	Green Fluorescence Protein
hcAb	Heavy-chain only antibodies
HRP	Horseradish peroxidase
HRSV	Human respiratory syncytial virus
Ig	Immunoglobulin
KDEL	(Lys-Asp-Glu-Leu) a C-terminal ER retention peptide
mAb	Monoclonal antibodies
MES	2-(N-morpholino) ethanesulfonic acid
mIgA	Monomeric IgA
MG	Fc domain of murine IgG
OD	Optical density
pAPN	Porcine aminopeptidase N
PA	Fc domain of Porcine IgA
PG	Fc domain of Porcine IgG
PBS	Phosphate-buffered saline
PMDA	Pharmaceuticals and Medical Devices Agency
PVDF	Polyvinylidene fluoride
scFv	Single-chain variable fragment
SDS-PAGE	Sodium dodecyl sulfate-polyacrylamide gel electrophoresis
sdAb	Single-domain antibodies
SEC	Size exclusion chromatography
SSL7	staphylococcal superantigen-like 7
TTC	Tetanus toxin fragment-C
Tnos	Terminator of the nopaline synthase gene
VHH	variable domain of camelid heavy chain-only antibody
VHH-PA	Variable domain of heavy-chain-only antibody fused to the Fc of a porcine IgA
VHH-PG	Variable domain of heavy-chain-only antibody fused to the Fc of a porcine IgG
VHH-MG	VHH fused to Fc domain of murine IgG
YPD	Yeast extract peptone dextrose

INTRODUCTION

Chapter 1

Single-domain antibodies: engineering, applications and different production platforms

Shruti Bakshi and Ann Depicker
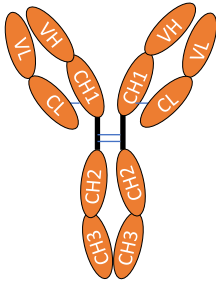
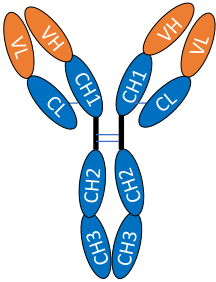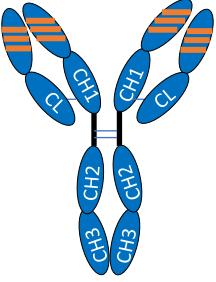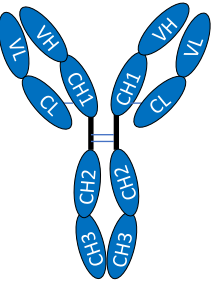**Author contribution:**

S.B. wrote the chapter. A.D. edited it.

Abstract

Monoclonal antibodies-based therapies have achieved several milestones since their discovery and have successfully been employed in various applications ranging from treating infectious diseases, curing cancer, molecular tools in research, as a delivery vehicle of toxins and so on. However, their complex structure and expensive mammalian-based production pose a great challenge towards their further development as broadly applicable ideal therapeutic agents. Since the past two decades, research efforts resulted in great advances into understanding the antibody structure. That gave rise to the identification of antibody fragments such as single chain of the variable fragments (scFv) and the variable domain of the heavy chain only antibodies (VHH). The scFv is a synthetic antibody protein that combines the variable antigen binding domains of the light and heavy chain, does not require post-translational modifications for its activity, and can be produced in a cost-effective manner in bacterial and yeast expression systems. The optimal length of the connecting linker between the variable regions in scFvs is very crucial for their proper folding and is dependent on the relative location of the 6 variable regions, thus determining antigen binding of the scFvs and functionality. Nevertheless, scFv has been receiving a lot of attention because the antibody-antigen interaction could be very well characterized with the monoclonal itself. However, things changed since the discovery of camelid-derived single domain antibody (sdAb). A variable domain of sdAb, referred to as VHH, has several advantages over scFv antibody fragments including their small size, high affinity for particular epitopes, difficult to reach with scFvs, ease of manipulation as the single domain contains all the information in 3 variable loops for antigen binding, high stability in harsh conditions, and cost-effective production in bacterial and yeast fermentation systems. Due to their peculiar properties, VHHs have been employed in various applications ranging from research, diagnosis, and therapeutics. Today, several VHH-based products are being developed and evaluated in preclinical and clinical phase and are anticipated to become the next generation of antibody-based biopharmaceuticals. This chapter intends to shed light on different aspects of the use of scFvs and VHHs, their engineering for improved functionality, their production in different platforms such as bacterial, mammalian, plant and yeast expression systems, and their potential applications and comparison with the conventional monoclonal antibodies (mAbs).

1. Antibodies and their derivatives

In 1975, Georges Kohler and Cesar Milstein succeeded in fusing myeloma cell lines with B cells, that gave rise to immortalized cells termed Hybridoma. The hybridomas were capable of producing antibodies against a specific antigen. These antibodies are known as monoclonal antibodies (mAbs). The first commercialized mAb, muromonab CD3 (Orthoclone OKT3) was developed in 1986 to prevent kidney transplant rejection (Liu, 2014). Since then, the monoclonal antibody market has witnessed continuous growth and represents a novel way for targeting a wide range of disease conditions including cancer, infectious diseases, cardiovascular diseases, transplantation, and chronic inflammatory diseases. Today, monoclonal antibodies own approximately 50% of the market share of the biopharmaceutical industry with more than 50 monoclonal antibody products currently approved. Every year, about 4 new mAbs get approval from the Food and Drug Administration (FDA) and reach the market. With this rate, the monoclonal antibody market is projected to grow even further with an estimated revenue of nearly $125 billion in 2020 for worldwide sale of biopharmaceuticals (Ecker et al., 2015).

Antibodies are expected to meet the stringent criteria of an ideal therapeutic protein for human use before reaching the market. These include their safe administration with optimal functional performance. Murine monoclonal antibodies raise an immune response in humans due to their murine specific epitopes. Muromonab CD3 (first licensed mAb) was a murine IgG2a antibody that posed some side effects in humans (e.g. human anti-mouse antibody response), thus urging humanization of the murine antibodies. (Smith, 1996). Since then, substantial efforts have been invested in generating chimeric, humanized or completely human antibodies to overcome the safety issues. To this end, murine sequences in the antibody are replaced with the human counterparts and their nomenclature is based on the percentage of the remaining murine part in the engineered antibody (Table 1) (Singh et al., 2018). The first fully human antibody was Humira (Adalimumab), developed for the treatment of rheumatoid arthritis, and approved in 2004. Today, most of the approved antibodies are either humanized or fully human. Despite the great progress in reducing immunogenicity risks by humanizing the antibodies, adverse reactions are unpredictable in some patients, and still may occur.

	Murine	Chimeric	Humanized	Fully Human
Table 1- Humanization of monoclonal antibodies (adapted from (Singh et al., 2018)				
	VL VH CH1 CL (antibody diagram)	VL VH CH1 CL (antibody diagram)	CH1 CL (antibody diagram)	VL VH CH1 CL (antibody diagram)
Murine part	100 %	30 %	10 %	0 %
Generic suffix	-omab	-ximab	-zumab	-umab
Example	-	Rituximab	Palivizumab	Adalimumab

Moreover, the production of early monoclonal antibodies was limited due to genetic instability of hybridomas and the low yield obtained upon fermentation, thus presenting major stumbling blocks in the development of this class of mAb- therapeutics. The complex structure of the full-length antibody, that contains intra- and interchain disulfide bonds does not allow their production in prokaryotic systems such as *E. coli*, the most rapid and cheapest production system by far. Thus, mAb production is limited to more complex eukaryotic host-based systems. Antibodies also require efficient post-translational modifications such as glycosylation for their proper functionality and efficient effector functions, which is not achievable in the bacterial expression systems. Moreover, the size of the full-length antibody is about 150 kDa, that prevents deep and efficient tissue penetration of the target sites.

The major advances in genetic engineering and a deeper understanding of the disease conditions have paved the way for the new and improved generation of therapeutic antibodies. In recent past, derivatives of monoclonal antibodies have been employed not only for the treatment of cancer, autoimmune and infectious diseases; but also, in immunodetection, and bioseparation techniques (de Marco, 2011). The most popular ones include single-chain variable fragment (scFv) and single-domain antibodies (sdAbs), as they are easy to manipulate and

produce in bacterial and yeast expression system, without compromising their antigen binding property.

1.1 Single-chain fragment variable (scFv)

The full-length antibodies, also known as immunoglobulins (Ig) are large Y-shaped glycoproteins and composed of four polypeptide chains (two light chains, LC and two heavy chains, HC), held together via interchain disulfide bridges and hydrophobic interactions. The N-terminal end of each chain is highly variable (termed VL for LC and VH for HC) and is involved in interaction with the antigen, while the CL for LC and CH1, CH2, CH3 for HC) are quite conserved in a given class of antibody. The Fab region consists of a light chain (VL and CL), and the variable and constant region of HC (VH and CH1). The Fc region (CH2-CH3 domain) of an antibody attributes the stability and important biological functions such as antibody-dependent cell-mediated cytotoxicity (ADCC) and Complement-Dependent Cytotoxicity (CDC). (Figure 1)

Nevertheless, the full-length antibody is not required for its antigen binding property, that led to the development of a smaller unit of an antibody (molecular mass of approximately 30 kDa), termed single-chain fragment variable (scFv). The scFv is composed of only variable fragments of both LC and HC (VL and VH) and it possesses full antigen binding property. The carboxyl terminus of one variable domain is connected to the amino terminus of another variable domain via a flexible peptide linker without having any detrimental effect on their fidelity. scFv lacks glycosylation and can easily be produced in a bacterial expression system. However, the length of the connecting linker is very crucial for the proper folding with minimal steric hindrance that determines the functionality and expression level of scFv (Ahmad et al., 2012). Peptide linkers can be of variable length, ranging from 10 to 25 amino acids and typically contain hydrophilic amino acids; short linkers have the advantage to make the scFv less susceptible to cleavage, but they often lead to multimer formation (Shen et al., 2008). Nowadays, the most extensively used linker is multiples of three Glycine (G) and one Serine (S) residues (Andris-Widhopf et al., 2011; Schaefer et al., 2010).

Conventionally, scFv were cloned from hybridoma cells, of which the produced monoclonal antibodies contained interesting binding or neutralization properties. The mRNA is isolated from hybridoma cells followed by cDNA synthesis by reverse transcription PCR. Then, VL and VH genes are PCR amplified using immunoglobulin-specific primers and cDNA as a template and cloned into an expression vector (Dubel et al., 1994). However, this method generates a large library with a heterogeneous population of PCR products, that demands the analysis of several randomly picked VH and VL clones (Toleikis and Frenzel, 2012). The subsequent successful approach developed is based on creating a phage display library where each phage expresses a gene for VL or VH at their surface; the best combinations can then be enriched upon biopanning and selected for their antigen specificity (McCafferty et al., 1990). Generally, VL and VH can be linked in any orientation (either VL-Linker-VH or VH-Linker-VL) although, it was reported that a VL-Linker-VH led to higher levels of scFv accumulation then a VH-Linker-VL combination in *Pichia* pastoris (McCafferty et al., 1990). The assembly of VL and VH gene fragments can be achieved by several methods including PCR (LeBoeuf et al., 1989), sequential cloning (Kobayashi et al., 2005) or combinatorial infection (Wang et al., 2005), and nowadays by DNA synthesis.

The scFvs have several advantages over monoclonal antibodies. They can be produced economically in both bacterial and yeast expression systems. Their small size offers better tissue penetration and low serum half-life. This results in rapid clearance, that may be beneficial for radiolabeling, but is a problem in therapy. This issue has been addressed by engineering them to yield multivalent scFv, or also by making fusions with albumin or the Fc domain of a conventional antibody. During the past years, numerous scFv constructs have been made for a variety of heterogeneous functions, such as medical therapy (i.e. cancer, Crohn's, disease, Rheumatoid Arthritis), and diagnostic applications (Ahmad et al., 2012; Monnier et al., 2013). Moreover, several studies were performed where scFvs were fused with different proteins for various applications including drug delivery, *in vivo* imaging by attaching to a fluorescent moiety (Monnier et al., 2013). Up till now, many scFv based therapies have made their way to market, while some are still in development or clinical trial phase (Table 2).

Table 2. Selected antibody fragments on the market or in clinical development (adapted from Sheridan, 2017)

Developer (location)	Molecule	Format	Target	Indication	Clinical status
Amgen (Thousand Oaks, California)	Blincyto (blinatumomab)	Bispecific T-cell engager (Bite) comprising two scFv fragments joined by a peptide linker	CD19 × CD3	Acute lymphoblastic leukemia	First FDA approval 12/03/14
Boehringer Ingelheim (Ingelheim, Germany)	Praxbind (idarucizumab)	Humanized IgG1 Fab fragment	Dabigatran	Reversal agent for anticoagulant Pradaxa (dabigatran)	First FDA approval 10/16/15
Ablynx, A Sanofi company (Zwijnaarde, Belgium)	Caplacizumab (Cablivi™)	Bivalent humanized single-variable-domain immunoglobulin (nanobody) derived from a heavy-chain-only Camelid antibody	von Willebrand factor	Acquired thrombotic thrombocytopenic purpura (aTTP)	FDA approval 06/02/19
AstraZeneca (Cambridge, UK)	Moxetumomab pasudotox	Fv monoclonal antibody fragment fused to 38-kDa fragment of *Pseudomonas* exotoxin A (PE38)	CD22	Hairy cell leukemia	FDA approval for some cases (13/09/18)
Eleven Biotherapeutics (Cambridge, Massachusetts)	Oportuzumab monatox; VB4-845 (Vicinum)	Single-chain variable fragment fused to a fragment of *Pseudomonas aeruginosa* exotoxin A (ETA$_{252-608}$)	Epithelial cell adhesion molecule (EpCAM)	Bladder cancer	Phase 3
Novartis	Brolucizumab; RTH258, formerly ESBA1008	Humanized single-chain antibody fragment (scFv)	VEGF-A	Neovascular AMD	Phase 3
Philogen (Sovicille, Italy)	Daromun (Darleukin + Fibromun)	Combination of two immunocytokines comprising scFv fragments of antibody L19 conjugated to interleukin-2 and tumor necrosis factor α, respectively	Fibronectin extra-domain B	Melanoma	Phase 3
Aptevo Therapeutics (Seattle)	Otlertuzumab	scFV antibody fragment	CD37	Chronic lymphocytic leukemia	Phase 2
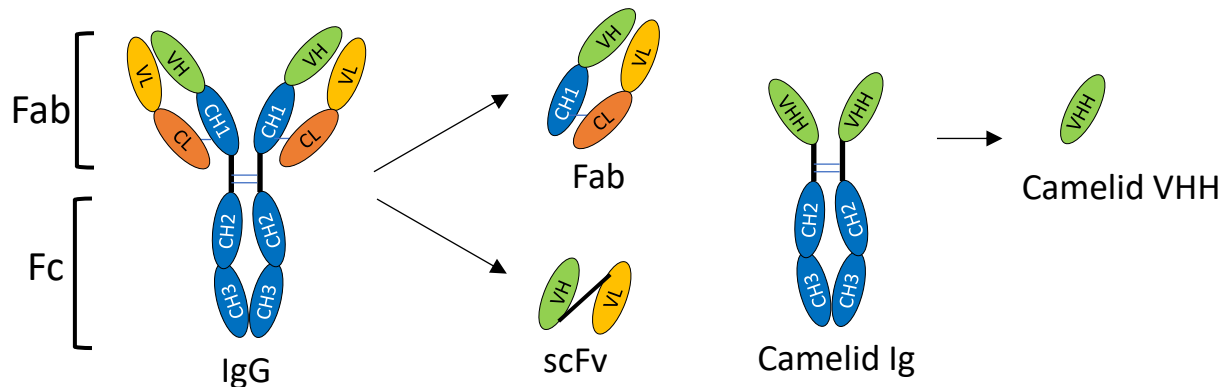
Figure 1. Schematic representation of antibodies and their derivatives.

1.2 Single domain antibodies

Besides these antibody derivatives, a unique kind of antibodies, termed as heavy chain only antibodies (HCAb) also exists in nature. These antibodies were first discovered in camelids (camels and llama), and comprise only a homo-dimer of heavy chains without light chains (Hamers-Casterman et al., 1993). In addition to HCAbs, conventional heterotetrameric antibodies are also naturally found in Camelidae. Few years later, the similar heavy chain only antibodies were also discovered in cartilaginous fishes (nurse sharks and wobbegong) (Greenberg et al., 1995). These antibodies were termed as Ig-NAR ('NAR stands for novel antigen receptor'). The variable domain of camelid HCAb and Ig-NAR are referred to as VHH and V-NAR, respectively. VHHs are also known as nanobodies and single domain antibodies (sdAb).

Moreover, the HCAbs are devoid of the CH1 domain, but contain both the CH2 and CH3 domains; the heavy chains are connected with disulfide bridges in an exceptionally long hinge region. Like the VH domain of conventional antibodies, the VHH domains of HCAbs are also composed of four highly conserved framework regions (FR1, FR2, FR3, and FR4), and three hypervariable regions, termed complementary determining regions (CDR1, CDR2 and CDR3) (**Figure 2**). The amino acid sequence of VHH framework regions is highly similar to that of the VH of conventional antibodies with few remarkable structural differences, rendering them superior to conventional antibodies and their fragments (Muyldermans, 2001). Within FR2, four amino acids (V, G, L, and W) known to interact with VL are substituted with smaller hydrophilic amino acids (F, E, G, and R) in VHHs, that contribute to high solubility. Besides these substitutions, CDR

14

regions in VHH also exhibit some striking differences. In contrast to CDR3 (typically 9-12 amino acids) in human and mouse (Wu et al., 1993), VHH in dromedary bears longer CDR3 with 16-18 amino acids. Whereas CDR3 of llama VHH is more variable in length (6-18 amino acids) (Muyldermans, 2001). The extended CDR3 in many camel VHH sequences is stabilized by an additional disulfide bond with CDR1 (Figure 2). However, this interloop disulfide bond occurs less frequently in llama VHH (Muyldermans, 2013).
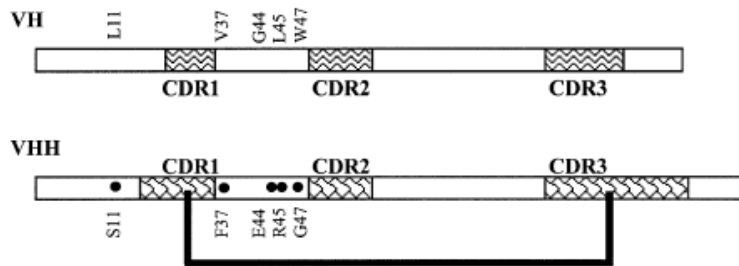

Figure 2. Schematic representation of the differences between VH and VHH based on the sequence comparison of cDNA clones. The position of the CDR in between the framework regions is indicated. The CDR1 and CDR3 of a VHH is larger than in VH genes and they are often connected by a disulfide bond (thick line). The hallmark amino acid substitutions in framework-one and -two are given. The numbering refers to the position of the amino acid along the sequence according to the Kabat numbering. (Figure reused from Muyldermans, 2001).

Since its discovery, VHHs have emerged as an alternative to monoclonal antibodies for developing biotherapeutics. Despite their limitations, monoclonal antibodies have occupied a large fraction of the biopharmaceutical market. VHHs provide a potential to circumvent those limitations as they are the smallest form of an antibody with a combination of some beneficial features of both full-length antibodies and the small biological molecules (Muyldermans, 2013). VHHs are small-sized (15 kDa) antibody fragments that are characterized by high affinities (in picomolar range) comparable or even superior to those of conventional antibodies or antibody fragments (Fab or scFv), high solubility and robustness in harsh conditions such as extremes of pH, or temperature. VHHs can be isolated from immune libraries with all their appealing properties and allow high production yields in bacteria or other expression hosts. The general protocol for isolation and selection of VHHs from immune libraries has been described elsewhere (Pardon et al., 2014).

Camelid VHHs exhibit a high degree of sequence homology with the VH domain of human immunoglobulins, rendering them less immunogenic than murine VHs. Nevertheless, their straightforward humanization is useful to make them suitable for chronic treatments (Vincke et al., 2009). Furthermore, their small size is favorable where a higher degree of tissue penetration is required (i.e. imaging tool) that enable them to reach those regions or molecules that are typically inaccessible to full-length antibodies. However, it is not desirable for chronic therapies. The size of a nanobody is below the cut-off limit of glomerular filtration system (~65 kDa), that leads to rapid clearance from the circulation. Therefore, substantial efforts have been made to extend their half-life. These include (PEG)-ylation (conjugation with polyethylene glycol), coupling to long-lived serum proteins such as IgG or albumin (human serum albumin) and conjugation to the Fc domain of conventional antibodies (extensively described in De Vlieger et al., 2019).

Moreover, their single domain and monomeric nature facilitate straightforward engineering into modular blocks with high affinity (termed as avidity) and improved physicochemical properties. There have been several examples where VHHs were formatted to make bivalent, trivalent or tetravalent fusions. Moreover, VHHs recognizing different epitopes can be fused together to obtain multispecific (e.g. bispecific) and versatile antibodies. Some of these engineered VHHs are at this moment being investigated in clinical trials (reviewed in (Steeland et al., 2016).

1.3 VHH-Fc fusion proteins

The small size and fast renal clearance of VHH are not favorable characteristics to provide long term protection in some diseases. Several approaches ensure the prolongation of half-life, while the Fc domain as a fusion partner for VHH-based therapeutics appears as the most straightforward strategy that also provides the fusion with a number of additional beneficial biological and pharmacological properties. Several studies have examined the merits of VHH-Fc fusions for treating various diseases (Gunaydin et al., 2016; Hussack et al., 2018; Laursen et al., 2018). To date, many Fc fusion proteins with other proteins such as TNF receptor, VEGFR1 have been developed and commercialized (reviewed in Czajkowsky et al., 2012). Enbrel and Orencia

are the most popular ones; both were developed to treat autoimmune diseases (Shukla et al., 2017); however, Fc fusions with VHHs are yet to reach the pipeline.

1.3.1 Valency

One of the major advantages of Fc fusion protein is that the Fc domain serves as a dimerization motif, that contributes to the avidity effect, that is often desirable for improved efficacy of the therapeutic protein. It has been noted previously that bivalent VHHs displayed 4000-fold better and broadened neutralization potency as compared to their monovalent VHH counterparts (Hultberg et al., 2011), and this was confirmed in an ample number of studies.

1.3.2 Half-life extension

The efficacy of the clinically relevant VHHs can be improved by fine-tuning the residence time. In this context, the IgG Fc domain seems qualified as it interacts with the neonatal FcRn receptor in a pH-dependent manner. The Fc domain binds FcRn tightly at acidic pH (<6.5) in the endosome, but not at physiological pH (7.4) and protects IgG from degradation (Roopenian and Akilesh, 2007), thereby contributing to its longer serum half-life. The binding site for FcRn resides at the CH2-CH3 interface of the IgG Fc domain. VHH-Fc fusions assemble as a homodimer and have a molecular mass of approximately 80 kDa, that is above the cutoff of glomerular filtration, thereby resulting in the increased half-life. Zhao et al. showed that a neutralizing VHH against Middle East respiratory syndrome coronavirus (MERS-CoV) fused with a human IgG1 Fc could be detected in serum 10 days post-injection, whereas it is not true for its monovalent VHH equivalent (Zhao et al., 2018). However, the half-life of Fc fusion proteins is relatively short (1-2 weeks), as compared to intact antibodies (3-4 weeks) (Suzuki et al., 2010).

1.3.3 Fc receptor-mediated effector functions

The antibody effector functions governed by the Fc tail are believed to play an important role in killing tumor and infected cells as a humoral arm of the immune response via interaction with specialized Fc-receptors and complement proteins and form a link between innate and adaptive immunity. To date, four different classes of Fcγ receptors have been defined in mouse: FcγRI

(CD64), FcγRII (CD32), FcγRIII (CD16) and FcγRIV (Figure 3). These receptors bind to different IgG subclasses with varying affinity and specificity. Whereas FcγRI displays nanomolar affinity for select IgG subclasses such as IgG1/3 in humans and IgG2a/c in mice, all the other receptors have low to medium affinity (in micromolar range) and a broader isotype binding pattern. However, the low-affinity receptors can only bind to IgG in form of immune complex. The high affinity receptor FcγRI on immune cells is saturated in the presence of serum IgG (Nimmerjahn and Ravetch, 2011).
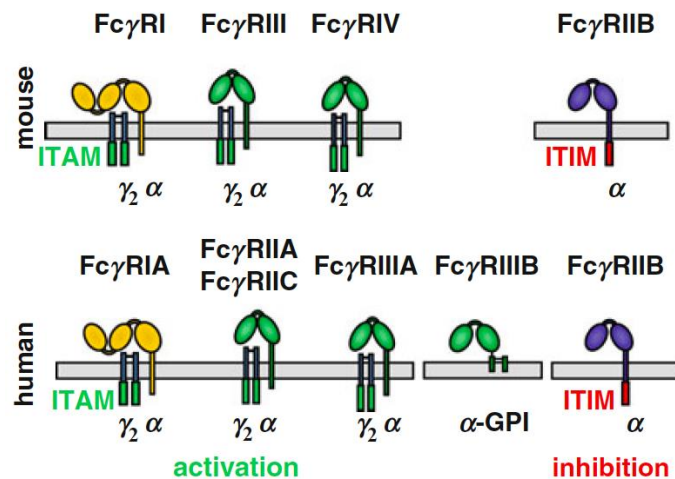
Figure 3. The extended family of mouse and human Fcγ-receptors. The family of classical FcγRs consists of several activating and one inhibitory member. In addition, humans have a glycosylphosphatidylinositol (GPI)-linked FcγR (FcγRIIIB) exclusively expressed on neutrophils (adapted from Nimmerjahn and Ravetch, 2011).

Besides these differences in affinity and specificity, other distinguishing feature among FcγR subtypes is their role in signal transduction. There are two different classes of Fc receptors: activation receptors (FcγRI, III, IV in mice and FcγRIA, IIA, IIC, IIIA, IIIB in humans) and inhibitory receptors (FcγRIIB). The majority of activating receptors transmit their signal via immunoreceptor tyrosine-base activation motifs (ITAM) such as the FcR common γ-chain. Whereas, the inhibitory FcγR has to associate with an immunoreceptor tyrosine-base inhibitory motifs (ITIM) in its cytosolic domain (Ravetch and Lanier, 2000). The coexpression of these receptors on the same immune effector cell is critical for simultaneous triggering of activating and inhibitory signaling pathways and to generate a balanced cellular effector function.

The IgG subclasses and their affinity for the Fc receptors varies widely between different species. For instance, four IgG subclasses are present in mice (IgG1, IgG2a, IgG2b and IgG3) and humans (IgG1-IgG4). Mouse IgG2a interacts strongly with activating receptors FcγRI, FcγRIV, but weakly with the inhibitory FcγRIIB receptor (Bruhns and Jonsson, 2015). Mouse and human FcγRs have quite different expression patterns and IgG binding characteristics. Interestingly, in contrast to poor binding of human FcγRs to mouse IgG subclasses, mouse FcγRs efficiently bind human IgG subclasses. For example, human FcγRI has affinity for mouse IgG2a and IgG2b, but not for mouse IgG1 (Bruhns, 2012).

Innate immune effector cells, such as dendritic cells (DCs), neutrophils, monocytes, macrophages, basophils and mast cells express activating and inhibitory FcγRs and their expression varies in different cell types. In mice, for example, monocytes and macrophages express all activating and inhibitory FcγRs (FcγRI–FcγRIV), DCs mainly express the activating FcγRI, FcγRIII and inhibitory FcγRIIB, whereas neutrophils express FcγRIIB, FcγRIII and FcγRIV. In contrast, B cells and NK cells do not co-express both activating and inhibitory receptors. B cells solely express inhibitory receptor FcγRIIB, whereas NK cells only express activating FcγRIII (Nimmerjahn and Ravetch, 2008). Inhibitory receptors have particular application in allergic reactions. For instance, activation of inhibitory FcγRIIB by Fc-fusion proteins is associated with the simultaneous downregulation of Fc receptor for IgE (FcεR) on mast cells that leads to decreased inflammatory response and may be crucial for treating allergic asthma (Daeron et al., 1995). A recent study demonstrated that several FDA-approved Fc-fusion proteins including TNFR-Fc (Etanercept), CTLA4-Fc 1 (Abatacept), CTLA4-Fc 2 (Belatacept), FIX-Fc (Coagulation factor IX, Fc-fusion protein) and FVIII-Fc (Antihemophilic factor, Fc-fusion protein) show diversity in binding to Fc receptors and C1q, and the fusion partner can influence the effector functions of the Fc-fusion proteins (Lagassé et al., 2019).

The important antibody-mediated effector mechanisms are antibody-dependent cell-mediated cytotoxicity (ADCC), antibody-dependent cellular phagocytosis (ADCP) and complement dependent cytotoxicity (CDC). ADCC is thought critical for destruction of the infected and tumor cells and dependent on binding to the Fc gamma receptors (FcγRs) localized on innate effector cells including monocytes, macrophages, neutrophils and natural killer (NK)

cells. However, NK cells are the most important contributor of ADCC which express only FcγRIIIA. Crosslinking with this receptor results in release of cytotoxic granules containing perforin and/or granzyme that triggers death of the target cancer cells. The antibody interaction with the Fc receptor can be improved further by either amino acid mutation in the Fc domain or alterations of the glycan structure (Strohl, 2009). For instance, ADCC can be enhanced by removing fucose from the Fc domain of IgG, resulting in increased affinity to FcγRIIIA (Shields et al., 2002; Zeitlin et al., 2011). ADCP is the uptake of antibody coated infected cells or antigen-antibody complexes by phagocytic cells including neutrophils, eosinophils, monocytes, macrophages and dendritic cells (DC) that express FcγRI, FcγRII and FcαRI. These cells mediate the transport of immune complexes to lysosome for degradation and antigen processing for presentation on major histocompatibility complex (MHC) on the cell surface. On the other hand, CDC triggers the cytolysis by immune complex interaction to the first component of the complement cascade (C1q) and subsequent activation of the classical pathway leading to phagocytosis and lysis of pathogens and infected cells.

Killing and/or uptake of infected cells or virions by leukocytes via FcγRs is considered to be of importance for the antiviral activity of at least some antibodies directed against multiple viruses including HIV-1, influenza, SARS and RSV (Tay et al., 2019). For example, FcγR have been shown to be essential for the protection offered by antibodies directed against the RSV small hydrophobic protein and most likely greatly contribute to the protective activity of Synagis (Schepens et al., 2014, Hiatt et al., 2014). In addition, antibodies directed against the RSV G protein were shown to enable ADPC *in vitro* (Cortjens et al., 2017).

1.3.4 Isotype dependent protection
Given the fact that secretory IgA is the predominant antibody isotype at the vulnerable mucosal membranes where the majority of pathogen initiate the infection, IgA-based fusions are believed to confer better protection against mucosal pathogens compared to other antibody isotypes. VHH-IgA fusions expressed in *Arabidopsis thaliana* seeds have been shown to protect weaned piglets against ETEC (enterotoxigenic *Escherichia coli*) infection upon oral delivery. Compared with the groups receiving VHH-IgG-based treatment, VHH-IgA groups showed reduced fecal

shedding of ETEC pathogen and lower seroconversion corroborating reduced ETEC exposure, suggesting the merits of IgAs at the intestinal mucosa (Virdi et al., 2013).

1.3.5 Purification of VHH-Fc fusions

Besides the above-mentioned advantages, Fc-fusions are also superior to VHH moieties by themselves in a technological viewpoint. Since, in most cases, the *in vivo* validation of a therapeutic protein requires highly pure protein the addition of an affinity tag (i.e. Histidine tag is needed in most cases. Alternatively, fusion of a VHH to the Fc domain enables the facile and cost-effective purification by commercially available affinity resins (Carter, 2011). For instance, VHH-IgG fusions can efficiently be purified by protein-G/A affinity chromatography. Likewise, most VHH-IgA fusions can be purified via IgA-specific resins such as SSL7 and Jacalin, however only at analytical scale. Note however that there are no affinity resins for mouse IgA-Fc based purification.

1.4 Potential applications of VHHs

The discovery of VHHs gave a momentum to the new era of engineered and personalized medicines for therapeutic interventions. VHHs offer several advantages over conventional antibodies. Given their peculiar characteristics including small size, ease of manipulation and selection from immune libraries, economic and efficient production in bacterial expression system, low immunogenicity, strong affinity, recognition of hidden epitopes, excellent tissue penetration capacity, high thermostability and solubility; VHHs are very convenient for a broad range of research, diagnostic and therapeutic applications.

1.4.1 VHHs in research and diagnosis

VHH fusions coupled to a fluorescent protein have an important implication in live cell microscopy and new functional studies. Such fusion proteins, also known as chromobodies, a VHH against an endogenous protein is fused to a fluorescent protein (i.e. GFP, RFP) that can efficiently express in the living cells and enables subcellular localization studies of the target protein (Rothbauer et al., 2006). Moreover, anti-GFP VHH has been employed in super-resolution

microscopy when coupled with an organic dye (Ries et al., 2012) and studying *in vivo* protein-protein interactions (Herce et al., 2013). Owing to their high stability, monomeric nature and oriented immobilization on the solid surface, VHHs have extensively been studied for developing affinity reagents for protein purification and immunoprecipitation. To this end, immobilized VHHs (commercially known as nanotrap) were developed against GFP that were commercialized by ChromoTek GmbH (Klooster et al., 2007; Rothbauer et al., 2008). Moreover, IgG purification was achieved with VHH-based affinity ligand that was commercialized by Thermo Fisher Scientific (CaptureSelect IgG-CH1 Affinity Matrix). LambdaFabSelect affinity ligand is another commercial VHH from GE Healthcare Life Sciences that is directed against the constant domain of the human λ light chain ($C_L\lambda$).

Recently, VHHs have gained much attention in developing a non-invasive *in vivo* imaging tool as they fulfill most of the requisites of an ideal imaging probe including their amenability for radiolabeling, deep tissue penetration, high solubility, and rapid renal clearance. These characteristics make them suitable for several imaging techniques such as PET (Positron-emission tomography) and SPET (Single photon emission tomography) (Van Audenhove and Gettemans, 2016) (Chakravarty et al., 2014). Many studies have attempted to utilize radiolabeled VHHs. For example, VHHs labeled at its C-terminal histidine tag with ^{99m}Tc was used to monitor EGFR (Epidermal Growth Factor Receptor) expression for *in vivo* tumor imaging (Huang et al., 2008). Moreover, VHHs are also used in biosensors as their small size and directional immobilization allow highest coating density on the sensor surface with maximal detection sensitivity, and their superior stability contributes to the longer shelf-life of the biosensor (Saerens et al., 2005).

1.4.2 VHHs in therapeutics

Although polyclonal and monoclonal antibodies have been ruling the therapeutic areas for ages with significant achievements, the single domain antibodies have gained popularity over the past decade due to their striking characteristics. In addition to the aforementioned applications as research and diagnostic tools, VHHs and derived fusions have also been exploited for therapeutic purposes to treat various disease conditions. These include cancer (Woodham et al., 2018), inflammatory diseases (Menzel et al., 2018), and neurological disorders (Rotman et al., 2015).

More recently, the first VHH, Caplacizumab (also known as ALX-0081) developed by Ablynx NV (Belgium) has been approved by FDA for the treatment of acquired thrombotic thrombocytopenic purpura (aTTP). Caplacizumab is a humanized bivalent VHH which is commercialized under the trade-name of Cablivi™ (Peyvandi et al., 2016). Fusions of VHHs against infectious diseases such as bacteria (Virdi et al., 2013; Virdi et al., 2019), viruses (Detalle et al., 2016), and parasites (Unciti-Broceta et al., 2015) are actively being studied. Interestingly, VHHs are endowed with the potential to reach undruggable targets such as G protein, which is a highly valued approach to block the GPCR signaling and treating multiple diseases (De Groof et al., 2019; Gulati et al., 2018).

2. Production platforms for recombinant antibodies and their derivatives

Nowadays, engineered antibody molecules and their derivatives are being increasingly exploited as a research tool for therapeutic development. Numerous products are already available in the market and many are currently being validated in clinical trials for the treatment of several diseases. However, the inability to produce large amounts of such proteins economically may limit the applicability of these technologies. Since, precise post-translational modifications, like glycosylation, has a significant influence on yield, stability, functionality, pharmacokinetic behavior and immunogenicity of the engineered proteins (de Marco, 2009; Frenzel et al., 2013), the selection of an appropriate expression platform is a very crucial step toward successful production of biotherapeutics. This section covers the general aspects of different recombinant protein production platforms and their comparison.

2.1 Bacterial expression system

The first biopharmaceutical reaching the market was Insulin (Humulin®, Eli Lilly & Co), and that was produced in *Escherichia coli*. Since then, bacterial expression systems have been very popular for the production of antibody fragments such as scFv, Fab, and single-domain antibodies (sdAbs) as they do not require human-like post-translational modification. Short generation time and ease of manipulation of *E. coli* allow rapid production, purification and analysis of large quantities of proteins in a shorter time compared to other expression platforms. Although the bacterial

expression system is the most inexpensive system, they are associated with some limitations. Some expressed proteins often end up in aggregates and form inclusion bodies due to the reducing cytoplasmic environment (Philibert et al., 2007; Schmidt, 2004). The inclusion bodies are then solubilized in an appropriate buffer and the functional proteins with correct disulfide bonds are recovered. This entire process is usually labor-intensive and time-consuming. An alternate method is to direct the secretion of the recombinant antibodies in the oxidizing environment of bacterial periplasm by fusing them with a secretion signal (e.g. PelB) (Sletta et al., 2007). Importantly, *E. coli* is not suitable for the production of glycoproteins such as full-length antibodies, or VHH-Fc fusions. Thus, it is necessary to produce them in eukaryotic platforms as discussed below.

2.2 Mammalian expression systems

The major advantage of using a mammalian expression system is their ability to produce antibodies with the glycosylation pattern that is naturally present in human proteins. The most common mammalian cell lines (non-human) include Chinese hamster ovary (CHO) cells, baby hamster kidney (BHK) cells, and murine myeloma cells (NS0 and Sp2/0). CHO cell lines are still the favored choice for large-scale production of the recombinant glycoproteins. However, these cell lines can also synthesize non-human-like glycoforms that can impact the immunogenicity, and thus result in rapid clearance of the therapeutic glycoproteins (Ghaderi et al., 2010; Ghaderi et al., 2012). Recently, human cell lines, such as human embryonic kidney (HEK) cells, have emerged as a powerful alternative that produces therapeutic proteins with fully human glycosylation (Swiech et al., 2012); but they are often associated with the potential risk of human-specific virus contamination (Dumont et al., 2016). The mammalian expression systems offer high yield (up to 10 g/L), high batch-to-batch consistency, and scalability in bioreactors (up to several thousand liters) (Zhu and Hatton, 2018); however, the initial capital and operating costs are very high due to rigid controls and maintenance of the sterile environment (Ecker et al., 2015). Thus, substantial efforts have been devoted to developing scalable production platforms such as plants expression system.

2.3 Plant expression systems

Plants are the most underestimated production platform for expression of therapeutic recombinant proteins, enzymes, and hormones (Dirisala et al., 2017; Tschofen et al., 2016), that have several advantages over bacterial and mammalian expression systems. The main argument is that plant systems are safe as they do not harbor mammalian pathogens, for instance when the proteins are required for controlling cell growth and differentiation to subsequently use in cell therapy. Plants are able to assemble functional antibodies with complex glycosylation. The first ever functional antibody production in transgenic plants was documented in 1989 (Hiatt et al., 1989). From then on, many antibodies and derivatives have been produced in plants (De Muynck et al., 2010; Rybicki, 2010; Yusibov et al., 2016). The proper folding and assembly of the functional antibodies in plants are orchestrated by ER-specific chaperones like BiP (binding protein) (Nuttall et al., 2002). However, the glycosylation accounts for the most significant difference between plant- and mammalian-derived glycosylation. The initial N-glycosylation in the endoplasmic reticulum (ER) is high-mannose type containing five to nine mannose residues and well conserved in both plant and mammalian system until the protein enters the Golgi apparatus. In the plant Golgi, the nascent glycoprotein undergoes species-specific glycosylation resulting in the addition of different plant-specific complex oligosaccharides such as core α(1,3)-linked fucose and β(1,2)-linked xylose that are never found in mammals (Gomord et al., 2010). The heterogeneity in glycosylation significantly influences the stability, physicochemical properties and immunogenicity of the plant-derived products, that raises concerns about their safety, especially for the parenteral administration (see ref. Walsh and Jefferis, 2006). Thus, the production of therapeutic glycoproteins with minimal adverse effects remains a considerable challenge. Two approaches have been employed to address the demerits of plant-derived therapeutic proteins- subcellular localization to avoid the addition of unwanted sugar and glycoengineering to replace plant-specific glycans to human-like glycans (Vukusic et al., 2016). In the first approach, the glycoprotein is retained in the ER by fusing with the C-terminal KDEL tag (ER retention motif, Lys-Asp-Glu-Leu), that prevents the transport to Golgi apparatus and addition of plant-specific complex glycans. However, in some cases, a significant amount of complex glycans could be detected, probably due to ER leakage and inaccessibility or partial

degradation of the KDEL tag (Abranches et al., 2008; De Meyer et al., 2015). Alternatively, a variety of strategies have been employed for glycoengineering of the plant glycosylation system, including conventional homologous recombination to generate knock-out plants lacking endogenous plant-specific glycosyltransferases and RNAi (RNA interference) mediated knock-down of the same enzymes (Bosch et al., 2013; Schahs et al., 2007; Strasser et al., 2008).

Many of the plant systems are cost-effective and scalable because they do not require maintenance of a sterile environment and large stainless-steel fermenters (Stoger et al., 2014). The cost for plant-derived mAbs production has been estimated to be about €100/g (Buyel et al., 2017), that is comparable to €50-200/g for mAbs production in CHO cells-based systems (Lim et al., 2010). It is important to note that initial investment and downstream processing costs for plant-derived products may be the same as the other production platforms, but their operating cost is much lower due to simple cultivation strategy of an intact plant, that substantially reduces the overall cost for the production at industrial scale. ELELYSO^{TM} (Protalix Biotherapeutics Inc., Israel) was the first plant-derived biopharmaceutical drug that was approved by the FDA in 2012 for human use to treat the rare genetic disorder, Gaucher's disease. ELELYSO^{TM} is a commercial name of the glucocerebrosidase enzyme which was produced in sterile grown carrot cells (Mor, 2015). This success story was an important breakthrough that opened the new avenues for plant-based manufacturing facilities.

There is a huge variety of plants and plant organs that are being explored for the production of therapeutic proteins to achieve high accumulation with low investment cost. These systems include seed-based systems such as *Arabidopsis* (Palaci et al., 2019; Virdi et al., 2016), tobacco (Ceballo et al., 2017), rice endosperms (Ou et al., 2014), corn (Zhong et al., 2006), crops like peas or soybeans (Daniell et al., 2001; Virdi et al., 2019); leaf-based systems such as tobacco (Bakshi et al., 2019; De Meyer et al., 2015), fruits like tomatoes (Juarez et al., 2012), plant cell-culture system such as tobacco cell lines BY-2 and NT-1 (Raven et al., 2015). Each of these systems has certain advantages, hence the particular expression system can be chosen depending on the objectives. In most cases, stable transgenic lines can be obtained either by *Agrobacterium*-mediated transformation or by particle bombardment protocols to integrate a foreign gene in the plant genome (reviewed in Ko and Koprowski, 2005). However, *Agrobacterium*-mediated

transformation is the preferred choice as it provides more stable transformants with low copy number and less silencing effects than the particle bombardment method (Travella et al., 2005).

2.3.1 Expression in seeds

Seed-based systems are very promising for the production of heterologous recombinant proteins. Seeds are natural storage organs for nutrients to allow the next generation embryos to develop, and this property ensures long-term storage of recombinant antibodies at ambient temperature without any significant loss of activity, thus they are also ideal for easy transportation without maintenance of cold chain (Boothe et al., 2010). Numerous antibodies, and engineered antibody fragments such as scFv, Fabs, sdAbs and their fusions with Fc tail have successfully been synthesized in Arabidopsis seeds (De Jaeger et al., 2002; De Meyer et al., 2015; Loos et al., 2011). Moreover, seeds would be very advantageous for oral delivery of antibodies to allow passive mucosal immunization against several infectious diseases (Juarez et al., 2016; Virdi et al., 2013; Virdi et al., 2019). Additionally, plant-based edible subunit vaccines have also been studied against various pathogens (including HIV, Plague, piglet enterotoxigenic *Escherichia coli* (ETEC) diarrhea) causing infectious diseases in humans or commercially important animals (Alvarez and Cardineau, 2010; Chan and Daniell, 2015). Edible vaccines are attractive alternatives for needle-based vaccination. The major disadvantage of the seed-based system is that it is time-consuming during the development phase because it takes several months to a year to obtain homozygous plants producing the seeds; however, after that, plants can be easily scaled-up (Palaci et al., 2019).

2.3.2 Expression in leaves

Recently, the leaf expression system has emerged as the most widely used method for inexpensive production of heterologous proteins in plants. Both stable and transient expression has been achieved in leaves. Several plants have been explored for this system and the tobacco plants (*Nicotiana* species) are the most suited for such applications. *Nicotiana tabacum* is the most reliable expression host for stable expression. However, it takes several months to obtain homozygous line, thus transient expression may be regarded as the most preferable method. In

addition to the merits of *in planta* expression, transient expression in leaves offers a high protein yield in a very short period of time (days to two weeks). Thus, this system significantly reduces the protein production timeline, that is not achievable with stable expression. However, transiently expressed proteins are often contaminated with alkaloids, therefore efficient downstream processing is required (Paul and Ma, 2011a). The leaf expression system is suitable for early discovery and refinement phase that allows validation of variety of engineered antibody formats in several *in vitro* assays (Virdi et al., 2016). However, for *in vivo* validation that requires antibodies in milligram amounts, one has to opt for seed-based expression systems. Arabidopsis seed enables accumulation levels of IgG and IgA antibodies up to 0.2% to 3% of total seed weight that suffice to perform pilot scale *in vivo* experiments (Virdi et al., 2013). However, crop plants such as soybean are much suited for bulk production that provide larger biomass compared to *Arabidopsis* seeds.

Nicotiana benthamiana is the widely used model for transient expression due to its amenability for agroinfiltration-mediated gene delivery, and this is based on the fact that this variety is a natural occurring mutant in the RNA dependent RNA polymerase gene, thus resulting in lower degrees of post transcriptional silencing. The traditional method for transient expression involves the utilization of standard, non-viral vectors comprised of the gene of interest under transcriptional control of strong constitutive promoters, and the highest yield is achieved by adding a KDEL peptide and ER-retention signal to the C-terminus of the gene of interest. The suspension of *Agrobacterium tumefaciens* bearing an expression cassette containing the gene of interest and a strong constitutive promoter (*i.e.* 35S CaMV (cauliflower mosaic virus) promoter) is delivered into the extracellular leaf spaces by syringe (physical) or vacuum infiltration, this process is known as agroinfiltration. Although flexibility with syringe infiltration allows the introduction of multiple constructs in the same leaf, thereby permitting multiple analyses with a single leaf (Vaghchhipawala et al., 2011). It is not possible with vacuum infiltration where the entire plant is infiltrated with the one construct. However, vacuum infiltration is more robust and has the potential for enormous scalability that facilitated the development of biopharmaceuticals at the industrial scale.

Antibody production by conventional plant-based systems has been considered as a very slow means of industrial scale manufacturing as compared to bioreactors using mammalian cell culture, until two major technological breakthroughs in Nicotiana-based manufacturing system. These include glycoengineered transgenic plants that can produce antibodies with mammalian glycoforms (Strasser et al., 2008) and viral-based transient expression system allowing high yield and upscaling of the antibodies in days (Hiatt and Pauly, 2006; Marillonnet et al., 2005). Besides the above-mentioned method, another strategy for transient expression utilizes plant viruses as adapted expression vectors. The earlier method was based on a mature virus particle carrying the gene of interest as an additional open reading frame in the functional genome (Lico et al., 2008). However, use of this method was hindered due to the limited packaging capacity of the viruses. The second, more advanced method allows the expression vector to contain only a few elements such as a promoter, terminator, enhancer and silencing suppressor gene that are crucial for transgene expression in the plant tissue. These vectors are referred to as the "deconstructed virus" (Gleba et al., 2007) that enables the development of a most advanced technology termed 'Magnifection' (Donini and Marusic, 2019) which was trademarked by Icon Genetics (Hale, Germany) as magnICON® technology and vectors (Klimyuk et al., 2014). The magnICON® technology allows the production of several heterologous proteins such as cytokines, growth hormones, single-chain antibodies and monoclonal antibodies at high levels in plants (1-5 g/kg FW) and is currently used by many industries and research laboratories worldwide. For example, Mapp Biopharmaceuticals Inc. developed an analogue of Palivizumab and produced in glycoengineered *N. benthamiana* plants using magnICON® to reduce the manufacturing cost and provide cost-effective treatment for respiratory syncytial virus (RSV) infection (Zeitlin et al., 2013). The virus neutralization activity and RSV F-binding affinity of plant-produced palivizumab (palivizumab-N) were comparable to that of conventional palivizumab produced by a mouse myeloma cell line. Moreover, palivizumab-N displayed protection against RSV infection in the cotton rat disease model in prophylactic and therapeutic settings (Zeitlin et al., 2013).

Currently, several plant-derived biopharmaceuticals based on 'MagnICON' are being validated in clinical trials. These include ZMapp (Mapp Biopharmaceutical, San Diego, United

States) against Ebola virus (clinical trial number- NCT03719586, https://clinicaltrials.gov), which comprise the cocktail of three chimeric neutralizing antibodies produced in *N. benthamiana* plants with knocked-down plant-specific glycosyl transferases (β1,2-xylosyltransferase; and α1,3-fucosyltransferase) (Qiu et al., 2014). These antibodies were first used to treat humans in the 2014 Ebola outbreak as alternative treatment was not yet available. HAI-05, subunit influenza vaccine against H5N1 was also produced in *N. benthamiana* (clinical trial number- NCT01250795, https://clinicaltrials.gov) (Shoji et al., 2012).

2.3.3 Yeast expression system

Another attractive platform for the production of therapeutic proteins is yeast expression that is useful for both basic laboratory research and industrial production. *Pichia pastoris* has gained enormous popularity in recent years due to its unique features that can be attributed to several features: these include ease of genetic manipulation, the rapid growth rate in relatively cheap and defined media thus decreasing the production cost, no susceptibility to contamination with endotoxins or viruses, stable expression and scalability in fermenters. Like other eukaryotic systems, *P. pastoris* is capable of diverse post-translational modifications including proteolytic processing, protein folding, disulfide bridge formation and oligomerization, glycosylation, methylation, and acylation (Wang et al., 2016).

Moreover, *P. pastoris* secretes large amount of active recombinant proteins with very few endogenous proteins, using the secretion signal, that eases downstream processing. The most commonly employed secretion signal is derived from the alpha mating factor (α-MF) leader sequence of *Saccharomyces cerevisiae* that has proven to direct and process heterologous protein through the secretion pathway effectively. The α-MF signal sequence composed of 19-amino acid pre- and 67 amino acid pro-peptides regions. First, the pre-signal directs the nascent protein to the ER and subsequently is cleaved off by signal peptidases, followed by transferring the protein to the Golgi by a pro-signal, where it is finally removed by the Kex2 endopeptidase (Kurjan and Herskowitz, 1982).

P. pastoris is a methylotrophic yeast, that is able to metabolize methanol as its sole carbon and energy source. Thus, the cloning system based on the inducible AOX1 promoter has been

extensively explored (Gomes et al., 2018). Methanol is oxidized to formaldehyde using molecular oxygen by the enzyme alcohol oxidase. The poorer affinity of this enzyme to O_2 is compensated by producing a large amount of alcohol oxidase. In *P. pastoris,* two genes (*AOX1 and AOX2*) code for alcohol oxidase, while the majority of production is regulated by *AOX1*. The strong and tightly regulation methanol inducible promoter for *AOX1* (P_{AOX1}) holds the advantage over other inducible promoters. Its repression and de-repression depend on the presence of carbon sources such as glucose, glycerol or ethanol. Upon depletion of the carbon sources, and the addition of methanol, P_{AOX1} is fully induced and drives the high expression of the heterologous protein (reviewed in Ahmad et al., 2014). However, its toxic and highly flammable nature makes methanol undesirable for industrial-scale production. To circumvent these disadvantages, several variants of P_{AOX1} have been explored that do not demand methanol for induction and allow high expression of the heterologous protein (Wang et al., 2017; Zahrl et al., 2017).

Since the majority of biopharmaceuticals are glycoproteins, the glycosylation machinery of the host is of tremendous interest. In contrast to homogenous and complex N-glycans in humans, *P. pastoris* provide their glycoproteins with heterogeneous high-mannose type which is detrimental to the pharmacokinetic behavior of the therapeutic proteins and leads to increased serum clearance in the human circulation due to interaction with human mannose receptors (De Pourcq et al., 2010). More recently, considerable efforts have been made towards the humanization of protein glycosylation pathways in order to produce therapeutic glycoproteins and antibodies with humanized glycosylation profiles (De Pourcq et al., 2010; Van Landuyt et al., 2018; Wildt and Gerngross, 2005).

Yeast expression systems have received approval from numerous regulatory agencies such as FDA, EMA, PMDA, CDSCO for production of a range of biopharmaceuticals (Sanchez-Garcia et al., 2016). In recent years, *Pichia pastoris* has gained attention for the production of numerous biopharmaceutical products including human serum albumin, human insulin, trypsin, collagen, hepatitis B vaccine, interferon-alpha 2b, and Nanobody® ALX-0061, among others (https://pichia.com/science-center/commercialized-products/). At present, several *P. pastoris* full-length antibodies are being studied in clinical trials. Eptinezumab (formerly known as ALD403) is currently in Phase III clinical trials (NCT02974153, https://clinicaltrials.gov/). It is a

humanized monoclonal antibody against calcitonin gene-related peptide (CGRP) that is being developed by Alder Biopharmaceuticals for the treatment of migraine (https://www.alderbio.com/pipeline/). Other examples are Vobarlizumab (ALX0061, recombinant sdAbs against IL6 receptor), and ALX0171 (recombinant anti-RSV sdAbs) used for rheumatoid arthritis and RSV infection treatment, respectively; both are developed by Ablynx NV. However, ALX0171 development program was stopped and the clinical trial has been discontinued. Moreover, anti-Ebola antibody cocktail, ZMapp has also been developed in glycoengineered *P. pastoris* strain (Glycoswitch); however, its *in vivo* efficacy has yet to be addressed in animal models (Purcell et al., 2017). To conclude, the characteristics of different expression platforms have been summarized in Table 3.

3. Conclusion

The global biopharmaceutical market accounted for $186,470 million in 2017 and is expected to rise up to $526,008 million by 2025. The increased demand of biopharmaceuticals is attributed to their ability to treat several untreatable diseases, that were incurable in the past. Full-length monoclonal antibody dominates the market that represent approximately half of the market share of total biopharmaceuticals, followed by vaccines, TNF blockers, hormones like insulin, and other small molecules (VHHs) (Ecker et al., 2015). Currently, nearly 50 monoclonal antibodies have been approved by the FDA and approximately 300 are in the stage of preclinical or clinical development. Despite capturing significant fraction of total market share, monoclonal antibodies are often associated with some limitations. Antibody fragments are attractive alternatives for new therapeutic and diagnostic applications. Over the past few years, there has been surging interest in the scientific community for developing VHH-based therapeutics as it offers several advantages such as small size, ease of manufacturing, high thermostability, ease of engineering to generate multivalent or multi specific moieties, and easy penetration. But, optimizing the production process with high productivity and desired properties such as optimal glycosylation is not an easy task. It is worthwhile to take a comparative view of different expression platforms into account to choose an appropriate production host. Although, both plants and yeast seem

cost-effective expression system for antibody production, yeast offers an advantage for rapid production and analysis. However, plants have the potential to store the functional proteins intact in seeds at ambient temperature for several years.

Table 3. Comparison of different expression platforms for therapeutic protein production (adapted from (Yao et al., 2015) and (Dingermann, 2008)				
Characteristics	*E. coli*	*Pichia pastoris*	**Plants**	**Mammalian cells (e.g. CHO)**
Classification	Gram-negative	Methylotrophic yeast	Higher eukaryotic	Higher eukaryotic
Disulfide bonds	only in periplasm	yes	yes	yes
Glycosylation	No	Yes, no terminal α1,3 mannose	Yes, terminal fucose	Yes, typically human-like
Protein folding accuracy	Low	Medium	High	High
Protein yield	Medium	High	High	Medium-High
Product quality	Low	Medium	High	High
Contamination risks	Endotoxins	Low	Low	Virus, Prions, oncogenic DNA
Cost of production	Low	Low	Moderate	High
Use of antibiotics	Typically required	Not required	Not required	Not required
Safety costs	Low	Low	Low	High
Scale-up capacity	High	High	Very High	Very low
Storage costs	Moderate	Moderate	Inexpensive	Expensive
Process developed	Industrial scale	Industrial scale	Industrial scale	Industrial scale
Production market	Yes	Yes	Yes	Yes

Chapter 2

Single domain antibodies: as vaccine delivery vehicles and antivirals

Shruti Bakshi, Bert Schepens and Ann Depicker

Author contribution:

S.B. wrote the chapter. A.D. and B.S. edited it.

Abstract

Owing to their appealing characteristics, VHHs have much to offer in various applications. Here, we exploited VHH-Fc fusions as a vaccine delivery vehicle and antivirals for the infectious agent. Antibodies are being used already for a long time as a precise selective targeting agent; however, their complex structure poses several obstacles. VHHs offer an attractive alternative due to their small size and ease of engineering. A triple fusion of VHH with a vaccine antigen and Fc domain enables the vaccine delivery to the tissue-specific receptors and also to the Fc receptors on antigen presenting cells, thereby eliciting focused immune response.

On the other hand, VHHs also have potential as antivirals to replace already available expensive therapies. For instance, VHHs against the respiratory syncytial virus have been shown to have a virus neutralization potency in the picomolar range by inhibiting fusion to the host cell membranes. Furthermore, Fc fusions to these VHHs not only improve the breadth of the neutralization by offering Fc-mediated effector functions, but also increase the half-life of the associated VHHs.

This chapter addresses the scope of VHH-Fc fusions to deliver vaccine antigens to a selected intestinal receptor allowing to fight against an enteric pathogen, and also the potential to develop improved VHH-antivirals for RSV infections.

Part 1. VHHs as vaccine delivery vehicle

Vaccination has been established as the most successful public health interventions for the prevention of a wide range of infectious diseases. The health benefits of vaccines are indisputable. Vaccination involves the administration of the antigenic preparation that subsequently results in activation of adaptive immunity and provides long-term protection against that pathogen. The very first development of a vaccine as a public health tool was demonstrated by Edward Jenner for smallpox in 1796. Since then, many milestones have been achieved in vaccine research yielding many cost-effective and safe vaccines with reduced adverse reactions induced by the vaccine material. There are several types of vaccines. The most traditional vaccine method utilizes live-attenuated/killed pathogens or inactivated bacterial toxins to initiate an immune response. The traditional methods became increasingly common and were employed to develop several successful vaccines such as vaccinia (Jacobs et al., 2009), tuberculosis (Luca and Mihaescu, 2013), and polio (Blume and Geesink, 2000). Despite these successes, the traditional methods started to lose interest among the scientific community as they failed to provide required protection without any adverse reactions. The risk of strain reversion to a more virulent phenotype and inefficient attenuation resulting in a more severe disease state (Pliaka et al., 2012; Unnikrishnan et al., 2012) is the major concerns with live-attenuated vaccines. Thus, with the advancements in biotechnology research and in search of an efficient vaccination strategy, the next generation vaccines such as recombinant/DNA vaccine, conjugated vaccines and subunit vaccines are being developed, all having their own advantages and disadvantages as summarized in Table 1.

Table 1. Comparison of different types of vaccines (Baxter, 2007; Vartak and Sucheck, 2016)

Vaccine type	Advantages	Disadvantages	Example
Live attenuated	• very potent, multiple doses are not required • immune response against all the antigens associated with the infection is generated	• Risk of reversion of the pathogen to infectious state that may cause illness	Measles, mumps, rubella (MMR combined vaccine), Varicella (Chickenpox), Influenza (nasal spray), Rotavirus
Killed/ inactivated	• Safe to use in immunocompromised patients • No risk of reversion thus can't cause a disease state. • Storage conditions are not critical compare to live attenuated vaccines.	• Require several doses • Inefficient • Adverse reaction at the vaccine site due to adjuvant • Do not give rise to cytotoxic T cells	Polio (IPV), Hepatitis A
Recombinant/ DNA	• Better stability compared to traditional vaccines. • No risk of reversion can't cause a disease state. • Storage conditions are not critical. • Better control on vaccine design as the desired gene can be added or deleted.	• High production cost compared to other vaccine types • Mutation in host DNA is possible in case of DNA vaccines	Vaccine to protect horses from West Nile virus
Conjugated	• Safe to use in immunocompromised patients • can't cause a disease state • Fewer chances of adverse reactions because of the purified antigenic components.	• Conjugation chemistry is difficult to control which could cause batch-wise variation. • Choice of the carrier protein is crucial as they could be immunogenic causing suppression of the antigenic immune response	*Haemophilus influenza* type b (Hib), Pneumococcal, Meningococcal
Subunit vaccine	• Safe to use in immunocompromised patients • can't cause a disease state • Fewer chances of adverse reactions because of the purified antigenic components.	• Less immunogenic than live attenuated vaccines • Particular antigens should be identified causing the disease	Hepatitis B, Human papillomavirus (Cervarix)

1.1 Targeted Subunit vaccines

Subunit vaccines are designed to possess only minimal microbial components (e.g. peptide, proteins or polysaccharides) that are necessary to produce an appropriate immune response, which makes them safer compared to traditional vaccines. Although subunits vaccines have the potential to circumvent the difficulties of classical vaccine development approach, they are often

poorly immunogenic due to the limited number of components and their non-replicating nature (Demento et al., 2011). This necessitates the co-administration of potent immunostimulatory agents (adjuvants or carrier), higher doses and multiple boosters to achieve prolonged immunity (Abdel-Aal et al., 2008; Boato et al., 2007; Demento et al., 2011; Skwarczynski et al., 2012).

The characteristics of subunit vaccines such as efficacy, immunogenicity, stability and the number of doses required can be further improved by incorporation with several other components including vaccine delivery system (e.g. emulsions, liposomes, and polymers) (Moyle and Toth, 2013; Vartak and Sucheck, 2016). Moreover, the subunit vaccines can be coupled to the targeting moieties capable of directing them to certain immune cells (e.g. antigen presenting cells) or organs (e.g. lymph nodes, mucosal-associated lymphoid tissue (MALT)) to generate a focused immune response. Antigen-presenting cells (APCs) such as dendritic cells (DCs), and macrophages are the vital components of the immune system that plays a crucial role in engulfing and processing the antigens. APCs ultimately present the processed antigens via major histocompatibility complex (MHC) molecules to T cells; thus, triggering their activation, expansion and differentiation into the effector cells (Bilsborough and Viney, 2004; Holmgren and Czerkinsky, 2005). APCs could also present the unprocessed antigens to B cells (Heesters et al., 2016). During the protective immune response, B-cell derived plasma cells secrete high-affinity antibodies (Abs), and T cells produce cytokines (CD4+ T cells) or show cytotoxic activity (CD8+ T cells) for pathogen clearance. While, for the adaptive immune response, some lymphocytes differentiate into memory cells that clear the pathogen upon secondary infections (Junt et al., 2008; Randolph et al., 2008).

The efficacy of the vaccine can be significantly enhanced by specific targeting to the cell surface receptors on APCs (Keler et al., 2007). Additionally, a precise targeting can also reduce the adverse effects and degradation of vaccine material by irrelevant cell types. Currently, therapeutics antibodies are being developed to fight against various infectious diseases by targeting disease-specific antigens in pathogens. The exquisite binding specificity of an antibody can be exploited for selective targeting of a vaccine antigen to APCs. The antigen payload that subsequently elicits the adaptive immune response can be coupled either genetically by producing recombinant antibody-antigen fusion constructs or chemically by linking the antigen

to APC-specific binding antibodies (Lehmann et al., 2016). The genetic fusion method has several advantages over chemical coupling. Genetic fusion allows more controlled coupling of an exact number of antigens, while this is unpredictable in the chemical coupling. Additionally, targeting antibodies can be engineered to contain improved characteristics such as high accumulation, host compatibility (humanization), appropriate folding and solubility by changing amino acid composition (Chiu and Gilliland, 2016; Ducancel and Muller, 2012; Teplyakov et al., 2018; Van der Weken et al., 2019). Antibodies possess several other features including complement fixation and effector functions of the Fc tail that also serves as a dimerization motif. For genetically engineered vaccines, the vaccine antigen may be fused to APC-specific full-length antibodies (Dudziak et al., 2007), antibody fragments such as single-chain variable fragments (scFv), Fabs, single-domain antibodies (VHH) (Fang et al., 2017b; Schjetne et al., 2007), or natural ligands against pattern recognition receptors (PRRs) expressed by APCs such as Toll-like receptors (TLRs) or C-type lectin receptors (CLRs) (Yu et al., 2018). VHH-Fc fusions seem superior due to their distinct properties, as described in Chapter 1 (Czajkowsky et al., 2012). Moreover, the choice of an Fc scaffold holds promise in directing the vaccine antigen to the Fc receptors on APCs. For instance, both human IgG1 and IgG3 exhibit higher affinity for FcγR than IgG2 and IgG4 (Bruhns and Jonsson, 2015), but IgG3 is not favored due to its short half-life (Morell et al., 1970) and susceptibility to proteolysis (Jefferis, 2007). The short half-life of IgG3 was explained by the presence of histidine residue at 435 position that results in reduced interaction with FcRn (Stapleton et al., 2011). Therefore, the human IgG1 isotype is the targeting antibody of choice.

1.2 Mucosal vs parenteral vaccination

In addition to vaccine targeting to APCs, the route of administration is equally important and strongly affects the quality of the immune response (Mohanan et al., 2010). Traditionally, the subcutaneous injection was the preferred method for all the adjuvanted vaccines, excluding BCG vaccine. It was later observed that the vaccines caused severe local adverse reactions at the site of injection due to the adjuvants used in the formulation. Therefore, the intramuscular injection was considered as an alternative route, that also elicited a better immune response with a reduced rate of adverse reactions compared to subcutaneous injection in some studies (Cook,

2008; Cook et al., 2006; Ruben et al., 2001). Although the traditional methods via parenteral routes (intramuscular, subcutaneous, and intradermal) have proven to be useful to stimulate the systemic immune response, the generated circulatory antibodies are not sufficient to fight against mucosal infections (Holmgren and Czerkinsky, 2005). Given that the majority of infections occur at the mucosal membranes, the establishment of protective mucosal immunity is of paramount importance.

Mucosal vaccines can not only trigger both antigen-specific humoral and cell-mediated immune responses at mucosal membranes, but they also result in systemic responses, that has been well documented in several studies. Moreover, mucosal vaccinations have the potential to achieve long-lasting B- and T-cell memory (Brandtzaeg, 2007; Sheridan and Lefrançois, 2011). The acquisition of mucosal homing property of B and T cells is dependent on the specialized dendritic cells that migrate from mucosa to draining lymph nodes and allow lymphocytes to enter the mucosal tissues (Mora and von Andrian, 2009). The mucosal vaccination is characterized by induction of pathogen-specific secretory IgA (SIgA), that also ensures cross-protection against viruses (Hasegawa et al., 2015).

Needle-free mucosal vaccines can be delivered via various routes based on the nature of the infection caused by the pathogen. For instances, vaccine administration via the oral route stimulates the immune response against intestinal infections caused by enteric pathogens such as enterotoxigenic *Escherichia coli* (ETEC), *Shigella* species, *Vibrio cholerae*, *Helicobacter pylori*, and rotaviruses. On the contrary, intranasal administration is effective at inducing an immune response against respiratory infections caused by *Mycoplasma pneumoniae*, influenza virus and respiratory syncytial virus; and sexually transmitted genital infections caused by HIV, *Chlamydia trachomatis*, *Neisseria gonorrhoeae* and herpes simplex virus (Holmgren and Czerkinsky, 2005; Lycke, 2012). In addition, sublingual vaccination is gaining a lot of interest because it evokes strong mucosal and systemic antibody responses, as well as T-cell mediated cytotoxic responses (Carmichael et al., 2011; Cho et al., 2010; Domm et al., 2011). One study even demonstrated that sublingual administration of adjuvanted subunit influenza vaccine evoked comparable B-cell memory responses to those elicited by intramuscular injection with conventional influenza vaccines (Gallorini et al., 2014). Moreover, it has been shown that pulmonary inoculation with

aerosolized virus-like particles (VLP)-based vaccines targeting the HIV coreceptor CCR5, could elicit both a mucosal as well as a systemic immune response resulting in high-titers of systemic antibodies (Hunter et al., 2009). These studies demonstrate the potential of mucosal vaccines to prevent infection at the portal of pathogen entry.

Furthermore, oral vaccines do not need extensive purification, as the gut is heavily populated with gut microflora. Thus, they are cost-effective and practical for mass vaccination. Moreover, needle-free administration reduces risks of transmitting blood-borne infections through the infected needle (Srivastava et al., 2015) and does not require the specific training for vaccination. However, the orally delivered subunit vaccines are poorly immunogenic due to degradation of most antigenic epitopes by the harsh environment in the gut-intestinal (GI) tract (Neutra and Kozlowski, 2006), thus they must be protected with supplemental materials or adjuvants to potentiate the vaccination capacity (Gutjahr et al., 2016).

Nevertheless, it is difficult to predict the *in vivo* efficacy of the vaccine protein, as multiple factors affect the functional outcome. Many mucosal vaccines candidates, that were successful in preclinical studies in animal models failed to confer protection in clinical trials (Czerkinsky and Holmgren, 2010; Pasetti et al., 2011), showing that results obtained in animal model systems cannot automatically be extrapolated to humans. Because of the low efficacy of most orally administered mucosal vaccines, only a few licensed oral vaccines currently exist. (summarized in Table 2), and more research is needed to make oral vaccines more potent and efficient.

Pathogen	Trade name	Composition	Dosage	Immunological mechanism	Efficacy
Rotavirus	Rotarix, RotaTeg	Live attenuated, monovalent or pentavalent rotaviruses	Oral, 3 doses	Mucosal IgA and systemic neutralizing IgG	Over 70%-90% against severe disease
Poliovirus	Orimune, OPV, Poliomyelitis vaccine	Live attenuated trivalent, bivalent, and monovalent polioviruses	Oral, 3 doses	Mucosal IgA and systemic IgG	Over 90% in most of the world
Salmonella Typhi	Vivotif, Ty21A	Live attenuated *S.* Typhi *bacteria*	Oral, 3-4 doses	Mucosal IgA, systemic IgG, and CTL responses	Variable, but more than 50%
Vibrio cholera	Dukoral, ORC-Vax, Shanchol	Inactivated *V. cholera* O1 classical and El Tor biotypes with or without CTB	Oral, 2-3 doses	Antibacterial, toxin-specific, and LPS-specific IgA	Strong herd protection over 85%
Influenza type A and B virus	FluMist	Live viral reassortant with the trivalent mix of H1, H3, and B strains of hemagglutinin and neuraminidase genes in an attenuated donor strain	Intranasal in young children, 2 doses	Hemagglutinin- and neuraminidase-specific mucosal IgA and systemic IgG responses	>85% in children, variable in adults

Table 2. Licensed mucosal vaccines for human use (reused from Kim and Jang, 2017)

1.3 Antigen sampling and immune responses in the gut

The mucosal immune system is composed of both inductive and effector sites based on their anatomical and functional characteristics. The inductive site in the GALT (Gut-associated lymphoid tissue) includes Peyer's patches and isolated lymphoid follicles that acquire the intestinal antigen and initiate a primary adaptive response; whereas effector sites such as lamina propria contain antigen-specific IgA-producing plasma cells and memory B and T cells. The gut epithelium is organized as crypt-villus structures and is composed of the four principle cell types:

enterocytes, goblet cells, Paneth cells and enteroendocrine cells. Enterocytes are the major cell type in the intestinal epithelium and have a primary function in nutrient absorption. However, these cells also express specific receptors on their surface to enable receptor-mediated endocytosis (Melkebeek et al., 2012). In addition, enterocytes express polymeric immunoglobulin receptor (pIgR) that facilitates the secretion of secretory IgA. Goblet cells secrete mucus, Paneth cells secrete antimicrobial peptides and proteins, whereas enteroendocrine cells produce hormone-like molecules (Kong et al., 2018). In addition to crypt-villus formation, a smaller proportion of intestinal epithelium exist as small flat sections that are called follicle-associated epithelium (FAE). The most distinguishing feature of the FAE is the presence of specialized antigen-sampling cells, known as M cells or 'microfold' cells. M cells are highly phagocytic and shuttle the intestinal antigen to underlying follicles. The basolateral membrane of the M cells is invaginated to form an intraepithelial pocket. Within these pockets, antigen-presenting cells (APCs) and lymphocytes are present that take up transcytosed antigens. In comparison to enterocytes, M cells are far less abundant and account for only 1% of all intestinal epithelial cell populations. Next to M cells and enterocytes, dendritic cells (DCs) in the lamina propria can also participate in sampling both pathogenic and commensal bacteria by extending their dendrites between epithelial cells (Rescigno et al., 2001).

Further, the transcytosed antigen is taken up by dendritic cells which play a crucial role in inducing immune responses to control the infection. Under steady-state conditions, production of local factors such as TGF-β and prostaglandin E_2 by intestinal epithelial cells results in partial maturation of DCs in Peyer's patches (PP) or lamina propria (LP). These semi-mature DCs present antigen to naïve $CD4^+$ T cells in the mesenteric lymph nodes (MLN) or PP and induce their differentiation into either tolerogenic T cells (T_H3) or regulatory T cells (T_{reg}). On the contrary, when pathogen is encountered, they are recognized by TLRs expressed by macrophages, DCs and intestinal epithelial cells, resulting in inflammation. This leads to the complete maturation of DCs and secretion of IL-12. These mature DCs migrate to MLN and subsequently activate the pathogen-specific effector T cells (T_H1, T_H2 and/or T_H17 cells) (Cerutti et al., 2011, Devriendt et al., 2011). Finally, effector T cells migrate to B cell follicles of germinal center and secrete cytokines to promote IgA class switching (Bemark et al., 2012). Moreover, IgA+ plasma cells

terminally differentiate in lamina propria to secrete secretory IgA (SIgA) that are the major immune effector component in the mucosa. SIgAs transport across the epithelial cells via pIgR and eliminate the pathogenic antigen by making antigen-IgA complexes, thereby inhibiting the antigen binding to the specific receptors (Kim and Jang, 2017) (Figure 1).
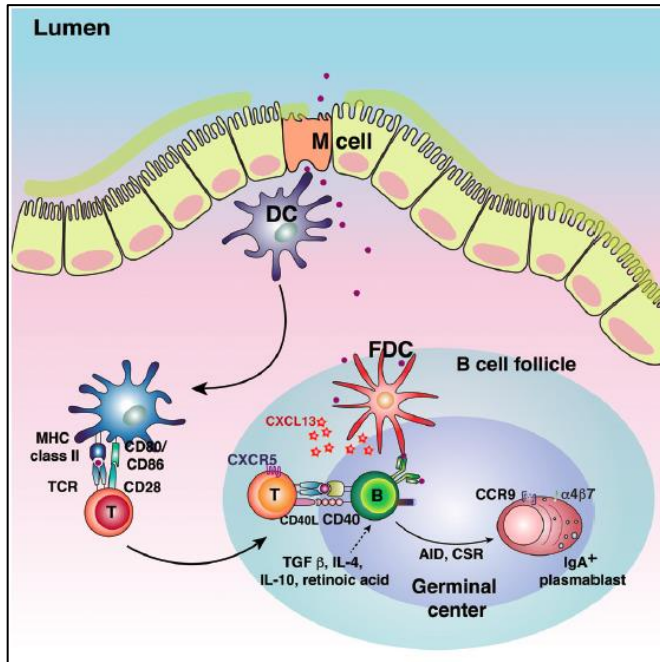
Figure 1. Schematic diagram of mucosal immune induction. The luminal antigens transcytosed by M cells encounter dendritic cells (DCs) in the subepithelial dome of Peyer's patch. DCs loaded with the antigens migrate to the interfollicular T cell zone and induce the effector T cells. Antigen-specific effector CD4+ T cells express CD40 ligand and induce the IgA+ plasmablasts. FDC, follicular dendritic cell; TCR, T-cell receptor; TGF β, transforming growth factor β; IL, interleukin; AID, activation-induced cytidine deaminase; CSR, class switch recombination; CXCL13, CXC chemokine ligand 13; CXCR5, CXC chemokine receptor 5. (reused from Kim and Jang, 2017).

1.4 VHHs as delivery vehicle to combat enteric pathogens

Given the fact that most pathogens colonize and invade the host at mucosal surfaces, it seems logical to pursue needle-free mucosal vaccination. In contrast to parenteral vaccination, oral immunization is capable of inducing a mucosal immune response to battle intestinal pathogens (Melkebeek et al., 2012). The oral route is more challenging due to the hostile environment in the gastrointestinal tract such as low gastric pH, degradation by proteolytic enzymes, rendering the oral vaccine ineffective. Thus, encapsulation of the vaccine antigens in biodegradable microparticles as delivery systems is of paramount importance. Nevertheless, the intestinal wall is almost impermeable except for the metabolites and small products from digestion. This results in poor uptake of such vaccine microparticles by intestinal cells and inefficient transport across the epithelial barrier to reach the underlying GALT. Repeated large dose administration of vaccine

antigens is the simplest method by far to overcome these difficulties. However, producing the vaccines in large quantities becomes very expensive, what makes this strategy unsuitable. M cell-mediated transport leads to induction of local and short-live antigen-specific IgA immune response and also systemic tolerance to the fed antigen; thus antigen-specific systemic response is not generated (Russell-Jones, 2000).

However, some molecules use a special mechanism and are capable of inducing good serum antibody response by crossing the intestinal barrier. These molecules bind to specific receptors on villous enterocytes, rather than on M cells. Selective targeting of vaccine antigens to a receptor on intestinal cells facilitates the induction of local as well as systemic immune responses towards the intestinal infection (Devriendt et al., 2012). A fusion protein comprised of a vaccine antigen and a receptor targeting ligand can be envisioned to provoke efficient adaptive immune responses both locally and systemically. The strong affinity and specificity of antibodies makes them ideal targeting moieties for vaccine delivery.

In the recent past, aminopeptidase N (APN) on enterocytes was identified as a receptor for F4ac fimbriae of F4+ ETEC (enterotoxigenic *E. coli*) that causes severe diarrhea in piglets. The orally delivered anti-APN rabbit polyclonal antibodies elicited a mucosal immune response (Melkebeek et al., 2012) that suggests a hypothesis to target an antigen to this receptor via antigen-antibody fusions to elicit the intestinal mucosal immune response. However, antigen fusions to a conventional antibody remains challenging owing to their complex structure. An alternative would be to use simplified antibody versions or antibody fragments such as VHHs, that offer several advantages as discussed earlier. For instance, Lipovaxin-MM (developed by Lipotek) is an antibody-conjugated vaccine formulation to treat metastatic melanoma. It is composed of DC-SIGN (C-type lectin receptors expressed on dendritic cells) targeting single domain antibody fragment (VH or VL of the antibody) and liposome nanoparticle-based vaccine encapsulating melanoma antigens and IFN-γ. Lipovaxin-MM has recently been successful in a phase I clinical trial (Gargett et al., 2018).

Although, VHH itself is enough to act as a targeting ligand, fusion to an Fc domain can further potentiate the immune response. Thus, a vaccine antigen fused to APN-targeting VHH-Fc would be an ideal mucosal vaccine for enteric pathogens that are taken up by enterocytes, and

the Fc domain would allow selective delivery of transcytosed antigens to the antigen presenting cells (APCs) such as dendritic cells. A first part of this thesis greatly concentrates on designing different permutations of antigen-antibody constructs to deliver antigen payloads to the intestinal mucosa.

Part 2. Passive immunization against Respiratory syncytial virus

Passive immunization has proven to be an extraordinary method to provide immediate protection against many human pathogens including bacteria, virus, fungi and parasites. Passive immunization is generally employed when a vaccination is not available for a certain disease or is not functional (for instance in immunocompromised individuals). Passive immunization involves the administration of IgG obtained from human plasma or human(ized) monoclonal antibodies. Although often expensive, passive immunization has been proved to be life-saving for several viral infections. For example, prophylactic administration of Palivizumab is the only proven means to protect against respiratory syncytial virus (RSV). Numerous advantages offered by VHHs make their use appealing for antiviral development. In this section, we focus on VHH-based antiviral development for the respiratory syncytial virus (RSV).

2.1 Respiratory syncytial virus - brief introduction

Respiratory syncytial virus (RSV) is one of the leading causes of lower respiratory tract illness (e.g. bronchiolitis, pneumonia) in infants and young children worldwide (Shi et al., 2017). Virtually, all children will have had an RSV infection by two years of age (Hall et al., 1991). As immunity induced by previous infections is not durable; recurring infections are common throughout life. The immature immune system as well as the early lung development of infants and neonates, correlate with increased susceptibility to respiratory tract infections (Levy, 2007). The most common lower respiratory tract infection (LRTI) in infants is bronchiolitis which is usually caused by RSV. However, children older than 2 years do not develop bronchiolitis upon RSV infection. RSV associated upper respiratory tract infection is more common in older children and young adults (Sidwell and Barnard, 2006). Although RSV is rarely lethal in healthy people, it can cause severe illness in high-risk groups (e.g. premature infants), immunocompromised individuals, frail and community-dwelling elderly persons (Falsey et al., 2005).

2.2 Clinical manifestations and pathogenesis

Children start to develop respiratory symptoms after 4-6 days of the incubation period (Meissner, 2016). Some common clinical manifestations in infants are tachypnea, cough, crackles, wheezing, fever, pharyngitis or respiratory distress. The disease is often associated with lethargy, irritability and poor feeding. Older children and adults present with cold-like symptoms such as cough, fever and congestion (Eiland, 2009). There is growing evidence that children who had severe RSV infection early in life are more likely to develop long term wheezing during early childhood, impaired lung function, hyper-reactive airways, and asthma later in life (Fauroux et al., 2017; Mohapatra and Boyapalle, 2008; Scheltema et al., 2018).

RSV is highly contagious and transmitted through direct contact with respiratory secretions from infected individuals. Factors that contribute to virus pathogenesis could be environmental, viral, and host factors. The weather has a significant impact on RSV spread and infection. In temperate climates, RSV circulates more in the winter season, typically peaking in January and February; compared to enterovirus infections that predominate in summer (van Drunen Littel-van den Hurk and Watkiss, 2012). Cigarette smoking or air pollution has a detrimental effect on respiratory health that results in necrotic cell death rather than RSV-induced apoptotic cell death (Groskreutz et al., 2009). Apoptosis is an efficient way to clear the airway from RSV infected cells and is associated with a less significant inflammatory response. Moreover, RSV-related infections are influenced by several host factors such as premature birth, young age (<6 months), chronic lung disease at prematurity, incomplete development of the respiratory system, T-cell immunodeficiency, immunosuppression or old age, and congenital heart disease (Simoes et al., 2015). Interestingly, an association between vitamin D deficiency and RSV-related bronchiolitis has been reported, typically during the first year of life (Belderbos et al., 2011). However, more recent evidence suggests otherwise as the study could not confirm this observation (Beigelman et al., 2015). Moreover, genetic predisposition of the host is also associated with the disease severity. Several single nucleotide polymorphism (SNPs) have been identified in the genes that are involved in innate immunity (TLR4 and VDR) and altered Th1/Th2 immune responses (IL4, IL13), surfactant protein genes (SPA and SPD), host cell receptor genes,

and cytokine or chemokine response genes (CCR5, IFN, IL6, IL10, TGFβ1) (Alvarez et al., 2018; Choi et al., 2013; Miyairi and DeVincenzo, 2008).

RSV infection occurs in both the bronchiole and alveolar epithelium and is associated with the obstruction of small airways by cellular debris (Johnson et al., 2017). Macrophages and epithelial cells secrete several cytokines and chemokines including IL-6, IL-8/CXCL8, IL-1α/β, IP-10/CXCL10, MCP-1/CCL2, MIP-1α/CCL3, MIP-1β/CCL4, RANTES/CCL5, TNF-α, and IFN-α/β and they were majorly found in respiratory secretions of hospitalized children (van Drunen Littel-van den Hurk and Watkiss, 2012). IL-8 upregulation correlates with the neutrophil recruitment that constitutes at least 84% of the total immune cell population. Although neutrophils are often protective in RSV infection by clearing RSV-infected cells, high number of these cells correlated with disease severity (van Drunen Littel-van den Hurk and Watkiss, 2012).

2.3 RSV burden on the health care system

Since its discovery about 60 years ago, RSV has been established as a major public health burden globally; however, reported incidence and mortality of RSV acute lower respiratory infection (ALRI) varies in different geographical locations (Nair et al., 2010; Stein et al., 2017). In 2015, RSV has been estimated to cause about 33.1 million ALRI incidences. 10 % of these cases (3.2 million) required hospitalization, with 59,600 in-hospital deaths in children younger than 5 years, resulting in a substantial burden on health-care industries (Shi et al., 2017). RSV-related mortality has been sporadically studied in developed countries (Lee et al., 2016; Leung et al., 2014); however, little is known about in-hospital fatality rate in developing or low-income countries where hospital-based surveillance is performed less frequently. Poorly defined data of disease severity in resource-limited settings might limit our ability to accurately access the overall burden in the full community. Therefore, it is possible that RSV-associated true case fatality rate is significantly higher than estimated (Karron and Black, 2017; Nokes et al., 2009). Finally, the global burden of RSV disease is overwhelming, therefore development of an effective therapeutic and preventive interventions are indispensable (Figure 2).
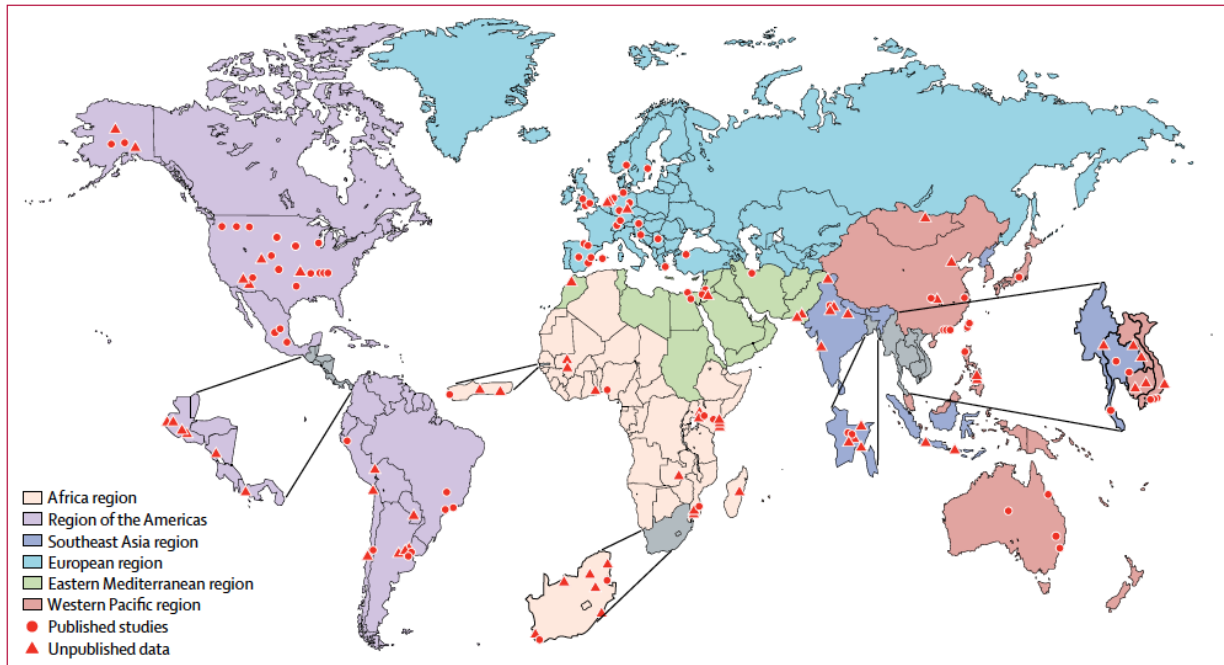
Figure 2. Location of studies reporting incidence, hospital admission, and in-house case fatality in children with RSV-associated acute lower respiratory infection (reused from Shi et al., 2017).

2.4 RSV Virology

RSV is a non-segmented negative-sense single-stranded RNA virus. It is an enveloped virus that belongs to the family *Pneumoviridae*, genus *Orthopneumovirus*. Its 15.2 kb long genome consists of 10 genes and encodes 11 proteins since two partially overlapping (upstream and downstream) open reading frames in the M2 mRNA yield two distinct matrix proteins, M2-1 and M2-2 (Borchers et al., 2013). Four genes code for intracellular proteins, namely N (nucleocapsid), P (phosphoprotein), M (matrix protein), and L ("large" protein, containing the RNA polymerase catalytic motifs) and are involved in genome transcription, replication and virus assembly. M2-1 is also a component of the mature assembly; however, the function of M2-2 is currently unknown. Non-structural proteins (NS1 and NS2) preferentially interfere with IFN-α/β signaling, thus play a significant role in evading immune responses (Lo et al., 2005). Three proteins contribute to the viral coat: glycoprotein (G), fusion (F), and small hydrophobic (SH) protein. The G and F surface proteins are responsible for viral entry by attachment and fusions, respectively to the host's cell membrane receptors, allowing the release of the viral genome in the cytoplasm. The role of SH protein is not well understood. Unlike protein G, protein F is highly conserved and

shares a significant level of sequence identity with its counterparts in other paramyxoviruses (Collins et al., 1984). (Figure 3)
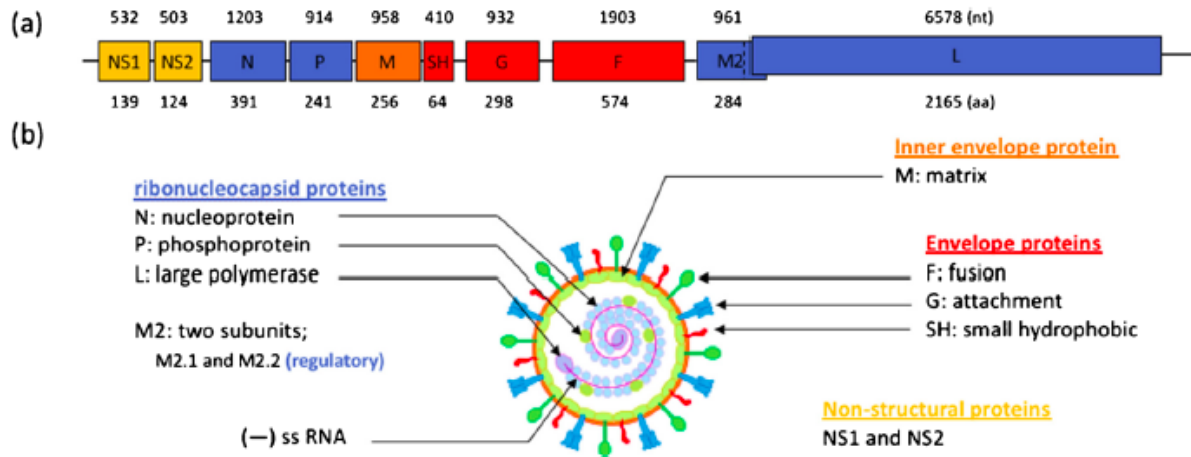
Figure 3. RSV genome and proteins. (a) negative-sense RNA genome encodes 11 proteins. The number above and below the map represent length in nucleotides (nt) and amino acids (aa) respectively. (b) Mapping of 11 proteins on RSV virion and their corresponding classes. (reused from Taleb et al., 2018)

Protein F is synthesized as an inactive precursor F_0 and activated by furin-like host proteases during transport to the cell surface to yield two disulfide-linked subunits, N-terminal F_2 and C-terminal F_1 (Gonzalez-Reyes et al., 2001). The newly generated F_1 subunit has a hydrophobic N terminus that represents the fusion peptide of the metastable prefusion conformation containing trimers of disulfide-linked heterodimers (F2-F1). This prefusion state is refolded to acquire a stable post-fusion confirmation during the subsequent fusion process. RSV infections in humans elicits antibodies that recognize preferentially either postfusion F, prefusion F or both. However, the RSV neutralizing activity of human sera is mainly mediated by antibodies that preferentially bind the F protein in its prefusion conformation (Ngwuta et al., 2015). Moreover, detailed analysis of a broad panel of RSV F-specific monoclonal antibodies isolated form human volunteers demonstrated that the most potent RSV neutralizing antibodies preferentially bind the prefusion F protein (Gilman et al., 2016). Hence, the prefusion state is an important target for developing antivirals or small molecules that can block the virus entry by inhibiting the refolding process (Krarup et al., 2015; Rossey et al., 2018).

RSV has been classified into two antigenic subgroups, A and B on the basis of the reaction with monoclonal antibodies against surface antigens (Mufson et al., 1985). Based on the genetic variability of the G protein, RSV A and B subtypes are further subdivided into 12 genotypes and 20 genotypes, respectively (Duvvuri et al., 2015). A relationship between RSV A and RSV B subtypes in terms of disease severity still remains controversial (Wright and Piedimonte, 2011), although some studies have reported that RSV A has a significant association with higher severity of illness and may more frequently increase the need of intensive care treatment (Jafri et al., 2013; Walsh et al., 1997). Both the subtypes can co-circulate during one epidemic, but in general, one predominates (Anderson et al., 1985; Kneyber et al., 1998; Laham et al., 2017; Ogunsemowo et al., 2018).

2.5 Treatment and prevention

RSV has a significant impact on global health. However, despite decades of research a vaccine or effective antiviral therapy for RSV is still missing. Consequently, the current primary treatment for RSV infection is still mainly supportive care with oxygen and fluid management. Different modalities such as antibiotics, hypertonic saline, and bronchodilators have failed in the past (Smith et al., 2017). Incomplete understanding of the body's immune response against RSV poses a challenge to RSV vaccine development efforts. The first formalin-inactivated (FI) RSV vaccine was developed in 1966, that resulted in increased disease severity in those children who were seronegative for RSV before vaccination and also caused the death of two infants (Kim et al., 1969). Thus, the vaccine was discontinued. Substantial effort is being devoted into RSV disease prevention; more than 15 RSV vaccines based on different strategies such as inactivated or live attenuated, subunit, virus-like particles (VLPs), and nanoparticles-based vaccines are currently in the pipeline as summarized in Figure 4 (obtained from RSV Vaccine snapshot—PATH Vaccine Resource Library', http://www.vaccineresources.org/).

RSV Vaccine and mAb Snapshot

TARGET INDICATION: (P) = PEDIATRIC (M) = MATERNAL (E) = ELDERLY

Category	PRECLINICAL	PHASE 1	PHASE 2	PHASE 3	MARKET APPROVED
LIVE-ATTENUATED/ CHIMERIC	Codagenix LID/NIAID/NIH — RSV; LID/NIAID/NIH — RSV; Meissa Vaccines LID/NIAID/NIH; PIV1-3/RSV — RSV	Intravacc (P) Delta-G RSV; Sanofi, LID/NIAID/NIH (P) RSV ΔNS2/Δ1313/I1314L; Sanofi, LID/NIAID/NIH (P) RSV 6120/ΔNS2/1030s; Pontificia Universidad Catolica de Chile (P) BCG/RSV; Sanofi LID/NIAID/NIH (P) RSV D46/NS2/N/ΔM2-2-HindIII; SIIPL, St. Jude Hospital (P) SeV/RSV			
WHOLE-INACTIVATED	Blue Willow Biologics RSV				
PARTICLE-BASED	AgilVax VLP; Fraunhofer VLP; TechnoVax VLP; VBI Vaccines VLP; Artificial Cell Technologies Peptide microparticles; Georgia State University VLP; University of Massachussetts Virometix VLP	Novavax (P) RSV F Nanoparticle	Novavax (E) RSV F Nanoparticle	Novavax (M) RSV F Nanoparticle	
SUBUNIT	Instituto de Salud Carlos III; University of Georgia; RSV F Protein; Sciogen RSV G Protein; University of Saskatchewan RSV F Protein	Beijing Advaccine Biotechnology (P)(E) RSV G Protein; Immunovaccine, VIB (E) DPX-RSV-SH Protein; NIH/NIAID/VRC (E)(M) RSV F Protein; GlaxoSmithKline (E)(M) RSV F Protein; Janssen Pharmaceutical (E) RSV F Protein	Pfizer (E)(M) RSV F Protein		
NUCLEIC ACID	CureVac RNA; Inovio Pharmaceuticals DNA				
RECOMBINANT VECTORS	BravoVax Adenovirus	Vaxart (E) Adenovirus	Bavarian Nordic (E) MVA; GlaxoSmithKline (P) Adenovirus; Janssen Pharmaceutical (P)(E) Adenovirus		
IMMUNO-PROPHYLAXIS/ COMBINATION	Arsanis Anti-F mAb; Biomedical Research Models DNA prime, Particla boost	Pontificia Universidad Catolica de Chile Anti-N mAb; UCAB, mAbXience Anti-F mAb; Merck (P) Anti-F mAb	MedImmune, Sanofi (P) Anti-F mAb		MedImmune (P); Synagis

Figure 4. RSV vaccines and therapeutic antibodies in clinical trial.

54

The most advanced RSV vaccine in development is the Novavax F-protein nanoparticle vaccine. This vaccine consists of insect cells produced postfusion F proteins that spontaneously arrange into nanoparticles. In cotton rats, this vaccine induces neutralizing antibodies and protects against RSV infections (Smith et al., 2012). Although immunogenic in elderly, this vaccine was not effective in reducing RSV infections in this population (Fries et al., 2017).

Maternal immunization allows to protect infants for a few months after birth. In this approach, a pregnant woman is vaccinated to increase her immunity and subsequent transfer of the neutralizing antibodies to the developing fetus. The half-life of the maternal antibodies and insufficient antibody transfer in case of premature birth are critical issues for this strategy. The Aluminum adjuvanted Novavax F-protein nanoparticle vaccine was shown to be safe and immunogenic in women of childbearing age (August et al., 2017). In a recent phase III clinical trial this vaccine could reduce RSV LRTI hospitalizations but did not met its primary objective to reduce the frequency of medically relevant RSV LRTI infections. New vaccine candidates based on the RSV F protein stabilized in its prefusion conformation are currently under clinical development (Graham, 2019).

Next to active vaccination, passive vaccination can be an effective strategy to protect from viral infections. Currently, a humanized monoclonal antibody, Palivizumab (Synagis from MedImmune) is the only available immunoprophylaxis for RSV disease. This antibody binds antigenic site II present on both the postfusion and prefusion conformation of the F protein and has moderate RSV neutralizing activity. Monthly intramuscular injections with this antibody (50 or 100 mg) can reduce hospitalizations of high-risk infants with about 55% (Null et al., 1998). However, its use is limited to only high-risk children, due to its expensive production based on mammalian expression system. Therefore, affordable antibodies that can protect newborns in the first few months after birth are being developed. MEDI8897 is a recombinant half-life extended human monoclonal antibody that specifically targets the perfusion RSV F protein (antigenic site ϕ) with an RSV neutralizing activity that is 50 times more potent than palivizumab. A 50 mg injection with this antibody is believed to be able to protect infants from RSV infections for the duration of a 5-month season (Domachowske et al., 2018).

VHHs have the potential to combat viral infections by interfering at several steps of the virus replication cycle. These include prevention of virus-cell attachment, virus uncoating and viral entry. For instance, a neutralizing bivalent VHH against H5N1, that was administered intranasally in mice, was shown to avert influenza A virus attachment to the host membrane, thus abrogating the subsequent virus replication (Ibanez et al., 2011). In another study, five neutralizing VHHs were analyzed for their mechanism to block the virus replication cycle of the polio virus. All of them were found to be involved in initial phases- attachment and uncoating, while the latter was dependent on capsid stabilization by VHH (Schotte et al., 2014).

Several studies have reported the RSV F-specific VHHs with neutralizing potency in the nanomolar range (Hultberg et al., 2011; Rossey et al., 2017). These VHHs were also developed in their oligomeric state and exerted at least a thousand fold better neutralization than their monovalent equivalent (Detalle et al., 2016; Hultberg et al., 2011). However, the short retention time and short half-life in circulation of VHHs impact the time-frame in which prophylactic VHH treatment can provide protection and impact the efficacy of single dose therapeutic VHH treatment (Schepens et al., 2011). Another example is MD3606 in which 4 different head-to-tail fused VHHs are linked to the Fc fragment of human IgG1. The individual VHHs can potently neutralize either group 1 influenza A viruses, group 2 influenza A viruses, Yamagata lineage influenza B viruses or Victoria lineage influenza B viruses. Consequently, prophylactic MD3606 treatment could protect mice from lethal infections with various influenza A and B viruses. Although MD3606 could potently neutralize these viruses in vitro, its protective activity *in vivo* appeared to be dependent on its Fc effector functions (Laursen et al., 2018).

3. Conclusion

VHH technology has grown significantly in the past few years and is estimated to grow even further, and that is quite evident as the number of published studies has exploded since its discovery. In this thesis, we have extended the use of VHH moieties to VHH-Fc fusion proteins to evaluate their efficiency to combat infectious diseases as antivirals and vaccine delivery systems.

RESEARCH AIMS

Single-domain antibodies or VHHs have emerged as a potential competitor of monoclonal antibodies-based therapeutics due to their peculiar properties. This thesis highlights the application of VHHs to combat infectious diseases. We took advantage of the single domain nature of the VHH to explore two different applications: engineer VHH derivative fusions into an effective antiviral agent against respiratory syncytial virus and characterize a transcytotic receptor binding VHH to construct a vaccine delivery vehicle for intestinal infections. The two major objectives were set to assess the feasibility of engineering a VHH to have added advantages.

Development of a VHH-based vaccine delivery vehicle

The prime aim of this project was to develop a vaccine delivery system against intestinal infections. Poor uptake of orally delivered subunit vaccines across the intestinal epithelium often poses a major hurdle in developing mucosal vaccines. Therefore, we aimed at targeting the vaccine antigen to a transcytotic receptor on small intestinal epithelial cells by making fusions with receptor-binding antibodies, that should enhance their uptake and subsequent immune response. For this purpose, two strategies based on single-chain variable fragment (scFv) and single-domain antibody (VHH) were designed to make antigen-antibody fusion constructs for targeted delivery. As a monoclonal antibody (IMM013) against an intestinal receptor Aminopeptidase N (APN) was already available and was shown to deliver antigens via β-glucan microparticles to APN (Baert et al., 2015), scFv-fusions would be first made for rapid screening of antigen-antibody fusions and their characterization. As an alternative strategy, we intended to generate VHHs as new binders against APN by immunizing llamas and screening phage library, which would allow to make and evaluate VHH-based vaccine antigen carriers. The scFv-based or VHH-based fusion proteins would be selected based on their accumulation levels and APN binding strength, followed by their characterization in cell-based binding and uptake assays. The best performing fusions would be evaluated for their capacity to induce focused immune response upon oral immunization in piglet models.

Development of VHH-Fc fusions against respiratory syncytial virus

The second objective of this thesis was to develop VHH-Fc fusions to combat RSV infection by using the plant-based expression systems. In addition to advantages over VHH alone, VHH-Fc fusions could be better than conventional monoclonal antibodies (mAbs). A multispecific construct can be created by fusing different VHHs in one molecule. Moreover, the isolation of VHHs by panning is more straightforward than selection of conventional mAbs which relies on a clone by clone approach. Here, as a proof of concept, we chose two RSV specific VHHs that were previously isolated and shown to have RSV neutralizing potency in the micromolar range (Hultberg et al., 2011). It was demonstrated that the neutralizing potency of VHH was improved by approximately 4000-fold when engineered into a bivalent construct (Hultberg et al., 2011). Therefore, we specifically aimed to make VHH fusions with the Fc domain of murine IgG to generate bivalent molecule with improved neutralization. As these fusions need a eukaryotic expression system, we wanted to evaluate their production in infiltrated *Nicotiana benthamiana* leaves via transient expression system, as this system is known to allow for rapid analysis (Virdi et al., 2016). Subsequently, the plan was to test these VHH-Fc fusions for their *in vitro* neutralizing potency with lab strains and binding to RSV fusion protein (RSV F) in ELISA and on cells, and to characterize them via *in vivo* settings in mice. Besides their protection against RSV infection, the VHH-Fc fusions would be compared with VHHs and conventional antibodies in terms of their thermostability, lung retention time and Fc-effector functions.

Additionally, we also aimed to assess the merits of IgA at the pulmonary mucosal surface. Since IgA are the predominant antibodies at mucosal membranes, they are believed to perform better compared to IgGs (Virdi et al., 2013). However, they cannot be purified due to unavailability of the affinity ligand. Thus, we aimed to provide a solution to this issue by introducing a mutation in IgA Fc domain to be able to purify on commercially available resin. The mutant IgA Fcs would be fused to RSV F binding VHHs and tested for their RSV F binding and neutralization potency.

RESULTS

Chapter 3

Single-chain Fv can make derived fusions unstable for recombinant protein production

Shruti Bakshi[1,2], Paloma Juarez[1,2], Bert Devriendt[3], Vikram Virdi[1,2], Eric Cox[3] and Ann Depicker[1,2]

[1] Department of Plant Biotechnology and Bioinformatics, Ghent University, 9052 Gent, Belgium
[2] VIB Center for Plant Systems Biology, 9052 Gent, Belgium.
[3] Laboratory of Immunology, Faculty of Veterinary Medicine, Ghent University, 9820 Merelbeke, Belgium.

Abstract

Mucosal vaccines have great potential to elicit both mucosal as well as systemic immune responses. Orally administered vaccines to fight against enteric pathogens are often unsuccessful due to the well-developed mucosal barriers of the gastrointestinal tract and their poor uptake by intestinal epithelial cells. Selective targeting of the vaccine antigen to a intestinal receptor such as aminopeptidase N (APN) can be a promising approach to circumvent the difficulties associated with oral vaccine development. This study involves the engineering of a novel antigen carrier, by fusing a target antigen to an anti-APN antibody. Although monoclonal antibodies have been used for ages as a targeting agent, their engineering to make antigen fusions is rather difficult due to their structural complexities. The antibody fragments such as scFv (single-chain variable fragment) and VHH (single domain antibody) offer several advantages over conventional antibodies including small size, ease of engineering and production. Here, we developed various permutations of antigen fused to the scFv derived from an anti-APN monoclonal antibody and Fc domains of a conventional antibody. This chapter describes the limitations of scFv-based fusion constructs such as low accumulation in several recombinant protein production platforms. Replacing the scFv with a VHH in several synthetic fusions resulted in improved accumulation levels in *Pichia pastoris* expression system. This suggests that the low production levels are most likely due to instability of the fused variable fragments often not resulting in correct folding and assembly.

Introduction

During the past decades, particular interest has been focused on the development of effective mucosal vaccines because of their efficiency in inducing mucosal as well as systemic immune responses (Neutra and Kozlowski, 2006). However, only a handful of mucosal vaccines are commercially available. Orally administered vaccines pass the same gauntlet of host defenses as do microbial pathogens. They are diluted in mucosal secretions, degraded by proteases, and subunit vaccines are often not very immunogenic. Moreover, poor uptake by intestinal cells hinders the transcytosis of vaccine antigen across the epithelium to reach underlying inductive sites. A promising approach to address this last issue is to target the antigen selectively to receptors at mucosal membranes as an antigen-ligand fusion (Longet et al., 2018). Since villus enterocytes are predominant in small intestine, transcytotic receptors on enterocytes may be an interesting target to deliver the vaccine antigen.

In the recent past, APN (Aminopeptidase N) was identified as a receptor on enterocytes through which some enteric pathogens make their entry. Moreover, antibodies against this APN receptor are known to be internalized across the mucosal surface through this receptor (Melkebeek et al., 2012). Although monoclonal antibodies have not lost their importance as targeting agents or as vaccine carriers, their large size and complex structure limit their application for genetic fusions. One approach that has potential to advance the antibody-based targeting is to reduce the size of the complex molecule and design simplified versions that can be easily produced with comparable binding characteristics as that of the monoclonal antibodies. The advancements in genetic engineering made it possible to envision the vaccine carrier with antibody fragments such as single-chain variable fragment (scFv) comprising variable domains of the heavy chain (VH) and light chain (VL).

Here we report the design of a targeted vaccine delivery system based on antibody engineering of an scFv that is derived from the APN-specific monoclonal antibody IMM013, which was shown to deliver antigen to APN via β-glucan microparticles (Baert et al., 2015). With our experience, we know that IMM013 does not bind well to immobilized antigen in ELISA, while it

was the best clone among other isolated anti-APN mAbs in terms of binding to APN expressed on cell lines, thus it was chosen to design the antigen carrier.

The antibody-antigen fusion constructs were designed to deliver vaccine antigen to APN receptor present at the intestinal mucosal membranes. The scFv derived from IMM013 was genetically fused to a model antigen (Green Fluorescent Proteins (GFP) in this case). GFP fusion allows to trace the molecule *in vivo*. Moreover, we chose to also fuse the fragment crystallizable (Fc) part of an antibody (Murine IgG2a, Porcine IgG3 and Porcine IgA) to this scFv::GFP fusions for several reasons. It enables the purification on commercially available Fc specific resins and also dimerization of the molecule, thereby generating avidity effect. Several permutations of antigen (GFP), antibody (scFv) and Fc tail has been made and production was compared in two production platforms – plant (*Nicotiana benthamiana*) and yeast (*Pichia pastoris*). Moreover, similar constructs were made with irrelevant VHH (variable domain of the heavy chain-only antibody) to compare with the production of scFv-based constructs. This chapter reports the construction of scFv-based fusions and their difficulties with the accumulation. Finally, replacing scFv with a VHH provides a solution to enhance accumulation level of fusion proteins.

Results and discussion

Cloning and expression of the scFv-fusions in Nicotiana benthamiana leaves
To design a novel antigen carrier, as a proof of concept, we genetically fused GFP to the scFv of an anti-APN IMM013 antibody (Baert et al., 2015) and the Fc part of a porcine IgG3 to be able to track the molecule (referred to as 13-G-PG). Porcine IgG3 is resistant to proteolytic degradation, that makes them ideal fusion partner for oral immunization (Butler et al 2009). In parallel, the control fusions GFP::Fc IgG3 without scFv (G-PG), scFv::GFP without Fc domain (13-G-) and two fusions without GFP (conventional like antibody with porcine IgG3 constant region (13HL-PG) and scFv fused to Fc part of porcine IgG3 (13-PG)) were designed via the GoldenBraid cloning system (Sarrion-Perdigones et al., 2011). We used the 18-amino acid long Cys Linker (L) to join V_H and V_L domain of scFv. CysL contains one cysteine residue at the C-terminus that promotes covalent stabilization of the bivalent scFv dimers. This linker has been previously described to efficiently

produce bispecific small immune proteins (bivalent- scFv fused to a CH3 domain of human IgG1), where the position of the terminal Cys residue was determined by molecular modelling (Li et al., 1997). Moreover, a helical linker was used to connect scFv with GFP, which is a helical domain derived from the C-terminal domain (CTD) of the nuclear antigen La. The helix linker was previously described to design a bispecific scFv fused with GFP for in vivo visualization of the retargeting processes and to improve the stability of the scFv fusion proteins (Stamova et al., 2012). The nomenclature for these fusions and cloning strategy is summarized in Figure 1 and Figure S4, respectively.
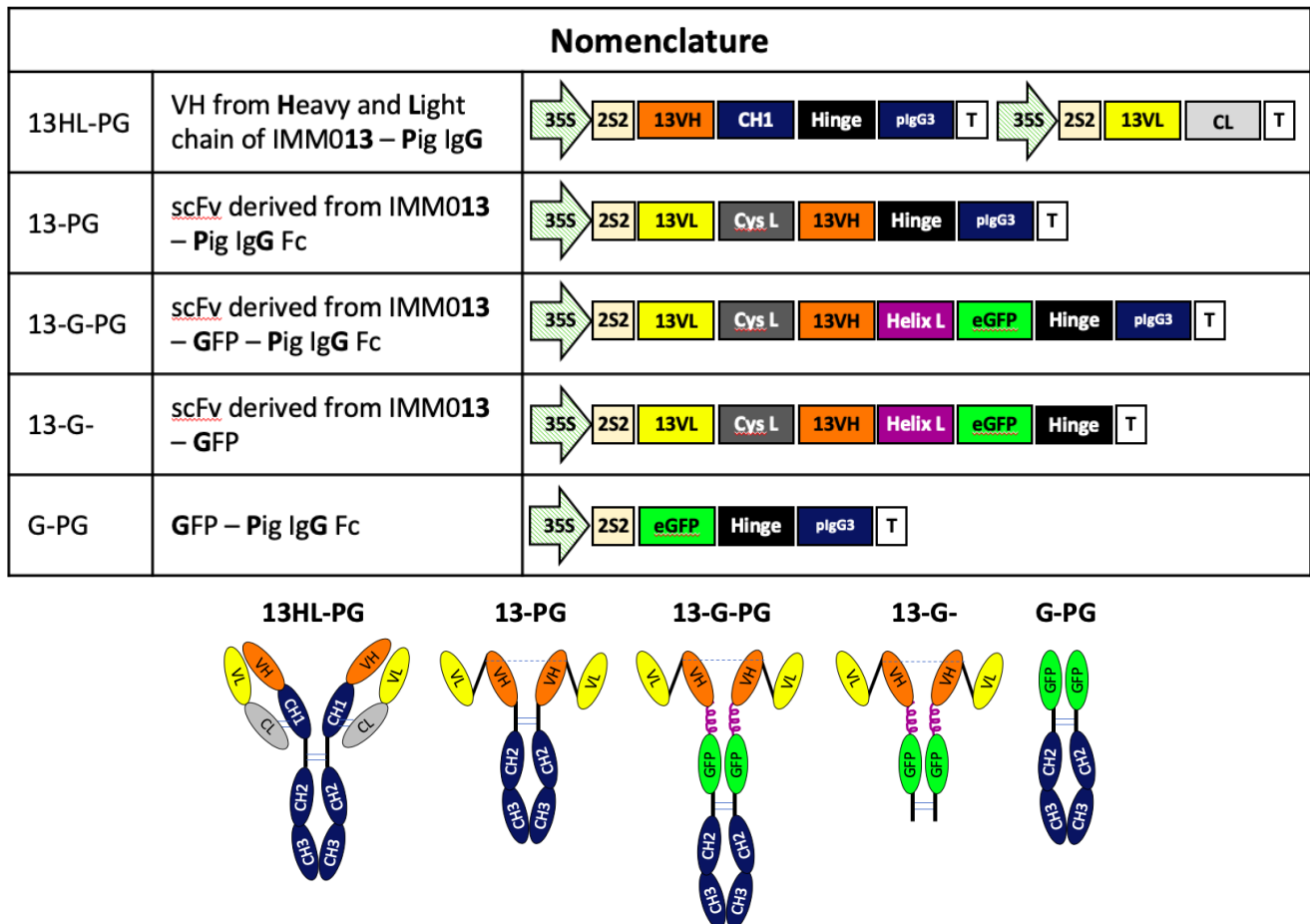

Figure 1. Nomenclature and schematic representation (not drawn to scale) of the expression cassettes for plant expression of the different recombinant fusions. 35S: the constitutive 35S promoter of cauliflower mosaic virus; 2S2: the signal peptide sequence of the 2S2 seed storage protein, VH and VL sequences from IMM013 anti-APN mAb, constant region of porcine lambda light chain (CL), green fluorescent protein (eGFP), the CH1, hinge and CH2-CH3 domain of porcine IgG3, the C-terminal endoplasmic reticulum retention motif (KDEL) and the nopaline synthase terminator (Tnos), connecting linkers (Cys L and Helix L). Dashed line represents the disulfide bridge between the CysL of the bivalent scFv.
CysL, GSTSGSGKPGSGEGSTGC; Helix L, EKEALKKIIEDQQESLNK.

These constructs were produced in infiltrated *Nicotiana benthamiana* leaves via *Agrobacterium tumefaciens* – mediated transient expression to facilitate the rapid analysis. Five days after infiltration, the crude leaf extracts were prepared and analyzed by western blotting in reducing conditions with the two different detection setups. The fusion proteins with Fc domain were probed with anti-pig IgG antibody, and GFP-fusions were probed with anti-GFP antibodies (Figure 2A). The G-PG fusion (GFP-Fc) with the expected molecular weight (56 kDa) was detected with both probes, although the band intensity with the anti-IgG probe was at least 10-fold weaker in comparison to anti-GFP detection, but this could be because of the sensitivity of the detection antibody. A high molecular weight band (~140 kDa) most likely corresponds to aggregates or a non-reduced bivalent form with glycosylation. 13-G- (scFv-GFP, 57.8 kDa) along with some degradation products was also detectable with anti-GFP. Moreover, the band intensity of the degradation products is quite high, suggesting that 13-G- could be unstable and more prone to proteolytic degradation. The other fusions (13HL-PG, 13-PG and 13-G-PG) were below the detection limit in both probe settings, suggesting a low accumulation level in the leaf extracts (Figure 2A).

Therefore, the expression of the engineered fusion products was confirmed in target binding ELISA. There were several detection possibilities based on the fusion proteins as indicated in Figure 2B, 2C and 2D. All the control fusion proteins and 13-G-PG (scFv-GFP-Fc) were detectable in their respective detection settings. 13-G-PG was analyzed by two methods. The first method in which the ELISA plates were coated with anti-GFP and detection was performed with anti-pig IgG antibody, indicates the presence of GFP-Fc fusion in the fusion protein (Figure 2B). The second method in which the plates were coated with porcine APN to capture the scFv allows to measure the bound 13-G-PG fusion protein with anti-pig IgG antibody (Figure 2C). This ELISA setup confirms the presence of anti-APN scFv and the Fc domain, that is only possible when the complete fusion molecule is properly folded and carrying all the fusion moieties including scFv, GFP and Fc domain. Moreover, 13HL-PG and 13-PG were also detected with the second detection method (Figure 2C). As observed in the western blotting, G-PG was readily detected in ELISA (Figure 2B), whereas 13-G- only gave a low signal-to-noise ratio, correlating with high degradation

in the western blotting (Figure 2B). Finally, the ELISA data allow to conclude that all the fusion products are properly folded and functional; however, the accumulation level is very low for all fusions containing the scFv '13' moiety.
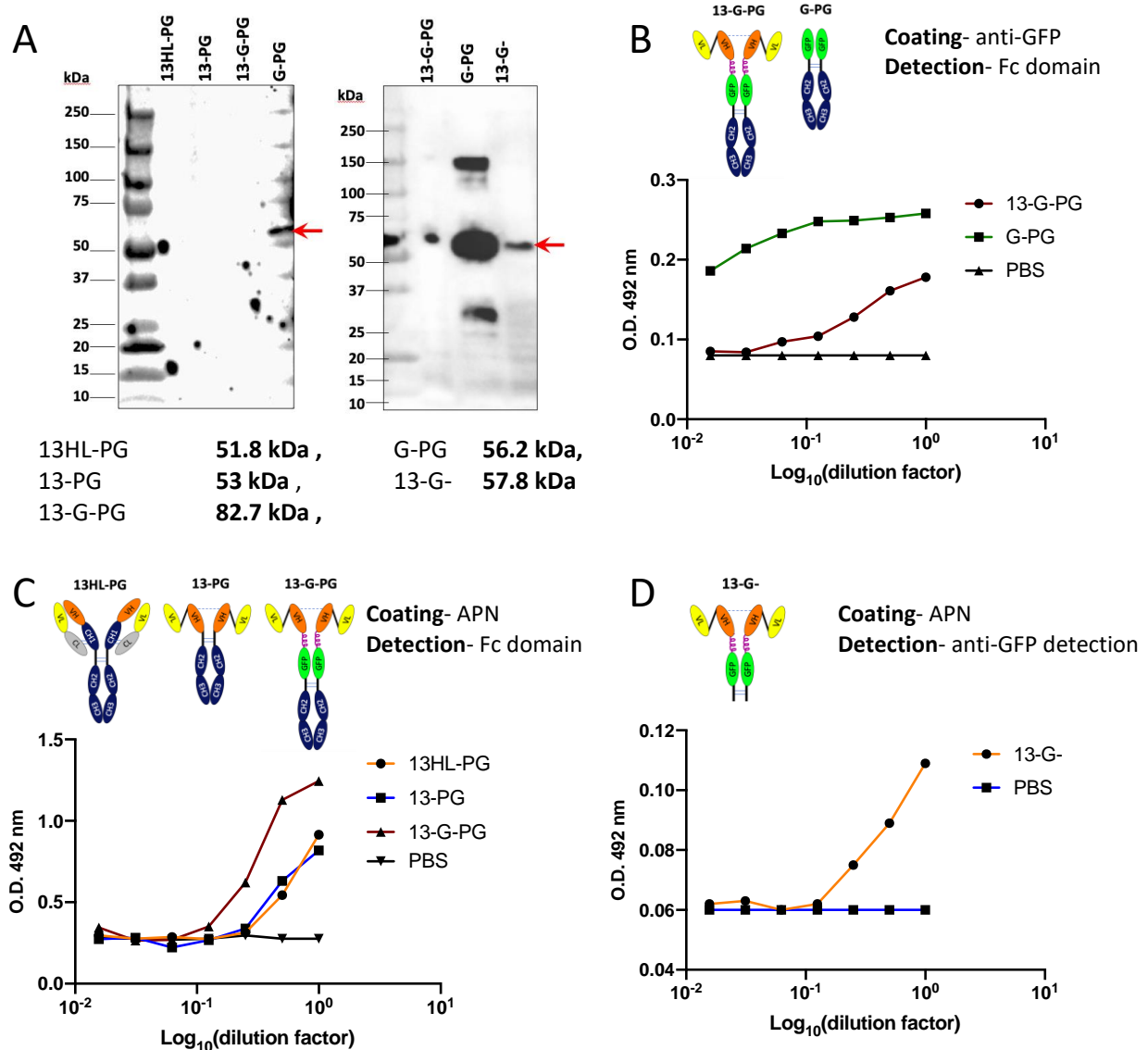

Figure 2. Characterization of plant-produced fusion proteins.
(A) Western blot analysis under reducing conditions with the crude leaf extracts obtained after transient expression with the fusion constructs. The blot was probed with anti-pig IgG antibody (left) and anti-GFP antibody (right). The theoretical molecular weights are shown below. Red, full-length protein (G-PG and 13-G-), black dots represent the artifacts; (B, C and D) ELISAs to analyze fusion proteins in crude leaf extracts in three different settings. (B) plates were coated with anti-GFP and bound proteins were detected with anti-pig IgG. (C, D), plates were coated with APN and bound proteins were detected with anti-pig IgG (C) and anti-GFP antibody (D). The graph shows the O.D. (492 nm) values obtained for each individual sample.

Enrichment and purification of the fusion proteins

Since the expression level for the engineered fusion proteins was very weak, they were enriched by affinity purification to perform further analyses. All the fusion proteins excluding 13-G- were purified using protein A affinity chromatography. The purification yield of 13-G-PG was in the range of 3 mg/Kg of fresh leaf weight, while the G-PG yielded 200 mg/Kg FW that is nearly 60-fold more than that of 13-G-PG. The purification yield for other proteins was also very low and is summarized in Figure 3A. 13-G- was purified by anti-GFP coupled agarose beads. Importantly, the low yield of all fusions containing the scFv module suggests that the scFv somehow influences the stability of the fusion proteins. Next, the purified samples were assessed in western blot to test their quality and integrity. The engineered fusion products of precise molecular weights were detected on western blots with some high molecular weight aggregates (Figure 3A). For 13-G-PG, a smaller fragment corresponding 50 kDa band was also observed that may be due to a cleavage between scFv and GFP, resulting in one 50 kDa band of cleaved -GFP-Fc and a smaller fragment for scFv that could not be detected by anti-pig IgG in the western blot.

Next, an ELISA was performed to confirm the binding of the purified scFv containing fusions to APN. G-PG was assessed for binding to anti-GFP. The 13-G-PG (also 13HL-PG and 13-PG) exhibited a very weak binding to APN, whereas anti-GFP coating displayed a stronger signal (Figure 3B). The poor binding of 13-G-PG to APN was not a complete surprise, because the parent IMM013 mAb also binds weakly to the immobilized APN in ELISA. For such clones, ELISA is not an ideal method, although it is informative for the initial screening. Furthermore, 13-G- was barely detectable in western blot and undetectable in ELISA (not shown). This suggests that either the anti-GFP purification is not efficient or the protein is very unstable and is completely degraded during the purification procedure.
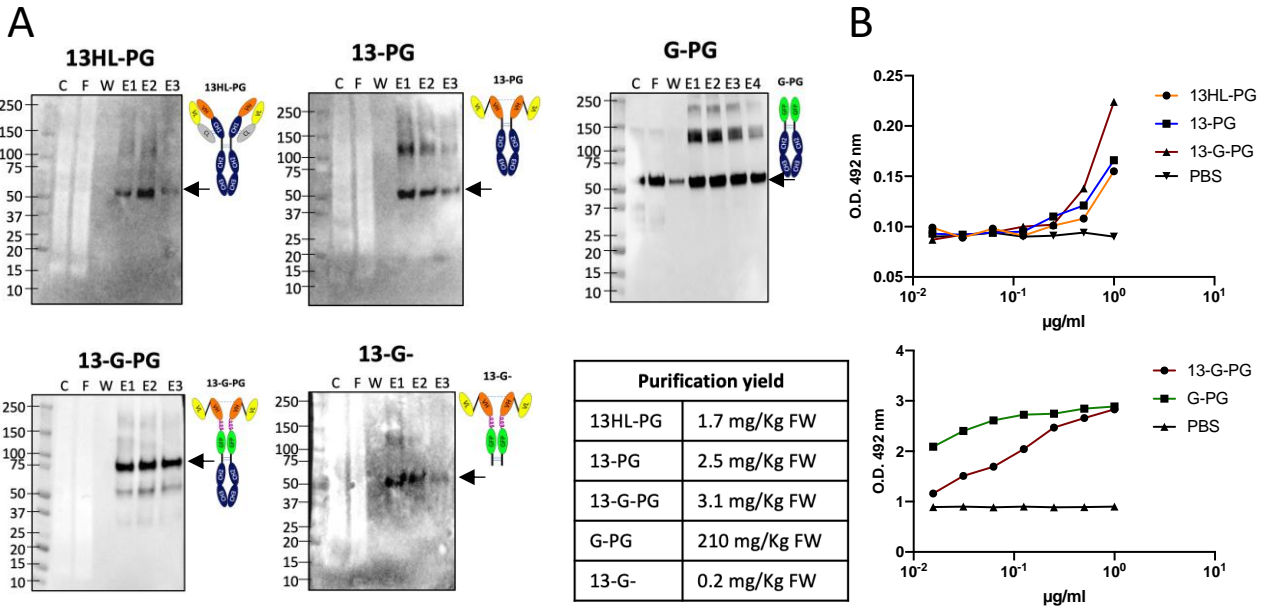
Figure 3. Affinity purification of fusion proteins. The proteins were purified on protein A except for 13-G, that was purified on anti-GFP coupled agarose beads. (A) The purified samples were analyzed in western blot under reducing condition and detected with anti-pig IgG. 13-G- was detected with anti-GFP antibody. C, crude leaf extract; F, flow-through; W, wash fractions; E1-E4, elution fractions. The arrow represents the expected molecular weight of the full-length protein. The purification yield is shown in the table. (B) ELISA was performed to analyze binding activity of the fusion antibodies. The ELISA plates were coated with APN (top) and anti-GFP (bottom), and bound proteins detected with anti-pig IgG antibody. The graph shows the O.D. (492 nm) values obtained for each individual sample.

Binding of the fusion proteins to APN-expressing cell lines

Next, the fusion proteins were assessed for their binding to full-length APN expressed on the biological membrane of cell lines via flow cytometry. APN-stable IPEC-J2 cell lines were used for this purpose (Melkebeek et al., 2012). The anti-APN monoclonal antibody IMM013 served as a positive control. Since the produced fusion antibodies contain GFP, they were directly detected by flow cytometry; whereas antibodies that do not carry an internal fluorescent tag (for instance – IMM013) were detected by fluorophore-labeled secondary antibody. 13-G-PG was able to stain 32% of the total cell population, whereas the negative control G-PG did not show any binding. The control proteins IMM013, 13HL-PG, 13-PG and 13-G- (with or without GFP) also displayed binding to APN-expressing cells (Figure 4). This assay was repeated with the new protein preparations and higher concentration (up to 10 μg). Moreover, the purified proteins were eluted in the high salt buffer, which is not recommended for cell-based analysis. The proteins were

71

dialyzed against PBS to perform subsequent analyses and protein integrity was tested in ELISA (Figure S1). However, no detectable binding could be achieved in flow cytometry. We assumed that 13-G-PG folds in such a manner that GFP fluorescence is undetectable by flow cytometry. Therefore, in the next assay setup, detection was also performed with fluorophore-labelled anti-pig IgG, but no binding could be observed. These data suggest that 13-G-PG is very unstable and/or affinity of scFv to APN is abolished due to improper folding. Moreover, the protein yield was very low and most of the protein was lost during downstream processing. Thus, batch-to-batch variation of the production process was also a limiting factor and results were not reproducible. Therefore, a production platform that resulted in high yield could allow for an easy characterization and subsequent production and purification.
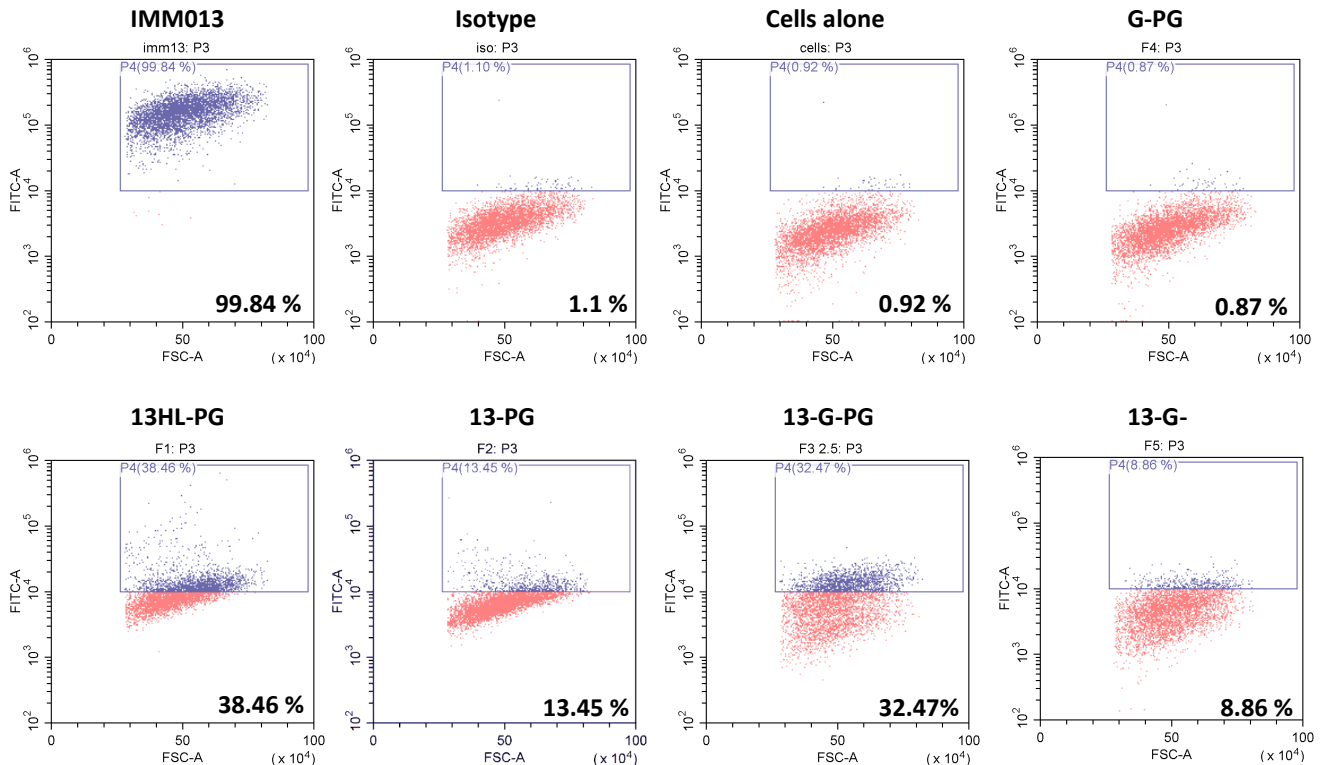
Figure 4. APN binding assay with APN-stable IPEC-J2 cell lines. The fusion antibodies were analyzed to test their binding to the APN expressed on the cell membrane. Cells were incubated with fusion antibodies. IMM013 is a positive control, whereas isotype and cells alone are negative controls. Bound antibodies were probed with fluorescently labelled secondary antibody and fluorescent was measured by flow cytometry. No secondary antibody was added for GFP-fusion antibodies (13-G-PG, G-PG, 13-G-) and cells were detected based on their GFP fluorescence. Each box represents the percentage of cells that were stained by the antibodies.

An alternative production platform and linkers connecting different domains do not improve the yield

Since the yield was very low in *N. benthamiana* and upscaling of the production process was very cumbersome, we decided to evaluate an alternative expression system. Based on the results of (De Meyer et al., 2015), recombinant protein expression in *P. pastoris* provides an interesting alternative (De Meyer et al., 2015). So, *P. pastoris* was chosen to produce the scFv-antigen-Fc fusion proteins with some additional permutations (Figure S2). Several aspects and components were compared including origin of the Fc domain (mouse vs porcine), isotype (IgG2a, IgG3 and IgA), position of the GFP fusion at either C- or N-terminal end of the Fc domain, scFv from IMM013 by itself and scFv from a different anti-APN monoclonal antibody C5C8. To this end, scFv-GFP-Fc was made with mouse IgG Fc (referred to as 13-G-MG) to compare the expression with mouse monoclonal antibody IMM013 which is the positive control, and with porcine IgA Fc (referred to as 13-G-PA) to improve the stability during oral immunization. In the constructs which included the model antigen GFP, GFP was fused at both N- and C-terminal end of the Fc part to see the effect of fusion position. 13-G- was made as before without any modification. Moreover, only scFv with a histidine tag was made to evaluate whether the scFv alone is functional or not. All these genes were cloned, checked for their sequence, transformed in Pichia, and finally the recombinant fusion proteins secreted in the culture supernatant were analyzed by western blot. The result was that only those fusion proteins without the scFv of IMM013 namely G-MG and MG-G were observed in western blot, whereas all scFv-fusions could not be detected (Figure 5).
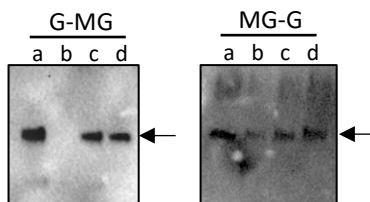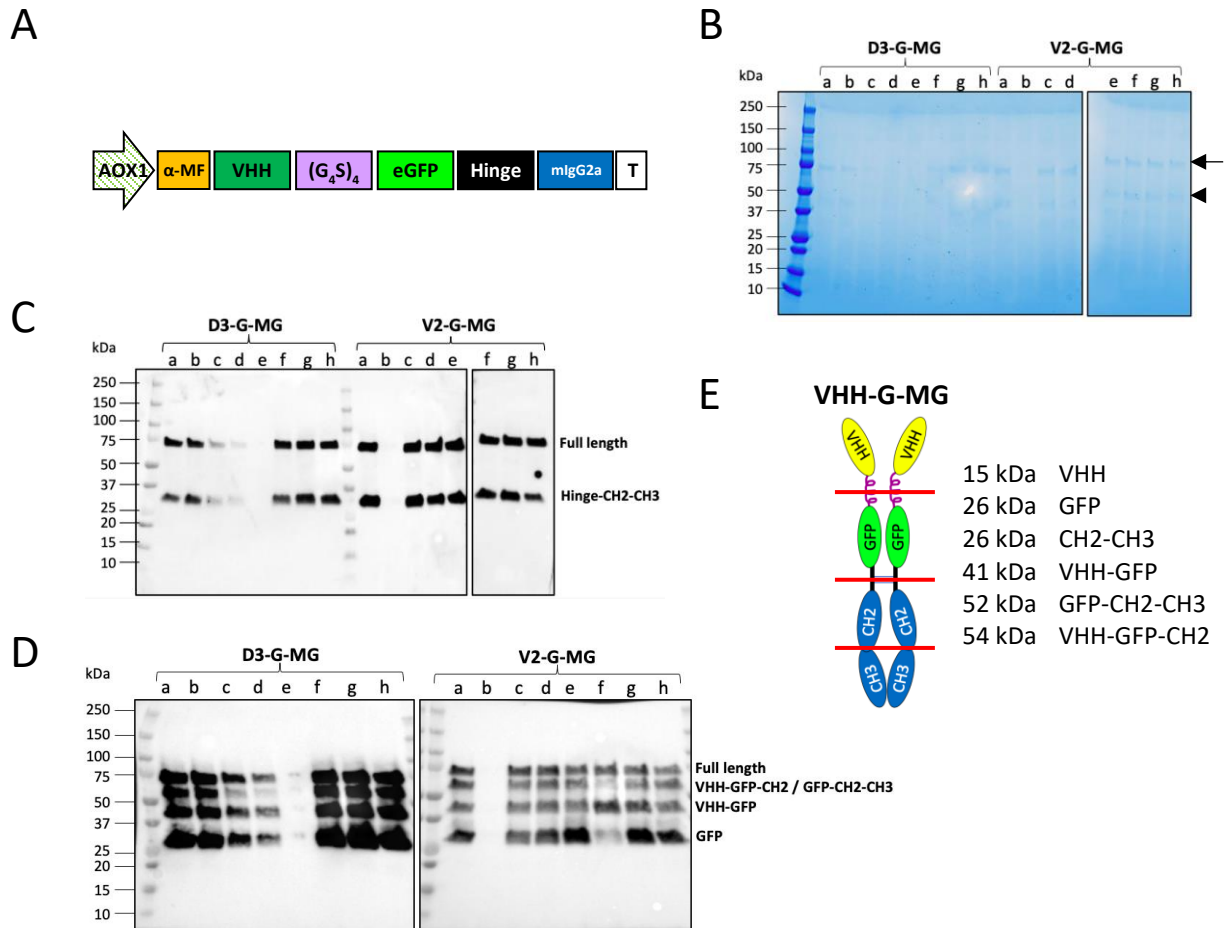

Figure 5. Expression of the fusion proteins in *Pichia pastoris*. The expression plasmids were transformed in *P. pastoris* and four clones each construct were analyzed via methanol induction to screen for the highest expressing clone. The secreted proteins in the culture supernatant were analyzed using western blot under reducing conditions and probed with anti-mouse IgG polyclonal antibody. Black arrow represents the full-length protein.

Furthermore, scFv of IMM013 alone was also not detectable via the his-tag in western blot, suggesting that scFv itself is not expressing well. Therefore, we sought to investigate whether the connecting linker between VH and VL influences the folding and assembly. For 13-G-MG, two new constructs were made as shown in Figure S3 where the linkers originally used were replaced with GGGGS linker. However, also this did not result in any significant improvement in the expression levels. These data led us to conclude that scFv of IMM013 and derived fusions cannot be produced regardless of the expression platforms and connecting linkers.

The transition from scFv to VHH improves the yield of the fusion protein

To confirm that incorrect folding of the scFv was the problem for expression, and to obtain more information on the feasibility to make such complex fusions composed of three domains, the anti-APN scFv of IMM013 was replaced with another affinity ligand. Here, we took advantage of the single domain nature of a VHH domain of heavy-chain only antibodies that does not require optimization of the connecting linker and also allow easy engineering due to their small size. To this end, the two irrelevant VHHs namely VHH V2 (Virdi et al., 2013) and VHH D3 (Moonens et al., 2014) were grafted on the GFP:Fc scaffold (GFP fused to the Fc domain of murine IgG2a) via GGGGS linker (referred to as V2-G-MG and D3-G-MG) (Figure 6A), and were examined for their expression levels in *P. pastoris*. The secreted proteins in the culture supernatant were analyzed by SDS-PAGE in reducing conditions, and bands were revealed by Coomassie staining and western blotting. Noteworthy is that detectable expression level was even accomplished after Coomassie staining, that was never the case with scFv derived fusions (Figure 6B), suggesting that VHH-fusions allow accumulation and good yield in *P. pastoris*. Likewise, western blots also revealed prominent bands with two different detection probes. The anti-IgG detection displayed a band for full-length protein and also a smaller fragment corresponding to the Fc domain (Figure 6C). The anti-GFP detection revealed four bands, of which the largest corresponds to the molecular weight of full-length fusion, the smaller fragment (approximately 26 kDa) most likely corresponds to GFP (Figure 6D). The two intermediate bands correspond to various cleavage patterns in such fusion molecules, of which some possibilities are indicated in Figure 6E. The cleavage might occur within the linker, hinge or the CH2-CH3 interface. Nevertheless, VHH fusions appear to be more

straightforward and provide clear information about the integrity of the fusion proteins. It is clear that with these accumulation levels, VHH-GFP-Fc fusions could be purified and upscaled.

Figure 6. Cloning and expression of the fusion proteins in *P. pastoris*. (A) Schematic representation (not drawn to scale) of the expression cassettes for cloning in the expression vector under control of AOX1 promoter (AOX1) and AOX1 terminator (T), and α-mating factor (α-MF) secretion signal. Two VHHs (VHH V2 and VHH D3) were used to make the fusions. (G$_4$S)$_4$, Glycine-Serine linker; eGFP, green fluorescence protein. The expression plasmids were transformed in *P. pastoris* and eight clones (a-h) each construct were analyzed via methanol induction to screen for highest expressing clone. The secreted proteins in the culture supernatant were analyzed using Coomassie staining (B) and western blot (C, D) under reducing conditions. The blot was probed with anti-mouse IgG antibody (C) and anti-GFP antibody (D). (E) represents the different proteolytic cleavage possibilities in the fusion proteins. Black arrow and arrowhead represent the full-length protein and the cleaved product, respectively.

Conclusion

In conclusion, this study shows the difficulties that can occur with the production of IMM013 scFv and derived scFv fusion proteins. It seems logical to pursue scFv-based fusions if the specific monoclonal antibody is already available, thereby the cumbersome process of immunizing llama and screening immune libraries to obtain a VHH can be avoided. However, scFv itself is associated with various limitations to obtain a fully functional and high expressed protein. We assessed the scFv fusions in different stages. First, the fusions were made in the plant expression system, and examined for their functionality in ELISA. However, the results were not reproducible due to the difficulty in producing large quantities. Next, the fusions were made in various permutations to gain more information about the fusion position, type and origin of the Fc domain, and the alternative production platform. In addition, two different linkers were also tested by replacing the previous linkers connecting the VH-VL in scFv and scFv to GFP. All these efforts did not result in any significant improvement in the yield. It is possible that shorter or longer linkers, or linkers with different amino acid compositions may have a positive effect on the solubility and folding; however, this is a trial-and-error approach. Thus, it is worthwhile to explore the various linkers before grafting the scFv on the fusion partner. Finally, it is important to note that the search of the high-expressing clones required to make more than 50 constructs, that somehow limits the practicality of the scFv-based antigen carrier with this system.

Thanks to their single domain nature, the VHHs are easily engineered and fusion molecules carrying both the antigen and Fc domain with VHH were possible to make in *P. pastoris*. Although the VHH-fusions also seem susceptible to cleavage, it is different from the scFv degradation, as observed in the western blot analysis. Perhaps, the scFv further augments the instability of the scFv-based fusion molecules. Thus, they were more prone to degradation as compared to VHH-fusions, and unable to be detected in western blot or ELISA. As a final note, VHH-based fusions offer a great potential to design a complex fusion protein and allow rapid analysis by their production in yeast expression systems.

Materials and Methods-

Vectors, strains, cell lines and DNA sequences

The plant expression vectors of GoldenBraid2.0 cloning system were used for protein expression in *N. benthamiana* (Sarrion-Perdigones et al., 2011). The yeast expression vector pPICZalphaH6E (NCBI accession number KM035419.1) modified for GoldenBraid cloning (named pKaiGG) was used for cloning the fusions under the control of the methanol inducible promoter AOX1 (Juarez et al., unpublished). The pKaiGG vector contains the Zeocin resistance marker for selection in bacterial as well as in yeast cells. *E. coli* strain DH5α was used for the construction and storage of the fusion expression vector (Meselson and Yuan, 1968). The fusions were expressed in *N. benthamiana* leaves and *P. pastoris* wild type strain NRRL Y-11430 (Kuberl et al., 2011). APN stable cell lines (IPEC-J2 and BHK-21) were cultured as described previously (Baert et al., 2015; Melkebeek et al., 2012).

DNA sequences corresponding to the fragment crystallizable (Fc) domain of porcine IgG3 (CH1-Hinge-CH2-CH3; NCBI accession number EU372658), porcine IgA (Hinge-CH2-CH3; NCBI accession number U12594), mouse IgG2a (Hinge-CH2-CH3; NCBI accession number KC295246.1), VL and VH of anti-APN monoclonal antibody IMM013 (Baert et al., 2015), constant region of porcine lambda light chain CL (NCBI accession number CU467669, 2693..3009), eGFP (NCBI accession number, GenBank- NC_025025.1, Protein- YP_009062989.1), Helix linker (Stamova et al., 2012), Cys linker (Li et al., 1997) were synthesized by Gen9 (Ginkgo Bioworks). VHH V2 (Virdi et al., 2013) and VHH D3 (Moonens et al., 2014) coding sequences were obtained from the previously cloned vector in our laboratory.

Construction of the plant expression plasmids harboring the coding sequence of the fusion proteins

The plant expression vectors were created by taking advantage of seamless assembly offered by GoldenBraid2.0 cloning system as described previously (Sarrion-Perdigones et al., 2011). Briefly, the DNA sequences corresponding to Fc domain of porcine IgG3, CL, VL and VH from IMM013 anti-APN mAb, Cys linker and Helix linker were assembled in a plant expression vector (Figure 1).

The N-terminal 2S2 plant signal peptide (Krebbers et al., 1988) and C-terminal KDEL sequence were added to the coding sequences of VHH and Fc, respectively. The fusions were cloned under the control of constitutive 35S promotor of cauliflower mosaic virus (CaMV-35S) and nopaline synthase terminator (Tnos). First, all the GB parts including VH, VL, CL, CH1-Hinge-CH2-CH3 domain, 35S promoter and Tnos terminator were cloned separately in the domesticator vector (pUPD) and then assembled into the destination vector (pDGBα2). To achieve high accumulation levels, the resulting transcriptional unit was subsequently fused to the silencing suppressor p19 cloned in another vector pDGBα1 (Sarrion-Perdigones et al., 2011). In this way, we obtained the final plant expression vector pDGBΩ2 harboring fusion proteins referred to as 13HL-PG (like full-length conventional antibody), 13-PG (scFv fused to porcine IgG3 Fc domain), 13-G-PG (scFv fused to eGFP and porcine IgG3 Fc domain), and G-PG (eGFP fused to porcine IgG3 Fc domain) (Figure S4). DH5α cells were transformed with the expression plasmid and transformants were screened on the media supplemented with spectinomycin selection. The plasmids were isolated using GeneJET plasmid miniprep kit (ThermoFisher- K0502) to confirm the recombinants by restriction analysis and sequencing. Finally, the expression vectors were transformed into heat shock competent *A. tumefaciens* cells (strain – LBA4404) for production in the plant expression system (Hoekema et al., 1983).

Expression of the fusion proteins in Nicotiana benthamiana

A. tumefaciens cells bearing the expression vector were infiltrated in *N. benthamiana* leaves as previously described (De Buck et al., 2012; Juarez et al., 2013). Briefly, overnight grown bacterial culture in YEB medium were sedimented and pellet was resuspended in certain volume of agroinfiltration buffer (10 mM MES pH 5.6, 10 mM $MgCl_2$, and 200 mM acetosyringone) needed to obtain an optical density of 0.2 at 600 nm, followed by gentle shaking for 2 hours at room temperature. The resulting suspension was used to infiltrate the abaxial surface of young leaves of 4-5-weeks old *N. benthamiana* plants. The leaves were harvested 5 days post infiltration and extracts were prepared to obtain total soluble protein in a ratio of 1:3 (w/v) in Dulbecco's phosphate buffered saline (Lonza- 17-512F) supplemented with cOmplete protease inhibitor

cocktail (Sigma-Aldrich- 11697498001). After centrifugation, the clarified extract was immediately used to examine for transgene expression via SDS-PAGE and ELISA.

Purification of the fusion proteins from crude leaf extract

The leaf extracts from about 5 g of infiltrated leaves were prepared as described above and filtered through 0.45-µm Millex® Syringe Filters (Merck) and incubated with pre-equilibrated protein A resin (GE Healthcare) on a shaker at 4°C for 1 h, except for 13-G- which was incubated with GBP-Fc coupled agarose beads (De Meyer et al., 2015). These extracts were then applied to PD10 columns (Pharmacia) by gravity flow, followed by washing with 10 ml wash buffer (Equilibration buffer DPBS, Lonza). The bound antibodies were eluted in three fractions with 250 µl of 1 M Arginine (pH 2.7) and neutralized immediately with 1 M Tris-HCl (tris (hydroxy methyl) aminomethane) pH 9. The protein concentration was determined by OD_{280} measurement. The purified antibodies were analyzed by western blot and ELISA.

Immunoblotting

Transiently expressed fusion proteins (10 µl of crude leaf extract) were analyzed on 4-20% precast protein gels (Bio-Rad- 4561096). Samples were prepared in NuPAGE LDS Sample buffer (ThermoFisher- NP0008) with a reducing agent (ThermoFisher- NP0009). For immunoblotting, the proteins were blotted onto a polyvinylidene difluoride membrane (Bio-Rad- 1704156) using the semidry transfer method (Bio-Rad). The membrane was subsequently blocked for one hour with 5% (w/v) of skimmed milk in PBS containing 0.05% Tween-20 (PBST) and probed with 1/5000 diluted HRP-conjugated anti-pig IgG (Bethyl- A100-104P) or 1/500 anti-GFP VHH-Fc (mouse IgG Fc) (De Meyer et al., 2015) followed by 1/5000 HRP-conjugated anti-mouse IgG (GE Healthcare, NXA931). The membrane was then washed three times with PBST, and bands were visualized by adding WesternBright ECL HRP substrate (Advansta- K-12045-D20). All incubation steps were performed at room temperature on the orbital shaker.

APN binding ELISA

96-well ELISA plates (Nunc Polysorp®) were coated for two hours at 37°C with 400 ng of APN (Sigma) diluted in PBS. Plates were then washed three times with PBST and blocked overnight at 4°C with 3% (w/v) gelatin prepared in PBS and 0.05% Tween-80. For another ELISA setup, the plates were coated overnight at 4°C with 200 ng of anti-GFP VHH-Fc (De Meyer et al., 2015). Following three washing steps with PBST, plates were blocked with 4% (w/v) skimmed milk prepared in PBST. Subsequently, the proteins were serially diluted in dilution buffer (2% skimmed milk + PBS + 0.05% Tween-20), added to each well and incubated for 1 hour at RT. After washing, bound fusion proteins were detected by anti-pig IgG (Bethyl- A100-104P), diluted 1:10000 in the dilution buffer. Following incubation for 1 hour at RT, plates were washed three times with PBST and developed by adding HRP substrate (SIGMA*FAST*^{TM} OPD tablets dissolved in 20 ml deionized water, Sigma-Aldrich- P9187). Finally, the reaction was stopped with 1 M hydrochloric acid and the optical density of the colorimetric reaction was measured at 492 nm (VersaMax, Molecular Devices, Sunnyvale, California).

Flow cytometry

Binding of the different fusions was analyzed using flow cytometry. The APN-expressing cell line IPEC-J2-APN was grown until 90% confluence and detached with StemPro accutase (Gibco). Detached cells (3.0×10^5) were transferred to a conical bottom 96-well microtiter plate (Gibco) in 200 µl culture medium and centrifuged for 3 min at 350 g and 4°C. Cells were incubated with 2.5 µg/ml of 13-G-PG and G-PG, and 1 µg/ml of other fusions, anti-APN monoclonal antibody (mAb, clone IMM013) and IgG1 isotype control on ice for 30 minutes. The GFP fusions were detected by measuring the GFP fluorescence, whereas the other bound antibodies were detected with FITC-labelled mouse anti-pig IgG antibody (Abcam) or sheep anti-mouse IgG (Sigma) to detect all antibodies including IMM013. Cells were incubated for 30 minutes on ice. Dead cells were excluded using Sytox blue staining (5 nM; Molecular probes). A total of 10000 viable, single cells were measured for each condition (Cytoflex, Beckman Coulter).

Construction of the yeast expression vector harboring scFv- and VHH-fusion proteins

The fusion proteins were cloned in the yeast expression vector pKaiGG (Juarez et al., unpublished) via GoldenBraid cloning system. Briefly, similar to the plant expression vector, all parts (coding sequences) were first cloned in a domesticator vector pUPD2, followed by the assembly in the yeast expression vector pKaiGG. Subsequently, the plasmids were transformed in *E. coli* DH5α. Upon plasmid preparation and sequence confirmation of the insert, yeast cells were transformed with the PmeI-linearized vectors and transformants were selected on YPD (1% yeast extract, 2% peptone, 2% Dextrose) supplemented with 50 mg/ml Zeocin (Invitrogen).

Expression of the scFv/VHH-fusion proteins produced in Pichia pastoris

Expression of scFv/VHH-IgG fusions was first analyzed in 2 ml cultures. On day one, 2 ml of BMGY medium (1% Bacto yeast extract, 2% peptone, 1.34% YNB, 0.1M potassium phosphate pH 6, 1% glycerol) with 25 mg/ml Zeocin was inoculated with individual transformants and incubated while shaking at 28°C for 48 h. For each fusion construct, four to eight independent transformants were grown in 24-well plates. Cells were then pelleted for 10 min at 1500 g and resuspended in 2 ml BMMY medium (1% Bacto yeast extract, 2% peptone, 1.34% YNB, 0.1M potassium phosphate pH 6, 1% methanol) to induce the expression. Cultures were incubated while shaking at 28°C for 48 h and spiked with 1% methanol (v/v) every 12 h. After 48 h of induction, the yeast cells were pelleted, and the supernatant was analyzed by SDS-PAGE, western blot and ELISA to assess the accumulation of secreted fusions.
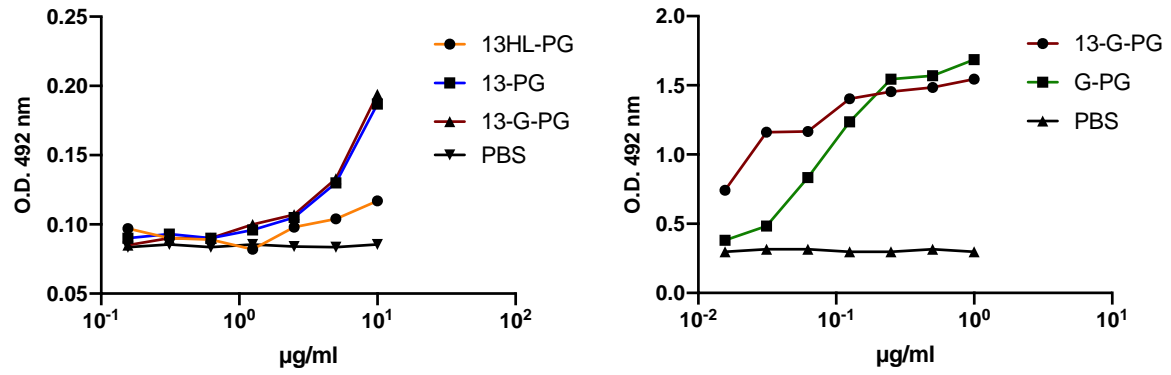
Figure S1. Binding activity of the fusion proteins after dialysis. The ELISA plates were coated with APN (left) and anti-GFP (right), and bound proteins were detected with anti-pig IgG antibody. The graph shows the O.D. (492 nm) values obtained for each individual sample.
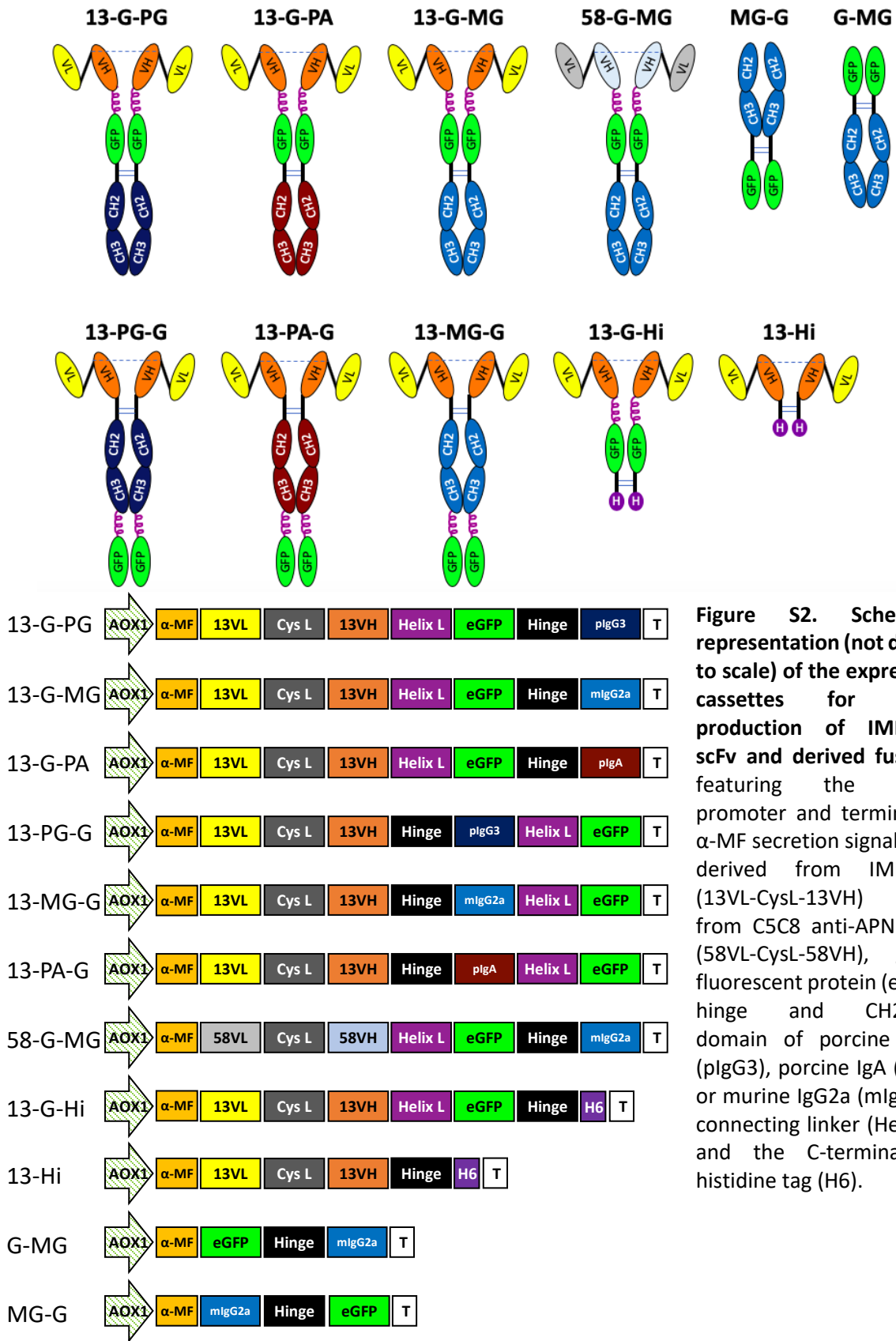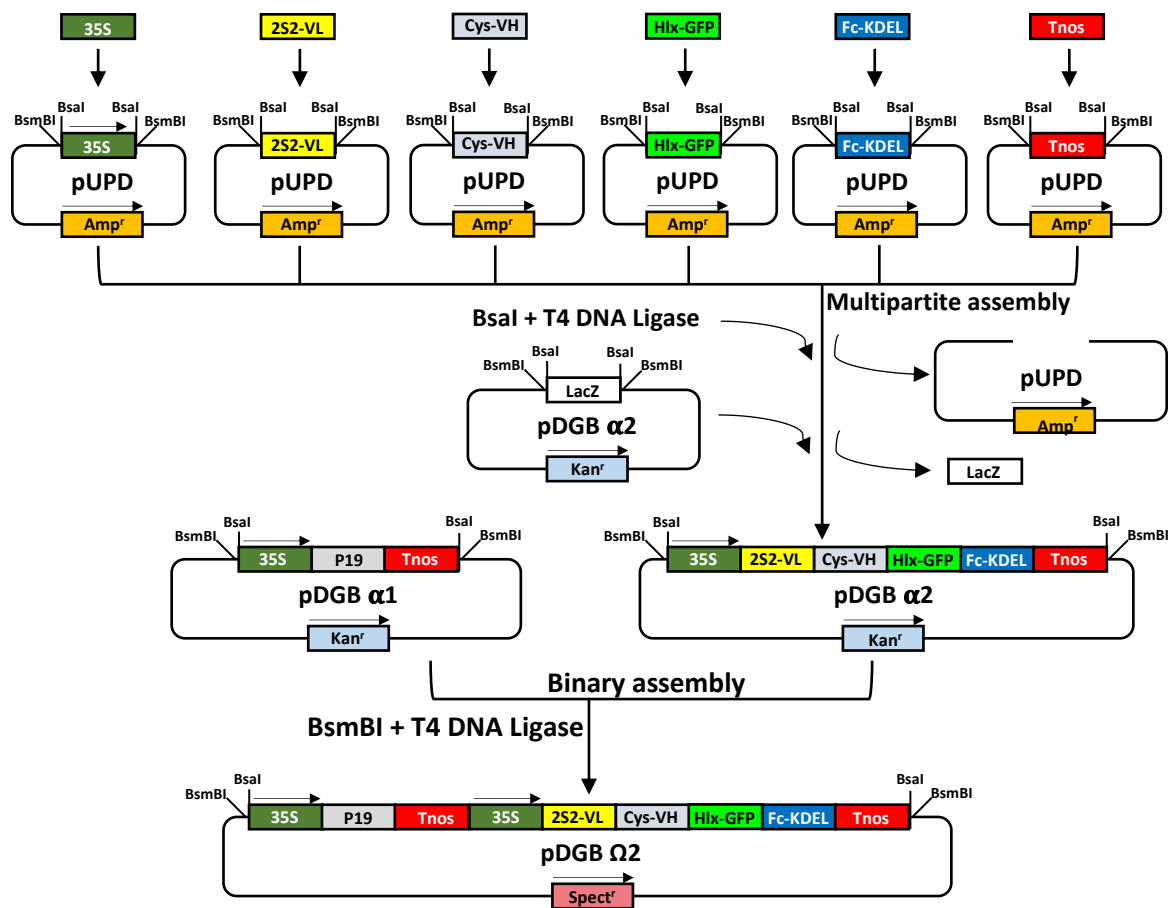
Figure S2. Schematic representation (not drawn to scale) of the expression cassettes for yeast production of IMM013 scFv and derived fusions, featuring the AOX1 promoter and terminator, α-MF secretion signal, scFv derived from IMM013 (13VL-CysL-13VH) and from C5C8 anti-APN mAb (58VL-CysL-58VH), green fluorescent protein (eGFP), hinge and CH2-CH3 domain of porcine IgG3 (pIgG3), porcine IgA (pIgA) or murine IgG2a (mIgG2a), connecting linker (Helix L), and the C-terminal 6x histidine tag (H6).
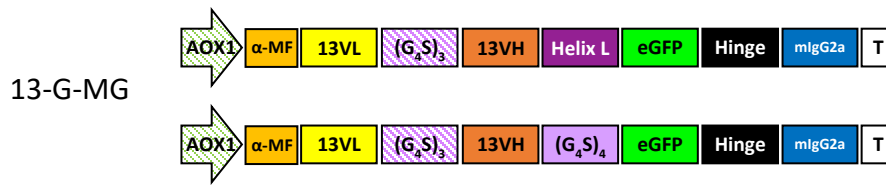
Figure S3. Expression cassettes with the replacement of connecting linkers with Gly-Ser linker. Two 13-G-MG constructs were cloned and expressed in *Pichia pastoris*. In the first construct, the scFv linker was replaced with Gly-Ser (GGGGS) linker; while in the second construct, both scFv linker and helix linker (linker connecting scFv to GFP) were replaced with a Gly-Ser linker.

Figure S4. Schematic representation of cloning scFv fusions (13-G-PG) into GoldenBraid 2.0 cloning vectors. 35S: the constitutive 35S promoter of cauliflower mosaic virus; 2S2-VL: the signal peptide sequence of the 2S2 seed storage protein fused with VL sequence from IMM013 anti-APN mAb, Cys-VH: Cys linker fused with VH sequence of IMM013, Hlx-GFP: Helix linker fused with green fluorescent protein (GFP), Fc-KDEL: hinge and Fc domain of porcine IgG3 and the KDEL at C-terminus. Tnos: the nopaline synthase terminator, P19: silencing suppressor, Amp[r]: ampicillin resistance marker, Kan[r]: kanamycin resistance marker, Spect[r]: spectinomycin resistance marker.

Chapter 4

Part I: Engineering single-domain antibodies as carriers for targeted vaccine delivery to the small intestinal epithelium

Shruti Bakshi[a,b], Hans Van der Weken[c], Raquel Sanz Garcia[c], Ashuwini Tharad[a,b], Shubham Pandey[a,b], Paloma Juarez[a,b,], Vikram Virdi[a,b], Bert Devriendt[c]*, Eric Cox[c]* and Ann Depicker[a,b]*

[a] *Department of Plant Biotechnology and Bioinformatics, Ghent University, 9052 Gent, Belgium*
[b] *VIB Center for Plant Systems Biology, 9052 Gent, Belgium.*
[c] *Laboratory of Immunology, Faculty of Veterinary Medicine, Ghent University, 9820 Merelbeke, Belgium.*

Author Contributions

A.D., E.C., B.D. and V.V. conceived the idea and designed the research; S.B., A.T. and S.P. performed cloning, production, purification and characterization; S.B, H.W. and A.T performed cell-based experiments; R.S. performed gut-ligated loop experiments and S.B. assisted in the experiment; P.J. designed the cloning vector; S.B., H.W., A.T., R.S., A.D., B.D. and E.C. analyzed the data; S.B. and A.D. wrote the chapter with contributions from H.W. and R.S.

ABSTRACT

Targeting a vaccine to the mucosal surface has recently been recognized as a promising approach to efficiently induce mucosal immune responses against enteric pathogens. However, poor uptake and inefficient transport of orally delivered subunit vaccines across the intestinal epithelium combined with weak immune responses still present important bottlenecks for mucosal vaccination. A possible strategy suggested to surmount these hurdles is to target the selected antigen to transcytotic receptors, such as aminopeptidase N (APN) present on enterocytes and antigen-presenting cells (APCs). Therefore, we aimed to identify potent and selective VHHs against porcine aminopeptidase N (pAPN), that were fused to the fragment crystallizable (Fc) domain of murine IgG2a, resulting in dimeric VHH-MG fusions. Out of a library of 30 VHH-MG fusion candidates, two fusions displaying the best binding on pAPN-expressing cells were selected and showed *in vivo* internalization across the porcine gut epithelium. Our results demonstrate the potential of bivalent VHH-MG fusions as delivery vehicles for vaccine antigens. VHH-mediated and APN-targeted antigens to generate focused immune responses at the mucosal membranes remains to be further validated via *in vivo* settings.

Introduction

The vast majority of pathogens and external noxious substances enter the body through the mucosal surfaces of the respiratory, gastrointestinal (GI) and urogenital tracts, and thus mucosal immunity is of paramount importance to counter infection. Currently, needle-free oral vaccine delivery is the most attractive route of administration for protection against intestinal pathogens, because it offers many advantages, such as ease of administration, no risk of blood-borne infection and practicality for mass vaccination (Juarez et al., 2016; Lycke, 2012). In contrast to subunit vaccines, only live attenuated vaccines or inactivated pathogen particles have been found to be effective in stimulating an efficient immune response. However, because of the safety issues associated with orally delivered live attenuated or inactivated pathogens, only a handful of such vaccines have been licensed. On the other hand, subunit vaccines are considered to be safe because they do not contain the live component of the pathogen, but poor transport of vaccine antigens across the intestinal epithelium to reach the underlying immune inductive sites resulting in a poor immune response pose a major hurdle to the development of oral vaccine delivery. Enterocytes or absorptive villus epithelial cells constitute ˜90% of all intestinal epithelium and they possess phagocytosis and transcytosis capacities to transport enteric pathogens or macromolecules across the epithelial barrier (Snoeck et al., 2008). Therefore, antigen targeting to transcytotic receptors on enterocytes is an interesting approach for vaccine delivery and inducing a strong mucosal as well as systemic immune response against intestinal pathogens (Devriendt et al., 2012)

In the recent past, aminopeptidase N (APN) has been identified as a receptor for F4 fimbriae that is expressed on a variety of cells including small intestinal enterocytes and APCs, but not on epithelial cells of other parts of the GI tract (Melkebeek et al., 2012). Oral immunization with APN-specific polyclonal antibodies triggered mucosal immunity (Melkebeek et al., 2012). Moreover, functionalization of microparticles with APN-specific mouse monoclonal antibodies also increased uptake of these particles by the intestinal epithelium and triggered systemic immune responses (Baert et al., 2015). These findings suggest that an APN-specific delivery agent conjugated with a vaccine antigen could be an interesting strategy to elicit a strong intestinal immune response. To date, several targeting mechanisms have been identified, such

as antibodies, cell-mediated targeting (DC immunotherapy, T cell adoptive transfer), and chemical conjugation of the antigen to small molecules such as glycans and amino acids (Narasimhan et al., 2016). Because of their strong affinity and specificity, antibodies are the ideal proteins to which an antigen of interest can be genetically fused for targeting to the APN-expressing enterocytes. Different antibody formats can be used, such as a monoclonal antibody (mAb), the single-chain variable fragments (scFvs), or the variable domain of heavy-chain-only antibodies (VHH, also known as nanobody). Although conventional mAbs have originally been preferred as a targeting vehicle, their production as fusion with the antigens turned out to be cumbersome and time-consuming. In addition, the structural complexity hampers their use as potential ligands. Therefore, other simpler forms such as scFvs and VHHs were considered as alternative approaches to full-sized antibodies. Although the advances in antibody engineering made it possible to easily design and clone scFv genes based on the targeting performance of mAbs, the stability and accumulation of the synthetic scFv proteins vary heavily, depending on several factors, including the unpredictable length of the requisite linker to obtain proper folding and the assembly of the two variable domains, and this often restricted scFv targeting applications (Cheng and Allen, 2010; Robinson and Sauer, 1998). On the other hand, the VHH immunoglobulin domain is only a 15-kDa variable fragment derived from the camelid heavy-chain only antibody (Duarte et al., 2016). Unlike scFv, VHH contains its antigen-binding properties in a single, long and variable loop rather than in two variable domains in conventional antibodies and derived scFvs, while retaining similar affinity. Owing to its peculiar properties such as small size, ease of production, good thermostability and efficient tissue penetration, VHH has received great interest for various applications compared with classical antibodies (De Meyer et al., 2014; Helma et al., 2015; Muyldermans, 2013)

The present study focuses on evaluating the VHH domain as a carrier for targeted vaccine delivery to the gut epithelium to induce strong mucosal immune responses. We identified a panel of 28 VHHs by immunizing llama with porcine APN (pAPN) and screening on pAPN-expressing cell lines. The selected binders belong to at least 14 different families based on their similarity (>80% sequence identity) in the epitope binding CDR3 sequence. In order to increase affinity and avidity

and at the same time allow easy purification, these VHH domains were fused to the Fc domain of murine IgG2a, hereafter, referred to as VHH-MG fusions.

Nowadays, different production platforms such as mammalian cells, yeast, plants, etc. are used for the production of complex assembled glycoproteins such as antibodies. Production based on mammalian cells, like Chinese Hamster Ovary (CHO) cells is straightforward for the production of mAbs but is complicated, expensive and often associated with the risk of animal-derived products when synthetic fusions need to be produced (Ellis and Gerety, 1990; Frenzel et al., 2013; Yusibov et al., 2016). Therefore, transgenic plants and yeast expression systems show a great potential. Yeast such as *Pichia pastoris* possesses a clear advantage over plant expression systems in terms of short generation time, cost effectiveness, ease of genetic manipulation and scalability (Schmidt, 2004; Weinacker et al., 2013). Moreover, *P. pastoris* secretes very low amount of endogenous proteins, therefore secreted recombinant proteins are highly enriched, which facilitates downstream processing (Cregg et al., 2000; Sallach et al., 2009). On the other hand, the glycosylation profile of recombinant proteins in plants is much more alike that of animal cells than the yeast expression platform (see ref. Donini and Marusic, 2019).

Here, we chose the Pichia platform as a more convenient, faster and flexible platform to test the production of different pAPN-binding VHH-MG fusion proteins and their capacity to raise mucosal immune responses. The yeast-produced VHH-MG fusions were further characterized for their binding to and uptake in pAPN-expressing cells. At least two VHH-MGs were produced to high levels, appeared to be stable and were efficiently endocytosed on cell lines and in loops of the porcine gut under physiological conditions.

Results

Construction of an APN-specific VHH library

To prepare an anti-APN VHH library, two llamas were immunized five times with commercially available kidney pAPN. However, because we wanted to target intestinal pAPN and not kidney pAPN, which are encoded by the same gene but might differ in glycosylation pattern and in the accessibility of particular antibody epitopes, the sixth booster was given with intestinal pAPN prepared by a lengthy procedure as described in the Materials and Methods section. Two independent VHH-phage display libraries were constructed, each consisting of about 10^8 transformants. After two consecutive rounds of panning, performed on stably transfected BHK21 cells expressing pig aminopeptidase N, 190 clones were randomly selected and sequenced. Through comparative alignment, VHHs having more than 80% sequence identity in their CDR3 region (B-cell lineages) were grouped as one family because they most likely recognize the same epitope (see ref. Pardon et al., 2014), but their characteristics (e.g. affinity, expression yield, stability etc.) can be different. In this way, we obtained 28 unique VHHs belonging to 14 different families as candidate binders to APN (Supplementary Fig. S1). These 28 unique VHHs were produced in *E. coli* cells and the crude periplasmic extracts were analyzed for their binding specificity via flow cytometry on pAPN-expressing BHK21 cells. The parental non-transfected BHK-21 cells served as negative control cells. An irrelevant VHH, (BCII10 specific for bacterial β-lactamase, described by Conrath et al. (2001) and a mouse anti-APN mAb IMM013 (Baert et al., 2015) were used as negative and positive control, respectively. This differential FACS analysis confirmed 22 of the originally 28 screened different VHHs belonging to 11 different families specific for porcine APN, demonstrating that the panning of the library on pAPN-transfected cells highly enriched for APN-binding VHH clones (Supplementary Fig. S1).

*Construction of a VHH-MG expression vector via the BioXP DNA printer*

Because the FACS analysis for the panning on APN-transfected BHK-21 cells was performed with crude periplasmic extracts containing an unknown concentration of phagemids, the quality of binding of the different VHHs had to be further analyzed with purified proteins to allow

comparison among the different VHHs and to rule out any experimental variables such as nanobody expression, periplasmic extraction efficiency, etc in the FACS analysis (Supplementary Fig. S1). Important to realize is that some of the VHHs may contain an amber stop codon within the VHH sequence, because the VHH library with C-terminal histidine tag was prepared in the suppressor *E. coli* strain TG1 that reads the amber stop codon (TAG) as glutamine (Q). Thus, when an amber codon was identified by sequencing, it was also replaced by the glutamine codon.

Classically the selected VHHs are sub-cloned in direct fusion with an affinity tag in a non-suppressor *E. coli* strain, but here we followed a new strategy. We sub-cloned the VHHs in direct fusion with an Fc fragment to have the fusions produced in the medium of *Pichia pastoris*, providing the following advantages: Fc can be used as an affinity tag for protein purification, it makes the VHH-Fc fusion bivalent providing an avidity effect, and it allows comparison with the mouse monoclonal antibody IMMO13 for APN binding as positive control. Twenty-eight selected VHHs were fused to the Fc domain of mouse IgG2a and cloned into an in-house *P. pastoris* expression vector. Two irrelevant VHHs, V2 (Virdi et al., 2013) and D3 (Moonens et al., 2014), specific for the F4 and F18 fimbriae of enterotoxigenic *E. coli,* respectively, were included as negative control.

The sequences of the VHH and Fc domain were synthesized using Gibson cloning strategy on the BioXP™ 3200 System and transformed into the yeast expression vector (Fig. 1a). All 30 constructs (with 28 selected VHHs and 2 negative controls) successfully built with the BioXP DNA printer were transformed into *E. coli* and four colonies per construct were analyzed by colony PCR or restriction digestion followed by sequencing to identify clones with the right insert. Twenty-three out of 30 constructs (77%) resulted in an error-free clone by sequencing only one colony, while for seven other VHH-MG constructs, two colonies had to be analyzed to obtain the right clone; for only one clone, i.e. 2L58MG (3%) the sequence was still incorrect in all four colonies, having one mutation in the coding sequence (Fig. 1b). Coincidently, this incorrect clone from family 12 was also negative in panning during VHH library preparation (Supplementary Fig. S1). Therefore, we omitted it from the further analyses.
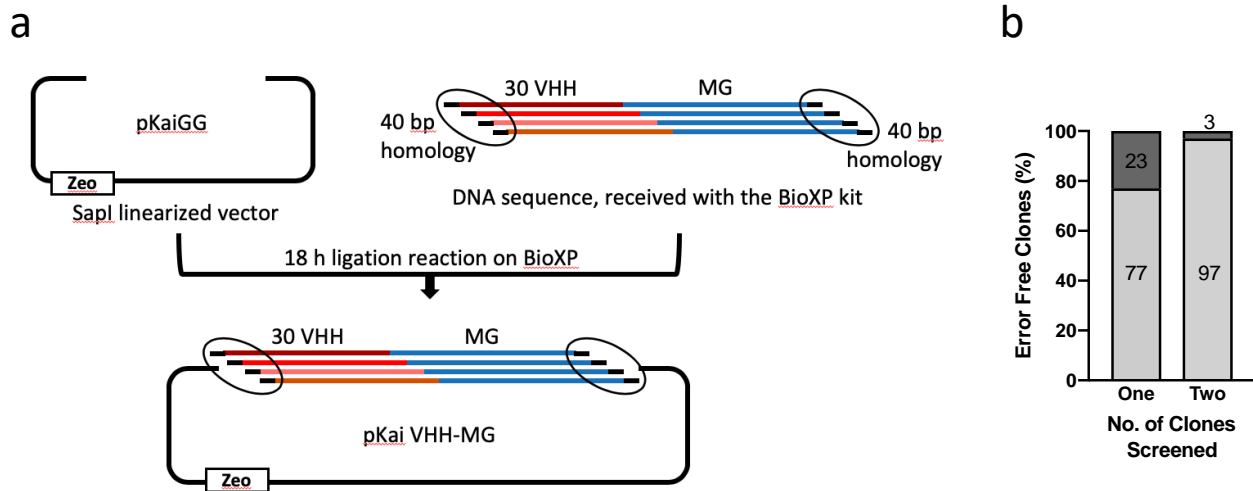
Figure 1. Schematic representation of the BioXp™ 3200 System-based Gibson cloning strategy to efficiently obtain VHH-MG fusions (a). The 40 bp at the ends of the VHH-MG fusion fragments are homologous with the ends of the SapI-linearized pKaiGG vector. MG represents the Fc domain of **M**ouse Ig**G**. VHH-MG fragments were synthesized and ligated into SapI-digested pKaiGG in an overnight run on the BioXP system. DH5α cells were transformed with ligation samples and transformants were screened on Zeocin (Zeo)-supplemented medium. Subsequently, DNA was isolated from four randomly selected clones and analyzed by restriction digestion or colony PCR and sequencing to screen for positive clones. (b) Efficiency of obtaining error-free clones via the BioXP cloning system. The probability to obtain error-free clones was 77% when one clone was screened and 97% when two clones were screened per construct via sequencing.

Yeast-produced VHH-MG fusions bind efficiently to full-length, surface-expressed APN

The 29 obtained VHH-MG encoding constructs were then transformed into Pichia, and for each, four individual yeast colonies were screened to identify the transformant producing the highest amount of VHH-MG accumulating in the culture medium. Therefore, equal amounts of supernatant were analyzed by SDS-PAGE and by western blotting to examine the intensity of the recombinant protein signal and the integrity of the protein (Supplementary Fig. S2). Only for the best expressing constructs, a band could be observed after SDS-PAGE; but for most constructs, a band was clearly present at the expected molecular weight after western blot analysis. The concentration of the different VHH-MGs produced in *P. pastoris* was determined using purified V2-MG and D3-MG reference proteins, and this ranged from 4 to 60 mg/l in 2-ml cultures, based on the analysis by ImageLab software. Only for some fusions, such as 3L11MG (family 9) and 2L22MG (family 5), a degradation product was detected besides the full-length product,

suggesting that the VHH has an effect on the stability of the VHH-MG fusion as was also seen for VHH-IgA fusions (Bakshi et al., 2019)
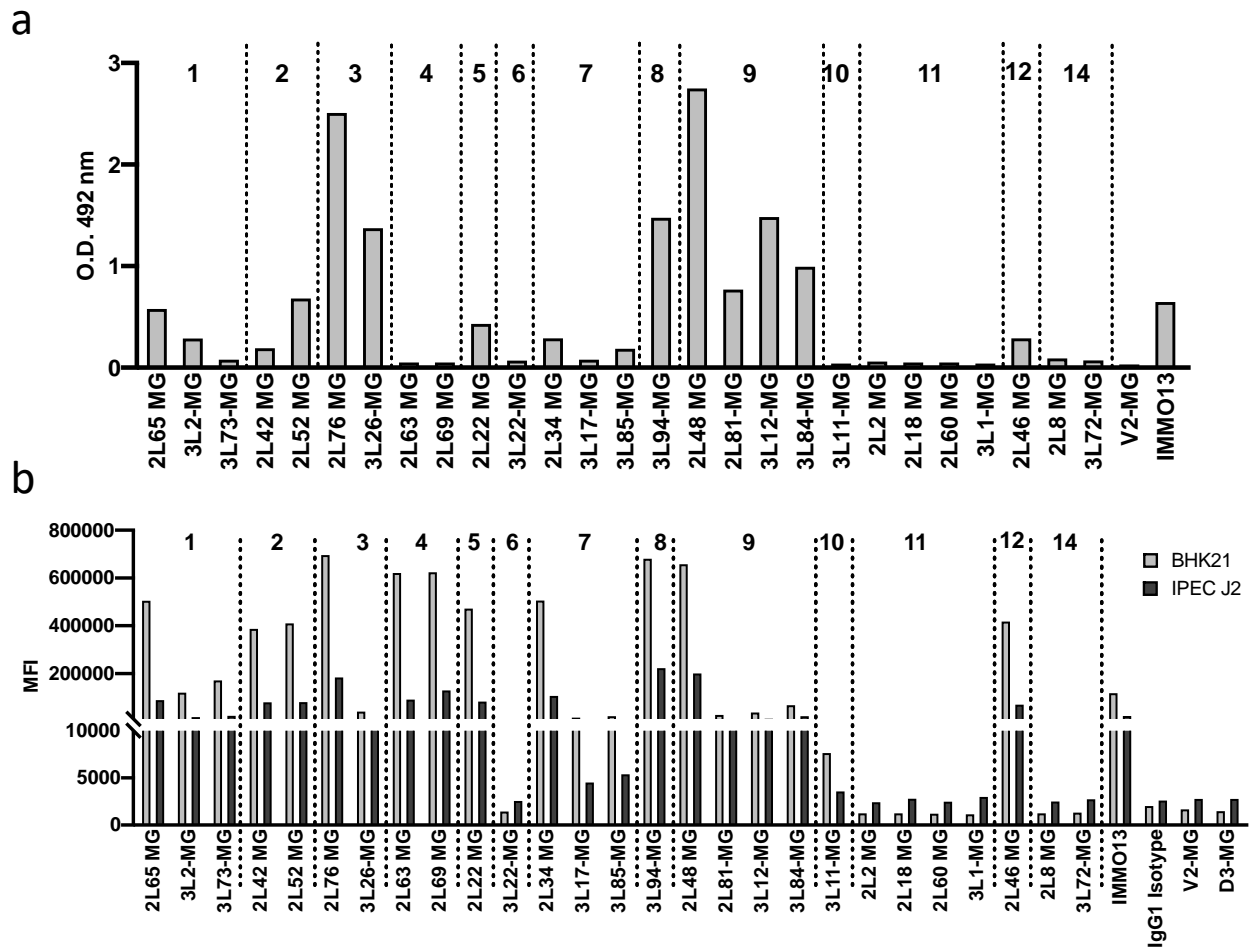
Figure 2. Selection of APN-specific VHH-MG via ELISA and flow cytometry. Clones are arranged according to the family they belong to and separated by a dotted line. (a) ELISA plates were coated with APN and incubated with the culture medium. APN binding of VHH-MG is depicted as O.D. values of the colorimetric reaction. (b) Flow cytometry screening for the VHH-MGs that bind to full-length APN expressed on the membrane of BHK21 (gray bars) and IPEC-J2 (black bars) cell lines. IMM013 (murine IgG1) is the positive control. IgG1 isotype, V2-MG and D3-MG are the negative controls. V2-MG and D3-MG fusions contain a VHH (V2 and D3, respectively) that binds an irrelevant target. The graph shows the mean fluorescence intensity (MFI).

Next, we determined the binding specificity of the VHH-MG fusions in a kidney APN-specific ELISA (Fig. 2a). Three-fold dilution series of VHH-MG in the culture supernatant were probed with anti-mouse IgG. The three strongest VHH-MGs, i.e. 2L48MG, 3L94MG and 2L76MG, displayed a strong binding activity to immobilized APN, each belonging to a different CDR3 group.

These three VHH-MGs also showed good binding in the FACS assay performed after the panning to screen for phage displayed VHHs (Supplementary Fig. S1). Interestingly however, some families of VHH-MG fusions were completely negative in the ELISA, for instance family 4 (2L63-MG, 2L69-MG), while they were strong binders in the FACS assay (Supplementary Fig. S1). It is thus important to note that the relative binding activity on APN-coated wells in the ELISA assay did not correlate with the affinity of the VHH-MG fusions for the cell-expressed APN. Notably, VHH screening was performed via FACS using the cells expressing APN on their surface, so binding on immobilized APN might differ with binding on cells, perhaps because epitopes become less accessible during immobilization. Also, because the experiments were performed with crude medium samples, in which the VHH-MG protein accumulation was not equilibrated, the ELISA signal could be related to the protein concentration in the culture medium rather than to the affinity. (Fig. 2a, Supplementary Fig. S1).

VHH-MG fusions were further assessed for their binding specificity and affinity on parent cell lines versus the derived transfected APN-expressing cell lines (BHK21 and IPEC-J2) via flow cytometry with equal amounts of VHH-MG protein (Fig. 2b). Of note, IPEC-J2 are porcine small intestinal epithelial cell lines which express low levels of APN on their surface and hence stably transfected cells were used. Based on the relative VHH-MG concentration, as determined by western blotting, equal molar amounts of the VHH-MG proteins and the positive control (IMM013) were spiked into spent medium of *P. pastoris*. Several strong APN-binders were identified based on the number of cells with bound VHH-MG through flow cytometry, whereas no binding was observed of spent medium with non-transfected BHK21/IPEC-J2 cells. Interestingly, family 4 (2L63 and 2L69), which was negative in an APN-specific ELISA, turned out to contain strong binders in the cell-based binding assay (Fig. 2b, Supplementary Fig. S2). These findings were in line with the FACS data obtained from the crude periplasmic extract during VHH library screening (Supplementary Fig. S1). We found that the amplitude of the binding activity on IPEC-J2-APN cells in comparison to BHK21-APN was significantly lower, which may be related to the amount of APN expressed on the IPEC-J2 cell membrane.

We selected different families showing binding activity in the flow cytometric screening to further assess their affinity for small intestinal tissue via immunohistochemistry (IHC).

However, only six families containing strong (1, 4, 8, 9) and moderate binders (5, 12) have been shown that were randomly selected for upscaling. As can be seen in Figure 3, each VHH-MG displayed binding to the intestinal ileum, whereas all controls were negative and did not show background; moreover, the intensity of the signal correlated with the binding activity in the FACS analysis (Fig. 2b).
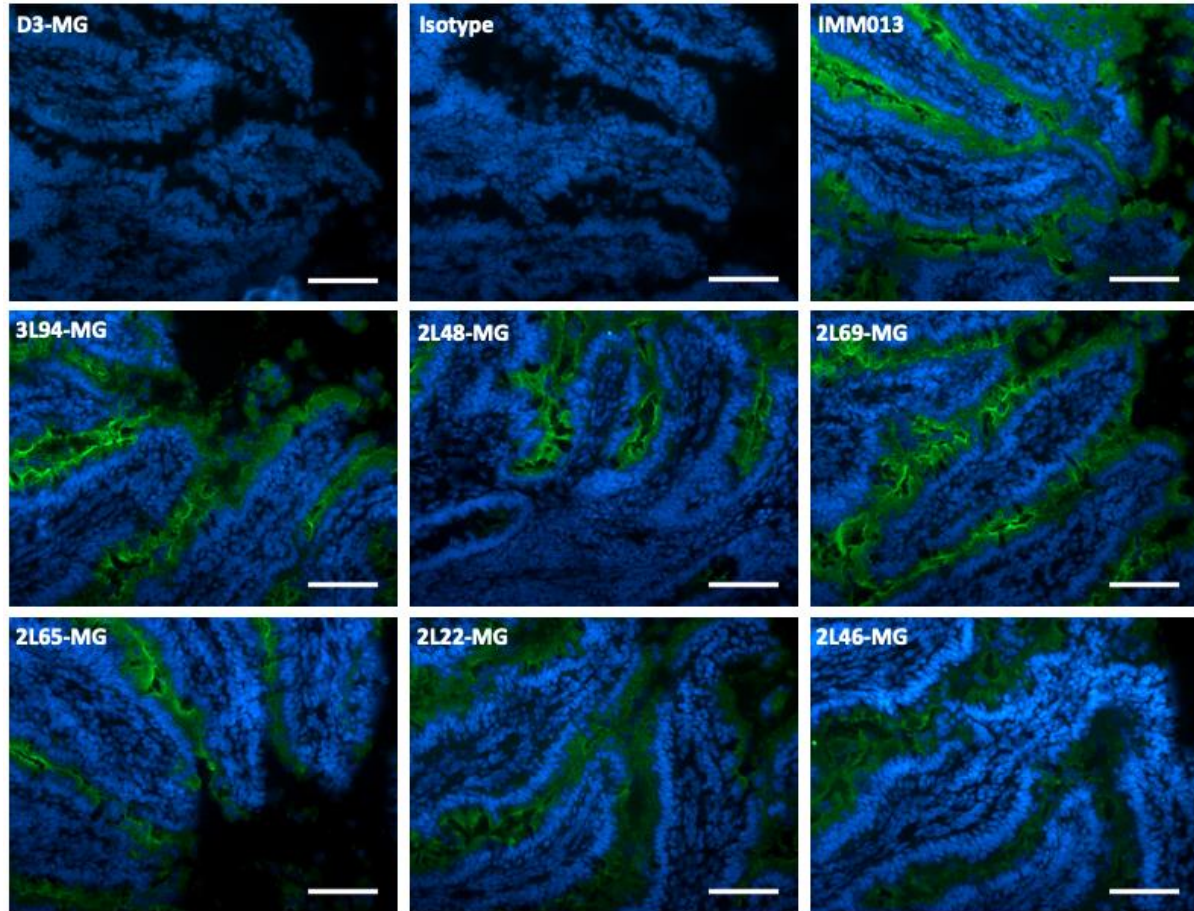
Figure 3. Binding analysis of anti-APN VHH-MG fusions on intestinal explants. Equal quantities of VHH-MG obtained after induction in yeast culture medium were assessed for binding on intestinal explants. IMM013 is a positive control, and Isotype and D3-MG are the negative controls. Binding of the VHH-Fc fusions to the explant was visualized by anti-mouse IgG-FITC (green) and counterstained with Hoechst (blue); scale bars: 100 µm.

Purified APN-binding VHH-MG fusions are internalized by intestinal epithelial cells

For each family, a single VHH-MG fusion displaying high expression and secretion in the spent Pichia medium and showing strong binding in FACS, was selected for upscaling. Secreted VHH-

MG fusions were affinity purified on protein A and further assessed by size exclusion chromatography (SEC) (Fig. 4a). For most fusions, the SEC profile showed two major peaks, one representing aggregates and multimers, and one representing the monomer with the corresponding molecular weight of two associated VHH-MG polypeptides. The major portion of the 2L76 VHH-MG was found in aggregates; therefore, we excluded it from further analysis (data not shown). For the remaining six fusions, the fractions corresponding to the monomeric VHH-MG were pooled and further analyzed by SDS-PAGE under both reducing and non-reducing conditions to verify dimerization. Because peaks for monomers and aggregates in the SEC profile slightly overlap, the pooled purified VHH-MGs still contain a small quantity of aggregates. The samples on the non-reducing gel nicely displayed an 80-kDa band (Fig. 4b), which corresponds to a monomeric VHH-MG composed of two VHH-MG polypeptides of 40 kDa, as seen in the SDS-PAGE under reducing conditions. Moreover, some high-molecular weight bands that most likely represent the aggregates or glycan variants were also observed.

Next, we tested the binding characteristics of the different purified VHH-MG fusions in ELISA and FACS (Fig. 5a and 5b, respectively). Although all of the six selected fusions showed strong binding on APN-expressing cells, the binding efficiency on the immobilized antigen in ELISA varied a lot, as was observed with the crude samples (Supplementary Fig. S1). These findings imply that screening for strong binders via ELISA would not be an ideal approach for applications aiming to target membrane proteins.

Because efficient endocytosis by the target cell population of the potential vaccine-carrying system is of high importance to obtain a strong immune response, we further investigated whether the APN-binding VHH-MG fusions showed specific uptake by cells via the APN receptor. We used APN-expressing BHK21 cells because of their strong binding capacity of VHH-MG in FACS (Fig. 5b). The VHH-MG proteins were stained with a different fluorescent molecule to discriminate between membrane-associated VHH-MG and internalized VHH-MG via the APN receptor. Confocal imaging clearly demonstrated the APN-dependent uptake of VHH-MG fusions, because uptake of irrelevant VHH-MG fusions could not be observed (Fig. 5c). Three VHH-MG fusions (3L94-MG, 2L65-MG and 2L48-MG) were found to be the most potent APN binders and they were taken up by APN-expressing cells (Fig. 5c).
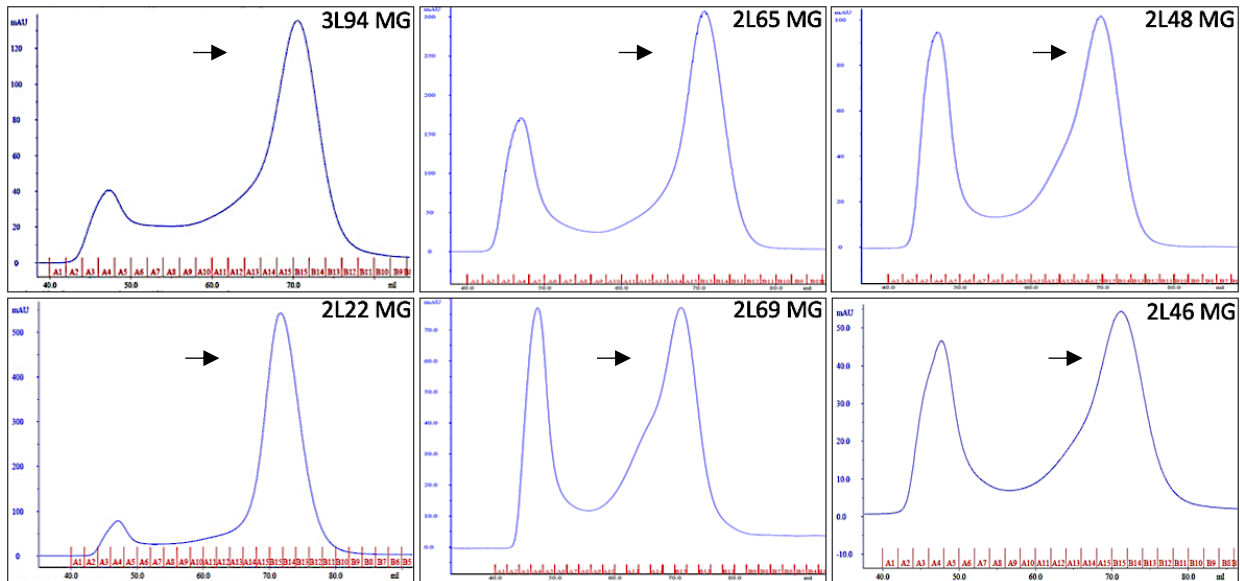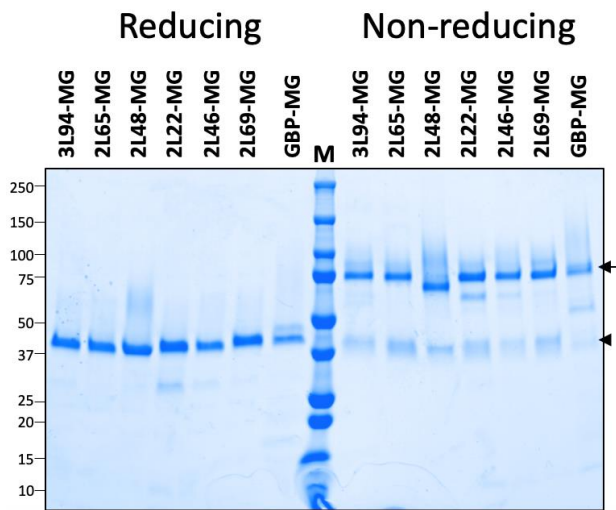
Figure 4. Purification of the different VHH-MG fusions. (a) Size exclusion chromatography (SEC) profile of six different VHH-MG fusions after protein A purification, labeled with its respective name at the top right corner. The arrows indicate the position and molecular weight of ~80 kDa, corresponding to monomeric VHH-MG fusions assembled by disulfide bridges between the hinge of two VHH-MG polypeptides (~40 kDa each). (b) SDS-PAGE analysis of pooled fractions of the 80-kDa peak after SEC on 4-20% polyacrylamide gel under both reducing (left) and non-reducing (right) conditions. The expected position of the intact full-length polypeptide is indicated by the arrowhead for monovalent VHH-MG (~40 kDa) in reducing conditions and by the arrow for bivalent VHH-MG (~80 kDa) in non-reducing conditions. M, molecular weight marker (kDa).
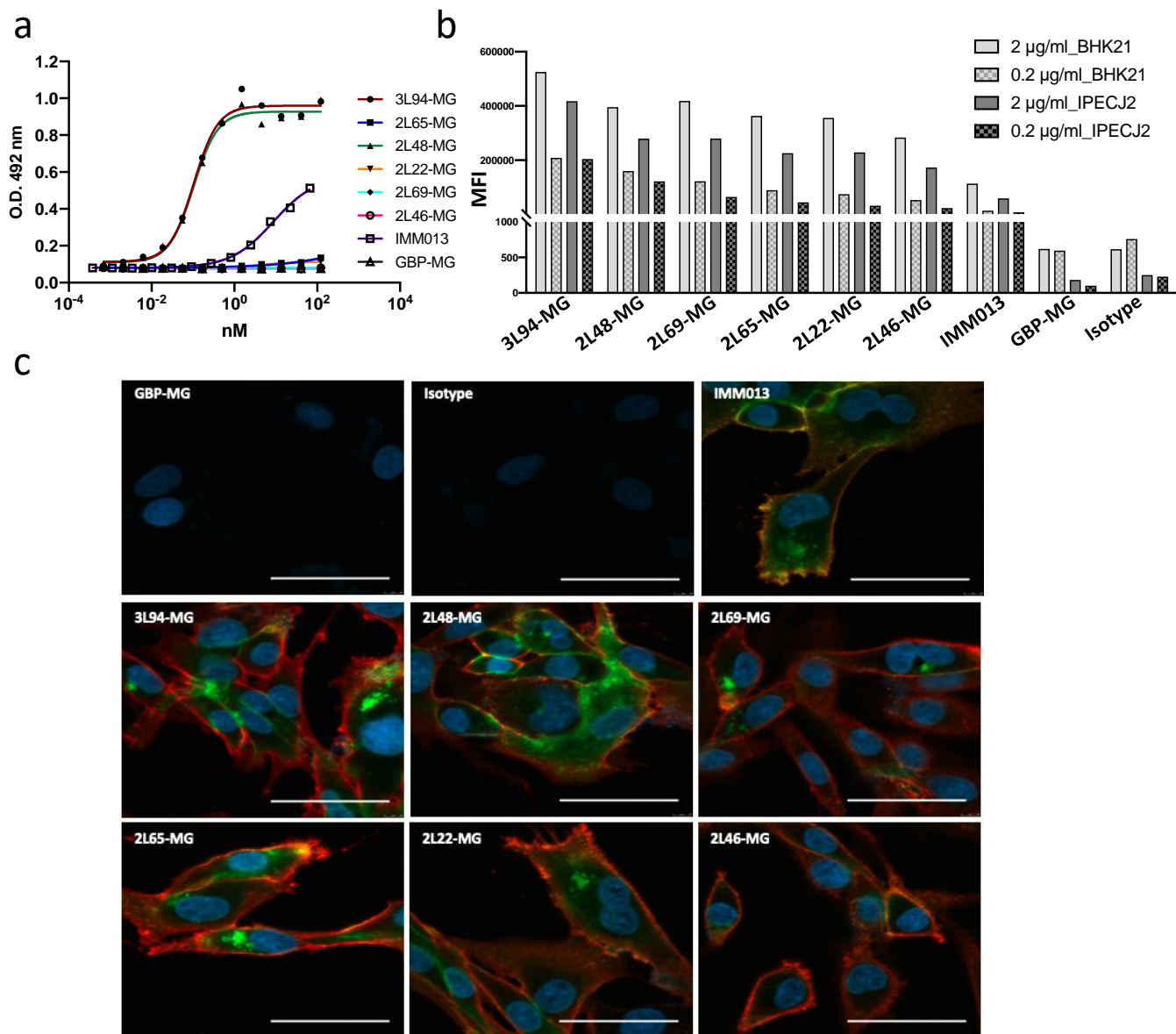
Figure 5. Binding analysis and APN-mediated endocytosis of purified VHH-MG fusions. (a) APN-binding ELISA with purified VHH-MG fusions. A three-fold dilution series of purified VHH-MGs were incubated on an APN-coated microtiter plate and probed with anti-mouse IgG conjugated with horse radish peroxidase. The binding of VHH-MG to immobilized antigen is depicted as OD (492 nm) values. IMM013 is a positive and GBP-MG is a negative control. The background threshold was determined as twice the OD (492 nm) value of the negative control. (b) Binding of the VHH-MG fusions to APN-expressing cells determined by flow cytometry. Graph shows the number of APN-positive cells that bind to VHH-MG at the indicated concentration (µg/ml). (c) Endocytosis of VHH-MG by APN-expressing cell lines. APN-expressing cells were incubated with VHH-MG on ice to allow binding followed by incubation at 37°C for 30 min to allow endocytosis. Cells were then fixed and stained with AF568-conjugated anti-mouse IgG (red) to visualize bound VHH-MG. Following permeabilization, cells were stained with anti-mouse IgG-FITC (green) to visualize endocytosed VHH-MG. Nucleus was stained with Hoechst (blue). IMM013 is the positive, and isotype and GBP-MG are the negative controls. Images represent a single confocal z-section, scale bars: 100 µm.

In vivo behavior of selected APN-specific VHH-Fc candidates in a gut ligated loop assay

To assess the *in vivo* behavior of the selected VHH-Fc IgG constructs, we performed a gut ligated loop assay in the small intestine (jejunum) of piglets. Figure 6 shows that 3L94-MG and 2L65-MG were able to bind to the entire apical epithelium of the villi, similar to the binding profile of IMM013. In contrast, 2L48 and 2L22 showed a more patchy binding profile. Supplementary Figure S3 shows that the binding profile is similar in different animals. We conclude that 3L94-MG and 2L65-MG are the best binders onto the small intestine enterocytes of a gut ligated loop assay.
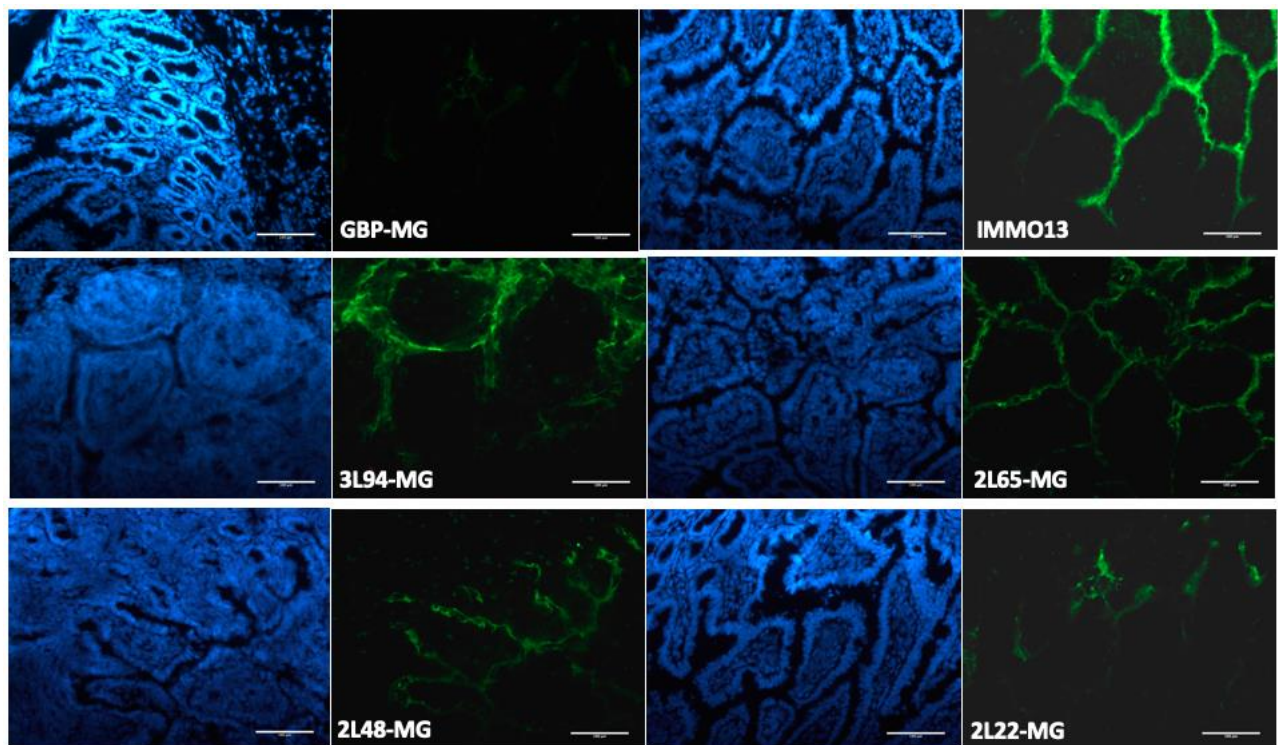
Figure 6. Gut ligated loop experiment to determine the uptake of VHH-MG by enterocytes. Sections from jejunal loops stained with sheep anti-mouse IgG (FITC, green) and counterstained with Hoechst (blue). The different anti-APN VHH-MG and anti-APN mAb (IMM013) are detected on the epithelial cells of the villi (scale bars: 100 µm)

Discussion

Despite their potential for generating both local and systemic immune responses, only few mucosal vaccines currently exist. The subunit vaccines very often trigger only a weak immunogenic response upon oral delivery, for which tolerance and the lack of uptake and presentation to the APCs are only two of the postulated reasons. Therefore, it was hypothesized that the selective targeting of subunit vaccines to intestinal receptors could help internalization of the vaccine to elicit more effective immune responses. Aminopeptidase N was previously described as a receptor for F4 fimbriae that is expressed on a variety of cells, including small intestinal enterocytes and APCs (see ref. Melkebeek et al., 2012), and as a target for oral delivery of mucosal vaccines. Very promising in this respect is that polyclonal antibodies raised against APN in rabbits were shown to be endocytosed by porcine enterocytes after oral administration to young piglets (Melkebeek et al., 2012). Moreover, a strong immune response against specific rabbit epitopes of the Fc portion of the polyclonal antibodies was found upon oral administration, whereas no immune response was observed upon oral administration of other polyclonal rabbit antibodies not binding to APN (Melkebeek et al., 2012). This led to the hypothesis that APN-dependent targeting of antigens might promote the efficacy of mucosal vaccines, for which a strong APN-binding carrier would be essential (Baert et al., 2015). Indeed, targeting with antigen loaded ß-glucan particles to APN enhanced their uptake and the immune response against the antigen.

Here, we demonstrate the isolation and characterization of APN-specific VHHs. VHHs have extensively been used for diagnostic and therapeutic applications because of their peculiar properties (Lafaye and Li, 2018; Steeland et al., 2016; Van Audenhove and Gettemans, 2016). Thanks to their small size, VHHs can easily be engineered to make genetic fusions with the model antigens. VHH against MHC class II proteins fused to a tumor-associated antigen has been shown to establish a strong and lasting immune response as a result of efficient processing and presentation of the exogenous antigen by APCs such as dendritic cells, B cells and macrophages (Fang et al., 2017a). Moreover, targeting an antigen via the Fc domain to Fcγ receptors on APCs has been shown to elicit both humoral and cell-mediated immune response (see ref. Czajkowsky

et al., 2012). Importantly, the Fc domain of an antibody has an added advantage over VHHs specific for Fcγ receptors, because they generate bivalent molecules that are often preferred for many applications owing to avidity effects and the capacity to cross-link. Fc fusions also offer many other advantages in terms of improved VHH serum half-life, purification on commercially available resins and recognition by Fc receptors present on the APCs (Narasimhan et al., 2016; Nimmerjahn and Ravetch, 2007). Thus, the VHHs identified in this study were fused to an Fc domain. We chose to first use the Fc fragment of a known mouse IgG (MG), enabling us to measure a specific immune response against mouse Fc epitopes upon oral delivery of APN-targeted VHH-mouse Fc fusions in pigs. The fact that there are many similarities between pigs and humans in terms of anatomy, physiology and genetics, raises the possibility to use pigs as an effective model system for preclinical studies of the human diseases (Guo et al., 2016; Meurens et al., 2012; Ober et al., 2001). However, the Fc domain from murine origin might not display efficient Fc-mediated effector functions in piglet models, because, in contrast to the information available about human and mouse Fc receptors, still little is known for pigs and especially on the interaction of the latter with murine IgG subclasses. It was recently reported that human IgG bind to human ortholog receptors with similar affinities than what is known for the human FcγR (Dekkers et al., 2017; Egli et al., 2019), suggesting that mouse IgG might show a similar binding to porcine FcγR. However, as long as experimental evidence is lacking on the interaction between murine Fc and porcine Fc receptors, the mouse Fc fragment should be replaced by a porcine Fc fragment in future experiments with other antigens when using pigs as a model system for *in vivo* validation of the vaccine targeting strategy.

We further determined the binding of VHH-MG fusions to pAPN via ELISA and to pAPN-expressing cells via flow cytometry. However, because binding to immobilized antigen may not be equivalent to binding to the cell membrane, flow cytometry data was the most reliable. It showed binding to the full-length protein in its native form that is expressed on the biological membrane. Moreover, we observed a clear correlation with the binding on intestinal tissue that further confirmed the flow cytometry data. Next, we demonstrated the uptake of VHH-MG on pAPN-expressing cells and porcine intestinal tissue in a gut ligated loop experiment. These data

support the efficient transport of the APN-targeted subunit vaccine across the intestinal epithelium.

Moreover, orally delivered subunit vaccines have to pass the gut epithelia that is protected by mucosal immune defense mechanisms and well-developed barriers such as low gastric pH and the presence of proteolytic enzymes resulting in the degradation of vaccine materials. Thus, oral delivery of VHH-based subunit vaccines might not generate a strong immune response that would otherwise be true when injected. To circumvent these hurdles, the subunit vaccine can be protected by encapsulation in a biodegradable particulate delivery system. Baert et al. (2015) reported that oral administration of β-glucan microparticles conjugated to mAb against APN (IMM013) can efficiently deliver the antigen payload and elicits a strong systemic immune response in piglets.

In conclusion, we have identified pAPN-specific VHHs and fused them to the Fc domain of a conventional antibody and showed efficient binding and uptake by the small intestinal epithelium under physiological conditions. The conjugation of a model antigen to these pAPN-specific VHHs can be envisioned as a next step to evaluate whether protein domains binding to the APN receptor of small intestinal enterocytes can trigger the targeted immune response at the gut epithelium. Finally, the present study extends the use of VHH as a delivery vehicle, thereby paving the way to develop a more rational approach to the broader basket of effective vaccine delivery systems.

Materials and methods

Vectors, strains, and cell lines

For the VHH library preparation, the pMECS phage display vector system was used that contains the pelB signal sequence to secrete the expressed VHH in bacterial periplasm and that adds an HA and His$_6$ tag at the VHH carboxy-terminal end, enabling purification. The yeast expression vector pPICZalphaH6E (NCBI accession number KM035419.1) modified for GoldenBraid cloning (named pKaiGG) was used for cloning the VHH-Fc fusions under the control of the methanol inducible promoter AOX1 (Juarez et al., unpublished). The vector contains the α-mating factor

secretion signal and Zeocin resistance marker for selection in bacterial as well as yeast cells. *E. coli* strains TG1 and DH5α (Meselson and Yuan, 1968) were used for construction of the VHH library and fusion expression vectors, respectively. The VHH-MG fusions were expressed in the *P. pastoris* wild-type strain NRRL Y-11430 (Kuberl et al., 2011). Stable APN-expressing cell lines (intestinal porcine epithelial cells IPEC-J2 and baby hamster kidney BHK-21) were obtained by transfection and cultured as previously described (Baert et al., 2015; Melkebeek et al., 2012).

Purification of intestinal APN

Enterocytes were isolated from the small intestine of a 3-week-old piglet following the method of Lundqvist et al. (1992). After analysis using light microscopy, more than 85% enterocyte purity was observed. Next, brush border membrane vesicles (BBMVs) were isolated from the enterocytes as described by Melkebeek et al. (2012). The obtained BBMVs were subsequently lysed in 9 volumes of lysis buffer (100 mM Tris-HCl, 300 mM NaCl, 1% Triton X-100, 0.5% sodium deoxycholate, 0.1% SDS, 2 mM leupeptin, 5 mM DTT, 1 mM AEBSF), sonicated for 2 min on ice, rotated for 30 min at 4°C and centrifuged at 17,400 g for 15 min at 4°C. Supernatant was collected and dialyzed in PBS using a 10-kDa MWCO dialysis cassette (Thermo scientific). Protein concentration was determined by BCA reaction (Pierce BCA protein assay kit), following the manufacturer's recommendations. Lysates were stored at -20°C until further use.

Intestinal pAPN was purified by immunoprecipitation from these lysates. First, affinity-purified rabbit anti-APN IgG (in house) was crosslinked to protein A Sepharose beads (CL-4B, Sigma). For this, 50 mg of beads were washed three times in 1 ml distilled water to remove salts by centrifugation at 400 g for 2 min. Rabbit anti-APN IgG (4 mg) was added to the beads for 1 h in PBS at room temperature (RT). Next, beads were washed twice with 1 ml 0.2 M sodium borate buffer (pH 8.0), after which 1 ml 0.2 M sodium borate (pH 9.0) + 20 mM dimethylpimelimidate (DMP, Sigma) was added for 30 min at RT. After crosslinking, the beads were washed twice for 1 h in 1 ml 0.2 M ethanolamine + 50 mM ammonium bicarbonate buffer (pH 8.0). Next, the beads were washed thrice in PBS before elution buffer (0.2 M Glycine-HCl, 50 mM L-arginine, 1 M NaCl (pH 2.0)) was added to remove non-crosslinked IgGs. Beads were washed again three times in PBS and stored at 4°C until further use. Finally, the anti-APN-beads were incubated with 1 ml of

BBMV lysate overnight at 4°C on a rotating wheel. Beads were centrifuged (400 g, 2 min, 4°C) and supernatant was collected. Beads were washed thrice with PBS to remove unbound proteins. Next, APN was eluted from the beads with elution buffer for 10 min at RT. After centrifugation, supernatant was collected and neutralized with 1 M Tris-HCl (pH 9.0). Eluted APN was dialyzed immediately in PBS and stored at -20°C. Concentration was determined with the Pierce BCA protein assay kit and purity (>95%) was assessed by performing a silver staining (Pierce® silver stain kit; Thermo Scientific), following the manufacturer's instructions.

Generation of a pAPN-specific VHH library

Porcine APN-specific VHHs were developed by the VIB Nanobody Core facility, Brussels (Belgium), as described previously (Pardon et al., 2014). Briefly, two llamas were immunized subcutaneously on days 0, 7, 14, 21 and 28, each time with 320 μg (per animal) APN isolated from porcine kidney (Sigma, cat. No. L6007-50UN). On day 35, each llama received a final booster with 200 μg of APN isolated from pig intestine. The porcine intestinal APN was purified as described above. For all immunizations, Gerbu P (GERBU Biotechnik) was used as adjuvant. On day 40, anticoagulated blood was collected for lymphocyte preparation. Total RNA from peripheral blood lymphocytes (PBLs) was used as template for first strand cDNA synthesis with an oligo(dT) primer. Using this cDNA, the VHH-encoding sequences were amplified by PCR, digested with PstI and NotI, and cloned into the PstI and NotI sites of the phagemid vector pMECS, and in this way fused to a histidine tag. Electrocompetent *E. coli* TG1 cells were transformed with the recombinant pMECS vector. An independent VHH library was obtained from each of the llamas, and each was subjected to a panning (in solution), performed on stably transfected BHK-21 cells expressing pAPN. The phage outputs of the first panning round from the two libraries were then pooled and the pool was used for further panning rounds. 190 randomly selected colonies from the second and third panning rounds (95 from each round) were sequenced and then grouped based on their CDR3 sequences. Using crude periplasmic extracts, 28 unique VHH (Nanobody) sequences were analyzed by flow cytometry for specificity to pAPN using pAPN-expressing BHK-21 cells.

Construction of the VHH-MG fusion expression vectors

To clone the *in silico* designed VHH-MG fusions in the yeast expression vector pKaiGG, customized reagents designed for Gibson Assembly® cloning were obtained from SGI-DNA (La Jolla, California), being synthetically produced DNA fragments of the VHH-encoding sequences fused to the Fc tail of mouse IgG2a with 40-base overlaps between the insert and the vector. The expression vector pKaiGG adapted for Golden Gate cloning was digested with SapI and column purified (GeneJET PCR purification kit, ThermoFisher Cat. No. K0701). The VHH fragments were always assembled with the same Fc fragment and were cloned at the 5'end in frame with the alpha factor secretion signal sequence (from novel *P. pastoris* expression vector named pPICZH6E; GenBank accession number KM035419) and at the 3'end with the transcription termination sequence into the in-house SapI-digested pKaiGG vector via the BioXp™ 3200 System in an approximately 18-h reaction and transformed into *E. coli* DH5α. Upon plasmid preparation and sequence confirmation of the insert, yeast cells were transformed with the PmeI-linearized vectors and positive transformants were selected on YPD (1% yeast extract, 2% peptone, 2% Dextrose) supplemented with 50 mg/ml Zeocin (Invitrogen).

Production of VHH-MG fusions in P. pastoris

Expression and secretion of the VHH-MG fusions in the medium was first analyzed in 2-ml cultures. On day one, 2 ml of BMGY medium (1% Bacto yeast extract, 2% peptone, 1.34% YNB, 0.1 M potassium phosphate (pH 6), 1% glycerol) with 25 mg/ml Zeocin was inoculated with individual transformants and incubated while shaking at 28℃ for 48 h. For each VHH-MG construct, four independent transformants were grown in 24-well plates. The cells were then pelleted for 10 min at 1500 g and resuspended in 2 ml BMMY medium (1% Bacto yeast extract, 2% peptone, 1.34% YNB, 0.1 M potassium phosphate (pH 6), 1% methanol) to induce expression of VHH-MG. Cultures were incubated while shaking at 28℃ for 48 h and spiked with 1% methanol (v/v) every 12 h. After 48 h of induction, the yeast cells were pelleted, and the supernatant was analyzed by SDS-PAGE, western blot and ELISA to assess the accumulation levels of the secreted VHH-MG fusions in the medium.

Affinity purification of VHH-MG fusions

Yeast transformants that yielded high levels of VHH-MG were selected for upscaling in 1-l cultures, using similar growth and induction conditions as described above for 2-ml cultures. *P. pastoris* cultures grown in baffled flasks were harvested after 48 h of induction. Culture supernatant was filtered using 0.22-μM PES membrane filters (Millipore) and affinity purified on a 1-ml HiTrap MabSelect SuRe Protein A column (GE healthcare), equilibrated with 20 mM sodium phosphate, 300 mM NaCl buffer, pH 7.8. Bound protein was eluted with 1 M arginine, pH 2.7 and immediately neutralized with 1 M Tris, pH 9. Relevant fractions with high concentration of VHH-MG were pooled and subjected to size-exclusion chromatography (Superdex 200, GE Healthcare). Fractions containing the major antibody peak in the chromatogram were pooled, concentrated by dialyzing against 20% polyethylene glycol in PBS and stored at -80℃ until use. The protein concentration was determined by OD_{280} measurement.

SDS-PAGE and western blotting

VHH-MG fusions (crude/purified) were analyzed on a commercial 4 to 20% gradient gel (Bio-Rad) under reducing conditions and stained with Coomassie G-250 following the manufacturer's instructions. For western blotting, proteins were transferred onto a polyvinylidene difluoride membrane (PVDF) using the semidry transfer method (Bio-Rad). Blotted membrane was blocked overnight with 2% skimmed milk in PBST (PBS + 0.1% (v/v) Tween-20) at 4℃. Thereafter, the membrane was probed with anti-mouse IgG (GE Healthcare, NXA931) conjugated to horseradish peroxidase (HRP), diluted 1:2000 in blocking solution and incubated for 1 h at RT. The membrane was then washed three times with PBST, and bands were visualized by adding HRP substrate (WesternBright ECL, Advansta). The membrane was imaged using a ChemiDoc MP imaging system (Bio-Rad) and analyzed by ImageLab software (Bio-Rad).

Antigen-binding ELISA

96-well ELISA plates (Nunc Polysorp®) were coated for two h at 37°C with 400 ng of APN (Sigma) diluted in PBS. Plates were then washed three times with PBST and blocked overnight at 4℃ with

3% (w/v) gelatin prepared in PBS and 0.05% Tween-80. Following three washes with PBST, VHH-MG fusions were serially diluted in dilution buffer (2% skimmed milk + PBS + 0.05% Tween-20), added to each well and incubated for 1 h at RT. An in-house produced pAPN-specific mAb (IMM013, see ref. Baert et al., 2015) was used as a positive control. After washing, bound VHH-MG fusions were detected by anti-mouse IgG (GE Healthcare, NXA931), diluted 1:5000 in the dilution buffer. Following incubation for 1 h at RT, plates were washed three times with PBST and developed by adding HRP substrate (one SIGMA*FAST*™ OPD tablet dissolved in 20 ml deionized water). Finally, the reaction was stopped with 1 M hydrochloric acid and the optical density of the colorimetric reaction was measured at 492 nm (VersaMax™).

Flow cytometry

Binding of the different VHH-MG fusions to APN-expressing cell lines was analyzed using flow cytometry. The wild-type and APN-transfected IPEC-J2 and BHK-21 cell lines were grown until reaching a 90% confluence and detached with StemPro accutase (Gibco). Detached cells (3.0 x 10^5) were transferred to a conical bottom 96-well microtiter plate (Gibco) in 200-μl culture medium and centrifuged for 3 min at 350 g and 4°C. Cells were incubated with 2 μg/ml VHH-MG fusions or anti-APN mAb (clone IMM013) on ice for 30 min. Detection of bound VHH-MG fusions was performed with an AF647-conjugated anti-mouse IgG2a antibody (4 μg/ml; Invitrogen, A21241) and with an AF647-conjugated anti-mouse IgG1 antibody (4 μg/ml; Invitrogen, A-21240) for IMM013. Cells were incubated for 30 min on ice. Dead cells were excluded using Sytox blue staining (5 nM; Molecular probes). A total of 10,000 viable, single cells was measured for each condition (Cytoflex, Beckman Coulter).

VHH-MG endocytosis assay

APN-expressing BHK-21 cells were seeded in 24-well plates (1.0 x 10^5 cells in 1 ml) on top of a sterile cover slip and cultured until a monolayer was formed. Cells were washed twice with ice-cold PBS and stored on ice before the VHH-MG fusions or IMM013 were added to the cells (250 μl; 100 μg/ml) in ice-cold culture medium. After a 60-min incubation at 4°C, cells were washed thrice with ice-cold PBS and incubated for 30 min at 37°C, 5% CO_2 in warm culture medium. After

washing twice in PBS, cells were fixed for 10 min with 500 µl 4% paraformaldehyde. Next, the presence of VHH-MGs or IMM013 on the cell membrane was detected with an AF568-conjugated anti-mouse IgG(H+L) (2 µg/ml; Invitrogen, A-11004) for 30 min at RT and protected from light. After washing three times with PBS + 1% FCS, cells were permeabilized with 250 µl 0.2% Triton-X100 for 2 min and washed again with PBS + 1% FCS. Both VHH-MG and IMM013 were then detected using a FITC-conjugated anti-mouse IgG (whole molecule) (Sigma, F2883) for 30 min at RT, protected from light. After washing three times, the cover slip was taken out and mounted on a microscope slide in mounting solution (DABCO). Images were taken with a confocal microscope (Leica).

In vivo uptake of anti-APN VHH-MG

Three female, 5-week-old piglets were used to assess the uptake of the VHH-MGs in gut ligated loops as described previously (Coddens et al., 2017). Briefly, following anesthesia and laparotomy, the jejunum was localized and six 3-cm loops with 10-cm intervals between each loop were made avoiding Peyer's patches. Blood supply was assured by placing the ligatures between the mesenteric arcades. The pAPN-specific mAb (IMM013, see ref. Baert et al., 2015) was used as a positive control, while a GFP-specific VHH was used as a negative control (De Meyer et al., 2015). The anti-APN mAb IMM013 (1 mg) or an equimolar amount of the different VHH-MGs were diluted in 3 ml of PBS and injected in the lumen of the loops. Upon injection, each loop was returned to the abdominal cavity and the abdomen was closed. After a 5-h incubation, the animals were euthanized with an overdose of sodium pentobarbital and tissue samples from intestines, loops and mesenteric lymph nodes were collected. Tissue samples were embedded in 2% Methocel® MC (Fluka), snap frozen in liquid nitrogen and stored at -80°C until use. All animal procedures were approved by the Ethical Committee of the Faculty of Veterinary Medicine of Ghent University (EC 2018-04).

Immunohistochemistry

Cryosections (8 µm) of porcine ileum and the ligated gut loops obtained from 3-week-old piglets were cut with a Leica CM3050 S cryostat, mounted on APES-coated glass slides, dried (30 min,

40°C) and fixed in acetone during 10 min at -20°C. Subsequently, the cryosections were incubated during 30 min in ammonium chloride buffer (50 mM, pH 8) and washed thoroughly. All washing steps were carried out at RT in PBS. Fc receptors were blocked for 30 min at 37°C with PBS containing 10% sheep or goat serum. Binding of the VHH-MG or IMM013 (10 µg/ml) was detected by incubation for 1 h at 37°C with a FITC-conjugated sheep anti-mouse IgG (Sigma; F2883) or goat anti-mouse IgG2a. Nuclei were counterstained with Hoechst (10 µg/ml). The sections were washed in ultrapure water and mounted in mounting solution (DABCO). Tissues were imaged with a Leica DC 100 fluorescence microscope mounted with a Scion Corporation camera. Images were analyzed and processed using Fiji.
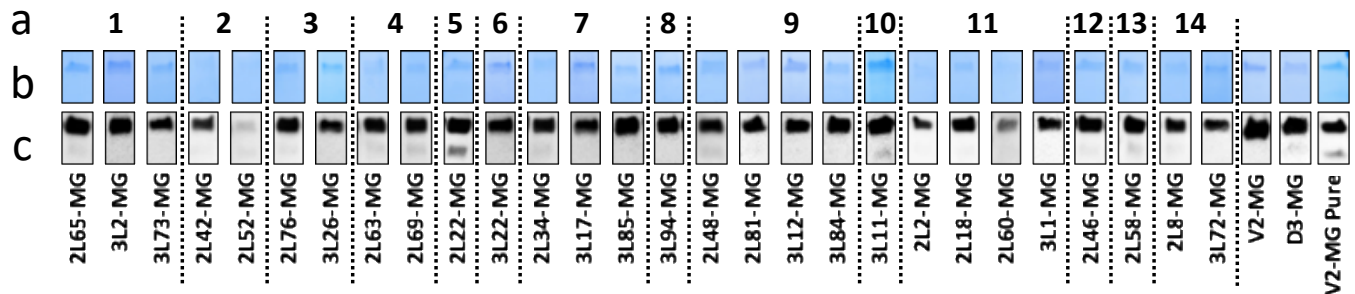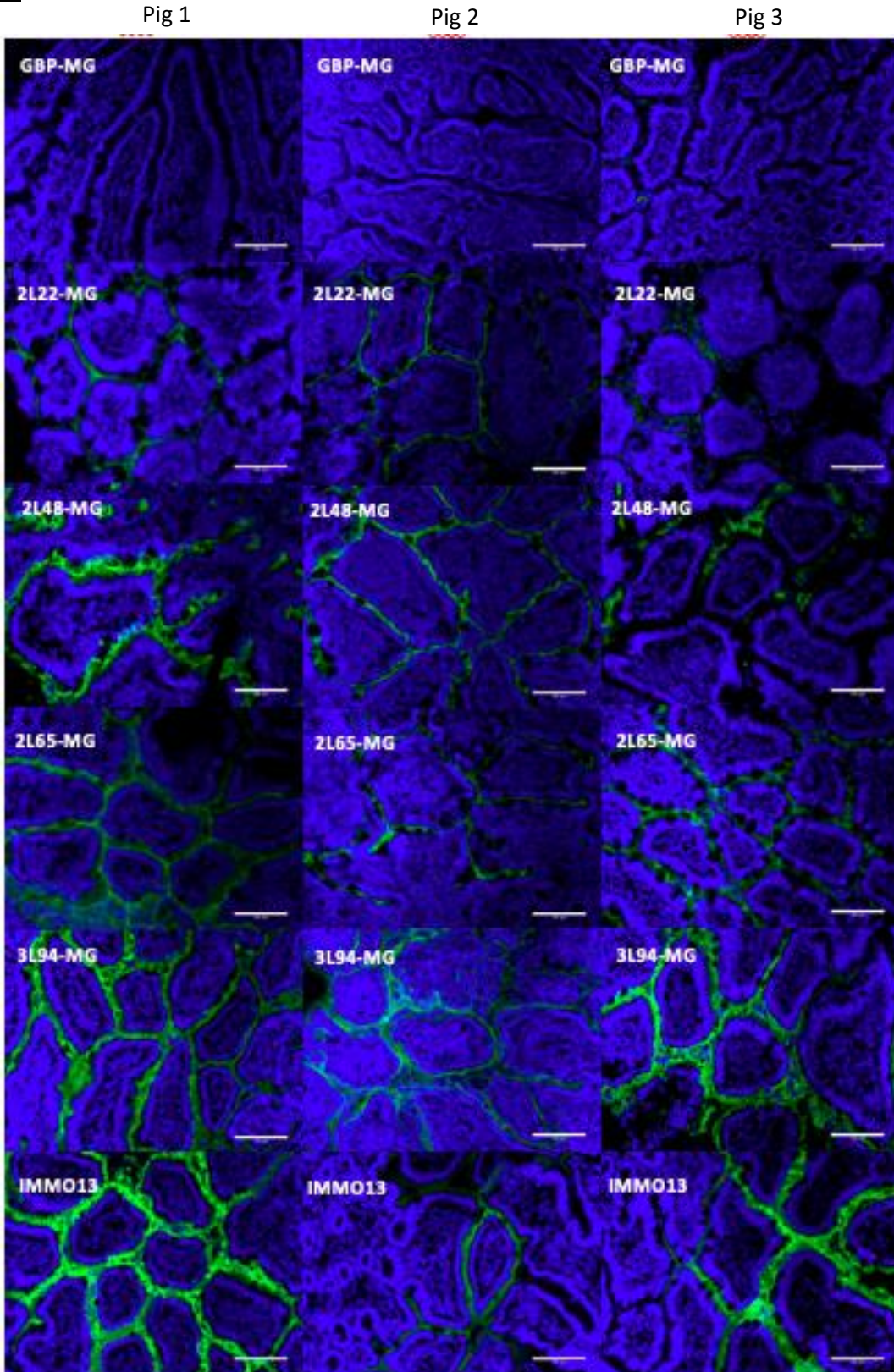
Supplementary figures

Figure S1
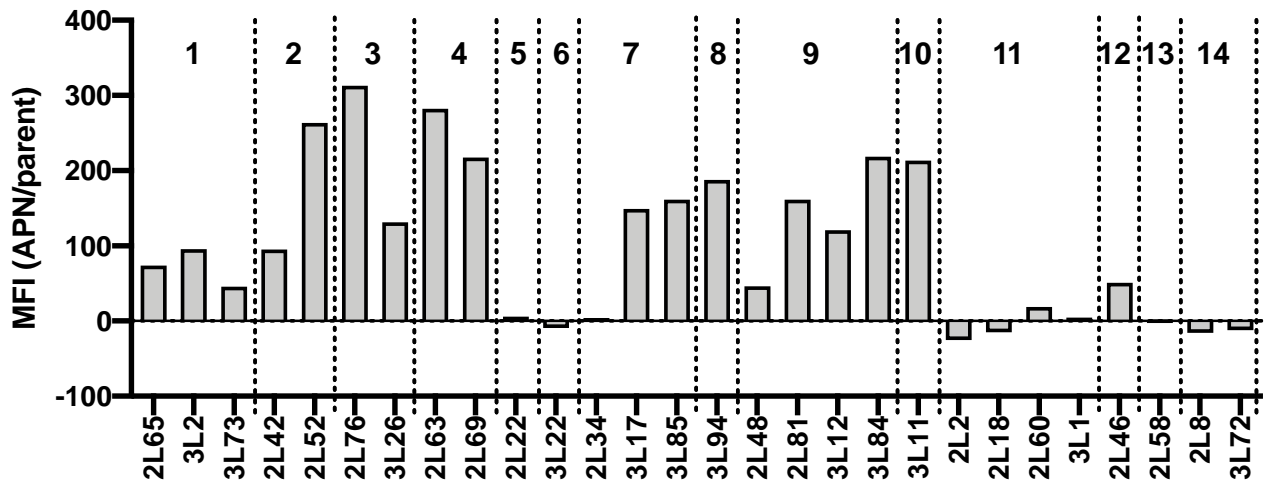
Supplementary Figure S1. Screening of VHHs that bind APN-expressing cell lines. Crude periplasmic extracts were prepared from TG1 cells harboring recombinant phagemids from the library. The 28 APN-binding VHH candidates were screened on APN-expressing cell lines by flow cytometry. The clones were grouped according to their similarity in CDR3 sequence; numbers on top between the dotted lines refer to the family to which the different clones belong. The Y-axis represents the ratio of median florescence intensity (MFI) of APN-transfected and parental non-transfected BHK21 cells.

Figure S2

Supplementary Figure S2. Expression of different variants of APN-specific VHH-MG fusions in *Pichia pastoris*. The culture medium of yeast transformants (4 colonies for each construct) were screened by Coomassie staining and western blot analysis to identify the highest expressing clone. Here, only one high expressing clone for each construct is shown and they were grouped according to their CDR3 similarity; the numbers between the dotted lines represent the family to which they belong (a). Protein expression was induced for 48 h with 1% methanol. Cultures were harvested and supernatant was analyzed by SDS-PAGE (b) and western blot (c). 'V2-MG Pure' was used as a loading control and 500 ng of samples were loaded for Coomassie staining and 200 ng for western blot. MG represents the Fc domain of **M**ouse Ig**G**.

110

Figure S3

Supplementary Figure S3. Sections from jejunal loops of three pigs. Merged images stained with goat anti-mouse (FITC, green) and counterstained with Hoechst (Blue). Scale bars: 100 μm.

Chapter 4

Part II: Up-scaling of APN binding VHH-Fc fusions for in vivo validation (follow-up)

Shruti Bakshi[1,2], Shubham Pandey[1,2], and Ann Depicker[1,2]

[1] Department of Plant Biotechnology and Bioinformatics, Ghent University, 9052 Gent, Belgium
[2] VIB Center for Plant Systems Biology, 9052 Gent, Belgium.

Author Contribution

S.B. and S.P. performed the large-scale production, purification and characterization; S.B. wrote the chapter.

In part I of this chapter, we described the characterization of the anti-APN VHH-MG fusions and identified two best performing fusions, 3L94-MG and 2L65-MG. These VHH-MG fusions displayed binding to and uptake in both APN-expressing cells and porcine intestinal epithelium. Here, we aimed to further characterize them for their potential to generate focused immune response *in vivo*. Therefore, 3L94-MG and 2L65-MG were up-scaled and purified.

Study design for oral immunization -

To test the oral immunogenicity of 3L94-MG and 2L65-MG, an oral immunization experiment in piglets was set up. We planned to test the immunogenicity in four experimental groups, as described in Table 1. A new negative control containing irrelevant VHH fused to mouse IgG2a Fc will be cloned, because Fc domain of GBP-MG was derived from mouse IgG3 that cannot be compared with 3L94-MG and 2L65-MG. Each group comprised of 3 pigs (5 weeks old) will be adjuvanted with 50 μg cholera toxin (CT). The piglets will be immunized on three consecutive days with intragastric administration of equimolar amounts and a booster immunization will be given on day 14. Immunogenicity will be evaluated by measuring serum antibody response against mouse IgG2a in ELISA as well as the increase in IgG2a-specific antibody secreting cells in blood and in the small intestine by ELIspot (Figure 1).

Table 1 Vaccination group and dosage

| Groups		Dose	Total protein required for 4 doses
3L94-MG	3 pigs	1 mg	12 mg
2L65-MG	3 pigs	1 mg	12 mg
3L94-MG + 2L65-MG	3 pigs	500 μg each	6 mg each
negative control	3 pigs	1 mg	12 mg
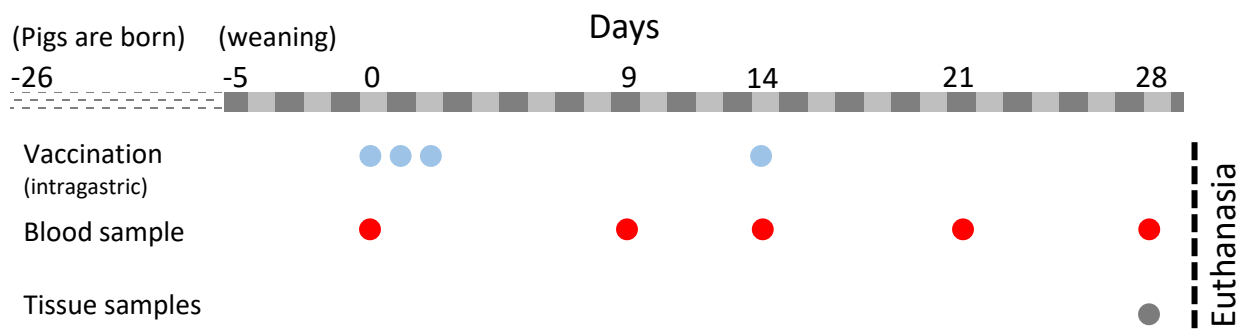
Figure 1. Schematic representation of the immunization experiment. All events have been depicted in reference to the first vaccination (day 0 in time line). Different time points for vaccination and sample collection (blood and intestinal tissue) are denoted with circles. At day 28, experiment ended, and pigs were euthanized.

Purification and characterization of purified 3L94-MG and 2L65-MG

To describe the proof of concept, both the fusions were upscaled to obtain a final amount of at least 20 mg. 10 liters of culture supernatants was first purified on protein A affinity chromatography, and then by size exclusion chromatography. Figure 2 shows the purification profile of only 3L94-MG, but a similar pattern was obtained for 2L65-MG. The pooled fractions from affinity purification of one liter of concentrated culture supernatant (Figure 2A) were subjected to size exclusion chromatography (Figure 2B). In SEC profile, two peaks were obtained, where the second peak represents the bivalent 3L94-MG, corresponding to 80 kDa. These results are consistent with the previous observation from small scale purification (Chapter 4, part I). All the SEC fractions were analyzed by SDS-PAGE, however only those corresponding to 80 kDa band were pooled and used for the immunization experiment (Figure 2C). Finally, we obtained about 200 mg of both 3L94-MG and 2L65-MG from 10 liters of *Pichia pastoris* culture. Figure 2D shows the SDS-PAGE analysis of 3L94-MG and 2L65-MG after purification as a quality check before proceeding to the immunization experiment. Both the profiles in reducing and non-reducing conditions are highly comparable with the previous data.
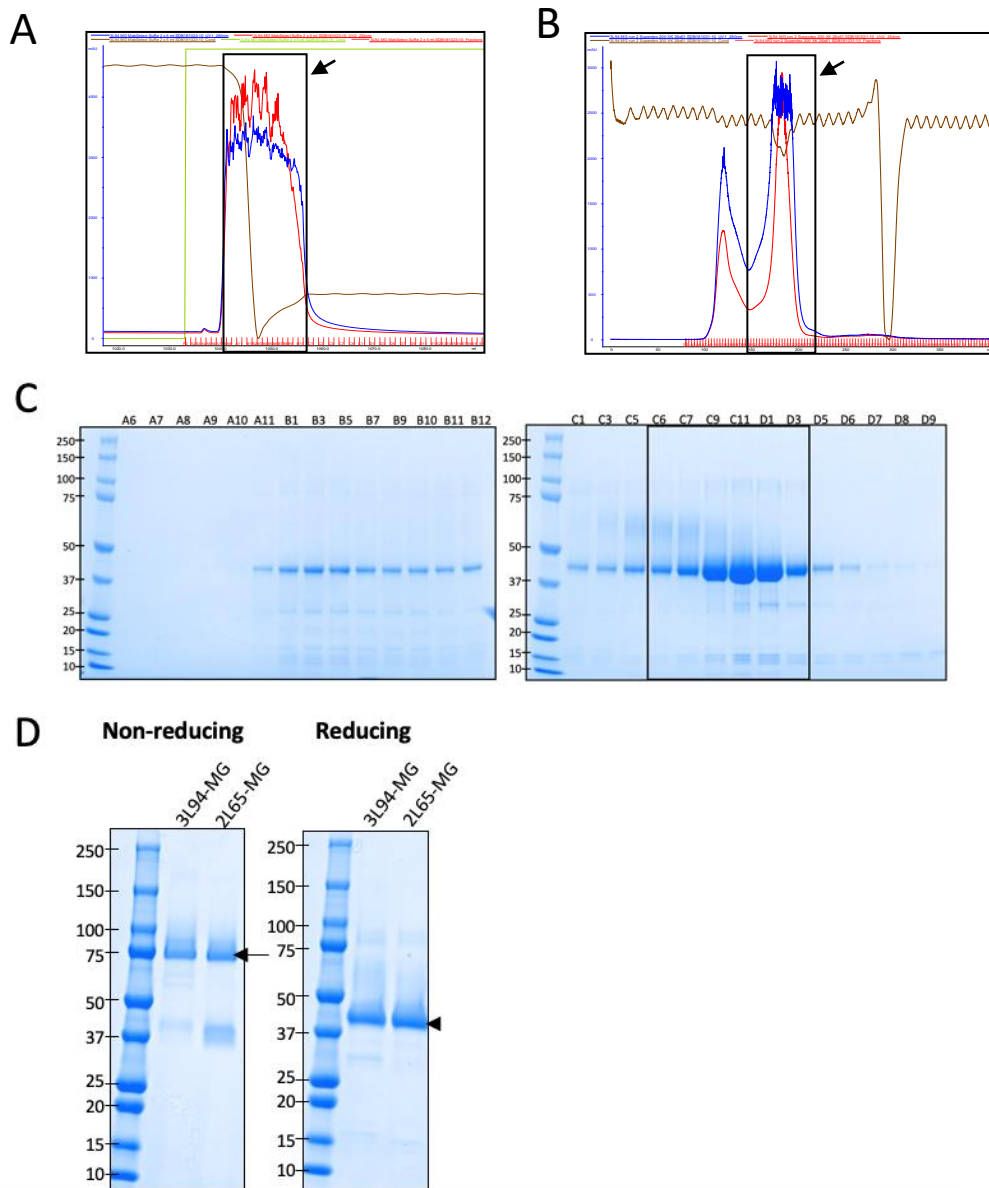
Figure 2. Purification of the VHH-MG fusions. Protein A chromatography (A) and size-exclusion chromatography (SEC) profile of 3L94-MG. The arrow and box indicate the pooled fractions corresponding to the eluted proteins. In SEC profile, the second peak indicated by box represents the position and molecular weight of 80 kDa, where monomeric 3L94-MG fusions assembled by disulfide bridges between the hinge of two 3L94-MG polypeptides (40 kDa each). (C) SDS-PAGE analysis of the SEC fractions on 4-12% Bis-Tris gels under reducing conditions. The box indicates the pooled fractions. (D) SDS-PAGE analysis of the 80 kDa peak of both 3L94-MG and 2L65-MG after SEC on 4-20% polyacrylamide gel under both non-reducing (left) and reducing (right) conditions. The expected position of the intact full-length polypeptide is indicated by arrowhead for monovalent VHH-MG (˜40 kDa) in reducing conditions and by arrow for bivalent VHH-MG (˜80 kDa) in non-reducing conditions.

Conclusion

A preliminary immunization experiment was performed as mentioned in the scheme (Figure 1, Table 1), but using the irrelevant conventional mouse IgG2a as a negative control. However, the results were not conclusive and no differential immunization responses were observed in the different groups. Therefore, the experiment will be repeated with the ideal control (irrelevant VHH fused with Fc domain of murine IgG2a) that would allow comparison with APN-binding VHH-Fc fusions.

Materials and methods

Production of 3L94-MG and 2L65-MG in Pichia pastoris

For upscaling, 10 liters of yeast cultures were grown in shake flasks. For this, 2 days grown preculture in YPD medium (1% Bacto yeast extract, 2% glucose, 25 mg/ml Zeocin) was used for 1/50 inoculation in 250 ml BMGY medium (1% Bacto yeast extract, 2% peptone, 1.34% YNB, 0.1M potassium phosphate pH 6, 1% glycerol, 0.002% biotine) per 2-liter shake flask (a total of 40 shake flasks were required) and incubated while shaking at 28°C for 24 h. The cells were then pelleted for 10 min at 1500 g and resuspended in 250 ml BMMY medium (1% Bacto yeast extract, 2% peptone, 1.34% YNB, 0.1M potassium phosphate pH 6, 1% methanol) to induce expression of VHH-MG. Cultures were incubated while shaking at 28°C for 48 h and spiked with 1.25% methanol (v/v) every 12 h. After 48 h of induction, the yeast cells were pelleted by centrifugation at 5000 rpm for 15 minutes and subsequently filtered using 0.22-µM PES membrane filters and concentrated to about 1 liter by diafiltration for first chromatographic step.

Purification of 3L94-MG and 2L65-MG

Concentrated *Pichia pastoris* culture supernatants were subjected to 2x 5 ml MabSelect SuRe Protein A columns (GE healthcare), equilibrated with 20 mM sodium phosphate, 300 mM NaCl buffer, pH 7.8. Bound protein was eluted with 1 M arginine, pH 2.7 and immediately neutralized with 1 M Tris, pH 9. Relevant fractions with high concentration of VHH-MG were pooled and

subjected to size-exclusion chromatography (Superdex 200, GE Healthcare). Fractions containing the major antibody peak in the chromatogram were pooled and stored at -80℃ until use. The protein concentration was determined by micro BCA kit (Pierce).

SDS-PAGE

The purified proteins were characterized by SDS-PAGE as described in chapter 4, Part I.

Chapter 5

The expression level of the APN binding VHH linked to the tetanus toxin C-fragment as antigen is negatively influenced by fusion to the Fc domain

Shruti Bakshi[1,2], Shubham Pandey[1,2], and Ann Depicker[1,2]

[1] Department of Plant Biotechnology and Bioinformatics, Ghent University, 9052 Gent, Belgium
[2] VIB Center for Plant Systems Biology, 9052 Gent, Belgium.

Abstract

Orally administered vaccines have great potential to fight against the enteric pathogens, however, poor uptake of the vaccine antigen by intestinal cells pose the huge challenge in their development. A promising approach to address this issue is to target vaccine antigens selectively to receptors on the mucosal membranes as an antigen-antibody fusion. Recent advances in antibody engineering allow the production of antigen fusions to single-chain variable fragments (scFv) derived from a monoclonal antibody, that overcomes the structural complexity of the conventional antibodies. However, optimization of the requisite linker to connect VH and VL domains is essential for their proper folding and functionality. On the other hand, single domain antibodies based on the variable region of the heavy chain only antibodies do not need this optimization of the linker between the variable regions in an scFv as all antigen binding hypervariable loops are located within a single compact small globular domain. Thus, VHH (single domain antibody) provides an easy solution to make such fusion constructs. This chapter describes the design and production of VHH-based vaccine carriers. The model antigen tetanus toxin C-fragment was fused to the anti-APN VHH 3L94 (characterized in the previous chapter) and Fc domains of porcine IgG and IgA. The fusions without the Fc domain and IgA-based fusions resulted in the high accumulation in *Pichia pastoris* as compared to IgG fusions. It is worthwhile to further characterize these fusions in *in vitro* (cell-based) and *in vivo* settings to demonstrate their potential as an ideal vaccine delivery system.

Introduction

Mucosal vaccines have the potential to elicit both local as well as systemic immune responses (Lycke, 2012). Since, the gut mucosa is protected by well-developed barriers including low pH, digestive enzymes, orally delivered subunit vaccines against the intestinal pathogens fail to develop a protective immunity as they encounter the same obstacles as do the other microorganisms. Moreover, poor uptake of the antigen payload by intestinal cells renders the oral vaccine unsuccessful. Thus, selective targeting of the vaccine antigen to transcytotic receptors on intestinal cells can be envisioned to facilitate the antigen uptake. Since the complex structure of the monoclonal antibodies limits their application as a targeting moiety, substantial efforts have been invested to reduce the size of the antibodies.

Chapter 1 described the cloning of fusion proteins with an APN targeting scFv and a model antigen (GFP), and their expression in *Pichia pastoris,* resulting in a very low yield. However, the similar fusions with an irrelevant VHH yielded better expression. Thus, rather than a single-chain variable fragment (scFv) derived from the anti-APN monoclonal antibody IMM013, we decided to opt for the single domain antibodies (VHH), that were isolated and characterized as described in the previous chapter (Chapter 4). The APN binding VHH 3L94 was grafted on the model antigen tetanus toxin C-fragment and produced in *Pichia pastoris*. Moreover, these VHH-antigen fusions were also fused to an Fc domain of an antibody, resulting in a bivalent molecule. Here, these fusions were produced in *P. pastoris*, analyzed for their specificity and integrity.

Results and discussion

IgA fusions accumulate better than IgG fusions

To design a novel antigen carrier, an anti-APN VHH (3L94) was genetically fused to a model antigen and an Fc domain derived from a conventional antibody of porcine origin. The recombinant C-fragment of tetanus toxin (TTC, 52 kDa) has been exploited as a model vaccine candidate in various studies (Jang et al., 2012; Lee et al., 2015). Owing to its immunogenic and non-toxigenic nature, TTC might be an ideal model antigen for developing a novel vaccine carrier. Moreover, both IgG3 and IgA[b] were reported to be resistant to proteolytic degradation, as compared to other isotypes (Brown et al., 1995; Butler et al., 2009). This attribute makes them ideal to use as a fusion partner to deliver antigens to the intestinal mucosa upon oral delivery. Thus, 3L94-TTC was fused to the N-terminal end of both IgG3 and IgA[b] (referred to as 94-T-PG and 94-T-PA, respectively) (Figure 1A). Additionally, two more fusions were made by linking the VHH 3L94 carrier and the Fc of IgG3 and IgA[b] to the N-terminal of the TTC (termed 94-PG-T and 94-PA-T, respectively) (Figure 1A). These fusion proteins were expressed in *P. pastoris* and four clones of each construct were screened for high expressers. The proteins expressed in the culture supernatant were analyzed by western blotting in reducing conditions with two detection systems. First, the Fc domain was detected by using anti-IgG antibody (for 94-T-PG and 94-PG-T) (Figure 1B) and anti-IgA antibody (for 94-T-PA and 94-PA-T) (Figure 1C). Although anti-IgG detection seems weaker as compared to anti-IgA detection, the bands corresponding to full-length protein were detected in clones of the four different constructs, except for two clones of 94-T-PG. Moreover, anti-IgA detection for 94-PA-T also revealed a smaller fragment of about 55 kDa. To compare the expression level, the proteins were also probed with an anti-TTC antibody (Figure 1D and 1E). In addition to the full-length band, a smaller fragment of different sizes was observed for all the fusions, that most likely represents a cleavage product. The cleavage might occur in G_4S linker, hinge or between CH2-CH3 interface. It appears that more than 50% of IgA-fusions are cleaved. Additional studies (such as N-terminal sequencing) are required to identify the cleavage pattern in the fusion molecule.
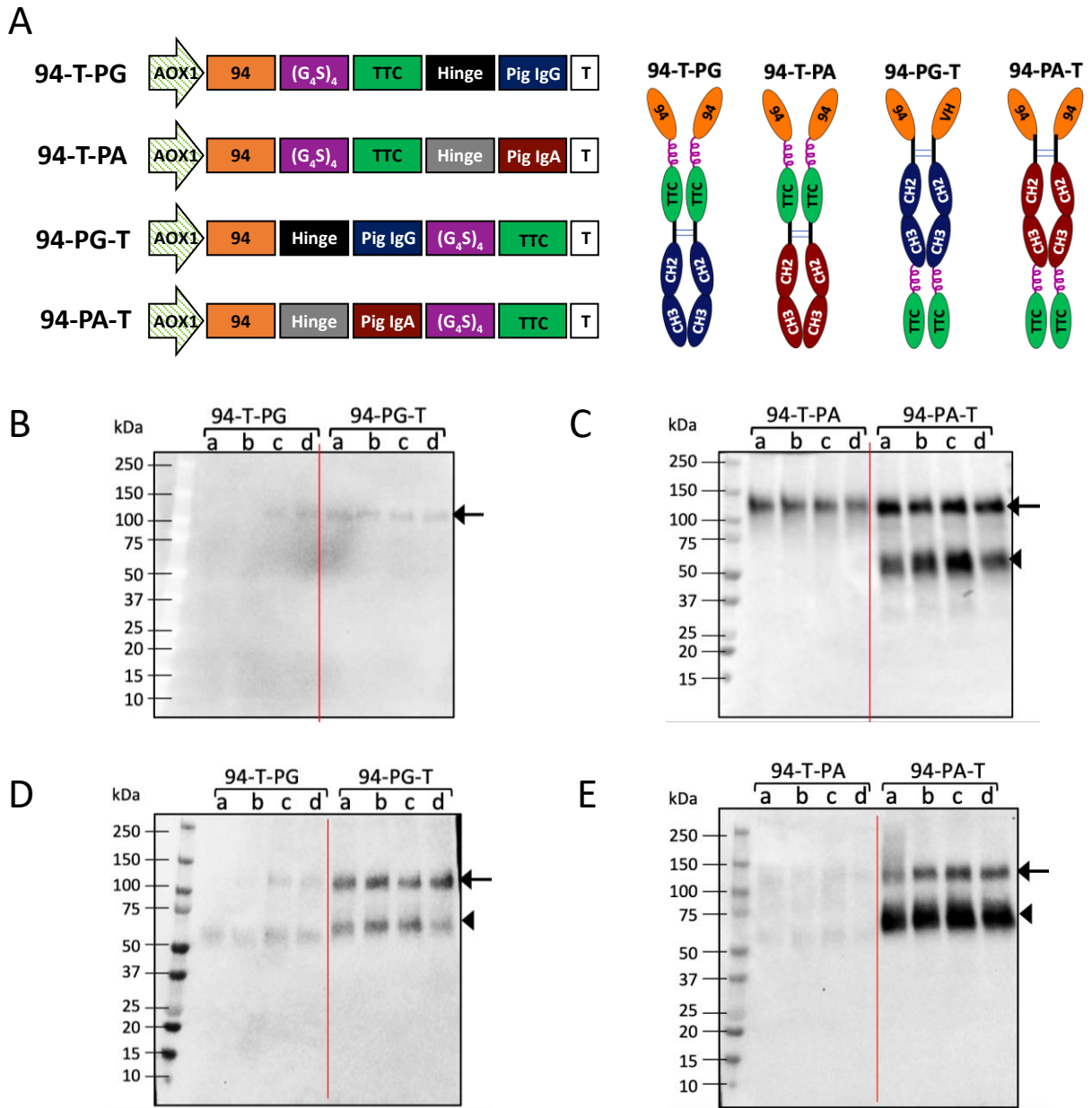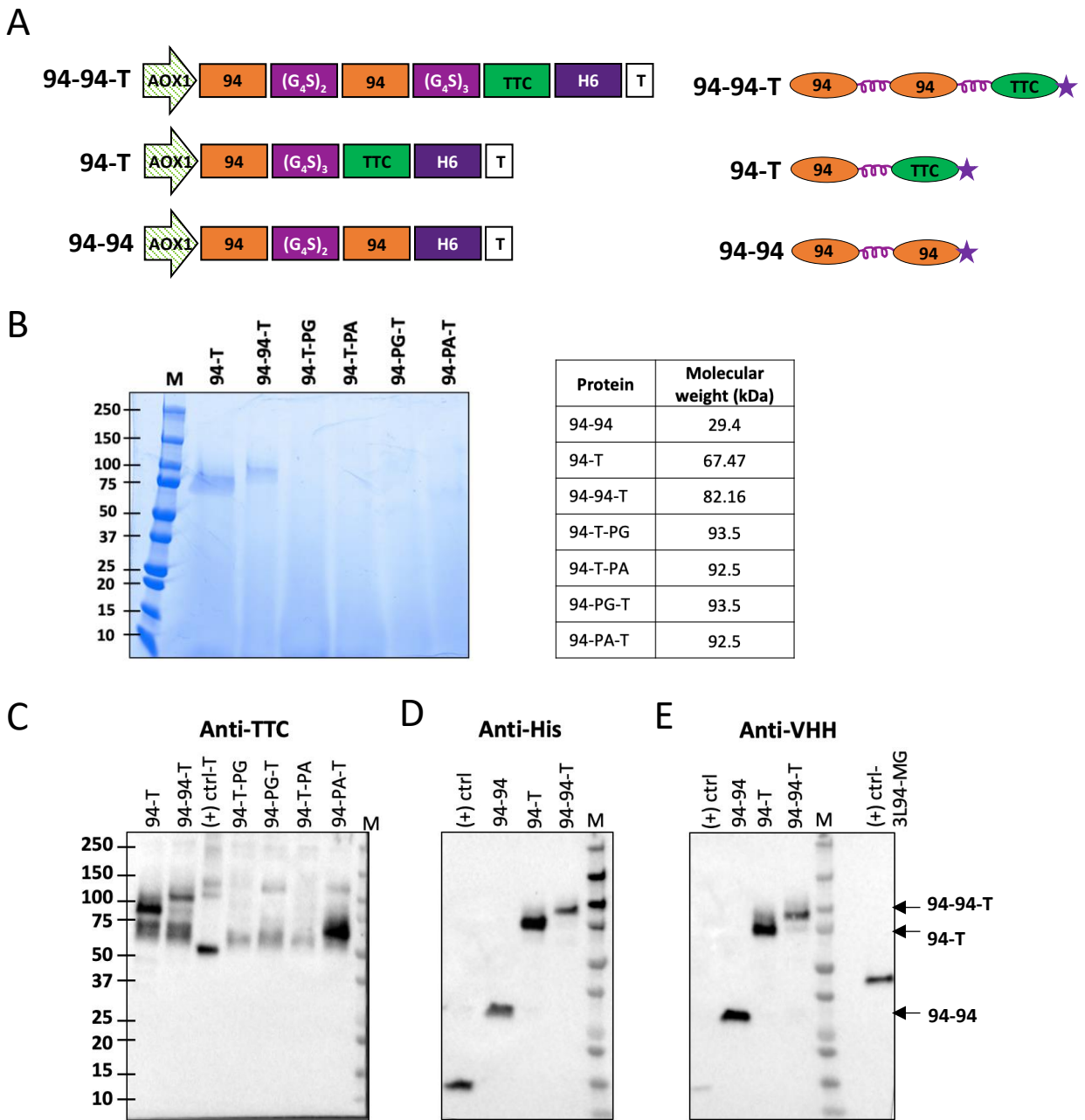
Figure 1. Cloning and expression of the fusion proteins in *Pichia pastoris*. (A) Schematic representation (not drawn to scale) of the expression cassettes for cloning in the expression vector under control of AOX1 promoter and terminator (T). 94, 3L94 (VHH); $(G_4S)_4$, Glycine-Serine linker; TTC, tetanus toxin C fragment. (B, C, D and E) The expression plasmids were transformed in *P. pastoris* and the culture medium of four clones (a, b, c, d) of each construct were analyzed to screen for highest expressing clone. The secreted proteins in the culture supernatant were analyzed using western blot under reducing conditions, in two different probe setups- with anti-Fc domain antibody (B, C); and with anti-TTC antibody (D, E). Black arrow represents the full-length protein, whereas arrowhead represents the cleavage product. Note that the intensity of the bands in B and C, and D and E, should not be compared as different detecting antibodies were used.

### *Removal of Fc domain leads to improved expression in P. pastoris*

Although the Fc fusions exhibited detectable expression levels in *P. pastoris*, the cleavage product may be hard to purify and may also interfere with the functionality. To address this issue, we made additional fusions without the Fc domain. Since, removal of Fc domain results in the monovalent molecule, a bivalent VHH (3L94) linked with the G_4S linker was also fused to TTC. 94-94 without TTC was made as a negative control. A C-terminal His-tag was fused to all the constructs to facilitate the purification (Figure 2A). The proteins expressed in culture supernatant were analyzed via Coomassie staining after SDS-PAGE and western blotting. Both 94-T and 94-94-T displayed clear bands corresponding to the full-length protein, while all fusions containing Fc were undetectable in Coomassie staining (Figure 2B). For western blot, the proteins were detected with anti-TTC antibody (Figure 2C), anti-his tag antibody (Figure 2D), and anti-VHH antibody (Figure 2E). In the three different probed blots, prominent bands are present for full-length proteins 94-T and 94-94-T. The anti-TTC detection exhibited some high molecular bands that possibly represent the aggregates or different glycan variants. However, noteworthy is that the anti-his detection only reveals the full-length protein suggesting that these could be separated from all other fragments and purified by affinity chromatography.

Figure 2. Expression of the VHH-TTC fusion proteins (lacking Fc domain) in *P. pastoris.* (A) Schematic representation (not drawn to scale) of the expression cassettes for cloning in the *Pichia pastoris* expression vector under control of AOX1 promoter and terminator (T). 94, 3L94 (VHH); $(G_4S)_{2/3}$, Glycine-Serine linker; TTC, tetanus toxin C fragment; H6, 6x histidine tag to facilitate the purification. (B, C, D, E) The expression plasmids were transformed in *Pichia pastoris* and four clones of each construct were expressed by methanol induction. Here, only one high expresser clone is shown. The secreted proteins in the culture supernatant were analyzed using Coomassie staining (B) and western blot under reducing conditions. In western blot, proteins were probed with three different probe setups- with anti-TTC antibody (C), anti-His tag antibody (D) and anti-VHH antibody (E). The table shows the expected molecular weight of the proteins. M, molecular weight marker; (+) ctrl, loading control (recombinant TTC from sigma for anti-TTC detection (C), and his-tagged VHH (irrelevant) for anti-his (D) and anti-VHH detection (E).)

The fusion proteins are functional in APN-binding ELISA

Next, all the proteins were analyzed for their binding to APN in ELISA. Depending on the fusion tag, the proteins were detected by different antibodies. First, the presence of anti-APN VHH in the fusion molecule was confirmed by anti-VHH antibody detection (Figure 3A). Although all the fusions displayed binding to APN, their binding strength cannot be compared as the crude samples were used for the ELISA. Interestingly, stronger ELISA signal of 94-94-T compared to 94-T does not correlate with the band intensity in western blot, suggesting the strong avidity effect of bivalent VHH in APN-binding ELISA. Moreover, all the fusions were also detected with anti-TTC detection. Interestingly, 94-T-PA, that display lower expression than 94-PA-T displayed stronger binding in ELISA, suggesting that most of the cleavage product doesn't carry anti-APN VHH, thus could not bind to APN and was undetectable in ELISA. The fusion proteins were further analyzed by detection of the Fc domain. The IgG-fusions displayed a very weak ELISA signal with anti-IgG detection (Figure 3C) that correlates with other two detections (Figure 3A and 3B) and their low expression as observed in western blot (Figure 1B). Surprisingly, anti-IgA detection displayed a very strong signal for 94-PA-T that confirms the full-length molecule containing anti-APN VHH (3L94), TTC and Fc domain of IgA; while 94-T-PA was below the detection limit (Figure 3D), indicating that 94-T-PA is either very unstable, thus completely degraded or its IgA Fc domain is cleaved therefore it was still detectable by anti-TTC, but unable to be detected by anti-IgA antibody. Despite being extensively cleaved, 94-PA-T appeared to be the best fusion among all other Fc-fusion proteins in terms of expression and APN-binding in ELISA.
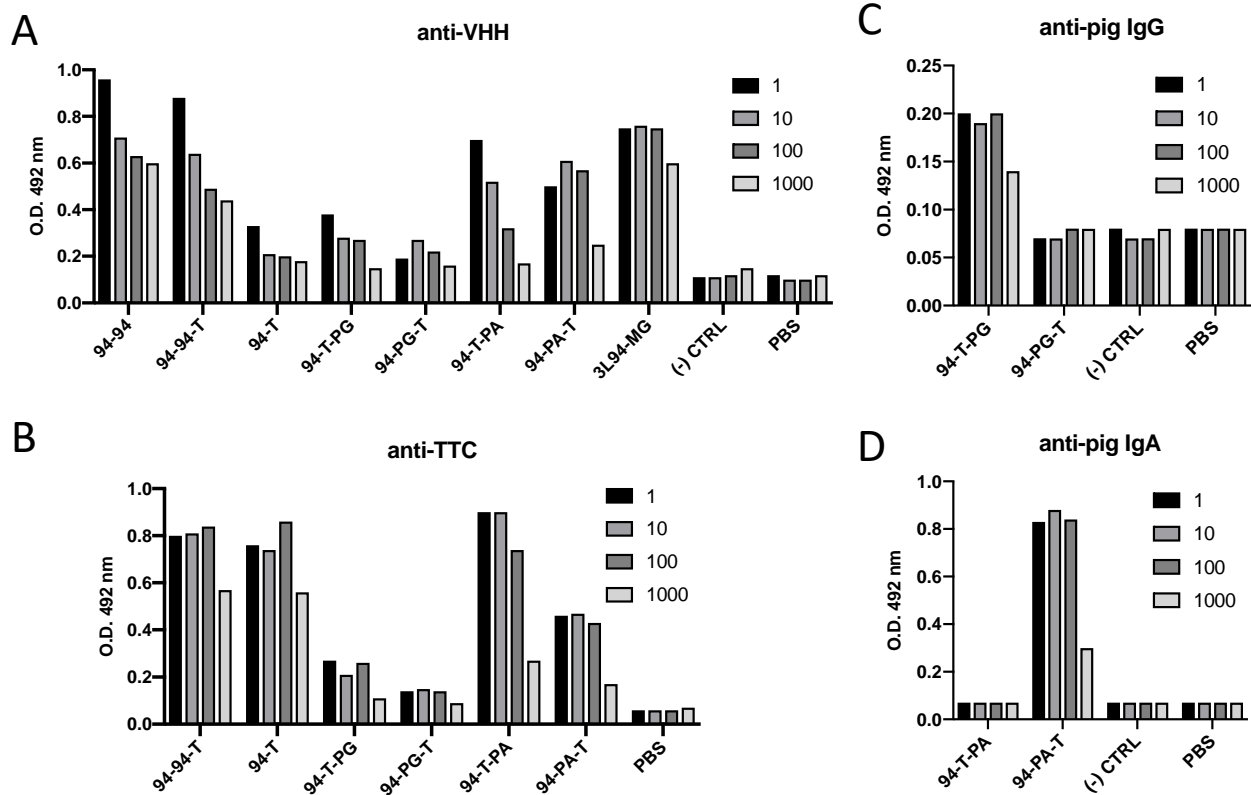
Figure 3. Characterization of the fusion proteins in ELISA. The fusion proteins expressed in *Pichia pastoris* were analyzed in ELISA to test their APN binding activity. The ELISA plates were coated with APN and a dilution series of the secreted proteins in culture supernatant was detected in four different setups- anti-VHH antibody (A), anti-TTC antibody (B), anti-pig IgG (C), and anti-pig IgA (D). (-), negative control = irrelevant VHH—murine IgG fusion (V2-MG) (A), pig IgG3 fusion (FaeG-IgG3) (C), VHH—pig IgA fusion (D3-IgA) (D). The graph shows the O.D. (492 nm) values obtained for each individual sample.

Conclusion

This chapter describes the effort to make a VHH-based vaccine carrier designed as either monovalent or bivalent by fusing to an Fc domain. The different expression patterns of the fusion molecules suggest that associated Fc domain impacts the integrity of the fusion molecule and its presence significantly reduced the accumulation. The Fc fusions appeared vulnerable to proteolytic cleavage, as evidenced by different fragments on reducing western blots. However, the different ELISAs show that the APN binding VHH 3L94 at the amino terminal end of the fusions is connected to the model antigen at the carboxyl terminal end of the fusion protein 94-PA-T, suggesting that some fraction of the full-length molecule remains intact in the solution by non-

covalent interactions. One might be puzzled by the different aspects affecting the integrity and functionality of the fusion proteins. Nevertheless, 94-PA-T and the two fusions without Fc domain 94-T and 94-94-T, which accumulate very well, may deserve further validation in *in vitro* and *in vivo* settings to assess their potential as a vaccine carrier to the intestinal membranes. As a final note to this section describing the production of innovative antibody-based fusion constructs, it is important to realize that the production and functionality of such fusions are very unpredictable, and extensive validation is required to identify the best candidate.

Materials and Methods-

Vectors, strains and DNA sequences

The yeast expression vector pPICZalphaH6E (NCBI accession number KM035419.1) modified for GoldenBraid cloning (named pKaiGG) was used for cloning the fusions under the control of the methanol inducible promoter AOX1 (Juarez et al., unpublished). The vector contains Zeocin resistance marker for selection in bacterial as well as in yeast cells. *E. coli* strain DH5α was used for construction and storage of the expression vector (Meselson and Yuan, 1968). The fusions were expressed in *P. pastoris* wild type strain NRRL Y-11430 (Kuberl et al., 2011). DNA sequences corresponding to the fragment crystallizable (Fc) domain of porcine IgG3 (CH1-Hinge-CH2-CH3; NCBI accession number EU372658), porcine IgA (Hinge-CH2-CH3; NCBI accession number U12594), VHH (3L94) coding sequences were obtained from the previously cloned vector in our laboratory. The coding sequence for C-fragment of tetanus toxin (TTC) (UniProtKB – P04958) was codon optimized for *P. pastoris* and synthesized by SGI-DNA (La Jolla, California).

Construction of the yeast expression vector harboring VHH-fusion proteins

The fusion proteins were cloned in the yeast expression vector pKaiGG via GoldenBraid cloning system (Sarrion-Perdigones et al., 2011). Briefly, all parts (coding sequences) were first cloned in a domesticator vector pUPD2, followed by assembly in the yeast expression vector pKaiGG. Subsequently, the plasmids were transformed in *E. coli* DH5α. Upon plasmid preparation and sequence confirmation of the insert, yeast cells were transformed with the PmeI-linearized

128

vectors and positive transformants were selected on YPD (1% yeast extract, 2% peptone, 2% Dextrose) supplemented with 50 mg/ml Zeocin (Invitrogen).

Expression of the VHH-fusion proteins produced in Pichia pastoris

Expression of VHH-IgG fusions was first analyzed in 2 ml cultures. On day one, 2 ml of BMGY medium (1% Bacto yeast extract, 2% peptone, 1.34% YNB, 0.1M potassium phosphate pH 6, 1% glycerol) with 25 mg/ml Zeocin was inoculated with individual transformants and incubated while shaking at 28°C for 48 h. For each fusion construct, four independent transformants were grown in 24-well plates. Cells were then pelleted for 10 min at 1500 g and resuspended in 2 ml BMMY medium (1% Bacto yeast extract, 2% peptone, 1.34% YNB, 0.1M potassium phosphate pH 6, 1% methanol) to induce the expression. Cultures were incubated while shaking at 28°C for 48 h and spiked with 1% methanol (v/v) in every 12 h. After 48 h of induction, the yeast cells were pelleted, and the supernatant was analyzed by SDS-PAGE, western blot and ELISA to assess the accumulation of secreted fusions.

Immunoblotting

10 μl of culture supernatant was analyzed on 4-20% precast protein gels (Bio-Rad- 4561096). Samples were prepared in NuPAGE LDS Sample buffer (ThermoFisher- NP0008) with a reducing agent (ThermoFisher- NP0009). For immunoblotting, the proteins were blotted onto a polyvinylidene difluoride membrane (Bio-Rad- 1704156) using the semidry transfer method (Bio-Rad). The membrane was subsequently blocked for one hour with 5% (w/v) of skimmed milk in PBS containing 0.05% Tween-20 (PBST) and probed with 1/5000 anti-Pig IgG + HRP (Bethyl, A100-104P) for IgG-fusions, 1/5000 anti-pig IgA + HRP (Bethyl, A100-102P) for IgA-fusions, 1/2000 anti-His + HRP (Thermo Scientific, MA1-21315-HRP) for His-tagged fusions, 1/5000 anti-VHH + HRP (GenScript, A01861) for VHH detection, and 1/5000 rabbit anti-TTC antibody (abm, Y054127) to detect TTC in the fusion proteins, followed by detection with 1/2000 anti-rabbit IgG + HRP (GE Healthcare, NA934). The membrane was then washed three times with PBST, and bands were visualized by adding WesternBright ECL HRP substrate (Advansta- K-12045-D20). All incubation steps were performed at room temperature on the orbital shaker.

APN binding ELISA

96-well ELISA plates (Nunc Polysorp®) were coated for two hours at 37^{0}C with 400 ng of APN (Sigma) diluted in PBS. Plates were then washed three times with PBST and blocked overnight at 4℃ with 3% (w/v) gelatin prepared in PBS and 0.05% Tween-80. Following three washing steps with PBST, the proteins were serially diluted in dilution buffer (2% skimmed milk + PBS + 0.05% Tween-20), added to each well and incubated for 1 hour at RT. Subsequently, the plates were washed three times with PBST and bound proteins were detected depending on the fusion tag, by 1/10000 anti-Pig IgG + HRP (Bethyl, A100-104P), 1/10000 anti-pig IgA + HRP (Bethyl, A100-102P), 1/5000 anti-VHH + HRP (GenScript, A01861) and 1/10000 rabbit anti-TTC antibody (abm, Y054127), followed by detection with 1/5000 anti-rabbit IgG + HRP (GE Healthcare, NA934). Following incubation for 1 hour at RT, plates were washed three times with PBST and developed by adding HRP substrate (SIGMA*FAST*^{TM} OPD tablets dissolved in 20 ml deionized water, Sigma-Aldrich- P9187). Finally, the reaction was stopped with 1 M hydrochloric acid and the optical density of the colorimetric reaction was measured at 492 nm (VersaMax, Molecular Devices, Sunnyvale, California).

Chapter 6

Plant-produced VHH-Fc fusions protect against Respiratory Syncytial Virus infection

Shruti Bakshi[a,b], Paloma Juarez[a,b], Dorien De Vlieger[c,e], Shubham Pandey[a,b], Vikram Virdi[a,b], Xavier Saelens[c,e], Ann Depicker[a,b] and Bert Schepens[d,e]

[a]Department of Plant Biotechnology and Bioinformatics, Ghent University, 9052 Ghent, Belgium

[b]VIB Center for Plant Systems Biology, 9052 Ghent, Belgium

[c]Department of Biochemistry and Microbiology, Ghent University, 9052 Ghent, Belgium

[d]Department of Biomedical Molecular Biology, Ghent University, 9052 Ghent, Belgium

[e]VIB Center for Medical Biotechnology, 9052 Ghent, Belgium

Abstract

Respiratory syncytial virus (RSV) is one of the leading causes of pediatric lower respiratory tract hospitalization throughout the world. Despite the overwhelming global burden of RSV infection, no vaccine or effective antiviral therapies are available. Owing to their high stability, the variable domains of camelid heavy-chain-only antibodies (VHHs) can be directly delivered to the lumen of the lungs. As this allows fast delivery of high amounts directly to the site of viral replication, VHHs represent an interesting type of antivirals to combat lung infections. However, as VHH lacks Fc fragments they have a short lung retention time and lack Fc associated effector functions that might be important to effectively control viral replication. To overcome these drawbacks, in the present study, a neutralizing (C4) and a non-neutralizing (E4) RSV F specific VHH and a control VHH, were fused to the mouse IgG2a CH2-CH3 Fc fragment and produced in a plant expression system. We demonstrate that these VHH-Fc fusion proteins (C4-Fc and E4-Fc) can be produced in *Nicotiana benthamiana* leaves and can efficiently bind to RSV F protein. Remarkably, 2 out of the 3 produced VHH-Fcs were highly thermostable, retaining full antigen-binding activity after heating to 90°C. The C4-Fc had far greater *in vitro* neutralizing activity than what is reported for its unformatted VHH counterpart and strongly protected mice against RSV infection. Remarkably, despite its lack of *in vitro* neutralizing activity, the E4-Fc could also reduce lung viral replication *in vivo*. This study sheds light on the potential of plant-produced VHH-Fc fusions as antiviral agents.

Introduction-

Respiratory syncytial virus (RSV) is one of the most important causes of lower respiratory tract infections and associated bronchiolitis and pneumonia in infants and young children worldwide (see ref. Battles and McLellan, 2019). By the age of two, virtually all children will have had at least one RSV infection (Glezen et al., 1986; Hall et al., 1991). As previous infection does not provide complete immunity, recurrence is common throughout life. Although RSV is rarely lethal in healthy people, it can cause severe illness in immunocompromised individuals, and elderly persons (Falsey et al., 2005). In 2015, RSV has been estimated to cause about 33.1 million ALRI incidence. 10% of these cases (3.2 million) required hospitalization, with 59,600 in-hospital deaths in children younger than 5 years, resulting in a substantial burden on health-care industries (Shi et al., 2017).

Although a vaccine and an effective antiviral treatment for RSV are still lacking, monthly passive immunoprophylaxis with palivizumab can reduce hospitalization of high-risk RSV infected infants by 55% (Null et al., 1998). Palivizumab (Synagis®) is a humanized mouse monoclonal antibody that targets the RSV fusion protein (F). The F protein is a conserved type I membrane protein that mediates the fusion of the viral membrane with the host cell membrane after attachment of the virus to the host cell. This fusion process is mediated by the refolding of the F protein from its prefusion to its postfusion conformation and starts with the insertion of the F protein fusion peptide into the membrane of the host cell. By subsequent joining of the heptad repeat regions that neighbor the inserted fusion peptide and the viral F protein transmembrane region, the viral and cell membrane are brought together and enabled to fuse. This fusion process can be blocked by antibodies like Palivizumab that bind to the prefusion conformation of the F protein (Battles and McLellan, 2019). Consequently, such antibodies can prevent virus infection. Although virus neutralization has also been demonstrated for antibodies that bind to the G protein involved in viral attachment, the vast neutralizing activity present in human sera is mediated by F specific antibodies (Ngwuta et al., 2015). New antibodies targeting the RSV F protein with high efficacy are currently under clinical development (Rossey et al., 2018).

The variable fragments of camelid heavy-chain-only antibodies (VHH) have received growing interest for a range of clinical applications (see ref. De Meyer et al., 2014; Vanlandschoot

et al., 2011) due to their peculiar properties such as high stability and solubility under different extreme conditions (Chapleau et al., 2015), easy penetration, high affinity, ease of engineering and production. Several recent studies have been reported the use of VHHs for prophylactic and therapeutic applications for many diseases including cancer, arthritis, bacterial zoonotic diseases and viral infections (Schepens et al., 2011; Zhao et al., 2018), and some are currently being evaluated in clinical trials (Detalle et al., 2016; Van Roy et al., 2015). Despite merits over conventional antibodies, the role of VHHs (either mono- or multivalent) as therapeutics providing long term immunity, remains elusive due to their rapid clearance from the circulation by renal infiltration. To surmount these hurdles, VHHs can be formatted by making fusions with Fc domain of conventional IgG antibodies that are widely acceptable to extend the half-life of biopharmaceuticals. Such bivalent fusions are equipped with Fc effector functions such as antibody-dependent cell-mediated cytotoxicity (ADCC), antibody-dependent cell-mediated phagocytosis (ADCP) and complement-dependent cytotoxicity (CDC); thereby provide better protection *in vivo* (Laursen et al., 2018).

Here, we report on the plant-based production of two RSV F targeting VHHs fused to the mouse IgG2a Fc fragment, and their *in vitro* and *in vivo* antiviral activity. The characterization of two RSV F specific VHHs- C4 and E4, former having the RSV-neutralization activity (Hultberg et al., 2011). The VHHs were fused to a mouse IgG2a Fc domain and produced in infiltrated leaves of *Nicotiana benthamiana* via Agrobacterium-mediated transient expression system. These plant-produced VHH-Fc fusions were evaluated for their *in vitro* RSV-neutralization potency, thermal stability and lung retention time. We further addressed the involvement of Fc domain in protection against RSV infection by comparing neutralizing (C4-Fc) and non-neutralizing (E4-Fc) VHH-Fc fusions in mouse models.

Results

The plant produced VHH-Fc assembles as bivalent

A neutralizing (C4) and a non-neutralizing (E4) VHH targeting the RSV F protein, isolated and described previously by Hultberg et al. (2011) were fused to the fragment crystallizable (Fc) domain of murine IgG2a (thereafter referred to as C4-Fc and E4-Fc, respectively). The VHH-Fc fusions were expressed in infiltrated tobacco leaves via Agrobacterium-mediated transient gene expression system (Supplementary Fig. S1A and S1B). An irrelevant VHH (V2), targeting the F4 fimbriae of enterotoxigenic *E. coli* served as a negative control (Virdi et al., 2013). The C-terminal ER retention motif (KDEL tag) was added to prevent the plant-specific N-glycan maturation in the Golgi apparatus and potential immunogenicity (Bardor et al., 2003; Jin et al., 2008; Landry et al., 2010). The crude leaf extracts were purified using protein A chromatography and subsequent size exclusion chromatography (SEC) (Supplementary Fig. S1C). The SEC profile has one major peak eluting after 65 ml (red box), which corresponds to the monomers containing bivalent VHH-Fc. Preceding peaks most likely represent dimers, multimers or aggregates that constitute a small fraction of the total purified protein (less than 5 %). Fractions derived from the major peak were pooled and the final yield of the pure protein varied from 10-30 mg/kg of fresh leaf weight. The purified proteins were analyzed by SDS-PAGE either by Coomassie staining and western blotting under both reducing and non-reducing conditions (Fig. 1). In reducing and non-reducing conditions, the full-length VHH-Fcs migrate respectively as 40-42 kDa bands and 80-82 kDa bands, verifying their assembly as a bivalent molecule. SDS-PAGE under reducing condition revealed additional band at 28 kDa that corresponds to the Fc moiety. This was confirmed by western blot analysis. Moreover, the band corresponding to bivalent Fc (approximately 56 kDa) was also observed under non-reducing conditions. Other low molecular and high molecular bands as detected in western blotting most likely represent the degradation and aggregates, respectively. Of note, the relative intensity of the cleavage product (smaller band) varied among the different VHH-Fc fusion proteins, indicating that the nature of the VHH might influence cleavage efficacy.
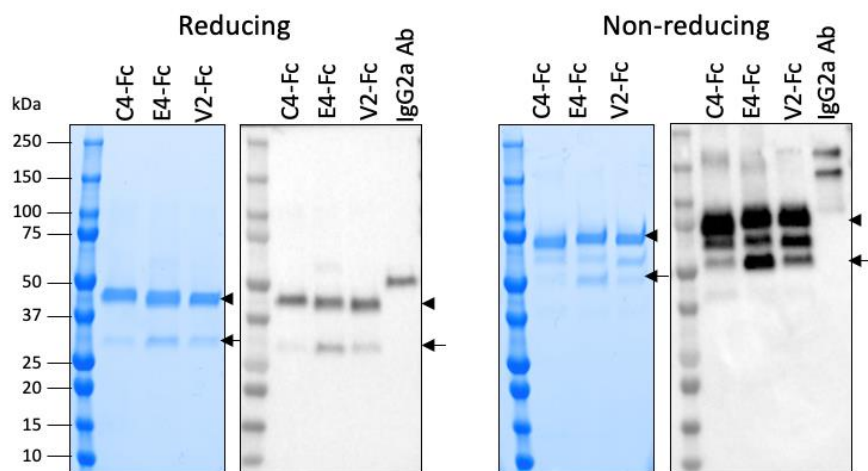
Figure 1 Characterization of purified VHH-Fc fusions. SDS-PAGE analysis of purified VHH-Fc fusions under reducing (left) and non-reducing conditions (right). The protein bands were revealed by Coomassie staining (blue) and western blotting (grey) using peroxidase conjugated anti-mouse IgG. A conventional full-length murine IgG2a was used as a reference in western blotting. The black arrowhead represents the full-length VHH-Fc and arrow represents the cleavage product.

C4-Fc and E4-Fc bind to full-length RSV F, whereas C4-Fc neutralizes both RSV A and B strain

VHH C4 and E4 both bind to the RSV F protein in its postfusion conformation. To test the binding of C4-Fc and E4-Fc to the RSV F protein, ELISA using postfusion F protein was performed. Palivizumab was used as a positive control. Figure 2A illustrates that next to Synagis, both C4-Fc (EC_{50} = 0.06 nM) and E4-Fc (EC_{50} = 0.24) but not the control V2-Fc bind to the RSV F protein in postfusion conformation (Fig. 2A). We also tested the binding of C4-Fc and E4-Fc to the F protein expressed at the surface of RSV infected cells. Flowcytometric analysis revealed that, in contrast to the V2-Fc control, both C4-Fc and E4-Fc can readily bind to the surface of RSV infected cells. (Fig. 2B).

Bivalent VHHs have been shown to neutralize viruses much more potently than their monovalent VHH equivalent (Hultberg et al., 2011). Therefore, we assessed the RSV neutralization activity of bivalent VHH-Fc. Palivizumab (Synagis) was used as positive control. C4-Fc neutralized RSV A2 and RSV A Long strain with EC_{50} of 0.6 nM and 0.14 nM respectively. This is far more potent than what is reported for its monovalent VHH equivalent (640 nM for RSV Long) (Fig. 3A, Supplementary Fig. S2) (Hultberg et al., 2011). Similar to what was reported for its monovalent VHH counterpart, no neutralizing activity could be detected for E4-Fc (Hultberg et al., 2011). Although monovalent C4 VHH was reported to have undetectable levels of neutralizing

activity for RSV subgroup B viruses, C4-Fc could neutralize RSV B ($EC_{50} = 144.7$ nM), yet with much lower activity than for RSV A viruses (Fig. 3B).
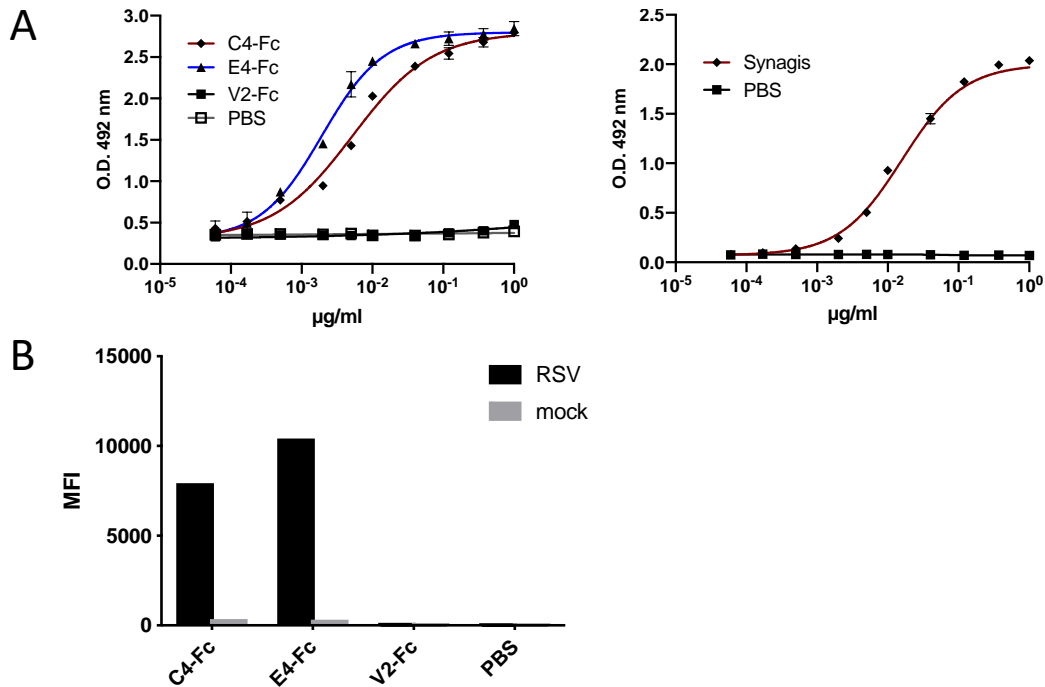

Figure 2 Both C4- and E4-Fc bind to RSV F. (A) RSV F binding ELISA. ELISA plates were coated with recombinant RSV F. VHH-Fc and Synagis were detected with anti-mouse IgG2a and anti-Human IgG, respectively. EC_{50} for C4-Fc = 0.064 nM and E4-Fc = 0.023 nM. **(B)** C4- and E4-Fc bind to RSV F-transfected cells. HEK293T cells, either infected with an RSV A2 or mock-infected were immunostained with VHH-Fc. The graph represents the median fluorescence intensity (MFI) of the GFP-positive cells determined by flow cytometry.

Next to testing the ability of VHH-Fc fusions to bind viral antigen and to neutralize RSV through the VHH, we also investigated the interaction of VHH-Fc fusions to antibody receptors through their Fc fragment. To test this, we investigated the binding of recombinant mouse FcγRI to VHH-Fc fusions or mouse IgG2a that were coated to the bottom of ELISA plates. Figure 4 illustrates that FcγRI can bind to the mouse IgG2a 65 mAb (with an EC_{50} of 8.3 nM which is in line with what has been reported) (Nimmerjahn et al., 2005), but also to the C4-Fc, E4-Fc and V2-Fc fusions proteins, although with a reduced affinity. The different glycosylation of plant-produced VHH-Fc and hybridoma secreted 65 mAb could be the reason for their variable affinity to FcγRI. Together, these data demonstrate that plant produced VHH-Fc are able to interact with their respective antigen and able to interact with Fcγ receptors.
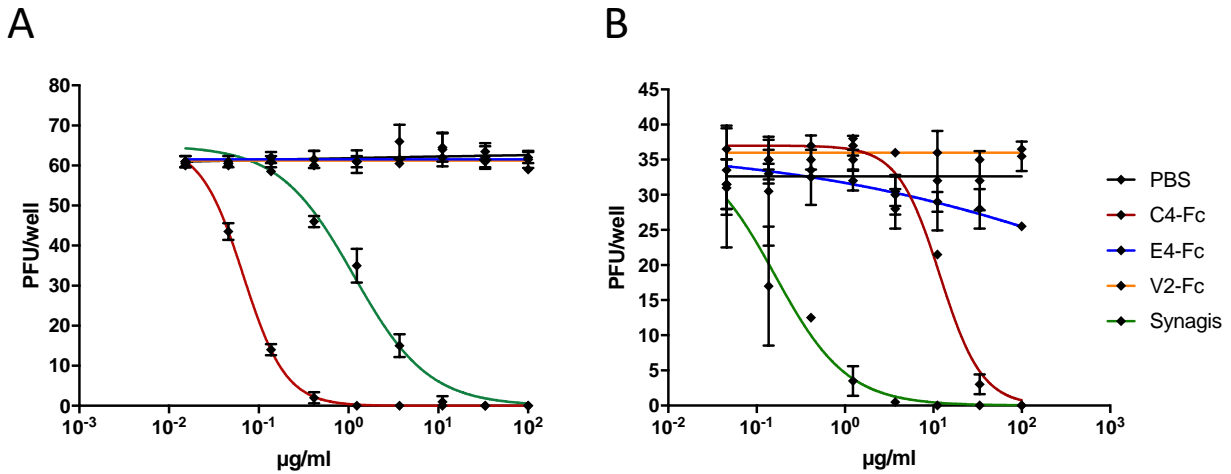
Figure 3 C4-Fc can neutralize RSV A and B strain *in vitro*. A microneutralization assay with (A) RSV A2 (50 pfu/well and (B) RSV B49 (40 pfu/well) strains. The virus was preincubated with a 3-fold dilution series of the antibodies and used to infect Vero cells. Three days later, plaques were stained with anti-RSV polyclonal serum and visualized by adding peroxidase substrate (n=2). (C4-Fc EC_{50} for RSV A2 = 0.82 nM and RSV B49 = 144.76 nM; Synagis EC_{50} for RSV A2 = 7.63 nM and RSV B49 = 1.08 nM).
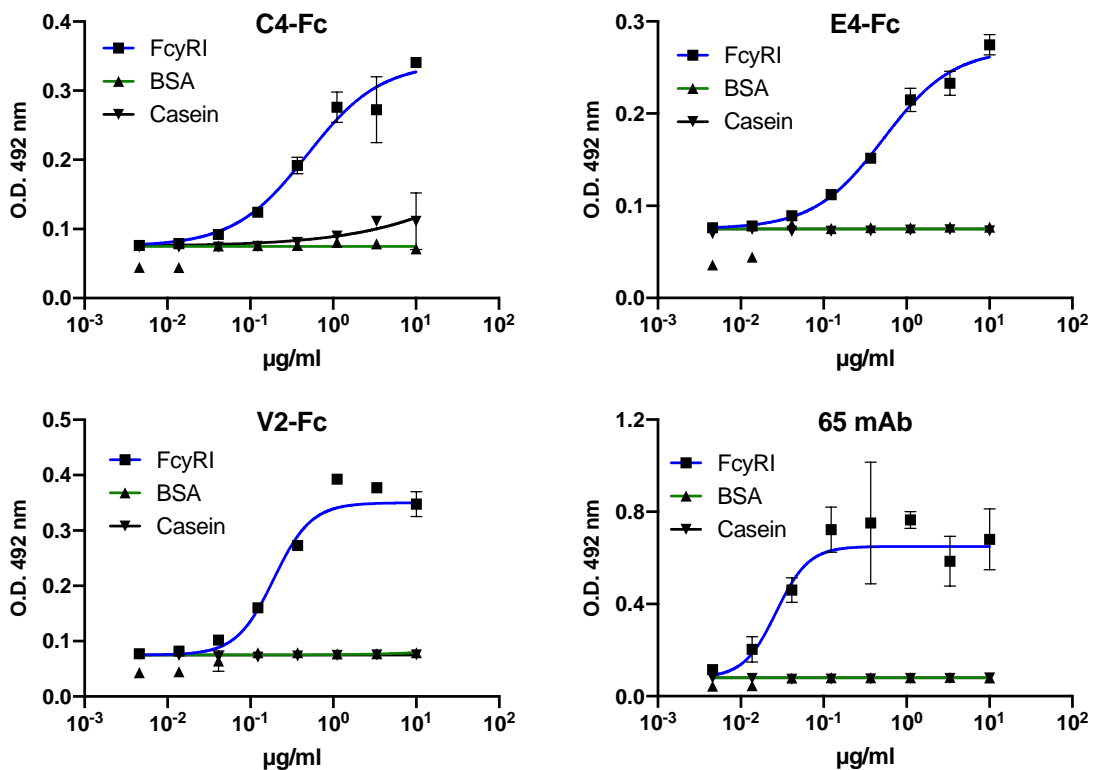
Figure 4. VHH-Fc bind to FcγRI receptor. ELISA plates were coated with VHH-Fc/65 mAb and three-fold dilution series of recombinant FcγRI (Histidine-tagged) was added. ELISA was developed by adding anti-his antibody. Casein and BSA (bovine serum albumin) were used as negative controls. (EC_{50} for C4-Fc – 5.95 nM; E4-Fc – 6.39 nM; V2-Fc – 2.33 nM; 65 mAb – 0.18 nM).

VHH-Fcs can have high thermostability

One major advantage of VHH over conventional antibodies is their high physical and chemical stability. Due to this feature VHHs are amiable for pulmonary delivery via nebulization. This allows quick administration of high amounts of VHH directly to the site of viral replication. To test the physical stability of the VHH-Fc fusions, their thermostability was tested. To this end, the VHH-Fc fusions, conventional mouse IgG2a antibodies targeting the influenza A M2e protein (65 mAb) and the RSV Small hydrophobic protein (3G8 mAb) and a GFP specific VHH (GBP) were heated at different temperatures for 20 minutes and subsequently analyzed for target binding activity by ELISA and compared with unheated samples (Fig. 5A). As expected, both conventional mouse IgG2a antibodies start losing antigen binding activity when incubated at temperatures between 60 and 65°C. Antigen binding of those mouse IgG2a antibodies was completely lost after incubation at 70°C. In sharp contrast, the GBP VHH retained almost full antigen-binding activity after incubation at the highest temperature (90°C). Similar results were also obtained for other VHHs (data not shown). E4-Fc and V2-Fc appeared to be remarkably stable and exhibited significant antigen binding activity after incubation at 90°C. Conversely, C4-Fc was less thermostable showing major loss in antigen binding after 75°C incubation. These data illustrate that depending on the VHH, the physical stability of VHH-Fc fusions can be remarkably high (Fig. 5A).

To better understand the differences in heat resistance among the VHH-Fc fusions and conventional mouse IgG2a antibodies, we analyzed heat induced protein unfolding and aggregation. Heat induced protein unfolding was examined by a SYPRO Orange thermal shift assay. This analysis revealed that the high thermostability of the E4-Fc and V2-Fc as compared to C4-Fc and mouse IgG2a antibodies is not associated with higher melting temperatures (Fig. 5B). To investigate protein aggregation, protein samples were incubated at either room temperature or at 70°C for 30 minutes and subsequently analyzed by size exclusion chromatography. As expected, the conventional mouse IgG2a antibodies and VHH-IgG2a fusions that were incubated at room temperature eluted at the expected volumes. Incubation of the 65 mAb and 3G8 mAb (conventional mouse IgG2a antibodies) and the heat sensitive C4-Fc fusion at 70°C resulted in the formation in aggregates that eluted at an earlier volume. In contrast, the E4-Fc and V2-Fc

fusions that retained strong antigen binding activity after heat treatment did not form aggregates when incubated at 70°C (Supplementary Fig. S3).
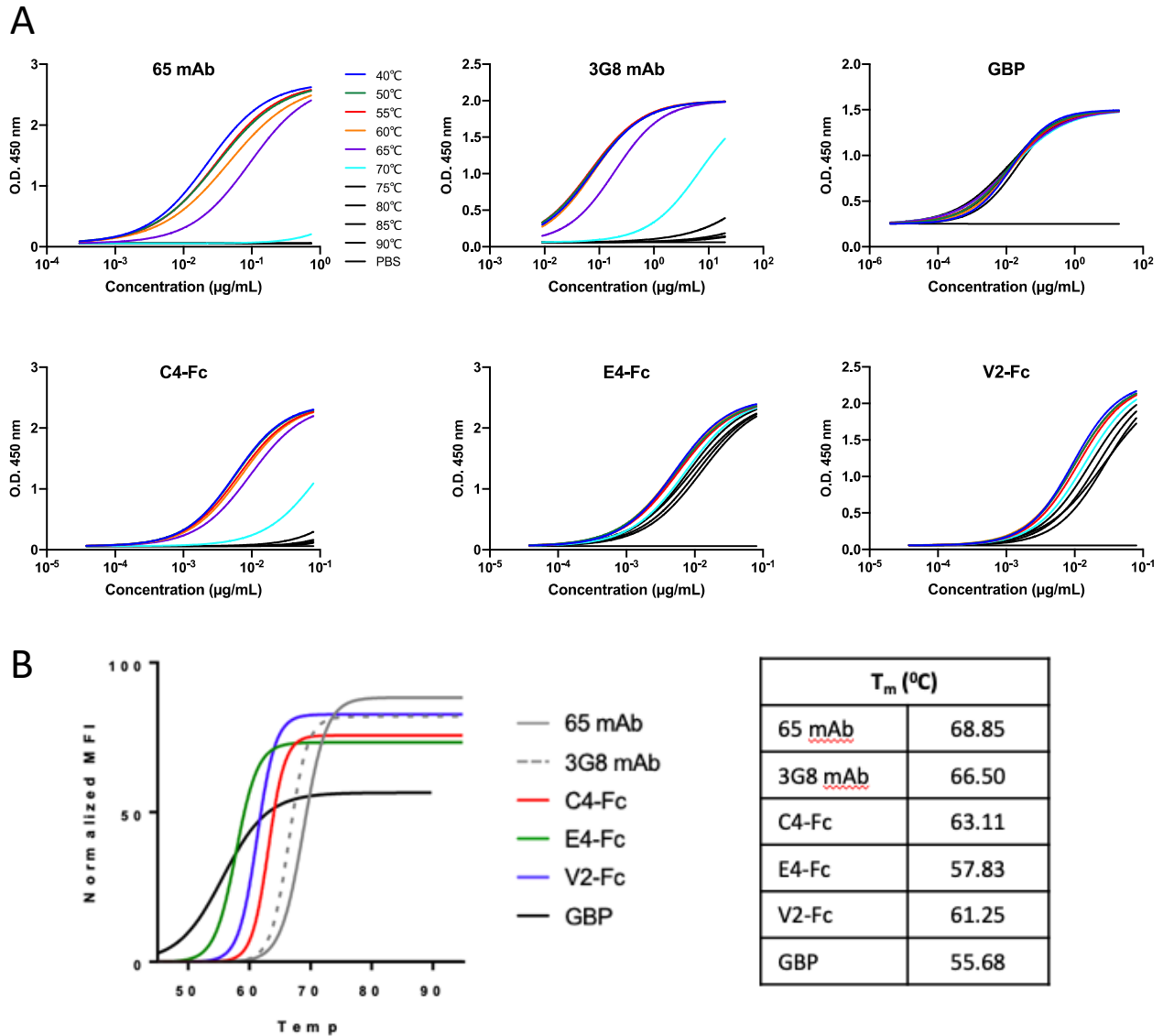
Figure 5 VHH-Fc are stable than conventional antibodies at elevated temperature. (A) Binding ELISA after thermal denaturation of antibodies. The antibodies were heated at indicated temperatures and binding activity was analyzed in target binding ELISA. GBP (GFP-binding protein) is a monomeric VHH. 65 mAb and 3G8 are conventional IgG2a. **(B)** Thermofluor assay. The graph shows the melting curve of VHH-Fcs (C4-Fc, E4-Fc and V2-Fc), GBP and conventional IgG2a (65 mAb and 3G8 mAb).

Prophylactic treatment with VHH-Fc protects mice from RSV infection

We next examined the potential of VHH-Fcs to prevent RSV replication *in vivo*. BALB/c mice were challenged with one million PFU of RSV A2 inoculation 4 hours after intranasal administration of the VHH-Fc fusions. Synagis and PBS were respectively used as positive and an additional negative control. Five days after RSV challenge, broncho-alveolar lavage fluid (BALF) and the lungs were collected to determine the level of pulmonary viral replication by plaque assay (Fig. 6A, Supplementary Fig. S4A). Prophylactic treatment with control V2-Fc did not impact RSV lung replication as compared to PBS treatment. In contrast, treatment with Synagis or the RSV neutralizing C4-Fc fusion strongly reduced lung viral replication to undetectable levels in the majority of infected mice. Remarkably, also the non-neutralizing RSV F specific E4-Fc fusion was able to control RSV replication in mice, albeit to lower extent as compared to C4-Fc. As residual VHH-Fc and Synagis could be detected in the BALF, we cannot exclude that these might interfere with the virus titration of the prepared lung homogenates (Supplementary Fig. S4C). Therefore, viral replication in the lungs was also analyzed via RT-qPCR. In agreement with the levels of live replication virus, the lungs of mice treated with C4-Fc and E4-Fc respectively have strongly and moderately reduced levels of RSV RNA (Fig. 6B, Supplementary Fig. S4B). For further validation of the protective effect of C4-Fc, RNA level of inflammation markers associated with RSV-infection was quantified by RT-qPCR and compared with the negative control group V2-Fc. The mRNA levels of IFNγ, IL-6, RANTES, MIP-1α and IFIT2 were significantly lower for C4-Fc treated group compared with V2-Fc treated control groups (Fig. 7 and Supplementary Fig. S5). These data demonstrate that prophylactic treatment with C4-Fc can strongly control RSV infection and associated inflammatory responses in mice.
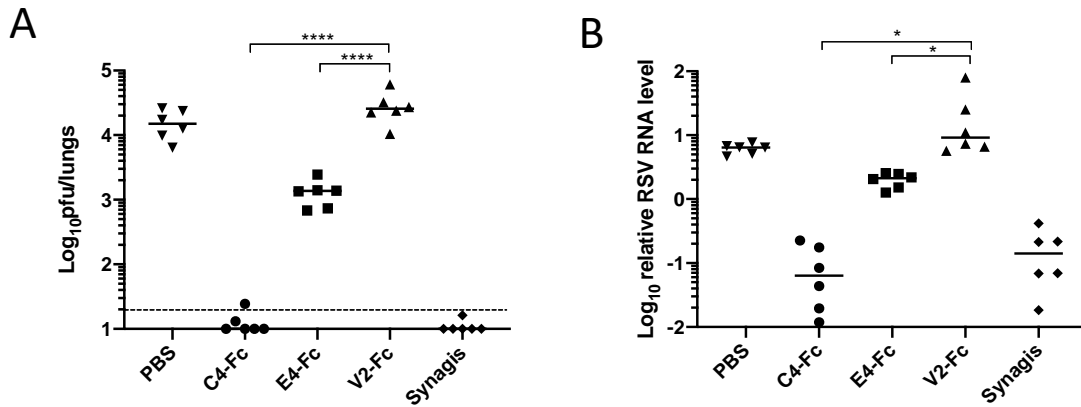
Figure 6. C4- and E4-Fc protect mice against RSV infection. BALB/c mice were treated intranasally with VHH-Fc/Synagis (dose= 20 µg/50 µl) four hours before the infection with RSV A2 (10^6 pfu). Five days later, lungs were harvested. RSV virus titer and RNA level were determined by plaque assay (A), and quantitative RT-PCR (B). Dashed line represents the detection limit (20 pfu). (**** ($P<0.0001$), * ($P<0.05$); one-way ANOVA) (n=6).
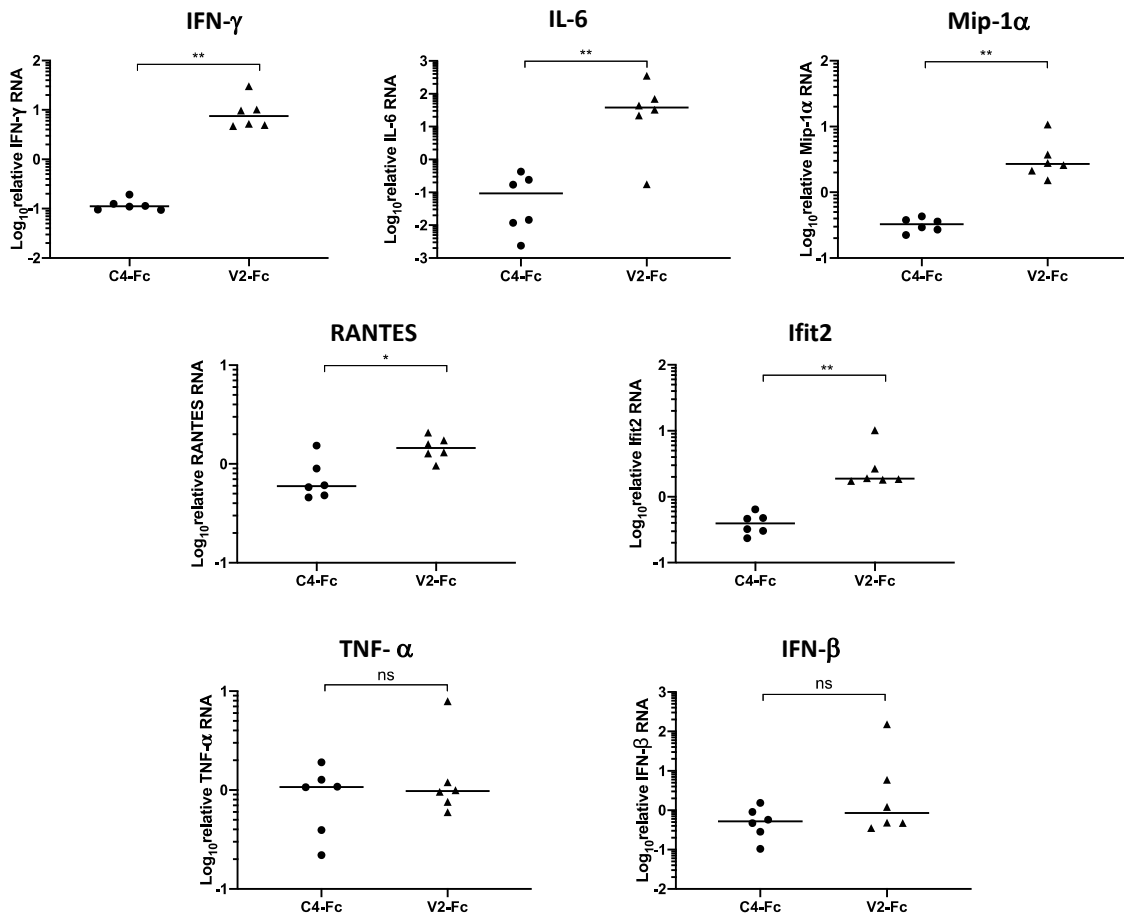

Figure 7. C4-Fc inhibits the expression of proinflammatory cytokines. BALB/c mice were treated intranasally with VHH-Fc/Synagis (dose= 20 µg/50 µl), four hours before the infection with RSV A2 (10^6 pfu). Five days later, RNA level of inflammatory cytokines in harvested lungs was quantified by RT-PCR. (n=6, ** ($P≤0.01$), * ($P=0.015$), ns= not significant; Mann-Whitney).

Fc domain contributes to prolongation of the lung retention time of the nanobody

One of the important aspects of successful IgG-based therapeutics is their remarkable longer serum half-life through the interaction of Fc domain with neonatal Fc receptor (FcRn). FcRn-mediated recycling and transcytosis of an antibody significantly contribute to the increased serum persistence (Challa et al., 2014). Moreover, FcRn also acts as a salvage receptor that rescues IgG from the default degradation pathway (see ref. Pyzik et al., 2015). VHH, due to its shorter half-life, is rapidly cleared from the circulation and has a very limited therapeutic value. Therefore, we evaluated whether plant-produced VHH-Fcs have this added advantage of the Fc domain. To this end, a mixture of one monovalent VHH (Nb-71 directed against RSV F), two VHH-Fcs (C4-Fc and V2-Fc), and conventional IgG2a (65 mAb) was administered intranasally to BALB/c mice. Thirty minutes, 24 and 48 hours after administration of the antibody mixture, BAL fluid was collected and analyzed by western blotting and ELISA. Western blot analysis revealed that the VHHs could by readily detected in the BALF samples collected 30 minutes after administration. In contrast, much lower and undetectable levels of VHH could be detected in the BALF samples collected 24 and 48 hours after administration, respectively (Fig. 8A, left panel). Due to the presence of endogenous mouse IgG2a antibodies in the BALF samples, detection of the administered 65 mAb was not possible (Fig. 8A, right panel). As the VHH-Fcs lack the CH1 domain they can be specifically detected in the BALF samples by anti-mouse IgG2a antibody staining. In contrast to the VHH, VHH-Fc fusions could still be detected in the BALF samples collected 48 hours after administration at moderately reduced levels as compared to those in the BALF samples collected 30 minutes and 24 hours after administration (Fig. 8A right panel). Whereas, VHH-Fcs and mAb 65 were clearly detectable at 48 hours after administration as 42 kDa and 50 kDa band, respectively. A band representing the cleaved Fc domain can also be detected as observed previously (Fig. 1). These data indicate that, compared to VHHs, VHH-Fc fusion have a substantially longer lung retention time.

To examine the lung retention time of the VHHs and VHH-Fcs in a more quantitative way, the BALF was analyzed by ELISA using their respective antigens. Each antibody (VHH/VHH-Fc/IgG2a) present in the BAL fluid either recognizes different antigen or can specifically be detected by either an anti-HIS-TAG antibody or an anti-IgG2a antibody. An equivalent amount of

the antibody mixture was used for the administration and individual antibodies were used as controls. At 30 minutes after administration, all samples showed levels of VHHs, VHH-Fcs and antibodies comparable to the equivalent administrated antibody mixture, indicating that the vast majority of administrated antibody (fragments) could be collected by bronchoalveolar lavage. In agreement with the western blot analysis, the levels of Nb-71 were substantially lower and undetectable in the BALF samples collected 24 and 48 hours after administration, respectively. In sharp contrast, the levels of both C4-Fc and V2-Fc decreased at much slower pace (Fig. 8C and D). Twenty-four hours after administration, 9.4% and 13.9% of C4-Fc and V2-Fc could still be detected in the BALF. These levels dropped to 2.4% and 2.8% at forty-eight hours after administration, respectively. Such a non-linear decrease was also observed for full-length IgG2a (65 mAb). The levels of 65 mAb in the BALF dropped to about 25% after 24 hours but to about 20% at 48 hours after administration (Fig. 8C and D). These data suggest that the Fc domain might have a significant contribution to prolong lung retention time of the VHH-Fc fusions. Moreover, VHH-Fcs could be detected in the BALF of RSV infected mice up to 5 days after administration (Supplementary Fig. S4C).
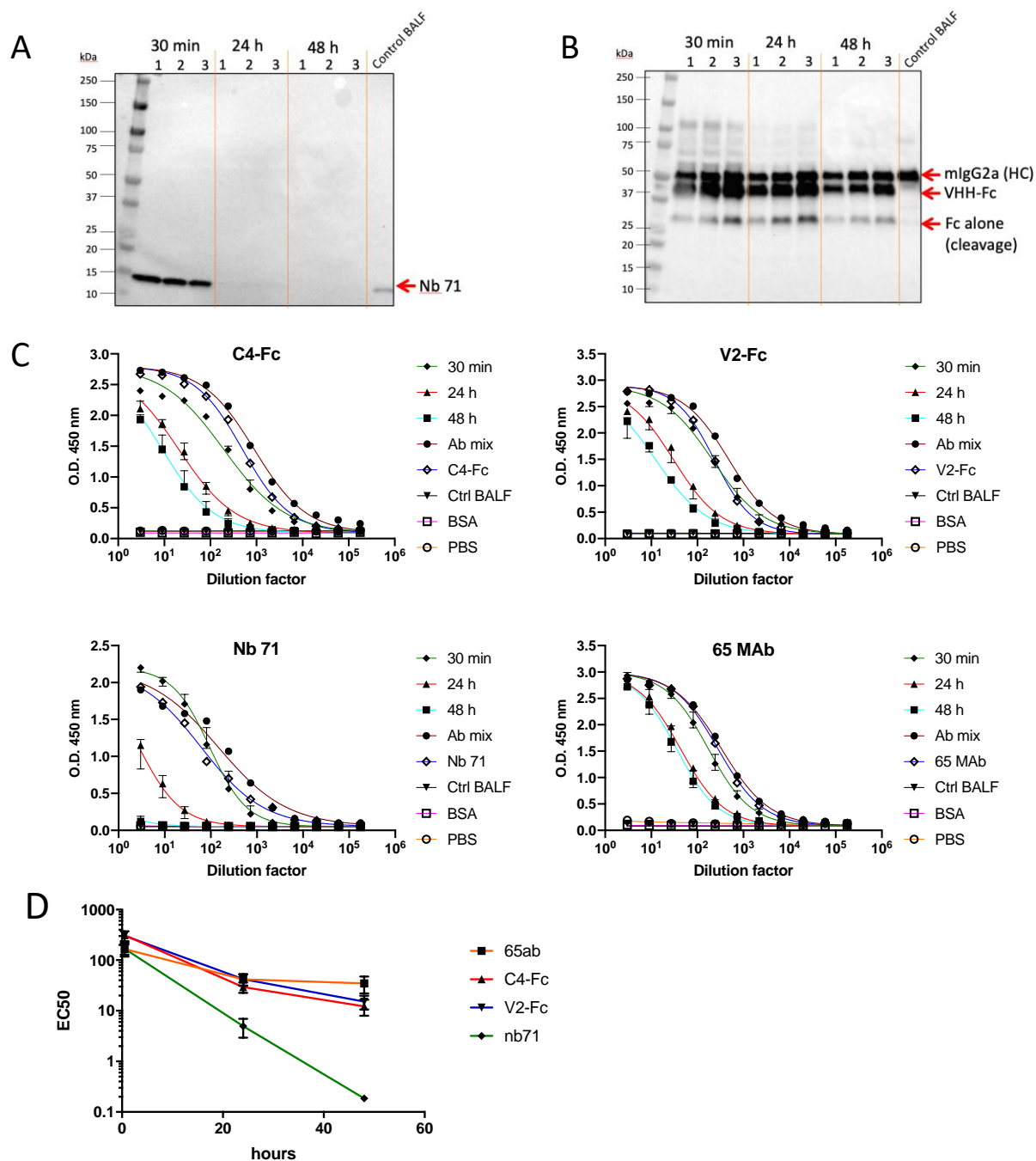
Figure 8. Fc domain increases lung retention time of the VHH. Three BALB/c mice received a mixture of four antibodies- 10 µg of VHH-Fc (C4-Fc and V2-Fc), 10 µg of VHH (Nb-71) and 10 µg conventional mouse IgG2a (65 mAb), intranasally. The BAL fluid was collected at indicated time points and analyzed in western blotting using anti-his tag antibody to detect VHH (Nb-71) (A) and anti-mouse IgG2a to detect C4-Fc, V2-Fc and 65 mAb (B). (C) The BAL fluid was also analyzed in target binding ELISA. Nb 71 was detected using anti-camelid antibody and other antibodies (C4-Fc, V2-Fc and 65 mAb) were detected using anti-mouse IgG2a. (D) EC$_{50}$ graph derived from the binding ELISA. EC$_{50}$ values for each curve in binding ELISA was calculated and a graph was plotted between EC$_{50}$ of the dilution factor and relative EC$_{50}$ values.

Discussion

VHH-based antiviral agents are of interest because of their merits over conventional antibodies including small size, facile genetic manipulation, cost-effective production and high physicochemical stability. However, their small size often leads to rapid clearance from the circulation. Thus, VHHs as such fail to provide lasting immunity and may not be suitable for therapeutic use. One possibility to increase the half-life of VHH is to fuse them to a serum albumin binding VHH. Alternatively, VHH can be fused to an Fc fragment. We have developed fusions of VHHs with Fc tail of murine IgG2a. These fusions assembled as bivalent moieties in plant expression system and exhibited *in vitro* RSV neutralization several folds better than what is reported for its monovalent VHH equivalent (Hultberg et al., 2011). This substantially increased potency is in line with the previous reports displaying better neutralization activity of bi- or multivalent VHHs (Detalle et al., 2016; Hultberg et al., 2011). We addressed the use of plant expression system for production of VHH-Fc fusions. To date, mammalian expression systems are the gold standard for the production of therapeutic antibodies. However, due to their high production cost, efforts are being made to evaluate alternative production system such as yeast, fungi, insect cells or plants, each having their own merits for development of immunoglobulin-like molecules (De Meyer et al., 2015; Schirrmann et al., 2008). Plant systems not only provide proper folding, assembly and precise glycosylation; but also offer several advantages such as low production cost and high scalability (Paul and Ma, 2011). However, only limited information is available about the actual production cost of biopharmaceuticals at industrial scale. Buyel et al. (2017) revealed that the cost of plant-produced mAbs can be as low as €100 g^{-1}, as compared to €200 g^{-1} for mAbs produced in CHO cells (Lim et al., 2010). It is important to note that the initial investment capital for the production facility and downstream processing cost of plant-derived products could be similar to that of other production systems. However, simple cultivation of an intact plant as compared to the expensive sterile environment for cell suspension cultures substantially reduce the overall operating costs of plant-based pharmaceuticals. Currently, several plant-based pharmaceuticals such as ZMApp against Ebola virus (NCT03719586) and HAI-

05 vaccine against H5N1 (NCT01250795) are being investigated under clinical trials (https://clinicaltrials.gov, Yao et al., 2015).

Immunogenicity against plant-specific glycans such as β-1,2-xylose and core α-1,3-fucose raises concerns about the safety of plant-derived products (Bardor et al., 2003; Jin et al., 2008; Landry et al., 2010). These complex glycans are modified in the Golgi apparatus that differ from the mammalian glycosylation. Since initial glycosylation in the ER is conserved in all eukaryotic cells, we added a C-terminal KDEL tag (ER retention motif) to the VHH-Fc to prevent plant specific glycosylation. Albeit, despite having a KDEL tag, there are a few studies reporting the presence of Golgi-specific glycosylation in plant-produced antibodies (De Meyer and Depicker, 2014; De Meyer et al., 2015). Another solution could be to use GlycoDelete plants to produce nonimmunogenic glycoforms by modifying the *N*-glycosylation pathway as described for *Arabidopsis thaliana* (Piron et al., 2015). Moreover, supporting evidence explaining the immunogenicity of plant-specific glycans in human are limited or conflicting (Rup et al., 2017; Shaaltiel and Tekoah, 2016; Wang et al., 2017). Nevertheless, plant-derived biotherapeutics deserve evaluation with more number of samples to make a definitive conclusion concerning the immunogenicity risk of plant-derived glycans.

A major advantage of VHHs to treat respiratory infections is their high physical stability that allows direct delivery to the site of viral replication, the lumen of the lungs by nebulization (Detalle et al., 2016; Van den Hoecke et al., 2017). To test if nebulization could also be an option for VHH-Fc proteins, we tested their physical stability. In the present study, we demonstrate that next to VHHs, also two of the tested VHH-Fc fusions can retain full antigen binding activity after 90°C heat treatment. In contrast, antigen binding of conventional IgG2a antibodies was almost completely lost after 70°C heat treatment. Whether high thermal stability is a general feature of VHH-Fcs or only occurs rarely needs to be determined in a more extensive study including multiple VHH-Fc fusions based on Fc fragments originating from different IgG subclasses. Although the high thermal stability of VHHs and VHH-Fc fusions was not associated with higher melting temperatures; it was rather associated with resistance to heat induced protein aggregation. In mouse and human antibodies, the CH2 domain is the first domain to unfold upon heating (Yang et al., 2017). As those domains are present in both conventional IgG2a and VHH-

Fc fusions, it is no surprise that both start to unfold at similar temperatures. The heat resistance of VHH-Fc fusions indicates that in contrast to conventional IgG2a, VHH-Fcs are able to refold into functional proteins after heat treatment. In conventional antibodies, the VH and VL interact via a hydrophobic interface created by hydrophobic amino acid patches on the VH and VL surface. As aggregation of globular proteins typically results from interactions between hydrophobic amino acids that normally reside in the protein core but are exposed during denaturation, hydrophobic amino acids on the VH antibody fragment might contribute to IgG aggregation (Vermeer et al., 2000). The hydrophobic amino acids involved in the VH/VL interface of conventional IgG are typically substituted for hydrophilic amino acids in VHHs (Hamers-Casterman et al., 1993). Thus, the absence of a hydrophobic patch on the surface of VHHs might contribute to the thermal stability of VHHs observed by us and others (Ewert et al., 2002; Perez et al., 2001; van der Linden et al., 1999). Remarkably, the thermal stability of isolated human VH antibody fragments could be considerably improved by replacing the hydrophobic amino acids that would interact with the VL domain by the corresponding hydrophilic amino acids present in VHHs (Davies and Riechmann, 1994). As such, the ability of some of the VHH-Fc fusions to retain antigen binding capacity and resist aggregation upon heat treatment might be partially attributed to their lack of a hydrophobic VH/VL interface of conventional IgGs. In addition, the absence of the CH1 domain and their dimeric instead of tetrameric nature might also contribute to the thermostability of VHH-Fc fusions. As antibody aggregation does not only impair antibody function but can also provoke immune responses, the physical stability of antibodies or antibody fragments is an important benchmark for therapeutic application (Bodier-Montagutelli et al., 2018). Although substantial efforts have been made to engineer IgG with improved thermal stability with minimal effect on target binding (McConnell et al., 2014), VHH-Fc fusions might be more suited due to easy engineering and production and their potentially higher intrinsic stability.

To examine if RSV neutralizing VHH-Fcs could be useful as immunoprophylaxis for RSV, we investigated if treatment of mice with neutralizing VHH-Fcs could protect mice against infection. In a prophylactic setting, C4-Fc (RSV neutralizing VHH), could abolish the RSV replication in the lungs as measured by both PFU assay and qPCR. Interestingly, also the non-

neutralizing, E4-Fc could control RSV replication in the lungs but to a lesser extent than the neutralizing C4-Fc. This indicates that next to direct viral neutralization, also Fc effector functions might be of importance. Non-neutralizing antibodies have been previously shown to confer protection against viral infections due to the Fc-dependent effector function such as ADCC (antibody dependent cell-mediated cytotoxicity), and CDC (complement dependent cytotoxicity) (Bootz et al., 2017; Carragher et al., 2008; Dunand et al., 2016; Hessell et al., 2007). Likewise, VHH engineered with a conventional Fc domain can protect mice against influenza infection even if the detectable influenza virus neuraminidase (NA)-inhibitory activity is absent (Cardoso et al., 2014). However, it needs further testing to investigate to which extent plant-produced VHH-Fcs designed to circumvent fucosylation, can interact with various Fc receptors and mediate Fc effector functions. In addition, VHH formatting as IgA fusions can be of further consideration to give significant protection at the pulmonary mucosa and broaden their application as a mucosal passive immunotherapeutic (Paul et al., 2014; Virdi et al., 2013).

A major disadvantage of antibody therapy for pulmonary diseases is that only a very small fraction (0.2%) of systemically administered antibody reaches the lumen of the lung (Dall'Acqua et al., 2006; Hart et al., 2001; Van Heeke et al., 2017). As such, it is no surprise that direct pulmonary delivery of RSV neutralizing antibodies is about 160 times more efficient than systemic administration (Crowe et al., 1994; Prince et al., 1987). However, the physical stress associated with nebulization can induce aggregation of antibodies (Maillet et al., 2008; Vermeer and Norde, 2000). Due to their high stability, VHHs are suited for pulmonary delivery by nebulization (Van Heeke et al., 2017). Unfortunately, the respiratory tract is highly permeable to small sized proteins resulting in fast absorption into circulation (Folkesson et al., 1990). Consequently, due to their small size, inhaled VHHs need to be re-administered frequently to attain therapeutic levels in the lung lumen (Mora et al., 2018; Van Heeke et al., 2017). We compared the lung retention of VHHs, conventional mouse IgG2a antibodies and mouse IgG2a based VHH-Fcs. Whereas VHHs were cleared very rapidly, about 2-3 % of the VHH-Fcs and about 20% of the conventional IgG2a antibodies was retained in lungs at 2 days after administration. For both VHH-Fcs and conventional antibodies, an initial phase of more rapid clearance was followed by a phase of much slower clearance. A similar biphasic pattern was also recently observed in a study by

(Guillon et al., 2019) who monitored the level of inhaled antibodies in the lungs of non-human primates by continuous sampling through lung microdialysis (Guillon et al., 2019). Whereas during the first 33 hours, the inhaled antibody was cleared in a linear mode, the antibody levels remained more or less stable thereafter. Multiple factors can contribute to the clearance of proteins from the lung lumen including passive diffusion of especially small-sized proteins through the tight junctions of the type I alveolar cells, mucociliary clearance, pulmonary proteases and uptake by lung epithelial cells and macrophages (Agu et al., 2001). Likely the longer lung retention time of VHH-Fcs compared to VHHs might be mainly attributed to their considerably bigger size. Whereas up to 50% of the inhaled small proteins like insulin can be absorbed into blood circulation via passive diffusion, larger inhaled proteins (e.g. IgG and serum albumin) remain retained in the lungs for longer period (Patton et al., 2004). Next to size, also the Fc fragment can impact lung retention. Through interaction with the FcRn, Fc fusions can be actively transported from the lung lumen to the circulation via transcytosis (Bitonti et al., 2004). Although IgGs and Fc fusions can also migrate from circulation to the lung lumen, FcRn-mediated transcytosis does not play a major role in this process (Dall'Acqua et al., 2006). In addition, through interaction with FcRn, IgG (and Fc fusion proteins) that have been taken up by lung cells can also recycled from the endosomes back to the lumen of the lung (Guilleminault et al., 2014). However, as we do not know the degree of interaction of plant-produced VHH-Fcs to FcRn; it remains unknown to which extent FcRn can contribute to transcytosis and recycling of VHH-Fc from and back to the lung lumen.

In conclusion, we demonstrate the advantages of VHH-Fc fusions and a solution to the limitations associated with VHH-based therapeutics. Thermostability of these fusions is comparable to VHH, with few exceptions. These VHH-Fc fusions provide better protection both *in vitro* and *in vivo* and hold great promise in therapeutic development due to their longer lung retention time, therefore it is worthwhile to test them in a therapeutic setting. We hope these results can make a significant impact on the new emerging era of VHH-based drug development.

Material and Methods

Construction of the expression plasmid harboring VHH-Fc coding sequence

The plant expression vector was created by taking advantage of seamless assembly offered by GoldenBraid2.0 cloning system as described previously (Sarrion-Perdigones et al., 2011) (Figure S6). Briefly, the DNA sequences corresponding to the fragment crystallizable (Fc) domain of mouse IgG2a (Hinge-CH2-CH3; NCBI accession number KC295246.1), VHH C4 and E4 were synthesized by Gen9 (Ginkgo Bioworks). VHH V2 coding sequence was obtained from the previously cloned vector in our laboratory (Virdi et al., 2013). The N-terminal 2S2 plant signal peptide (Krebbers et al., 1988) and C-terminal KDEL sequence were added to the coding sequences of VHH and Fc, respectively. The VHH-Fc fusions were cloned under the control of constitutive 35S promoter of cauliflower mosaic virus (CaMV-35S) and Nopaline synthase terminator (Tnos). First, all the GB parts including VHH, Fc domain, 35S promoter and Tnos terminator were cloned separately in the domesticator vector (pUPD) and then assembled into the destination vector (pDGBα2). To achieve high accumulation level, the resulting transcriptional unit was subsequently fused to the silencing suppressor p19 cloned in another vector pDGBα1 (Sarrion-Perdigones et al., 2011). In this way, we obtained the final plant expression vector pDGBΩ2 harboring VHH-Fc fusion. DH5α cells were transformed with the expression plasmid (Meselson and Yuan, 1968) and transformants were screened on the media supplemented with spectinomycin selection. The plasmids were isolated using GeneJET plasmid miniprep kit (ThermoFisher- K0502) to confirm the recombinants by restriction analysis and sequencing. Finally, the expression vectors were transformed into heat shock competent *A. tumefaciens* cells (strain – LBA4404) for production in the plant expression system (Hoekema et al., 1983).

Expression of VHH-Fc in Nicotiana benthamiana

A. tumefaciens cells bearing expression vector were infiltrated in *N. benthamiana* leaves as previously described (De Buck et al., 2012; Juarez et al., 2013). Briefly, overnight grown bacterial culture in YEB medium were sedimented and pellet was resuspended in the certain volume of

agroinfiltration buffer (10 mM MES pH 5.6, 10 mM MgCl$_2$, and 200 mM acetosyringone) needed to obtain an optical density of 0.2 at 600 nm, followed by gentle shaking for 2 hours at room temperature. The resulting suspension was used to infiltrate the abaxial surface of the young leaves of 4-5-weeks old *N. benthamiana* plants. The leaves were harvested 5 days post infiltration and extracts were prepared to obtain total soluble protein in a ratio of 1:3 (w/v) in Dulbecco's phosphate buffered saline (DPBS, Lonza- 17-512F) supplemented with cOmplete protease inhibitor cocktail (Sigma-Aldrich- 11697498001). After centrifugation, the clarified extract was immediately used to examine for transgene expression via SDS-PAGE and ELISA.

Purification of VHH-Fc from crude leaf extract

The extracts from about 100 g of infiltrated leaves were prepared as described above and filtered through a 0.22 µm membrane filter (Steritop, Millipore- SCGPT01RE). The cleared leaf extract then loaded on a pre-equilibrated HiTrap MabSelect SuRe protein A column (GE Healthcare- 11003493), connected to the AKTAexplorer purification system (GE Healthcare). All purification steps were performed at 4^{0}C. The extraction buffer (DPBS) was used for equilibration and washing steps, and bound antibodies were eluted with 1 M arginine, pH 2.7 that was immediately neutralized with 1 M Tris, pH 9. Elution fractions containing antibodies were pooled and subjected to size exclusion chromatography (HiLoad 16/600 Superdex 200 column, GE healthcare- 28989335) in DPBS. The relevant fractions containing monomeric VHH-Fc were pooled and concentrated by dialyzing against 20% polyethylene glycol in DPBS. The protein concentration was determined by OD$_{280}$ measurement. The purified antibodies were aliquoted and stored at -80℃ until further use.

SDS-PAGE and immunoblotting

Transiently expressed VHH-Fc fusions (10 µl of crude leaf extract or 1 µg of purified) were analyzed on 4-20% precast protein gels (Bio-Rad- 4561096). Samples were prepared in NuPAGE LDS Sample buffer (ThermoFisher- NP0008) with or without reducing agent (ThermoFisher- NP0009). The proteins were visualized by Coomassie brilliant blue staining. For immunoblotting, the proteins were blotted onto a polyvinylidene difluoride membrane (Bio-Rad- 1704156) using

the semidry transfer method (Bio-Rad). The membrane was subsequently blocked for one hour with 5% (w/v) of skimmed milk in PBS containing 0.05% Tween-20 (PBST) and probed with 1/2000 diluted HRP-conjugated anti-mouse IgG2a (SouthernBiotech- 1080-05). The membrane was then washed three times with PBST, and bands were visualized by adding WesternBright ECL HRP substrate (Advansta- K-12045-D20). All incubation steps were performed at room temperature on an orbital shaker.

RSV F binding ELISA

96-well ELISA plates (Nunc Maxisorb- 44-2404-21) were coated overnight at 4°C with 20 ng of RSV F prepared in PBS. All sequential ELISA steps were followed by three washing steps in PBST and one-hour incubation at room temperature. The wells were then blocked with freshly prepared 5 % (w/v) skimmed-milk in PBST and incubated with three-fold dilution series of purified VHH-Fc prepared in 2.5% (w/v) skimmed milk with PBST. After washing, the bound VHH-Fcs were detected with 1/4000 diluted HRP-conjugated anti-mouse IgG2a and the reaction was finally revealed at 492 or 450 nm after adding HRP substrate (SIGMA*FAST*™ OPD tablets, Sigma-Aldrich- P9187 or TMB- BD Biosciences, 555214), respectively.

SYPRO Orange thermal shift assay

To assess the stability of the different antibodies and antibody formats, a fluoroshift assay was performed. Briefly, 12.5 µl reaction mixtures were prepared containing either PBS or 0.1 µg/µl of the antibodies or antibody formats in HEPES-buffered saline (HBS, 20 mM HEPES pH 7 and 150 mM NaCl) and 10X SYPRO Orange dye (Life Technologies). Dye uptake by unfolding protein was followed in a Roche LightCycler 480 qPCR machine over a temperature gradient from 20°C to 98°C. For analysis the background fluorescence (PBS sample) was subtracted from recorded sample fluorescence intensity. Boltzman sigmoidal non-linear curve fitting was used to calculate the V50 melting temperature Tm (°C).

Aggregation analysis

To test resistance of heat induced aggregation, the antibodies and antibody fragments (10 μg / 50 μl) were either incubated at room temperature or heated at 70°C for 20 minutes and allowed to cool down to room temperature. The samples were analyzed by analytic size exclusion chromatography using an agilent Bio SEC-3 (3um) column on which 670, 158, 44, 17 and 1.3 kDa biorad gel filtration standard proteins elute at respectively 5.4, 5.9, 6.7, 7.8 and 10.8 minutes.

Thermal stability test

To test the thermal stability, VHH-Fc fusions (at a concentration of 20 μg/ml) were incubated at indicated temperatures for 20 minutes. Conventional VHH and antibodies were included for the comparison. Antibodies were subsequently centrifuged at 400 g for 1 minute and cooled down to room temperature. The impact of high temperature was assessed as the residual target-binding activity of the antibody in ELISA. The antigen was GFP-Fc (GFP conjugated to Fc tail of porcine IgG3) for GBP (VHH against GFP) and GBP-Fc (GBP fused with Fc tail of murine IgG3 (De Meyer et al., 2015)), M2e (Van den Hoecke et al., 2017) and SHe (Schepens et al., 2014) peptides for mAb 65 (Kolpe et al., 2018; Van den Hoecke et al., 2017) and 3G8 (Kolpe et al., 2018) (conventional murine IgG2a), respectively and RSV F for Synagis (conventional human IgG1). Bound VHHs were detected with 1/3000 mouse anti-His antibodies (AbD Serotec), followed by 1/5000 anti-mouse IgG conjugated to HRP. VHH-Fc (fused to murine IgG2a) and conventional murine IgG2a were detected in the single step with 1/4000 HRP-conjugated anti-mouse IgG2a, and GBP-Fc was detected with 1/4000 HRP-conjugated anti-mouse IgG3. Synagis was detected by HRP conjugated anti-Human IgG (1/5000).

Cells and viruses

HEp-2 cells (ATCC, CCL-23), Vero cells (ATCC, CCL-81), and HEK-293 T cells (a gift from Dr M. Hall, University of Birmingham, Birmingham, UK) were cultured in Dulbecco's modified Eagle medium (DMEM) supplemented with 10% heat-inactivated fetal calf serum (FCS), 2 mM L-glutamine, non-essential amino acids (Invitrogen, Carlsbad, CA, USA) and 1mM sodium pyruvate at 37⁰C in the presence of 5% carbon dioxide. RSV A2, an A subtype of RSV (ATCC, VR-1540, Rockville), RSV B49, a B subtype of RSV (BE/5649/08 clinical strain – source described in (Tan et al., 2013), obtained

from Prof. Marc Van Ranst, KU Leuven, Leuven, Belgium), and RSV A Long (ATCC, VR-26, kind gift from Dr. Rik De Swart, Erasmus MC, Rotterdam, The Netherlands) were propagated in HEp-2 cells and quantified on Vero cells by plaque assay using goat anti-RSV serum (Chemicon International-AB1128).

Plaque-reduction assay

HEp-2 or vero cells were seeded at a density of 10^4 cells per well into 96-well plates in DMEM (Gibco) supplemented with 10% FCS, antibiotics (penicillin-streptomycin), 2 mM L-glutamine, 1 mM sodium pyruvate and non-essential amino acids, and incubated for 48 h at 37°C in a 5% CO_2 incubator. A three-fold dilution series of purified VHH-Fc fusions were incubated with RSV in a total volume of 50 µl Opti-MEM (Gibco) for 1 h at 37°C. Synagis® mAb was included as a positive control. The premix was used to infect confluent HEp-2 or vero cells. After 3 h of incubation at 37⁰C, equal volumes of 1.2 % Avicel (FMC Biopolymers- RC 581) in DMEM medium containing 2% FCS, 2mM L-glutamine, non-essential amino acids and 1mM sodium pyruvate was added to each well and infection was allowed to continue for 3 days at 37°C in a CO_2 incubator. The cells were then fixed with 2% paraformaldehyde and viral infection was tested by immunostaining of the viral plaques. Fixed HEp-2 cells were blocked with 4% skimmed milk solution in PBS for 1 hour at RT, incubated for 1 h with goat anti-RSV serum (Chemicon International- AB1128) and HRP-conjugated anti-goat antibody (Santa Cruz Biotechnology- sc-2354). The plaques were visualized by applying the TrueBlue peroxidase substrate (KPL- 5510-0030) and counted. The plates were washed three times with PBS and developed with the standard ELISA procedure using the same anti-RSV antibodies. The IC_{50} was calculated using GraphPad Prism (GraphPad Software Inc., San Diego. CA) and non-linear regression curve fit. All experiments were performed at least twice.

Flow cytometry

HEK293T cells were either infected with RSV A2 or mock-infected. Forty-two hours after transfection, the cells were detached with the trypsin-EDTA solution (0.05% trypsin and 0.5 mM EDTA pH 8.0) and washed once with PBS and fixed using 1% PFA for 30 minutes at room temperature. After washing twice with PBS, the cells were blocked for 30 min with 1% (w/v) BSA

in PBS and incubated with a 2 µg / ml of VHH-Fc in BSA-PBS. One hour later the cells were washed and stained with anti-mouse IgG Alexa Fluor 633 (Invitrogen- A-21235). The stained cells were analyzed using a BD LSRII Flow cytometer.

Mice

Female BALB/c mice were purchased from Charles River (Charles River Wiga, Sulzfeld, Germany). The animals were housed under specific pathogen-free conditions and in a temperature-controlled environment with 12 h light/dark cycles; food and water were provided ad libitum. The animal facility operates under the Flemish Government License Number LA1400536. All experiments were authorized by the Institutional Ethical Committee on Experimental Animals (Ethical application EC2018-049).

Administration of VHH-Fcs and RSV A2 infection in mice

Nine weeks old mice were randomly distributed in experimental groups of six animals. They were slightly sedated by isoflurane before intranasal administration of antibodies and virus in a total volume of 50 µl PBS. Each group received an equimolar amount of antibodies (10 µg of VHH-Fc and 20 µg of palivizumab). The mock-treated group was also included that received only PBS. 4 hours later, mice were challenged with 10^6 PFU of RSV A2 and body weight was monitored every day.

Determination of infectious viral load by plaque assay

Monolayers of Vero cells were infected with 50 µl of serial threefold dilutions of the lung homogenates in a 96-well plate in serum-free OptiMEM medium (Invitrogen) supplemented with penicillin and streptomycin. After 3 h, the medium was removed, and the cells were washed twice with PBS. After adding 150 µl of growth medium containing 2% FCS and 0.6% avicel RC-851 (FMC Biopolymers), the cells were incubated for 4–5 days at 37°C. After infection, the cells were washed twice with PBS and subsequently fixed in 2% paraformaldehyde. After overnight fixation at 4°C, the paraformaldehyde solution was removed, and the cells were washed twice with PBS. Subsequently, the cells were permeabilized with PBS containing 0.2% Triton X-100 for 5 min and

blocked with PBS containing 1% BSA. The viral plaques were stained with a polyclonal goat anti-HRSV serum (AB1128, Chemicon International) (1/4,000). After washing three times with 1% BSA in PBS, the cells were incubated with HRP-conjugated anti-goat IgG antibodies (SC2020, Santa Cruz) for 30 min. Non-binding antibodies were removed by washing four times with PBS containing 1% BSA and 0.01% Triton X-100 and once with PBS. Finally, the plaques were visualized by using TrueBlue peroxidase substrate (KPL, Gaithersburg). The plaques of different dilutions were counted, and for each dilution, the number of PFU per lung (1 ml of lung homogenate) was calculated as the number of plaques present in the dilution × the factor of dilution × 20 (20 = 1,000 μl total supernatant volume/50 μl of supernatant used to infect the first well of the dilution series). The number of PFU/lung was then calculated as the average number of PFU/lung calculated for the different dilutions. As each supernatant of the homogenized lungs was tested in duplicate, the final number of PFU/lung was calculated as the average of these duplicates. A value of 10 was attributed to the samples for which no plaques could be detected.

qRT-PCR for determination of lung viral titer and cytokines expression

To determine the lung RSV load by qRT-PCR, total RNA from cleared lung homogenates was extracted by the use of High Pure RNA Tissue kit (Roche- 12033674001) according to the manufacturer's protocol and RNA samples were quantified using a NanoDrop® ND-1000 spectrophotometer (ThermoFisher). The first strand of cDNA was synthesized by using SensiFAST™ cDNA synthesis kit (Bioline- BIO-65054). Next, qRT-PCR was set up with SensiFAST Sybr No-ROX mix (Bioline- BIO-98005) and primers specific for RSV A2 M gene (Schepens et al., 2011) and cytokines (IFN-β, IFN-γ, Mip-1α, RANTES, Ifit2, IL-6, TNF-α) (Supplementary table 1). The qRT-PCR data were normalized to HPRT1 and UBC mRNA levels using the qbase program (Hellemans et al., 2007).

Determination of lung retention time

BALB/c mice were randomly distributed in three groups of three mice. Each group received a mixture of antibodies (10 μg each) prepared in 50 μl of PBS intranasally. Antibody mixture contained one VHH (Nb71), two VHH-Fcs (C4-Fc and V2-Fc) and one conventional mouse IgG2a

(mAb 65). BAL fluid was collected at 30 minutes, 24 hours and 48 hours, and samples were analyzed using western blot and ELISA. The coating antigen was RSV F (20 ng/well) for C4-Fc, Penta-His tag monoclonal antibody (100 ng/well, ThermoFisher- P21315) for Nb71, FaeG (100 ng/well) for V2-Fc and M2e peptide (100 ng/well) for mAb 65. Nb71 was detected with HRP conjugated 1/1000 anti-His antibody (ThermoFisher- MA1-21315) in western blot and 1/5000 anti-camelid VHH antibody (Genscript- A01861) in ELISA. All other antibodies (VHH-Fc and mAb 65) were detected with anti-mouse IgG2a (SouthernBiotech- 1080-05).

Statistical analysis

We used GraphPad Prism 8 for all statistical analyses using the Mann-Whitney *U* test and one-way ANOVA to evaluate differences between two groups and more than two groups, respectively.

Supplementary Table and Figures-

Supplementary Table 1. Primers used in this study.		
Gene	Primer	Sequence (5'→ 3')
RSV A2 M	hRSVM.F	TCACGAAGGCTCCACATACA
	hRSVM.R	GCAGGGTCATCGTCTTTTTC
IFN-γ	mIFNgamma.F	GCCAAGCGGCTGACTGA
	mIFNgamma.R	TCAGTGAAGTAAAGGTACAAGCTACAATCT
IL-6	mIL6.F	TAGTCCTTCCTACCCCAATTTCC
	mIL6.R	TTGGTCCTTAGCCACTCCTTC
TNF-α	mTNFalpha.F	CACCCCGGCCTTCCAAATAAATAC
	mTNFalpha.R	GCAATGCACAGCCTTCCTCACAG
Ifit2	mIfit2.F	ATCTCTCCCTACTCTGCCCTCCTA
	mIfit2.R	GCGTATAAATCAGCAATCCCTTCA
IFN-β	mIFNbeta1.F	TGGGTGGAATGAGACTATTGTTG
	mIFNbeta1.R	CTCCCACGTCAATCTTTCCTC
RANTES	mRANTES.F	GCTGCTTTGCCTACCTCTCC
	mRANTES.R	TCGAGGTGACAAACACGACTGC
Mip-1α	mMIP1a.1F	CTTGGAGGCAGCGAGGAA
	mMIP1a.1R	GGCAGCAAACAGCTTATAGGAGAT

Figure S1

A

B

C
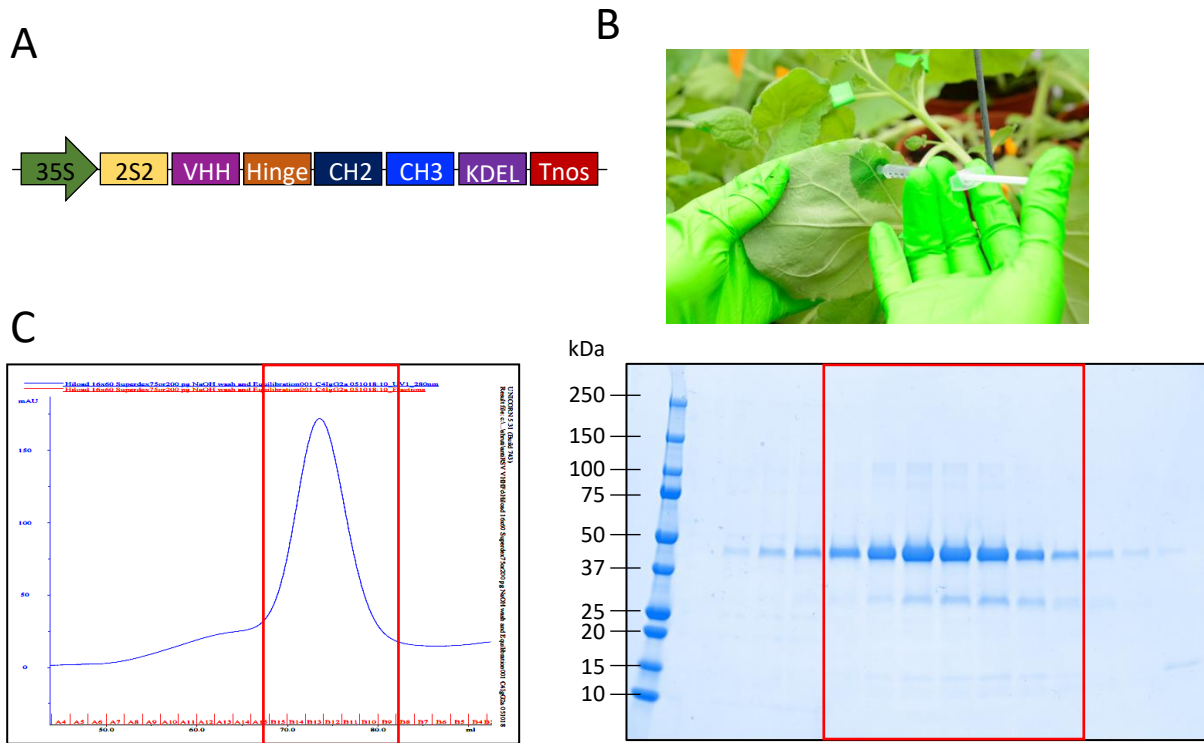
Figure S1 Cloning, production and purification of VHH-Fc. (A) Schematic representation (not drawn to scale) of the expression cassette, representing the constitutive 35S promoter of cauliflower mosaic virus, the signal peptide sequence of the 2S2 seed storage protein, VHH directed against the fusion protein of HRSV, the hinge and CH2-CH3 domain of murine IgG2a, the C-terminal endoplasmic reticulum retention motif (KDEL) and the nopaline synthase terminator (Tnos). (B) Infiltration of *N. benthamiana* leaves with agrobacterium suspension bearing expression vector for VHH-Fc fusions. (C) Size exclusions chromatography to enrich monomeric VHH-Fc (bivalent) form affinity purified fractions. Chromatogram showing fraction numbers and volume on X-axis and UV absorbance on Y-axis (left) and SDS-PAGE analysis of the major peak under reducing conditions (right) are shown for C4-Fc.

Figure S2
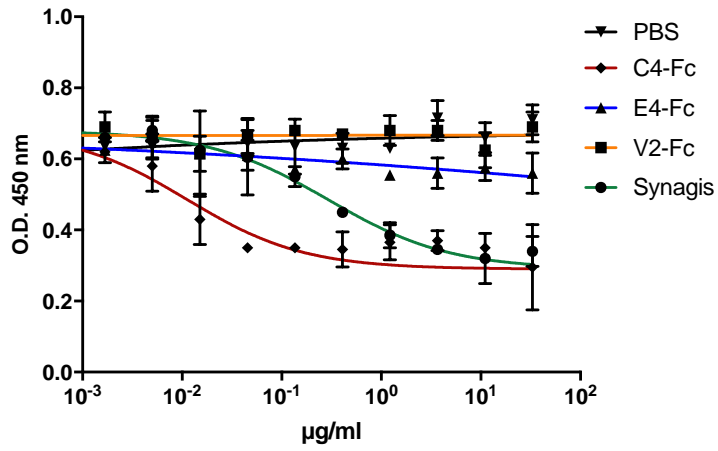
Figure S2. A microneutralization assay with RSV A long (200 pfu/well). The virus was preincubated with a 3-fold dilution series of the antibodies and used to infect Vero cells. After three days, plaques were stained with anti-RSV polyclonal serum (n=2). (C4-Fc EC_{50} = 0.138 nM; Synagis EC_{50} = 1.96 nM).
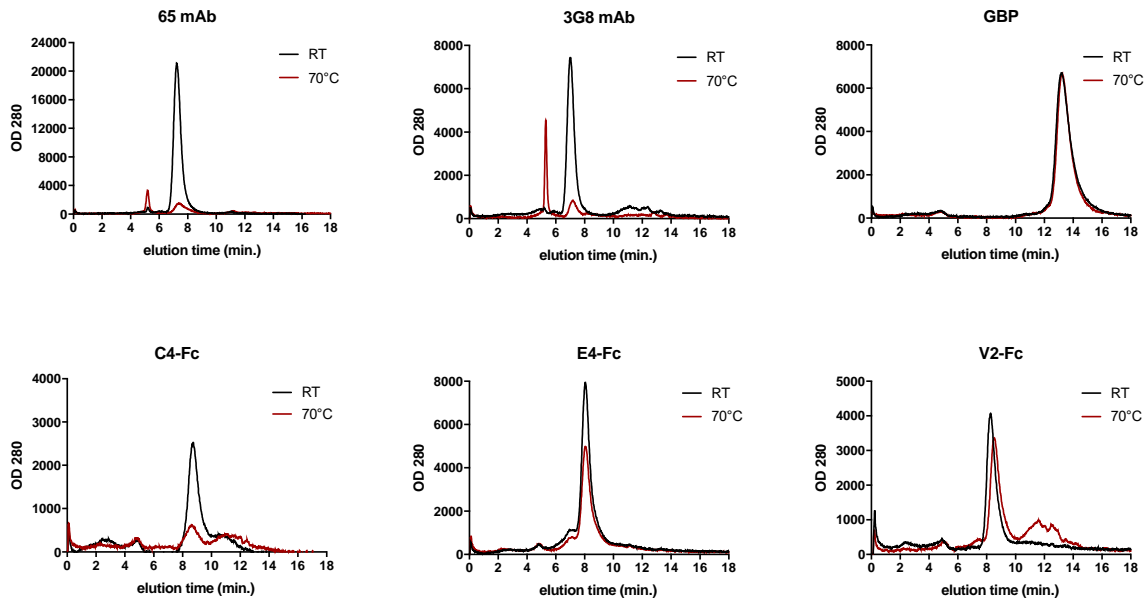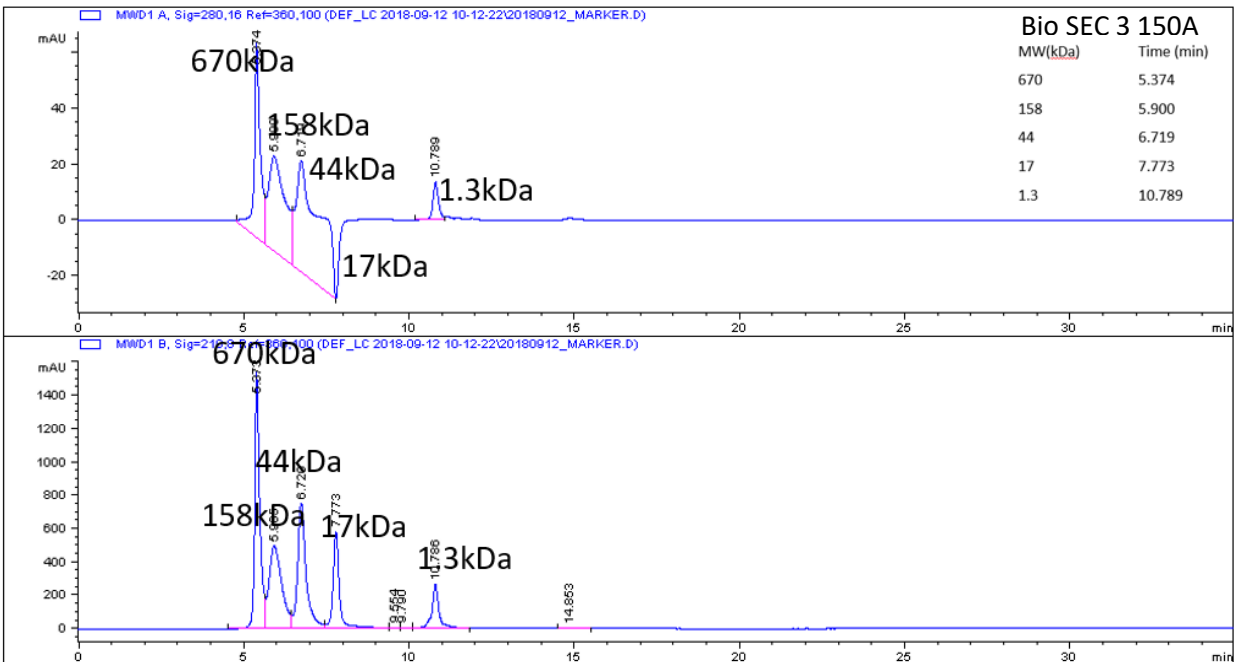
Figure S3 Aggregation analysis. (A) E4-Fc and V2-Fc do not aggregate after 20 minutes incubation at 70°C. The chromatograms (280 nm) show the elution profiles of the indicated antibodies, VHH-Fc fusions and the GBP VHH that were either incubated at room temperature (RT, black) or at 70°C (red). (B) The elution profiles of references proteins of different molecular weights.

Figure S4
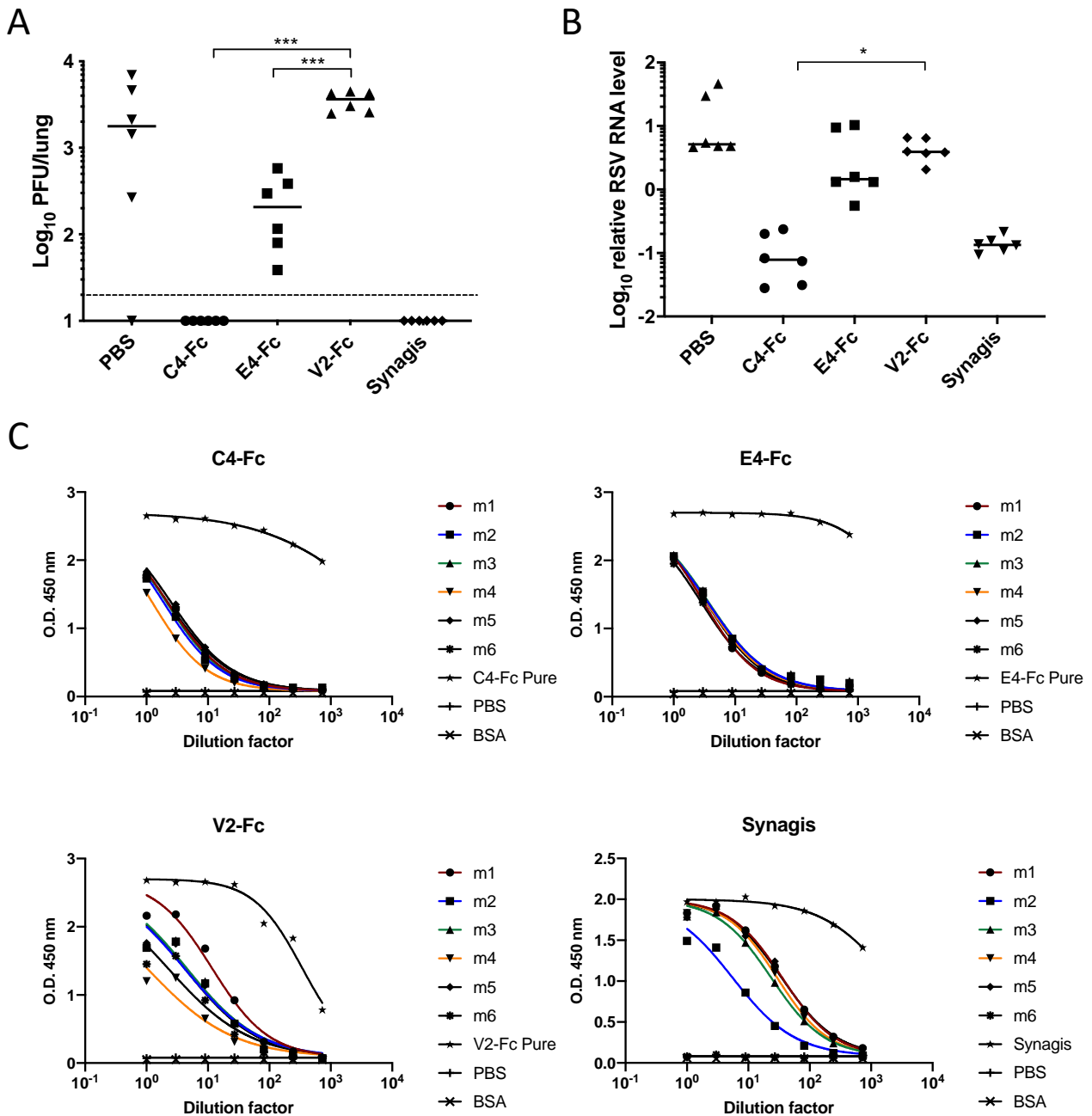
Figure S4. C4- and E4-Fc protect from RSV infection and retain in lungs till 5 days. BALB/c mice were treated intranasally with VHH-Fc/Synagis (dose= 20 µg/50 µl) four hours before the infection with RSV A2 (10^6pfu). Five days later, lungs were harvested, and BAL fluid was collected (n=6). (A) RSV virus titer was determined by plaque assay (*** (P≤0.0006), one-way ANOVA. Dashed line represents the detection limit (20 pfu). (B) RNA level was quantified by quantitative RT-PCR (* (P<0.05); Kruskal-Wallis test). (C) Antibody titer in BAL fluid was determined in RSV F binding ELISA.

162
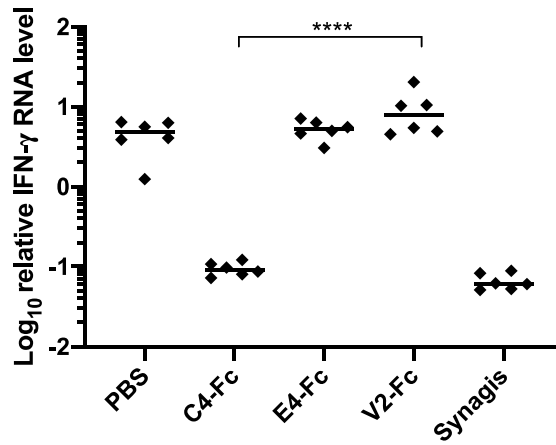
Figure S5

Figure S5. C4-Fc inhibits the expression of IFN-γ upon RSV infection. BALB/c mice were treated intranasally with VHH-Fc/Synagis (dose= 20 µg/50 µl), four hours before the infection with RSV A2 (10^6 pfu). Five days later, RNA level of IFN-γ in harvested lungs was quantified by RT-PCR. (n=6, **** (P<0.0001), one-way ANOVA).

Figure S6
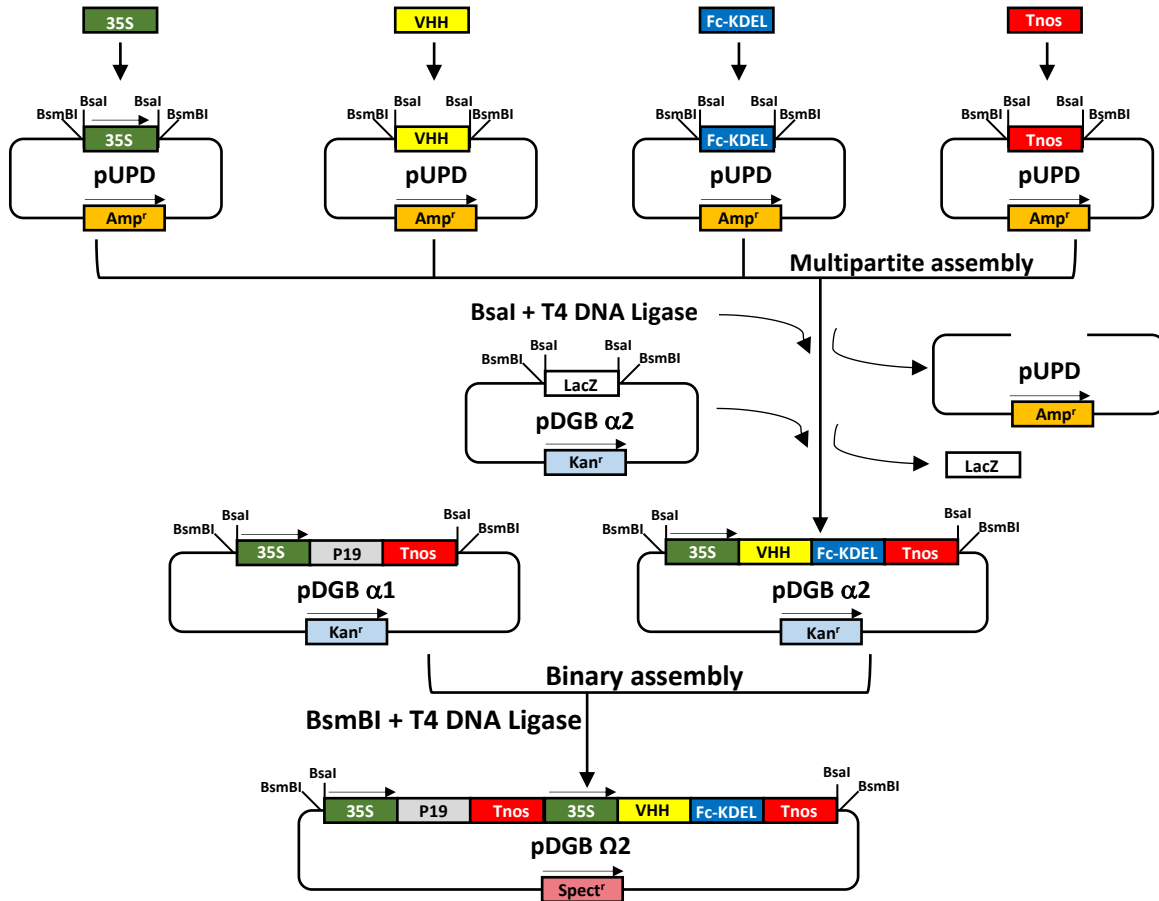
Figure S6. Schematic representation of cloning VHH-Fc fusions into GoldenBraid 2.0 cloning vectors.
35S: the constitutive 35S promoter of cauliflower mosaic virus; VHH: VHH C4/E4/V2, Fc-KDEL: hinge and Fc domain of murine IgG2a and KDEL at the C-terminus, Tnos: the nopaline synthase terminator, P19: silencing suppressor, Amp^r: ampicillin resistance marker, Kan^r: kanamycin resistance marker, Spect^r: spectinomycin resistance marker.

Chapter 7

A Two-Amino Acid Mutation in Murine IgA Enables Downstream Processing and Purification on Staphylococcal Superantigen-Like Protein 7

Shruti Bakshi [A], Ann Depicker [A], Bert Schepens [B], Xavier Saelens [B,C] and Paloma Juarez [A,D]*

[A]Ghent University, Department of Plant Biotechnology and Bioinformatics, 9052 Ghent, Belgium

VIB Center for Plant Systems Biology, 9052 Ghent, Belgium

[B]Ghent University, Department of Biomedical Molecular Biology, 9052 Ghent, Belgium

VIB Center for Medical Biotechnology, 9052 Ghent, Belgium

[C]Ghent University, Department of Biochemistry and Microbiology, 9052 Ghent, Belgium

[D]Instituto de Biología Molecular y Celular de Plantas (IBMCP), Consejo Superior de Investigaciones Científicas (CSIC), Universidad Politécnica de Valencia, Camino de Vera s/n, 46022 Valencia, Spain.

Author contribution:

P.J. conceived the idea. S.B. and B.S. performed the research and analyzed the data. A.D. and X.S. provided the mentorship. S.B. wrote the manuscript. P.J. and A.D edited it.

Abstract

With few exceptions, all currently marketed antibody therapeutics are IgG molecules. One of the reasons that other antibody isotypes are less developed are the difficulties associated with their purification. While commercial resins like staphylococcal superantigen-like 7 (SSL7) protein allow purification of IgAs from many animal species, these are not useful for murine IgAs. Because the mouse model is predominantly used for preclinical evaluation of IgA-based therapeutics, there is a need to develop an effective purification method for mouse IgA. Here, we adapted the sequence of a mouse IgA by mutating two amino acid residues in the fragment crystallizable (Fc) sequence to facilitate its purification on SSL7 resin. The mutated IgA Fc (hereafter referred to as IgA*) was then genetically fused with the variable domain of a llama heavy chain-only antibody (VHH) directed against the fusion protein of human respiratory syncytial virus (HRSV) resulting in VHH-IgA*, and transiently produced in infiltrated *N. benthamiana* leaves. These plant-produced mouse VHH-IgA* fusions were enriched by SSL7 affinity chromatography and were found to be functional in ELISA and could neutralize RSV *in vitro*, suggesting no detrimental effect of the mutation on their antigen-binding properties. This approach for the purification of murine IgA will facilitate downstream processing steps when designing innovative murine IgA-based fusions.

Introduction

Most of the commercial antibody therapeutics are based on IgG, which can readily be produced and purified in bulk amounts. Other interesting isotypes such as IgA are not so easy to purify because of the unavailability of efficient commercial affinity ligands, which creates a bottleneck for the manufacturing of IgA-based therapeutics. All available affinity capture methods for IgA have some limitations. For example, Skea et al. (1988) investigated the specificity of Jackfruit lectin, Jacalin, for IgA from various species and found that Jacalin specifically binds to a galactose-terminal oligosaccharide in the hinge region of human IgA1, which is not present in IgA2. Also, Jacalin does not show any binding affinity to IgAs from rat and mice (Kerr, 1990; Skea et al., 1988; Wilkinson and Neville, 1988) and because recombinant proteins produced in plants like tobacco lack terminal galactose residues, Jacalin-based purification is also unsuitable for plant-made proteins (Paul et al., 2014). Therefore, Jacalin can only be used for separation of the human IgA1 subclasses.

Another affinity ligand is protein L, a surface protein of *Peptococcus magnus*, which has been shown to bind specifically to the Ig light chains, independent of the class-specific heavy chain (Björck, 1988). Although protein L shows affinity to IgAs from many species, including human, mouse, rat and rabbit (Nilson et al., 1993), its binding is limited only to the kappa light chain. Boes et al. (2011) demonstrated that a given antibody can be engineered for purification with protein L by grafting the protein L-binding domain into the framework region of the variable light chains without affecting the antigen-binding property of the antibody. However, certain IgA formats, such as IgA fusions with variable domains of llama heavy chain-only antibodies (VHHs) that lack a light chain, cannot be purified using this affinity capture method. Peptide M, which is derived from the surface protein of *Streptococcus pyogenes*, is another affinity resin to purify IgA. This synthetic 50-amino acid (AA)-long peptide contains a cysteine residue at its C-terminus and binds exclusively to the Fc domain of human and bovine IgA, but not of murine IgA (Virdi et al., 2016). Staphylococcal superantigen-like 7 (SSL7) is a toxin isolated from *Staphylococcus aureus* that has been shown to have affinity for a wide range of IgAs. SSL7 competes with the leucocyte FcαRI to bind at the same site in the Fc of IgA, thereby suppressing the IgA-mediated effector

function (Ramsland et al., 2007). However, because mouse IgA does not contain the site for SSL7 binding, SSL7 is not suitable for the purification of mouse IgAs.

To study and evaluate new antibodies as therapeutics *in vivo*, the mouse is the main mammalian model used. Therefore, in order to develop murine IgA-based therapeutics, new downstream processing and characterization methods for murine antibodies, specifically for their heavy chain isotypes, should be developed. It has been reported that SSL7 has high affinity for the monomeric form of human IgAs and primarily interacts with a region of the Fc that contains the conserved amino acid sequence 'PLAFT' (Wines et al., 2006). However, in mouse IgAs, this sequence is replaced by a site for N-linked glycosylation, which is the main reason that SSL7 binding is abolished (Wines et al., 2011). To circumvent this, we mutated the mouse IgA Fc to contain the binding site of the commercially available SSL7 resin and fused it with a single domain antibody directed against the fusion protein of HRSV. The resulting VHH-IgA* fusion constructs were successfully purified on a SSL7 resin, and the integrity of these antibody constructs was confirmed by ELISA, western blot and an *in vitro* RSV neutralization assay, showing that removal of the N-linked glycosylation did not affect functionality.

Results and Discussion

Mutated VHH-IgA* Fusion Proteins in Crude Leaf Extract Bind Their Target

To enable purification of murine IgA with SSL7, the wild-type 'PMNFT' sequence of the mouse Fc part of IgA was substituted by the 'PLAFT' coding sequence (Figure 1A). The Fc domain of wild-type IgA and mutated IgA* were synthesized, and genetically fused to VHH C4 and VHH E4, two different single domain antibodies (also known as Nanobodies®) that bind the surface protein F of HRSV (Hultberg et al., 2011). Whereas VHH C4 can neutralize RSV *in vitro*, VHH E4 binds to RSV F but does not neutralize the virus (Hultberg et al., 2011). C4-IgA and E4-IgA fusions and their respective mutated IgA* counterparts (C4-IgA* and E4-IgA*) were cloned using GoldenBraid cloning strategy and transiently expressed in tobacco leaves by infiltration. The C-terminal ER retention motif (KDEL tag) was added to prevent the plant-specific N-glycan maturation in the Golgi apparatus. The accumulated levels in crude leave extracts were determined by western

blot. VHH-Fc fusions normally assemble as bivalent molecules as a result of the disulfide bonds in the hinge region. Therefore, western blot analysis was performed under reducing conditions (Figure 1B). In the E4-IgA, C4-IgA and E4-IgA* extracts, both the full-length fusion protein (42 kDa) and a fragment of 25 kDa could be detected. The latter most likely represents a cleavage product of the fusion protein. Extracts of leaves infiltrated with a C4-IgA* expression vector contained only a smaller band (about 25 kDa), suggesting extensive proteolytic cleavage. VHH fusions with both wild-type IgA and mutated IgA* yielded similar cleavage profiles, indicating that it is not the mutation in the IgA-Fc part but rather the VHH that affects the fusion protein accumulation and proteolysis sensitivity (Figure 1B).
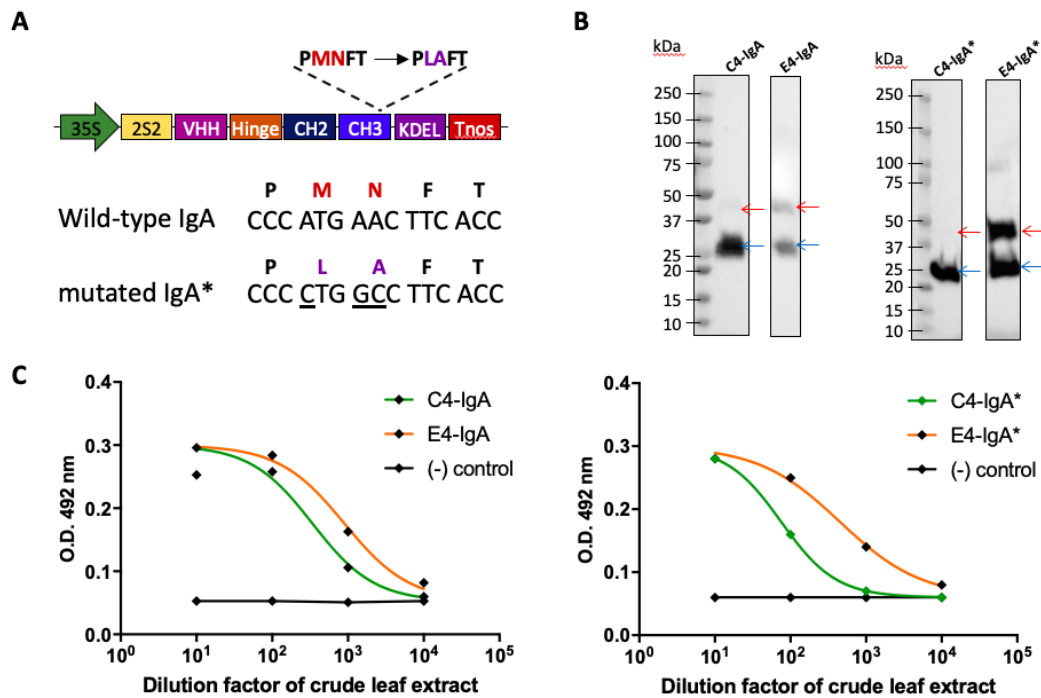
Figure 1. Production of mutated VHH-IgA* antibodies does not influence antigen-binding capacity. (**A**) Schematic representation (not drawn to scale) of the expression cassette, featuring the constitutive 35S promoter of cauliflower mosaic virus, the signal peptide sequence of the 2S2 seed storage protein, VHH directed against the fusion protein of HRSV, the hinge and CH2-CH3 domain of murine IgA, the C-terminal endoplasmic reticulum retention motif (KDEL) and the nopaline synthase terminator (Tnos). PMNFT → PLAFT represents the substitution of the PMNFT coding sequence from the CH3 domain of murine IgA by the SSL7-binding domain (PLAFT) of human IgA. (**B**) Western blot analysis of VHH-IgA (left) and VHH-IgA* (right) fusions in crude leaf extracts. The blot was probed with anti-mouse IgA conjugated with HRP. Red, full-length protein; Blue, cleavage product; (**C**) RSV F-binding ELISA to analyze functionality of VHH-IgA (left) and VHH-IgA* (right) fusions in crude leaf extracts. (-) control is the crude leaf extract from the non-transfected *N. benthamiana* leaves. Detection was performed with peroxidase-conjugated polyclonal anti-mouse IgA immune serum.

Subsequently, the antigen-binding activity of the fusion proteins in crude extracts was examined by ELISA using coated RSV F and a polyclonal anti-mouse IgA immune serum for detection of C4-IgA* and E4-IgA* binding. Binding to immobilized RSV F was detectable, although both C4-IgA and C4-IgA* showed a weaker signal than E4-IgA and E4-IgA* (Figure 1C), which correlated with the lower amount of full-length molecules detected in the western blot analysis (Figure 1B). We can conclude that mutation of the 'PMNFT' AA sequence in the Fc part of the mouse IgA into the conserved human 'PLAFT' sequence, does not influence the production or antigen-binding capacity of the VHH-IgA Fc antibody constructs.

VHH-IgA* Fusion Proteins Allow Purification with SSL7 Resin

To evaluate purification of the mutated VHH-IgA* molecules using SSL7 resin, a crude extract derived from approximately two grams of infiltrated leaves for each construct was passed over an SSL7 column, and the flow-through and subsequent eluted fractions were analyzed by SDS-PAGE followed by western blot under reducing conditions. The wild-type VHH-IgA fusions could clearly be demonstrated in the crude extracts and in the flow-through, and no VHH-IgA fusions were recovered from the eluted fractions (Figure 2A). On the other hand, mutant VHH-IgA* fusions for both VHH C4 and E4 could be eluted from the SSL7 column (Figure 2B). No remarkable difference in band intensity was observed between the crude extract and flow-through, suggesting that the SSL7 binds IgA* with relatively low affinity, which is in line with what has been observed for IgAs from other species. Both intact full-length protein and proteolytic fragments were enriched upon SSL7 purification, and a very faint double band indicated as yellow arrow may represent a glycosylation form of the antibody (Figure 2B). Some high-molecular weight bands were also detected, which likely represent the non-reduced forms or aggregates of the antibody fusion. We can conclude that the two-AA mutation in the Fc part of the IgA enables purification over SSL7 resin. Subsequently, a protein F-binding ELISA was performed to further evaluate the antigen-binding activity of the purified VHH-IgA* fusions. C4-IgA* and E4-IgA* showed specific binding to protein F (Figure 2C), which correlates with the results obtained for crude extracts (Figure 1C).
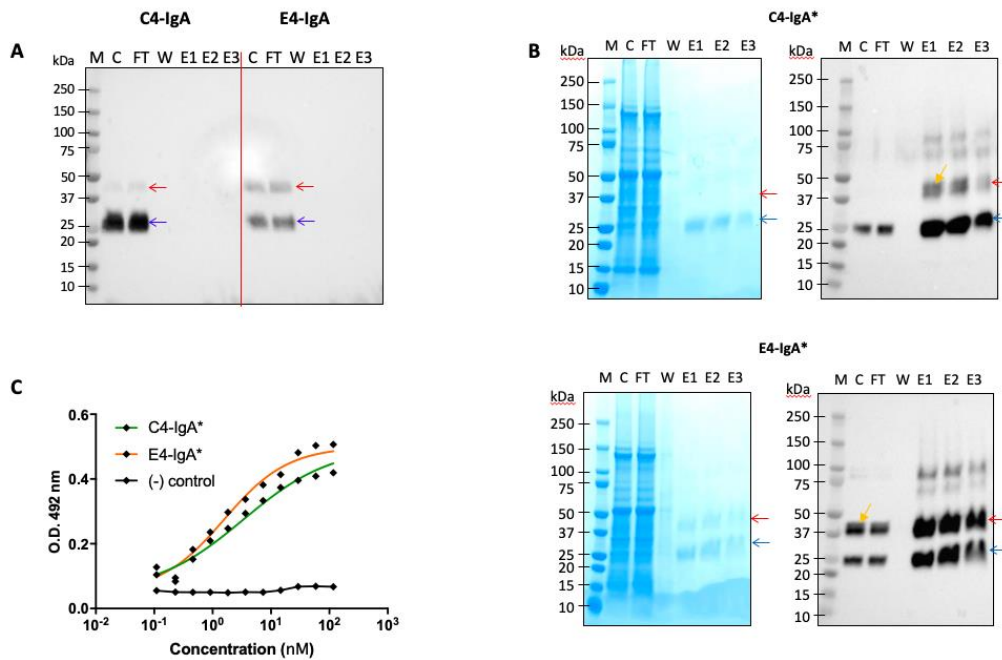
Figure 2. Purification and characterization of VHH-IgA/A* purified on SSL7 resin.
A) Western blot analysis of wild-type C4-IgA (left) and E4-IgA (right); **B)** Coomassie staining (left) and western blot analysis (right) of SSL7-purified C4-IgA* (top) and E4-IgA* (bottom). The high-molecular weight bands above the yellow arrows are the non-reduced forms or multimers of the antibody fusion. **C)** RSV F-binding ELISA was performed with purified VHH-IgA* fusions as described in **Figure 1C**. Protein concentration of the pure protein was determined by OD_{280} measurements. (M, marker (kDa); C, crude leaf extract; FT, flow-through; W, wash fraction; acid eluted fractions (E1, E2, E3); red, full-length; blue, cleavage products)

VHH-IgA* Fusion Proteins Can Neutralize RSV

To test the RSV A2 strain neutralization potency of C4-IgA* and E4-IgA*, an *in vitro* micro-neutralization assay was performed. The VHH-IgA* fusions were compared with Synagis®, an RSV-neutralizing humanized mouse monoclonal antibody that is used as prophylaxis in high-risk infants, which was used as a positive control. C4-IgA* but not E4-IgA* could neutralize RSV A2 (Figure 3). The deduced IC_{50} value of C4-IgA* was 10.94 nM, which was about 50-fold lower than that reported for its monovalent VHH C4 equivalent (640 nM) (Hultberg et al., 2011) suggesting that the bivalent C4-IgA* is 50-fold more potent in neutralizing RSV A2 strain as compared to the monovalent VHH C4. Of note, neutralization potency of C4-IgA* was about 13-fold lower as

compared to C4-IgG, as described previously in Chapter 6. This could be because of the integrity of C4-IgA* fusions.
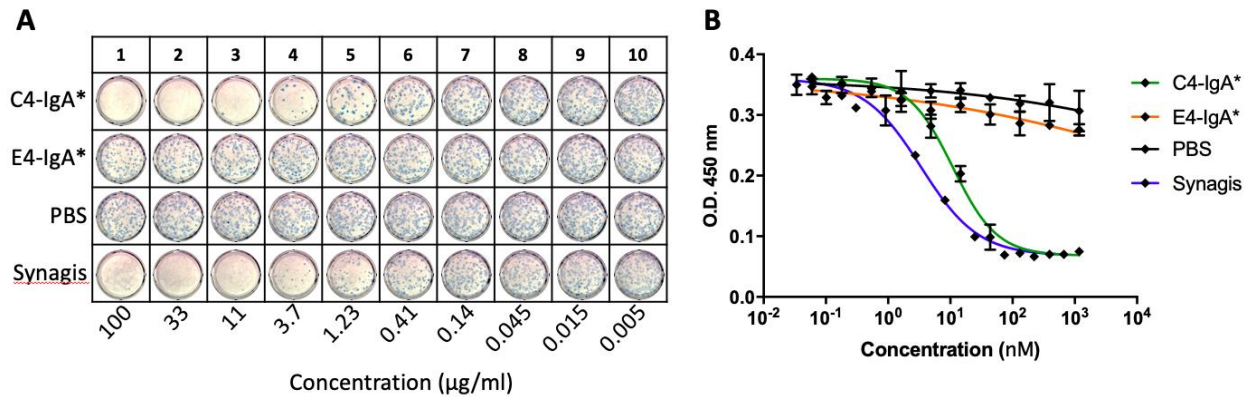
Figure 3. C4-IgA* can neutralize RSV A2 *in vitro*. A) C4-IgA*-neutralizing RSV A2 in a microneutralization assay. RSV A2 strain (50 pfu per well) was pre-incubated with different concentrations of VHH-IgA* before infection of HEp-2 cells. Three days after infection, the viral plaques were stained with polyclonal anti-RSV serum and visualized by TrueBlue staining. The RSV A2 plaque-reduction activity of C4-IgA* was compared with Synagis mAb. The VHH E4-IgA* and PBS were used as negative control. **B)** RSV neutralization curves of VHH-IgA* fusions derived from a microneutralization assay. Virus neutralization was measured as the reduction of the OD of the samples compared to the OD of the controls in the ELISA. The IC_{50} values were determined by curve fitting with GraphPad Prism software.

Conclusions

Murine IgA-based fusions can be functionally assessed in the mouse model, *e.g.* to select the best-performing immunotherapeutic candidates. However, their development is hampered because of the lack of a ligand for affinity purification of mouse IgA. To overcome this bottleneck for IgA purification, we mutated two AA residues of the Fc tail of mouse IgA to generate the PLAFT sequence found in the IgAs of many other species and known to interact with SSL7. We have shown that mutated VHH-IgA* fusions could successfully be purified on SSL7, without any deleterious effect on the antigen-binding property of the VHHs, even without the presence of the wild-type PMNFT glycosylation site. Although it has been shown that removal of N-glycan in human IgA does not affect its interaction with neutrophil FcαR (Mattu et al., 1998), the *in vivo*

functions of IgA* will have to be explored in transgenic mice expressing FcαR to make sure that the mutation does not impact the effector function of mutant IgA*. In the context of the RSV neutralizing VHH-IgA fusions studied here, it is relevant to mention that prophylactic treatment with a Palivizumab derived IgA in FcαRI transgenic mice did not result in better protection against RSV infection compared to wild-type mice (Jacobino et al., 2018). To summarize, we have designed a strategy for efficient IgA purification on SSL7, an effort that opens the door for advancements in the development of future IgA-based therapeutics.

Materials and Methods

Construction of VHH-IgA Fusions and Transient Expression in Tobacco Leaves

The DNA sequences corresponding to the wild-type and mutated Fc fragment of mouse IgA (NCBI Accession No. AB644393.1, UniProt Accession No. P01878) were synthesized and obtained from Gen9 (Ginkgo Bioworks), and ligated to VHH C4 and VHH E4 in the pDGBα1 vector using the GoldenBraid cloning strategy, as previously described (Figure 1A) (Sarrion-Perdigones et al., 2011). The resulting expression vectors containing VHH-IgA* fusions were introduced into *Agrobacterium tumefaciens* strain LBA4404 (Hoekema et al., 1983) and infiltrated in *Nicotiana benthamiana* leaves. Infiltrated leaves were harvested six days post infiltration and extracts were prepared in Dulbecco phosphate-buffered saline (DPBS, Lonza Biosciences) supplemented with cOmplete Protease Inhibitor (Roche) as described earlier (De Buck et al., 2012; De Meyer et al., 2015).

SDS-PAGE, Western Blotting and ELISA

Transiently expressed VHH-IgA fusions (10 μl of crude leaf extracts or purified proteins) were separated on 4-20% gradient gel (Bio-Rad) under reducing conditions and stained with Coomassie blue stain. The proteins were characterized via immunoblotting and ELISA using the standard procedure (De Buck et al., 2012; De Meyer et al., 2015).

Affinity Purification on SSL7 Resin

Fifty ml of crude leaf extract were filtered through 0.45-μm Millex® Syringe Filters (Merck) and incubated with pre-equilibrated SSL7 resin (InvivoGen) on a shaker at 4°C for 1 h. These extracts were then applied to PD10 columns (Pharmacia) by gravity flow, followed by washing with 10 ml wash buffer (Equilibration buffer DPBS, Lonza). Bound antibodies were eluted with 1 ml of 1 M Arginine (pH 2.7) and neutralized immediately with 1 M Tris-HCl (tris (hydroxy methyl) aminomethane) pH 9. Purified proteins were analyzed by SDS-PAGE and western blot.

HRSV Micro-Neutralization Assay

HRSV neuralization potency of the VHH-IgA* fusions was tested in plaque reduction assay using the protocol described earlier (Hultberg et al., 2011).

GENERAL CONCLUSIONS AND PERSPECTIVES

This Ph.D. thesis describes the engineering of VHHs for improved functionality for two different applications. We highlighted the ease of VHH engineering to develop a vaccine delivery system compared to conventional antibody platforms. APN-specific VHHs were screened from phage library and characterized for their potential to bind intestinal epithelium and generate specific immune response. On the other hands, anti-RSV VHHs were also developed as fusions with IgG2a Fc domain and produced in the plant expression system for cost-effective production. Moreover, the effect of Fc domain on the pharmacokinetic behavior of the associated VHH and their *in vivo* functionality was tested in RSV disease model.

Engineering of a single-chain variable fragment (scFv) is unpredictable

In search for APN binding domains as vaccine delivery system for intestinal infections, we followed two approaches: Chapter 3 describes the design of a vaccine carrier based on single-chain variable fragments (scFv) derived from an anti-porcine APN mouse IgG1 monoclonal antibody (IMM013), while chapter 4 and 5 describe the isolation of APN binding VHH domains and their feasibility to engineer as a vaccine carrier. To test the immune response, antigens were produced without and with these APN binding domains, and the major focus of this thesis was to produce these vaccines to test their immunization capacity upon oral delivery, in collaboration with the lab of Prof. Eric Cox.

Various studies have highlighted the application of scFv as a targeting moiety (Cheng and Allen, 2010). A flexible linker connecting VL and VH domain plays a crucial role in maintaining intrinsic binding and stability of the scFv (Robinson and Sauer, 1998). Although Glycine–Serine linker of varying lengths has been reported to be effective in making scFv fusions (Peipp et al., 2004; Shan et al., 1999), introducing an additional disulfide bond between VH and VL is often beneficial in improving scFv stability. Thus, we used a unique linker containing one Cys residue at the terminal position that induced the covalent stabilization of the bivalent scFv fusions with CH3 domain of human IgG1 (Li et al., 1997). In our study, whenever the scFv was present in the fusions, the yield was very low; while other fusions without scFv gave very high expression levels. These results were in line with our parallel study where similar constructs with another model antigen (adhesin proteins of $F4^+$ and $F18^+$ETEC fimbriae) were transformed in Arabidopsis to be expressed in seeds, however, only small amounts of the scFv fusions could be obtained (Tharad

et al, unpublished). The low expression can be attributed to unstable folding of scFv and is independent of the expression platforms. An additional disulfide bond can also lead to unexpected challenges such as the formation of intermolecular disulfide bond resulting in aggregation and reduced bioactivity (Cao et al., 2018). The scFv was fused to the model antigen GFP via a flexible helical linker that has been successfully used to produce functional bivalent scFv-GFP fusions (Stamova et al., 2012). In parallel, we also used Glycine-Serine linker to make these scFv fusions. Despite all these efforts, no high production levels were obtained in any expression system, suggesting that scFv engineering is difficult and requires various optimizations to identify a suitable peptide linker. As a result, we decided to generate pig APN-specific VHHs as our alternative strategy.

VHH engineering is straightforward

VHHs are highly stable and because of their modularity and single domain nature, they can be easily engineered. In this project, the APN binding VHHs selected from phage display library were re-cloned with mouse IgG2a Fc domain (MG) along with two negative controls VHH V2 and D3, both targeting adhesin proteins of Enterotoxigenic *E. coli* (ETEC). All the initial studies with crude extracts were performed using V2-Fc and D3-Fc as controls. However, due to ETEC infections in pig stables and difficulty in finding seronegative pigs, V2 and D3 were not the ideal controls for piglet models. Therefore, rather than cloning and producing new negative control, we used a GFP binding VHH (GBP) fused to mouse IgG3 Fc for subsequent studies which was previously produced in our laboratory (De Meyer et al., 2015). The small-scale production and purification of the VHH-Fc fusion proteins from the medium allowed their further functional analysis in ELISA, flow cytometry, immunohistochemistry on small intestinal tissues and endocytosis with APN-expressing cell lines and gut-ligated loops. Some clones, that did not bind well in ELISA, displayed very strong binding to APN-stable cell lines. These data were in line with our experience with IMM013. For instance, both 3L94-MG and 2L65-MG, bind to APN-expressing cells, while only 3L94-MG binds to immobilized APN in ELISA plates. Since both VHHs belong to two different families, they most likely recognize different epitopes (Pardon et al., 2014). It is possible that the

epitope for 2L65 is not accessible in coated APN, resulting in low or no binding activity of the VHH.

Since APN-binding VHH-Fc fusions showed significant binding and uptake on APN in the *in vitro* characterization, a preliminary oral immunization experiment was planned to test the immunogenicity of mouse IgG2a Fc domain in piglet models via APN targeting capacity of 3L94-MG and 2L65-MG fusions. An irrelevant VHH fusion with murine IgG2a will be cloned to use as a negative control because the Fc domain of GBP-MG was derived from mouse IgG3 that would differ with IgG2a Fc in terms of interaction with Fc receptors. The anatomical, physiological and genetic similarity between human and pig suggest that pig Fc receptors most likely function similar to that of humans. Notably, human FcγR and FcRn have very low or no affinity for mouse IgG isotypes. For instance, human FcγRIIA binds mouse IgG1, 2a and 2b, but not IgG3 (reviewed in Bruhns, 2012), suggesting that mouse IgG3 Fc of GBP-MG may have different effects *in vivo*. The phylogenetic relationship of human and porcine FcRn showed that they are more closely related than rodents (Guo et al., 2016) and porcine FcRn can bind to murine, human and bovine IgG (Stirling et al., 2005); however, no information about IgG isotype was reported in this study. Another study reported that human FcRn do not bind mouse IgG1, but has low affinity for mouse IgG2a and IgG2b (Ober et al., 2001). However, experimental evidences about interaction between murine IgG and porcine Fc receptors are still lacking. Therefore, we chose to produce a new negative control for *in vivo* validation. Moreover, different isolated VHH-Fc fusions can also be included as a cocktail to identify the best combination to assess the additive or synergistic effects. Alternatively, bi- or multi-specific VHH-Fc fusions can be designed with the best performing VHHs, as developed against influenza by Laursen et al. (2018).

After characterization of the VHHs (as described in chapter 4), the best VHH 3L94 was fused to model antigen C-fragment of tetanus toxin (TTC) and Fc domain of pig IgG and IgA. Besides their high accumulation, IgA-based fusions are more prone to proteolysis compared to IgG-fusions. These findings are consistent with our previous results with VHH-IgA fusions showing cleavage in the significant part of the total soluble proteins (Bakshi et al., 2019; De Buck et al., 2013; Virdi et al., 2019). However, their binding activity to APN in ELISA indicates that IgA fusion proteins are still functional even after excessive proteolysis. The efficacy of these fusions remains

to be further determined in cell-based assays and *in vivo* settings. In summary, VHH engineering is straightforward and offers the potential for designing complex fusion molecules such as vaccine carriers described in this thesis.

VHH-Fc fusions for the potential control of respiratory syncytial virus infection.

This PhD thesis lays the foundation for the development of effective antivirals for RSV infection. Previous studies have already shown the potential of VHHs as an antiviral agent and some were successful in entering clinical trial (Detalle et al., 2016). Despite their several advantages over conventional antibodies, VHHs are only limited to prophylactic treatment due to their short half-life. VHH fusions with Fc tail not only increase the half-life of associated VHH, but also improve the *in vivo* efficacy by Fc effector functions.

In this study, we chose RSV neutralizing VHH C4 to make VHH-Fc fusions as a proof-of-principle. However, VHHs more potent than C4 have already been identified that bind RSV F with picomolar affinity. Nb017, for example, is a VHH developed by Ablynx that binds both the pre- and postfusion conformation of RSV F (Detalle et al., 2016). Reformatting of Nb017 in a trivalent VHH, termed ALX-0171 resulted in increased neutralizing potency. ALX-0171 greatly outperformed Palivizumab in terms of both plaque reduction and complete inhibition of RSV replication *in vivo* (Detalle et al., 2016). Another VHH, F-VHH-4 selectively binds the prefusion conformation of RSV F and exerted higher neutralization potency in its monovalent state than that reported for trivalent ALX-0171 (Rossey et al., 2017). Thus, it would be worthwhile to make Fc fusions with such potent VHHs and further validate the effects of Fc tail via *in vivo* settings.

Moreover, ALX-0171 could withstand the nebulization process and displayed protection upon prophylactic administration by inhalation, which is attributed to the robustness of VHH. VHH-Fc fusions have not been studied so far for such applications. In chapter 6, we demonstrated the high physical stability of VHH-Fc fusions which is dependent on linked VHH. VHH-Fcs are highly stable and retain their antigen binding property at elevated temperature, while conventional antibodies fail to demonstrate such effects. It would be interesting to test their stability via nebulization to deliver them straight to the site of infection.

Importantly, E4-Fc fusions, which is a non-neutralizing VHH, also displayed prophylactic protection in mice, although weaker than that of C4-Fc. This data indicates the role of Fc tail by inducing effector functions such as antibody-dependent cellular cytotoxicity and phagocytosis (ADCC and ADCP respectively), and complement dependent cytotoxicity (CDC), thereby inducing faster clearance of RSV-infected cells. In this project, the interaction of VHH-Fc fusions with Fcγ receptor (FcγRI) was tested in ELISA, that can be further confirmed *in vitro* by cell-based assays. Furthermore, Fcγ receptor knockout mice would also be useful to study *in vivo* effect of VHH-Fc fusion. E4-Fc can act as a negative control in such experiments and is expected to display no protection if the Fc domain plays a crucial role to inhibit RSV replication *in vivo*. Many studies have demonstrated the importance of Fc-effector functions in virus clearance. A study shows a comparison of the conventional palivizumab with their different glycan variants produced in *N. benthamiana* (Hiatt et al., 2014). These variants had augmented binding to Fcγ receptor that resulted in reduction of RSV titers in cotton rat lungs compared to the conventional palivizumab. These findings suggested that rather than *in vitro* RSV neutralization potency, Fcγ receptor binding activity plays a significant role in determining the *in vivo* efficacy of an antiviral. In another study, a vaccine based on the extracellular domain (SHe) of the small hydrophobic protein of HRSV induces immune protection in mice and cotton rats which was solely dependent on the interaction of neutralizing antibodies with FcγRI and FcγRIII (Schepens et al., 2014). A multidomain VHH-Fc fusion developed for influenza virus infection protected all mice from disease lethality, whereas mutants lacking FcγR binding resulted in decreased survival rate (Laursen et al., 2018). A higher dose of the mutant antibody was needed to provide full protection.

VHH-Fc fusions offer the great therapeutic potential due to their longer lung retention time compared to VHHs and need to be studied further in a suitable animal model. A monovalent and bivalent VHHs without an Fc domain may serve as controls for more information about the impact of the Fc domain in therapeutic settings. Although most of the preclinical animal studies are performed in mouse, low permissiveness of RSV makes it difficult to demonstrate a therapeutic effect. Cotton rats have proven useful in many studies. In fact, the advancement of both palivizumab (Synagis®) and RSVIg (RespiGam®) to clinical trials was solely based on the

preclinical data from cotton rats (Niewiesk and Prince, 2002). However, extrapolation of the results from preclinical species to human depends on several factors such as breathing patterns, airway anatomy and administration device characteristics. Recently, neonatal lambs were successfully used to validate therapeutic efficacy of ALX-0171 (Mora et al., 2018). Lambs share many physiological, anatomical and developmental features with human and can be considered as a valuable RSV-infection model for preclinical studies of vaccines or therapeutics. In addition to half-life and animal models, route of administration and dose also affect the therapeutic efficacy of an antibody.

Merits of IgA at pulmonary mucosal membranes

In addition to VHH, choice of Fc domain may also have different effects at pulmonary mucosa. The predominant antibodies at mucosal surfaces are the secretory IgA (SIgA) that are believed to be functional at harsh environments at the mucosal membranes and also contribute to longer retention time as compared to IgG isotype (Corthesy, 2010; Strugnell and Wijburg, 2010). Moreover, their dimeric structure with a secretory component (SC) also helps in higher stability and avidity. Recombinant production of SIgA is achievable in the plant expression system such as Arabidopsis (Virdi et al., 2013). However, obtaining a homozygous line encoding three genes (IgA Fc, SC, and J chain) for SIgA might take several years, especially with crop species such as soybean (*Glycine max*) having life cycle of up to 6 months (Palaci et al., 2019). It was recently reported that VHH fusion with monomeric IgA produced in either soybean or *P. pastoris* could protect piglets from enterotoxigenic *E. coli* infection (Virdi et al., 2019). This study gives hope to take advantage of IgA properties while omitting all the tedious process of making SIgA at the same time. Thus, it would be of great interest to make VHH-based fusions with Fc domains derived from conventional IgG, monomeric and secretory IgA; and comparing their potency to assess the merits of IgA at the pulmonary mucosal surfaces.

One of the major hurdles in developing IgA-based therapeutics is lack of efficient purification method. We addressed this issue in this thesis (Chapter 7). A two amino acid mutation in Fc domain of murine IgA resulted in purification of VHH-IgA fusions on commercial

affinity ligand SSL7 without any detrimental effect on the antigen-binding property of the VHH. However, *in vivo* effect of mutated IgA will have to be explored further.

Plants and yeasts as alternatives to mammalian-based expression system for recombinant antibody production.

This thesis describes the expression of chimeric antibodies in both *P. pastoris* and *N. benthamiana*. Both the systems offer unlimited scalability and cost-effective protein production and are easy to be engineered to allow mammalian-like glycosylation. The purpose of this thesis was to take advantage of plant-based expression system as an alternative production platform for recombinant antibodies. Both the RSV neutralizing VHH-Fc and APN-specific scFv-antigen fusions were initially produced in infiltrated *N. benthamiana* leaves via *Agrobacterium*-mediated transient expression system for rapid analysis. However, due to difficulty with a very low accumulation of scFv-based fusions, several other fusions with scFv and VHHs were designed and produced in *P. pastoris* allowing convenient and rapid screening of multiple constructs and VHH library. Both plant and yeast expression systems have their own advantages and disadvantages.

Transient expression in plants is a favorable alternative to stable transformation because of the high accumulation of the recombinant protein in few days. This system is successfully used by Medicago, Inc using a plastocynin promoter from *Medicago sativa* sp. that provided the accumulation of recombinant antibody ranging from 0.6-0.7 g/kg of FW by syringe infiltration and 0.2-0.3 g/kg FW by vacuum infiltration to assess the scalability (Vezina et al., 2009). Production of RSV-specific VHH-Fc fusions in *N. benthamiana* yielded only 0.01-0.03 mg/kg of FW, about 10-fold lower than what was reported with plastocynin promoter by (Vezina et al., 2009). Thus, it would be interesting to test different promoters to improve the accumulation of VHH-Fc fusions.

In contrast to plant-based expression system, the yeast-based expression has been utilized for manufacturing a variety of novel recombinant therapeutics that are already in the market. Large amounts of recombinant proteins can be produced in growth medium and concentrated using ammonium sulfate at a small scale before mixing in the feed of piglets for oral immunization. However, on large scale production, lyophilization is the most suitable

method for protein concentration and generating powder form of the antibodies. Recently, it has been reported that VHH-IgA fusions produced in *Pichia pastoris* can be used without purification for oral administration (Virdi et al., 2019).

Finally, this thesis shows that VHH-Fc fusions can be produced in both production platforms. Since we did not compare the expression level of the same protein in different platforms, one cannot be considered better than the other. Moreover, accumulation level and protein integrity of the fusion protein were highly dependent on the associated VHH, as observed in both *N. benthamiana* for anti-RSV and *P. pastoris* for anti-APN VHH-Fc. These data were in accordance with our previous findings (De Meyer et al., 2015). The results obtained from one VHH-Fc fusions cannot be extrapolated to other and need to be studied on a case-by-case basis.

BIBLIOGRAPHY

Abdel-Aal, A.B., Batzloff, M.R., Fujita, Y., Barozzi, N., Faria, A., Simerska, P., Moyle, P.M., Good, M.F. and Toth, I. (2008) Structure-activity relationship of a series of synthetic lipopeptide self-adjuvanting group a streptococcal vaccine candidates. *J. Med. Chem.* **51**, 167-172.

Abranches, R., Arcalis, E., Marcel, S., Altmann, F., Ribeiro-Pedro, M., Rodriguez, J. and Stoger, E. (2008) Functional specialization of Medicago truncatula leaves and seeds does not affect the subcellular localization of a recombinant protein. *Planta* **227**, 649-658.

Agu, R.U., Ugwoke, M.I., Armand, M., Kinget, R. and Verbeke, N. (2001) The lung as a route for systemic delivery of therapeutic proteins and peptides. *Respiratory research* **2**, 198.

Ahmad, M., Hirz, M., Pichler, H. and Schwab, H. (2014) Protein expression in Pichia pastoris: recent achievements and perspectives for heterologous protein production. *Appl. Microbiol. Biotechnol.* **98**, 5301-5317.

Ahmad, Z.A., Yeap, S.K., Ali, A.M., Ho, W.Y., Alitheen, N.B. and Hamid, M. (2012) scFv antibody: principles and clinical application. *Clinical & developmental immunology* **2012**, 980250.

Alvarez, A.E., Marson, F.A.L., Bertuzzo, C.S., Bastos, J.C.S., Baracat, E.C.E., Brandao, M.B., Tresoldi, A.T., das Neves Romaneli, M.T., Almeida, C.C.B., de Oliveira, T., Schlodtmann, P.G., Correa, E., de Miranda, M.L.F., Dos Reis, M.C., De Pieri, J.V., Arns, C.W. and Ribeiro, J.D. (2018) Association between single nucleotide polymorphisms in TLR4, TLR2, TLR9, VDR, NOS2 and CCL5 genes with acute viral bronchiolitis. *Gene* **645**, 7-17.

Alvarez, M.L. and Cardineau, G.A. (2010) Prevention of bubonic and pneumonic plague using plant-derived vaccines. *Biotechnol. Adv.* **28**, 184-196.

Anderson, L.J., Hierholzer, J.C., Tsou, C., Hendry, R.M., Fernie, B.F., Stone, Y. and McIntosh, K. (1985) Antigenic characterization of respiratory syncytial virus strains with monoclonal antibodies. *The Journal of infectious diseases* **151**, 626-633.

Andris-Widhopf, J., Steinberger, P., Fuller, R., Rader, C. and Barbas, C.F. (2011) Generation of human scFv antibody libraries: PCR amplification and assembly of light-and heavy-chain coding sequences. *Cold Spring Harb. Protoc.* **2011**, pdb. prot065573.

August, A., Glenn, G.M., Kpamegan, E., Hickman, S.P., Jani, D., Lu, H., Thomas, D.N., Wen, J., Piedra, P.A. and Fries, L.F. (2017) A Phase 2 randomized, observer-blind, placebo-controlled, dose-ranging trial of aluminum-adjuvanted respiratory syncytial virus F particle vaccine formulations in healthy women of childbearing age. *Vaccine* **35**, 3749-3759.

Baert, K., de Geest, B.G., de Rycke, R., da Fonseca Antunes, A.B., de Greve, H., Cox, E. and Devriendt, B. (2015) β-glucan microparticles targeted to epithelial APN as oral antigen delivery system. *J. Control. Release* **220**, 149-159.

Bakshi, S., Depicker, A., Schepens, B., Saelens, X. and Juarez, P. (2019) A two-amino acid mutation in murine IgA enables downstream processing and purification on staphylococcal superantigen- like protein 7. *J. Biotechnol.* **294**, 26-29.

Bardor, M., Faveeuw, C., Fitchette, A.C., Gilbert, D., Galas, L., Trottein, F., Faye, L. and Lerouge, P. (2003) Immunoreactivity in mammals of two typical plant glyco-epitopes, core alpha(1,3)-fucose and core xylose. *Glycobiology* **13**, 427-434.

Battles, M.B. and McLellan, J.S. (2019) Respiratory syncytial virus entry and how to block it. *Nat. Rev. Microbiol.* **17**, 233-245.

Baxter, D. (2007) Active and passive immunity, vaccine types, excipients and licensing. *Occupational Medicine* **57**, 552-556.

Beigelman, A., Castro, M., Schweiger, T.L., Wilson, B.S., Zheng, J., Yin-DeClue, H., Sajol, G., Giri, T., Sierra, O.L., Isaacson-Schmid, M., Sumino, K., Schechtman, K.B. and Bacharier, L.B. (2015) Vitamin D Levels Are Unrelated to the Severity of Respiratory Syncytial Virus Bronchiolitis Among Hospitalized Infants. *J Pediatric Infect Dis Soc* **4**, 182-188.

Belderbos, M.E., Houben, M.L., Wilbrink, B., Lentjes, E., Bloemen, E.M., Kimpen, J.L., Rovers, M. and Bont, L. (2011) Cord blood vitamin D deficiency is associated with respiratory syncytial virus bronchiolitis. *Pediatrics* **127**, e1513-1520.

Bemark, M., Boysen, P. and Lycke, N.Y. (2012) Induction of gut IgA production through T cell-dependent and T cell-independent pathways. *Ann. NY Acad.Sci.* **1247**, 97-116.

Bilsborough, J. and Viney, J.L. (2004) Gastrointestinal dendritic cells play a role in immunity, tolerance, and disease. *Gastroenterology* **127**, 300-309.

Bitonti, A.J., Dumont, J.A., Low, S.C., Peters, R.T., Kropp, K.E., Palombella, V.J., Stattel, J.M., Lu, Y., Tan, C.A., Song, J.J., Garcia, A.M., Simister, N.E., Spiekermann, G.M., Lencer, W.I. and Blumberg, R.S. (2004) Pulmonary delivery of an erythropoietin Fc fusion protein in non-human primates through an immunoglobulin transport pathway. *Proc Natl Acad Sci U S A* **101**, 9763-9768.

Björck, L. (1988) Protein L. A novel bacterial cell wall protein with affinity for Ig L chains. *J. Immunol.* **140**, 1194-1197.

Blume, S. and Geesink, I. (2000) A brief history of polio vaccines. *Science (New York, N.Y.)* **288**, 1593-1594.

Boato, F., Thomas, R.M., Ghasparian, A., Freund-Renard, A., Moehle, K. and Robinson, J.A. (2007) Synthetic virus-like particles from self-assembling coiled-coil lipopeptides and their use in antigen display to the immune system. *Angew Chem Int Edit* **46**, 9015-9018.

Bodier-Montagutelli, E., Mayor, A., Vecellio, L., Respaud, R. and Heuze-Vourc'h, N. (2018) Designing inhaled protein therapeutics for topical lung delivery: what are the next steps? *Expert Opin Drug Deliv* **15**, 729-736.

Boes, A., Spiegel, H., Delbruck, H., Fischer, R., Schillberg, S. and Sack, M. (2011) Affinity purification of a framework 1 engineered mouse/human chimeric IgA2 antibody from tobacco. *Biotechnol. Bioeng.* **108**, 2804-2814.

Boothe, J., Nykiforuk, C., Shen, Y., Zaplachinski, S., Szarka, S., Kuhlman, P., Murray, E., Morck, D. and Moloney, M.M. (2010) Seed-based expression systems for plant molecular farming. *Plant Biotechnol. J.* **8**, 588-606.

Bootz, A., Karbach, A., Spindler, J., Kropff, B., Reuter, N., Sticht, H., Winkler, T.H., Britt, W.J. and Mach, M. (2017) Protective capacity of neutralizing and non-neutralizing antibodies against glycoprotein B of cytomegalovirus. *PLoS Pathog.* **13**.

Borchers, A.T., Chang, C., Gershwin, M.E. and Gershwin, L.J. (2013) Respiratory syncytial virus - A comprehensive review. *Clinical Reviews in Allergy & Immunology* **45**, 331-379.

Bosch, D., Castilho, A., Loos, A., Schots, A. and Steinkellner, H. (2013) N-Glycosylation of Plant-produced Recombinant Proteins. *Curr. Pharm. Design* **19**, 5503-5512.

Brandtzaeg, P. (2007) Induction of secretory immunity and memory at mucosal surfaces. *Vaccine* **25**, 5467-5484.

Brown, W.R., Kacskovics, I., Amendt, B.A., Blackmore, N.B., Rothschild, M., Shinde, R. and Butler, J.E. (1995) The hinge deletion allelic variant of porcine IgA results from a mutation at the splice acceptor site in the first C alpha intron. *J Immunol* **154**, 3836-3842.

Bruhns, P. (2012) Properties of mouse and human IgG receptors and their contribution to disease models. *Blood* **119**, 5640-5649.

Bruhns, P. and Jonsson, F. (2015) Mouse and human FcR effector functions. *Immunol. Rev.* **268**, 25-51.

Butler, J.E., Wertz, N., Deschacht, N. and Kacskovics, I. (2009) Porcine IgG: structure, genetics, and evolution. *Immunogenetics* **61**, 209-230.

Buyel, J.F., Twyman, R.M. and Fischer, R. (2017) Very-large-scale production of antibodies in plants: The biologization of manufacturing. *Biotechnol Adv* **35**, 458-465.

Cao, M., Wang, C., Chung, W.K., Motabar, D., Wang, J., Christian, E., Lin, S., Hunter, A., Wang, X. and Liu, D. (2018) Characterization and analysis of scFv-IgG bispecific antibody size variants. *Mabs-Austin* **10**, 1236-1247.

Cardoso, F.M., Ibanez, L.I., Van den Hoecke, S., De Baets, S., Smet, A., Roose, K., Schepens, B., Descamps, F.J., Fiers, W., Muyldermans, S., Depicker, A. and Saelens, X. (2014) Single-Domain Antibodies Targeting Neuraminidase Protect against an H5N1 Influenza Virus Challenge. *J. Virol.* **88**, 8278-8296.

Carmichael, J.R., Pal, S., Tifrea, D. and Luis, M. (2011) Induction of protection against vaginal shedding and infertility by a recombinant Chlamydia vaccine. *Vaccine* **29**, 5276-5283.

Carragher, D.M., Kaminski, D.A., Moquin, A., Hartson, L. and Randall, T.D. (2008) A novel role for non-neutralizing antibodies against nucleoprotein in facilitating resistance to influenza virus. *J. Immunol.* **181**, 4168-4176.

Carter, P.J. (2011) Introduction to current and future protein therapeutics: a protein engineering perspective. *Exp Cell Res* **317**, 1261-1269.

Ceballo, Y., Tiel, K., López, A., Cabrera, G., Pérez, M., Ramos, O., Rosabal, Y., Montero, C., Menassa, R. and Depicker, A. (2017) High accumulation in tobacco seeds of hemagglutinin antigen from avian (H5N1) influenza. *Transgenic Res.* **26**, 775-789.

Cerutti, A., Chen, K. and Chorny, A. (2011) Immunoglobulin responses at the mucosal interface. *Annual review of immunology* **29**, 273-293.

Chakravarty, R., Goel, S. and Cai, W.B. (2014) Nanobody: The "Magic Bullet" for Molecular Imaging? *Theranostics* **4**, 386-398.

Challa, D.K., Velmurugan, R., Ober, R.J. and Ward, E.S. (2014) FcRn: From Molecular Interactions to Regulation of IgG Pharmacokinetics and Functions. *Fc Receptors* **382**, 249-272.

Chan, H.T. and Daniell, H. (2015) Plant-made oral vaccines against human infectious diseases-Are we there yet? *Plant Biotechnol. J.* **13**, 1056-1070.

Chapleau, R.R., Frey, J.S., Riddle, D.S., Ruiz, O.N. and Mauzy, C.A. (2015) Measuring Single-Domain Antibody Interactions with Epitopes in Jet Fuel Using Microscale Thermophoresis. *Anal Lett* **48**, 526-530.

Cheng, W.W. and Allen, T.M. (2010) The use of single chain Fv as targeting agents for immunoliposomes: an update on immunoliposomal drugs for cancer treatment. *Expert Opin. Drug Deliv.* **7**, 461-478.

Chiu, M.L. and Gilliland, G.L. (2016) Engineering antibody therapeutics. *Curr. Opin. Struct. Biol.* **38**, 163-173.

Cho, H.-J., Kim, J.-Y., Lee, Y., Kim, J.M., Kim, Y.B., Chun, T. and Oh, Y.-K. (2010) Enhanced humoral and cellular immune responses after sublingual immunization against human papillomavirus 16 L1 protein with adjuvants. *Vaccine* **28**, 2598-2606.

Choi, E.H., Lee, H.J. and Chanock, S.J. (2013) Human genetics and respiratory syncytial virus disease: current findings and future approaches. *Curr Top Microbiol Immunol* **372**, 121-137.

Coddens, A., Loos, M., Vanrompay, D., Remon, J.P. and Cox, E. (2017) Cranberry extract inhibits *in vitro* adhesion of F4 and F18[+] *Escherichia coli* to pig intestinal epithelium and reduces *in vivo* excretion of pigs orally challenged with F18[+] verotoxigenic *E. coli*. *Vet. Microbiol.* **202**, 64-71.

Collins, P.L., Huang, Y.T. and Wertz, G.W. (1984) Nucleotide sequence of the gene encoding the fusion (F) glycoprotein of human respiratory syncytial virus. *Proceedings of the National Academy of Sciences* **81**, 7683-7687.

Conrath, K.E., Lauwereys, M., Galleni, M., Matagne, A., Frère, J.-M., Kinne, J., Wyns, L. and Muyldermans, S. (2001) β-Lactamase inhibitors derived from single-domain antibody fragments elicited in the *Camelidae*. *Antimicrob. Agents Chemother.* **45**, 2807-2812.

Cook, I.F. (2008) Evidence based route of administration of vaccines. *Hum. Vaccin.* **4**, 67-73.

Cook, I.F., Barr, I., Hartel, G., Pond, D. and Hampson, A.W. (2006) Reactogenicity and immunogenicity of an inactivated influenza vaccine administered by intramuscular or subcutaneous injection in elderly adults. *Vaccine* **24**, 2395-2402.

Corthesy, B. (2010) Role of secretory immunoglobulin A and secretory component in the protection of mucosal surfaces. *Future Microbiol.* **5**, 817-829.

Cortjens, B., Yasuda, E., Yu, X., Wagner, K., Claassen, Y.B., Bakker, A.Q., van Woensel, J.B.M. and Beaumont, T. (2017) Broadly Reactive Anti-Respiratory Syncytial Virus G Antibodies from Exposed Individuals Effectively Inhibit Infection of Primary Airway Epithelial Cells. *J. Virol.* **91**.

Cregg, J.M., Cereghino, J.L., Shi, J. and Higgins, D.R. (2000) Recombinant protein expression in *Pichia pastoris*. *Mol. Biotechnol.* **16**, 23-52.

Crowe, J.E., Murphy, B.R., Chanock, R.M., Williamson, R.A., Barbas, C.F. and Burton, D.R. (1994) Recombinant Human Respiratory Syncytial Virus (Rsv) Monoclonal-Antibody Fab Is Effective Therapeutically When Introduced Directly into the Lungs of Rsv-Infected Mice. *Proc. Natl. Acad. Sci. USA* **91**, 1386-1390.

Czajkowsky, D.M., Hu, J., Shao, Z.F. and Pleass, R.J. (2012) Fc-fusion proteins: new developments and future perspectives. *EMBO Mol. Med.* **4**, 1015-1028.

Czerkinsky, C. and Holmgren, J. (2010) Mucosal delivery routes for optimal immunization: targeting immunity to the right tissues. In: *Mucosal Vaccines* pp. 1-18. Springer.

Daeron, M., Latour, S., Malbec, O., Espinosa, E., Pina, P., Pasmans, S. and Fridman, W.H. (1995) The Same Tyrosine-Based Inhibition Motif, in the Intracytoplasmic Domain of Fc-Gamma-Riib, Regulates Negatively Bcr-Dependent, Tcr-Dependent, and Fcr-Dependent Cell Activation. *Immunity* **3**, 635-646.

Dall'Acqua, W.F., Kiener, P.A. and Wu, H. (2006) Properties of human IgG1s engineered for enhanced binding to the neonatal Fc receptor (FcRn). *J Biol Chem* **281**, 23514-23524.

Daniell, H., Streatfield, S.J. and Wycoff, K. (2001) Medical molecular farming: production of antibodies, biopharmaceuticals and edible vaccines in plants. *Trends Plant Sci.* **6**, 219-226.

Davies, J. and Riechmann, L. (1994) 'Camelising' human antibody fragments: NMR studies on VH domains. *FEBS Lett* **339**, 285-290.

De Buck, S., Nolf, J., De Meyer, T., Virdi, V., De Wilde, K., Van Lerberge, E., Van Droogenbroeck, B. and Depicker, A. (2013) Fusion of an Fc chain to a VHH boosts the accumulation levels in Arabidopsis seeds. *Plant Biotechnol J* **11**, 1006-1016.

De Buck, S., Virdi, V., De Meyer, T., De Wilde, K., Piron, R., Nolf, J., Van Lerberge, E., De Paepe, A. and Depicker, A. (2012) Production of camel-like antibodies in plants. *Methods Mol. Biol.* **911**, 305-324.

De Groof, T.W.M., Bobkov, V., Heukers, R. and Smit, M.J. (2019) Nanobodies: New avenues for imaging, stabilizing and modulating GPCRs. *Mol Cell Endocrinol* **484**, 15-24.

De Jaeger, G., Scheffer, S., Jacobs, A., Zambre, M., Zobell, O., Goossens, A., Depicker, A. and Angenon, G. (2002) Boosting heterologous protein production in transgenic dicotyledonous seeds using Phaseolus vulgaris regulatory sequences. *Nat. Biotechnol.* **20**, 1265-1268.

de Marco, A. (2009) Strategies for successful recombinant expression of disulfide bond-dependent proteins in Escherichia coli. *Microb. Cell Fact.* **8**.

de Marco, A. (2011) Biotechnological applications of recombinant single-domain antibody fragments. *Microb Cell Fact* **10**, 44.

De Meyer, T. and Depicker, A. (2014) Trafficking of endoplasmic reticulum-retained recombinant proteins is unpredictable in Arabidopsis thaliana. *Front. Plant Sci.* **5**.

De Meyer, T., Laukens, B., Nolf, J., Van Lerberge, E., De Rycke, R., De Beuckelaer, A., De Buck, S., Callewaert, N. and Depicker, A. (2015) Comparison of VHH-Fc antibody production in *Arabidopsis thaliana*, *Nicotiana benthamiana* and *Pichia pastoris*. *Plant Biotechnol. J.* **13**, 938-947.

De Meyer, T., Muyldermans, S. and Depicker, A. (2014) Nanobody-based products as research and diagnostic tools. *Trends Biotechnol.* **32**, 263-270.

De Muynck, B., Navarre, C. and Boutry, M. (2010) Production of antibodies in plants: status after twenty years. *Plant Biotechnol. J.* **8**, 529-563.

De Pourcq, K., De Schutter, K. and Callewaert, N. (2010) Engineering of glycosylation in yeast and other fungi: current state and perspectives. *Appl Microbiol Biotechnol* **87**, 1617-1631.

De Vlieger, D., Ballegeer, M., Rossey, I., Schepens, B. and Saelens, X. (2019) Single-Domain Antibodies and Their Formatting to Combat Viral Infections. *Antibodies* **8**, 1.

Dekkers, G., Bentlage, A.E.H., Stegmann, T.C., Howie, H.L., Lissenberg-Thunnissen, S., Zimring, J., Rispens, T. and Vidarsson, G. (2017) Affinity of human IgG subclasses to mouse Fc gamma receptors. *Mabs-Austin* **9**, 767-773.

Demento, S.L., Siefert, A.L., Bandyopadhyay, A., Sharp, F.A. and Fahmy, T.M. (2011) Pathogen-associated molecular patterns on biomaterials: a paradigm for engineering new vaccines. *Trends Biotechnol.* **29**, 294-306.

Detalle, L., Stohr, T., Palomo, C., Piedra, P.A., Gilbert, B.E., Mas, V., Millar, A., Power, U.F., Stortelers, C., Allosery, K., Melero, J.A. and Depla, E. (2016) Generation and Characterization of ALX-0171, a Potent Novel Therapeutic Nanobody for the Treatment of Respiratory Syncytial Virus Infection. *Antimicrob. Agents Chemother.* **60**, 6-13.

Devriendt, B., De Geest, B.G. and Cox, E. (2011) Designing oral vaccines targeting intestinal dendritic cells. *Expert Opin. Drug Deliv.* **8**, 467-483.

Devriendt, B., De Geest, B.G., Goddeeris, B.M. and Cox, E. (2012) Crossing the barrier: Targeting epithelial receptors for enhanced oral vaccine delivery. *J. Control. Release* **160**, 431-439.

Dingermann, T. (2008) Recombinant therapeutic proteins: production platforms and challenges. *Biotechnology Journal: Healthcare Nutrition Technology* **3**, 90-97.

Dirisala, V.R., Nair, R.R., Srirama, K., Reddy, P.N., Rao, K.R.S.S., Kumar, N.S.S. and Parvatam, G. (2017) Recombinant pharmaceutical protein production in plants: unraveling the therapeutic potential of molecular pharming. *Acta Physiol. Plant.* **39**.

Domachowske, J.B., Khan, A.A., Esser, M.T., Jensen, K., Takas, T., Villafana, T., Dubovsky, F. and Griffin, M.P. (2018) Safety, Tolerability and Pharmacokinetics of MEDI8897, an Extended Half-life Single-dose Respiratory Syncytial Virus Prefusion F-targeting Monoclonal Antibody Administered as a Single Dose to Healthy Preterm Infants. *Pediatr Infect Dis J* **37**, 886-892.

Domm, W., Brooks, L., Chung, H.L., Feng, C., Bowers, W.J., Watson, G., McGrath, J.L. and Dewhurst, S. (2011) Robust antigen-specific humoral immune responses to sublingually delivered adenoviral vectors encoding HIV-1 Env: association with mucoadhesion and efficient penetration of the sublingual barrier. *Vaccine* **29**, 7080-7089.

Donini, M. and Marusic, C. (2019) Current state-of-the-art in plant-based antibody production systems. *Biotechnol. Lett.* **41**, 335-346.

Duarte, J.N., Cragnolini, J.J., Swee, L.K., Bilate, A.M., Bader, J., Ingram, J.R., Rashidfarrokhi, A., Fang, T., Schiepers, A., Hanke, L. and Ploegh, H.L. (2016) Generation of immunity against pathogens via single-domain antibody–antigen constructs. *J. Immunol.* **197**, 4838-4847.

Dubel, S., Breitling, F., Fuchs, P., Zewe, M., Gotter, S., Welschof, M., Moldenhauer, G. and Little, M. (1994) Isolation of Igg Antibody Fv-DNA from Various Mouse and Rat Hybridoma Cell-Lines Using the Polymerase Chain-Reaction with a Simple Set of Primers. *J. Immunol. Methods* **175**, 89-95.

Ducancel, F. and Muller, B.H. (2012) Molecular engineering of antibodies for therapeutic and diagnostic purposes. In: *Mabs-Austin* pp. 445-457. Taylor & Francis.

Dudziak, D., Kamphorst, A.O., Heidkamp, G.F., Buchholz, V.R., Trumpfheller, C., Yamazaki, S., Cheong, C., Liu, K., Lee, H.-W. and Park, C.G. (2007) Differential antigen processing by dendritic cell subsets in vivo. *Science* **315**, 107-111.

Dumont, J., Euwart, D., Mei, B., Estes, S. and Kshirsagar, R. (2016) Human cell lines for biopharmaceutical manufacturing: history, status, and future perspectives. *Crit. Rev. Biotechnol.* **36**, 1110-1122.

Dunand, C.J.H., Leon, P.E., Huang, M., Choi, A., Chromikova, V., Ho, I.Y., Tan, G.S., Cruz, J., Hirsh, A., Zheng, N.Y., Mullarkey, C.E., Ennis, F.A., Terajima, M., Treanor, J.J., Topham, D.J., Subbarao, K., Palese, P., Krammer, F. and Wilson, P.C. (2016) Both Neutralizing and Non-Neutralizing Human H7N9 Influenza Vaccine-Induced Monoclonal Antibodies Confer Protection. *Cell Host Microbe* **19**, 800-813.

Duvvuri, V.R., Granados, A., Rosenfeld, P., Bahl, J., Eshaghi, A. and Gubbay, J.B. (2015) Genetic diversity and evolutionary insights of respiratory syncytial virus A ON1 genotype: global and local transmission dynamics. *Sci. Rep.* **5**.

Ecker, D.M., Jones, S.D. and Levine, H.L. (2015) The therapeutic monoclonal antibody market. *Mabs-Austin* **7**, 9-14.

Egli, J., Schlothauer, T., Spick, C., Seeber, S., Singer, T., Odermatt, A. and Iglesias, A. (2019) The Binding of Human IgG to Minipig FcRs - Implications for Preclinical Assessment of Therapeutic Antibodies. *Pharm. Res.* **36**.

Eiland, L.S. (2009) Respiratory syncytial virus: diagnosis, treatment and prevention. *J Pediatr Pharmacol Ther* **14**, 75-85.

Ellis, R.W. and Gerety, R.J. (1990) Key issues in the selection of an expression system for vaccine antigens. *J. Med. Virol.* **31**, 54-58.

Ewert, S., Cambillau, C., Conrath, K. and Pluckthun, A. (2002) Biophysical properties of camelid V-HH domains compared to those of human V(H)3 domains. *Biochemistry* **41**, 3628-3636.

Falsey, A.R., Hennessey, P.A., Formica, M.A., Cox, C. and Walsh, E.E. (2005) Respiratory syncytial virus infection in elderly and high-risk adults. *N. Engl. J. Med.* **352**, 1749-1759.

Fang, T., Van Elssen, C.H.M.J., Duarte, J.N., Guzman, J.S., Chahal, J.S., Ling, J. and Ploegh, H.L. (2017a) Targeted antigen delivery by an anti-class II MHC VHH elicits focused αMUC1(Tn) immunity. *Chem. Sci.* **8**, 5591-5597.

Fauroux, B., Simoes, E.A.F., Checchia, P.A., Paes, B., Figueras-Aloy, J., Manzoni, P., Bont, L. and Carbonell-Estrany, X. (2017) The Burden and Long-term Respiratory Morbidity Associated with Respiratory Syncytial Virus Infection in Early Childhood. *Infect Dis Ther* **6**, 173-197.

Folkesson, H.G., Westrom, B.R. and Karlsson, B.W. (1990) Permeability of the respiratory tract to different-sized macromolecules after intratracheal instillation in young and adult rats. *Acta Physiol Scand* **139**, 347-354.

Frenzel, A., Hust, M. and Schirrmann, T. (2013) Expression of recombinant antibodies. *Front. Immunol.* **4**, 217.

Fries, L., Shinde, V., Stoddard, J.J., Thomas, D.N., Kpamegan, E., Lu, H., Smith, G., Hickman, S.P., Piedra, P. and Glenn, G.M. (2017) Immunogenicity and safety of a respiratory syncytial virus fusion protein (RSV F) nanoparticle vaccine in older adults. *Immunity & ageing : I & A* **14**, 8.

Gallorini, S., Taccone, M., Bonci, A., Nardelli, F., Casini, D., Bonificio, A., Kommareddy, S., Bertholet, S., O'Hagan, D.T. and Baudner, B.C. (2014) Sublingual immunization with a subunit influenza vaccine elicits comparable systemic immune response as intramuscular immunization, but also induces local IgA and TH17 responses. *Vaccine* **32**, 2382-2388.

Gargett, T., Abbas, M.N., Rolan, P., Price, J.D., Gosling, K.M., Ferrante, A., Ruszkiewicz, A., Atmosukarto, I.I.C., Altin, J., Parish, C.R. and Brown, M.P. (2018) Phase I trial of Lipovaxin-MM, a novel dendritic cell-targeted liposomal vaccine for malignant melanoma. *Cancer Immunol. Immunother.* **67**, 1461-1472.

Geison, G.L. (1978) Pasteur Work on Rabies - Reexamining Ethical Issues. *Hastings Cent Rep* **8**, 26-33.

Ghaderi, D., Taylor, R.E., Padler-Karavani, V., Diaz, S. and Varki, A. (2010) Implications of the presence of N-glycolylneuraminic acid in recombinant therapeutic glycoproteins. *Nat. Biotechnol.* **28**, 863-U145.

Ghaderi, D., Zhang, M., Hurtado-Ziola, N. and Varki, A. (2012) Production platforms for biotherapeutic glycoproteins. Occurrence, impact, and challenges of non-human sialylation. *Biotechnol Genet Eng* **28**, 147-175.

Gilman, M.S., Castellanos, C.A., Chen, M., Ngwuta, J.O., Goodwin, E., Moin, S.M., Mas, V., Melero, J.A., Wright, P.F., Graham, B.S., McLellan, J.S. and Walker, L.M. (2016) Rapid profiling of RSV antibody repertoires from the memory B cells of naturally infected adult donors. *Science immunology* **1**.

Gleba, Y., Klimyuk, V. and Marillonnet, S. (2007) Viral vectors for the expression of proteins in plants. *Curr. Opin. Biotechnol.* **18**, 134-141.

Glezen, W.P., Taber, L.H., Frank, A.L. and Kasel, J.A. (1986) Risk of Primary Infection and Reinfection with Respiratory Syncytial Virus. *American Journal of Diseases of Children* **140**, 543-546.

Gomes, A.M.V., Carmo, T.S., Carvalho, L.S., Bahia, F.M. and Parachin, N.S. (2018) Comparison of Yeasts as Hosts for Recombinant Protein Production. *Microorganisms* **6**.

Gomord, V., Fitchette, A.C., Menu-Bouaouiche, L., Saint-Jore-Dupas, C., Plasson, C., Michaud, D. and Faye, L. (2010) Plant-specific glycosylation patterns in the context of therapeutic protein production. *Plant Biotechnol. J.* **8**, 564-587.

Gonzalez-Reyes, L., Ruiz-Arguello, M.B., Garcia-Barreno, B., Calder, L., Lopez, J.A., Albar, J.P., Skehel, J.J., Wiley, D.C. and Melero, J.A. (2001) Cleavage of the human respiratory syncytial virus fusion protein at two distinct sites is required for activation of membrane fusion. *Proc. Natl. Acad. Sci. USA* **98**, 9859-9864.

Graham, B.S. (2019) Immunological goals for respiratory syncytial virus vaccine development. *Curr. Opin. Immunol.* **59**, 57-64.

Greenberg, A.S., Avila, D., Hughes, M., Hughes, A., Mckinney, E.C. and Flajnik, M.F. (1995) A New Antigen Receptor Gene Family That Undergoes Rearrangement and Extensive Somatic Diversification in Sharks. *Nature* **374**, 168-173.

Groskreutz, D.J., Monick, M.M., Babor, E.C., Nyunoya, T., Varga, S.M., Look, D.C. and Hunninghake, G.W. (2009) Cigarette Smoke Alters Respiratory Syncytial Virus-Induced Apoptosis and Replication. *Am. J. Respir. Cell Mol. Biol.* **41**, 189-198.

Guilleminault, L., Azzopardi, N., Arnoult, C., Sobilo, J., Herve, V., Montharu, J., Guillon, A., Andres, C., Herault, O., Le Pape, A., Diot, P., Lemarie, E., Paintaud, G., Gouilleux-Gruart, V. and Heuze-Vourc'h, N. (2014) Fate of inhaled monoclonal antibodies after the deposition of aerosolized particles in the respiratory system. *J Control Release* **196**, 344-354.

Guillon, A., Pardessus, J., Lhommet, P., Parent, C., Respaud, R., Marchand, D., Montharu, J., De Monte, M., Janiak, P., Boixel, C., Audat, H., Huille, S., Guillot, E. and Heuze-Vourc'h, N. (2019) Exploring the fate of inhaled monoclonal antibody in the lung parenchyma by microdialysis. *Mabs-Austin* **11**, 297-304.

Gulati, S., Jin, H., Masuho, I., Orban, T., Cai, Y., Pardon, E., Martemyanov, K.A., Kiser, P.D., Stewart, P.L., Ford, C.P., Steyaert, J. and Palczewski, K. (2018) Targeting G protein-coupled receptor signaling at the G protein level with a selective nanobody inhibitor. *Nat. Commun.* **9**.

Gunaydin, G., Yu, S.Z., Graslund, T., Hammarstrom, L. and Marcotte, H. (2016) Fusion of the mouse IgG1 Fc domain to the VHH fragment (ARP1) enhances protection in a mouse model of rotavirus. *Sci. Rep.* **6**.

Guo, J., Li, F., He, Q., Jin, H., Liu, M., Li, S., Hu, S., Xiao, Y., Bi, D. and Li, Z. (2016) Neonatal Fc receptor-mediated IgG transport across porcine intestinal epithelial cells: potentially provide the mucosal protection. *DNA Cell Biol.* **35**, 301-309.

Gutjahr, A., Tiraby, G., Perouzel, E., Verrier, B. and Paul, S. (2016) Triggering intracellular receptors for vaccine adjuvantation. *Trends Immunol.* **37**, 573-587.

Hall, C.B., Walsh, E.E., Long, C.E. and Schnabel, K.C. (1991) Immunity to and Frequency of Reinfection with Respiratory Syncytial Virus. *J. Infect. Dis.* **163**, 693-698.

Hamers-Casterman, C., Atarhouch, T., Muyldermans, S., Robinson, G., Hammers, C., Songa, E.B., Bendahman, N. and Hammers, R. (1993) Naturally occurring antibodies devoid of light chains. *Nature* **363**, 446.

Hart, T.K., Cook, R.M., Zia-Amirhosseini, P., Minthorn, E., Sellers, T.S., Maleeff, B.E., Eustis, S., Schwartz, L.W., Tsui, P., Appelbaum, E.R., Martin, E.C., Bugelski, P.J. and Herzyk, D.J. (2001) Preclinical efficacy and safety of mepolizumab (SB-240563), a humanized monoclonal antibody to IL-5, in cynomolgus monkeys. *J Allergy Clin Immunol* **108**, 250-257.

Hasegawa, H., van Reit, E. and Kida, H. (2015) Mucosal Immunization and Adjuvants. *Curr Top Microbiol* **386**, 371-380.

Heesters, B.A., van der Poel, C.E., Das, A. and Carroll, M.C. (2016) Antigen Presentation to B Cells. *Trends Immunol.* **37**, 844-854.

Hellemans, J., Mortier, G., De Paepe, A., Speleman, F. and Vandesompele, J. (2007) qBase relative quantification framework and software for management and automated analysis of real-time quantitative PCR data. *Genome Biol* **8**, R19.

Helma, J., Cardoso, M.C., Muyldermans, S. and Leonhardt, H. (2015) Nanobodies and recombinant binders in cell biology. *J. Cell Biol.* **209**, 633-644.

Herce, H.D., Deng, W., Helma, J., Leonhardt, H. and Cardoso, M.C. (2013) Visualization and targeted disruption of protein interactions in living cells. *Nat. Commun.* **4**.

Hessell, A.J., Hangartner, L., Hunter, M., Havenith, C.E., Beurskens, F.J., Bakker, J.M., Lanigan, C.M., Landucci, G., Forthal, D.N., Parren, P.W., Marx, P.A. and Burton, D.R. (2007) Fc receptor but not complement binding is important in antibody protection against HIV. *Nature* **449**, 101-104.

Hiatt, A., Bohorova, N., Bohorov, O., Goodman, C., Kim, D., Pauly, M.H., Velasco, J., Whaley, K.J., Piedra, P.A., Gilbert, B.E. and Zeitlin, L. (2014) Glycan variants of a respiratory syncytial virus antibody with enhanced effector function and in vivo efficacy. *Proc. Natl. Acad. Sci. USA* **111**, 5992-5997.

Hiatt, A., Cafferkey, R. and Bowdish, K. (1989) Production of Antibodies in Transgenic Plants. *Nature* **342**, 76-78.

Hiatt, A. and Pauly, M. (2006) Monoclonal antibodies from plants: A new speed record. *Proc. Natl. Acad. Sci. USA* **103**, 14645-14646.

Hoekema, A., Hirsch, P.R., Hooykaas, P.J.J. and Schilperoort, R.A. (1983) A Binary Plant Vector Strategy Based on Separation of Vir-Region and T-Region of the Agrobacterium-Tumefaciens Ti-Plasmid. *Nature* **303**, 179-180

Holmgren, J. and Czerkinsky, C. (2005) Mucosal immunity and vaccines. *Nat. Med.* **11**, S45.

Huang, L., Gainkam, L.O.T., Caveliers, V., Vanhove, C., Keyaerts, M., De Baetselier, P., Bossuyt, A., Revets, H. and Lahoutte, T. (2008) SPECT imaging with Tc-99m-labeled EGFR-specific nanobody for in vivo monitoring of EGFR expression. *Mol. Imaging Biol.* **10**, 167-175.

Hultberg, A., Temperton, N.J., Rosseels, V., Koenders, M., Gonzalez-Pajuelo, M., Schepens, B., Ibanez, L.I., Vanlandschoot, P., Schillemans, J., Saunders, M., Weiss, R.A., Saelens, X., Melero, J.A., Verrips, C.T., Van Gucht, S. and de Haard, H.J. (2011) Llama-Derived Single Domain Antibodies to Build Multivalent, Superpotent and Broadened Neutralizing Anti-Viral Molecules. *PLoS ONE* **6**.

Hunter, Z., Smyth, H.D., Durfee, P. and Chackerian, B. (2009) Induction of mucosal and systemic antibody responses against the HIV coreceptor CCR5 upon intramuscular immunization and aerosol delivery of a virus-like particle based vaccine. *Vaccine* **28**, 403-414.

Hussack, G., Ryan, S., van Faassen, H., Rossotti, M., MacKenzie, C.R. and Tanha, J. (2018) Neutralization of Clostridium difficile toxin B with VHH-Fc fusions targeting the delivery and CROPs domains. *PLoS ONE* **13**.

Ibanez, L.I., De Filette, M., Hultberg, A., Verrips, T., Temperton, N., Weiss, R.A., Vandevelde, W., Schepens, B., Vanlandschoot, P. and Saelens, X. (2011) Nanobodies With In Vitro Neutralizing Activity Protect Mice Against H5N1 Influenza Virus Infection. *J. Infect. Dis.* **203**, 1063-1072.

Jacobino, S.R., Nederend, M., Reijneveld, J.F., Augustijn, D., Jansen, J.H.M., Meeldijk, J., Reiding, K.R., Wuhrer, M., Coenjaerts, F.E.J., Hack, C.E., Bont, L.J. and Leusen, J.H.W. (2018) Reformatting palivizumab and motavizumab from IgG to human IgA impairs their efficacy against RSV infection in vitro and in vivo. *Mabs-Austin* **10**, 453-462.

Jacobs, B.L., Langland, J.O., Kibler, K.V., Denzler, K.L., White, S.D., Holechek, S.A., Wong, S., Huynh, T. and Baskin, C.R. (2009) Vaccinia virus vaccines: past, present and future. *Antiviral Res.* **84**, 1-13.

Jafri, H.S., Wu, X.H., Makari, D. and Henrickson, K.J. (2013) Distribution of Respiratory Syncytial Virus Subtypes A and B Among Infants Presenting to the Emergency Department With Lower Respiratory Tract Infection or Apnea. *Pediatr Infect Dis J* **32**, 335-340.

Jang, J.I., Kim, J.S., Eom, J.S., Kim, H.G., Kim, B.H., Lim, S., Bang, I.S. and Park, Y.K. (2012) Expression and delivery of tetanus toxin fragment C fused to the N-terminal domain of SipB enhances specific immune responses in mice. *Microbiol Immunol* **56**, 595-604.

Jefferis, R. (2007) Antibody therapeutics: isotype and glycoform selection. *Expert Opin. Biol. Ther.* **7**, 1401-1413.

Jin, C., Altmann, F., Strasser, R., Mach, L., Schahs, M., Kunert, R., Rademacher, T., Glossl, J. and Steinkellner, H. (2008) A plant-derived human monoclonal antibody induces an anti-carbohydrate immune response in rabbits. *Glycobiology* **18**, 235-241.

Johnson, J.N., Barrett, C.S., Franklin, W.H., Graham, E.M., Halnon, N.J., Hattendorf, B.A., Krawczeski, C.D., McGovern, J.J., O'Connor, M.J., Schultz, A.H., Vinocur, J.M., Chowdhury, D. and Anderson, J.B. (2017) Development of quality metrics for ambulatory pediatric cardiology: Infection prevention. *Congenit Heart Dis* **12**, 756-761.

Juarez, P., Huet-Trujillo, E., Sarrion-Perdigones, A., Falconi, E.E., Granell, A. and Orzaez, D. (2013) Combinatorial Analysis of Secretory Immunoglobulin A (sIgA) Expression in Plants. *Int J Mol Sci* **14**, 6205-6222.

Juarez, P., Presa, S., Espi, J., Pineda, B., Anton, M.T., Moreno, V., Buesa, J., Granell, A. and Orzaez, D. (2012) Neutralizing antibodies against rotavirus produced in transgenically labelled purple tomatoes. *Plant Biotechnol. J.* **10**, 341-352.

Juarez, P., Virdi, V., Depicker, A. and Orzaez, D. (2016) Biomanufacturing of protective antibodies and other therapeutics in edible plant tissues for oral applications. *Plant Biotechnol. J.* **14**, 1791-1799.

Junt, T., Scandella, E. and Ludewig, B. (2008) Form follows function: lymphoid tissue microarchitecture in antimicrobial immune defence. *Nat. Rev. Immunol.* **8**, 764.

Karron, R.A. and Black, R.E. (2017) Determining the burden of respiratory syncytial virus disease: the known and the unknown. *Lancet* **390**, 917-918.

Keler, T., He, L., Ramakrishna, V. and Champion, B. (2007) Antibody-targeted vaccines. *Oncogene* **26**, 3758.

Kerr, M.A. (1990) The structure and function of human IgA. *Biochem. J.* **271**, 285-296.

Kim, H.W., Canchola, J.G., Brandt, C.D., Pyles, G., Chanock, R.M., Jensen, K. and Parrott, R.H. (1969) Respiratory syncytial virus disease in infants despite prior administration of antigenic inactivated vaccine. *Am J Epidemiol* **89**, 422-434.

Kim, S.-H. and Jang, Y.-S. (2017) The development of mucosal vaccines for both mucosal and systemic immune induction and the roles played by adjuvants. *Clin. Exp. Vaccine Res.* **6**, 15-21.

Klimyuk, V., Pogue, G., Herz, S., Butler, J. and Haydon, H. (2014) Production of recombinant antigens and antibodies in Nicotiana benthamiana using 'magnifection' technology: GMP-compliant facilities for small- and large-scale manufacturing. *Curr Top Microbiol Immunol* **375**, 127-154.

Klooster, R., Maassen, B.T., Stam, J.C., Hermans, P.W., Ten Haaft, M.R., Detmers, F.J., de Haard, H.J., Post, J.A. and Theo Verrips, C. (2007) Improved anti-IgG and HSA affinity ligands: clinical application of VHH antibody technology. *J Immunol Methods* **324**, 1-12.

Kneyber, M.C., Brandenburg, A.H., de Groot, R., Joosten, K.F., Rothbarth, P.H., Ott, A. and Moll, H.A. (1998) Risk factors for respiratory syncytial virus associated apnoea. *European journal of pediatrics* **157**, 331-335.

Ko, K. and Koprowski, H. (2005) Plant biopharming of monoclonal antibodies. *Virus Res.* **111**, 93-100.

Kobayashi, N., Ohtoyo, M., Wada, E., Kato, Y., Mano, N. and Goto, J. (2005) Generation of a single-chain Fv fragment for the monitoring of deoxycholic acid residues anchored on endogenous proteins. *Steroids* **70**, 285-294.

Kolpe, A., Schepens, B., Ye, L., Staeheli, P. and Saelens, X. (2018) Passively transferred M2e-specific monoclonal antibody reduces influenza A virus transmission in mice. *Antiviral Res* **158**, 244-254.

Kong, S., Zhang, Y.H. and Zhang, W. (2018) Regulation of Intestinal Epithelial Cells Properties and Functions by Amino Acids. *Biomed Res. Int.* **2018**, 2819154.

Krarup, A., Truan, D., Furmanova-Hollenstein, P., Bogaert, L., Bouchier, P., Bisschop, I.J.M., Widjojoatmodjo, M.N., Zahn, R., Schuitemaker, H., McLellan, J.S. and Langedijk, J.P.M. (2015) A highly stable prefusion RSV F vaccine derived from structural analysis of the fusion mechanism. *Nat Commun* **6**, 8143.

Krebbers, E., Herdies, L., De Clercq, A., Seurinck, J., Leemans, J., Van Damme, J., Segura, M., Gheysen, G., Van Montagu, M. and Vandekerckhove, J. (1988) Determination of the Processing Sites of an Arabidopsis 2S Albumin and Characterization of the Complete Gene Family. *Plant Physiol* **87**, 859-866.

Kuberl, A., Schneider, J., Thallinger, G.G., Anderl, I., Wibberg, D., Hajek, T., Jaenicke, S., Brinkrolf, K., Goesmann, A., Szczepanowski, R., Puhler, A., Schwab, H., Glieder, A. and Pichler, H. (2011) High-quality genome sequence of Pichia pastoris CBS7435. *J. Biotechnol.* **154**, 312-320.

Kurjan, J. and Herskowitz, I. (1982) Structure of a yeast pheromone gene (MFα): a putative α-factor precursor contains four tandem copies of mature α-factor. *Cell* **30**, 933-943.

Lafaye, P. and Li, T. (2018) Use of camel single-domain antibodies for the diagnosis and treatment of zoonotic diseases. *Comp. Immunol. Microbiol. Infect. Dis.* **60**, 17-22.

Lagassé, H.D., Hengel, H., Golding, B. and Sauna, Z.E. (2019) Fc-Fusion Drugs Have FcγR/C1q Binding and Signaling Properties That May Affect Their Immunogenicity. *The AAPS journal* **21**, 62.

Laham, F.R., Mansbach, J.M., Piedra, P.A., Hasegawa, K., Sullivan, A.F., Espinola, J.A. and Camargo, C.A. (2017) Clinical Profiles of Respiratory Syncytial Virus Subtypes a and B among Children Hospitalized with Bronchiolitis. *Pediatr Infect Dis J* **36**, 808-810.

Landry, N., Ward, B.J., Trepanier, S., Montomoli, E., Dargis, M., Lapini, G. and Vezina, L.P. (2010) Preclinical and Clinical Development of Plant-Made Virus-Like Particle Vaccine against Avian H5N1 Influenza. *PLoS ONE* **5**.

Laursen, N.S., Friesen, R.H.E., Zhu, X., Jongeneelen, M., Blokland, S., Vermond, J., van Eijgen, A., Tang, C., van Diepen, H., Obmolova, G., van der Neut Kolfschoten, M., Zuijdgeest, D., Straetemans, R., Hoffman, R.M.B., Nieusma, T., Pallesen, J., Turner, H.L., Bernard, S.M., Ward, A.B., Luo, J., Poon, L.L.M., Tretiakova, A.P., Wilson, J.M., Limberis, M.P., Vogels, R., Brandenburg, B., Kolkman, J.A. and Wilson, I.A. (2018) Universal protection against influenza infection by a multidomain antibody to influenza hemagglutinin. *Science* **362**, 598-602.

LeBoeuf, R.D., Galin, F.S., Hollinger, S.K., Peiper, S.C. and Blalock, J.E. (1989) Cloning and sequencing of immunoglobulin variable-region genes using degenerate oligodeoxyribonucleotides and polymerase chain reaction. *Gene* **82**, 371-377.

Lee, S.E., Nguyen, C.T., Kim, S.Y., Thi, T.N. and Rhee, J.H. (2015) Tetanus toxin fragment C fused to flagellin makes a potent mucosal vaccine. *Clin Exp Vaccine Res* **4**, 59-67.

Lee, Y.I., Peng, C.C., Chiu, N.C., Huang, D.T.N., Huang, F.Y. and Chi, H. (2016) Risk factors associated with death in patients with severe respiratory syncytial virus infection. *J Microbiol Immunol* **49**, 737-742.

Lehmann, C., Heger, L., Heidkamp, G., Baranska, A., Lühr, J., Hoffmann, A. and Dudziak, D. (2016) Direct delivery of antigens to dendritic cells via antibodies specific for endocytic receptors as a promising strategy for future therapies. *Vaccines* **4**, 8.

Lery, L. and Richard, M. (1978) Rabies Vaccinations at Pasteur Institute of Lyon. *Ann. Microbiol.* **B129**, 291-295.

Leung, T.F., Lam, D.S.Y., Miu, T.Y., Hon, K.L., Chau, C.S.K., Ku, S.W., Lee, R.S.Y., Chow, P.Y., Chiu, W.K., Ng, D.K.K. and Respirology, H.K.S.P. (2014) Epidemiology and risk factors for severe respiratory syncytial virus infections requiring pediatric intensive care admission in Hong Kong children. *Infection* **42**, 343-350.

Levy, O. (2007) Innate immunity of the newborn: basic mechanisms and clinical correlates. *Nat. Rev. Immunol.* **7**, 379-390.

Li, E., Pedraza, A., Bestagno, M., Mancardi, S., Sanchez, R. and Burrone, O. (1997) Mammalian cell expression of dimeric small immune proteins (SIP). *Protein Eng* **10**, 731-736.

Lico, C., Chen, Q. and Santi, L. (2008) Viral vectors for production of recombinant proteins in plants. *J. Cell. Physiol.* **216**, 366-377.

Lim, J.A., Patkar, A., McDonagh, G. and Sinclair, A. (2010) Modeling Bioprocess Cost.

Liu, J.K. (2014) The history of monoclonal antibody development - Progress, remaining challenges and future innovations. *Annals of medicine and surgery* **3**, 113-116.

Lo, M.S., Brazas, R.M. and Holtzman, M.J. (2005) Respiratory syncytial virus nonstructural proteins NS1 and NS2 mediate inhibition of Stat2 expression and alpha/beta interferon responsiveness. *J. Virol.* **79**, 9315-9319.

Longet, S., Lundahl, M.L.E. and Lavelle, E.C. (2018) Targeted Strategies for Mucosal Vaccination. *Bioconjug Chem* **29**, 613-623.

Loos, A., Van Droogenbroeck, B., Hillmer, S., Grass, J., Pabst, M., Castilho, A., Kunert, R., Liang, M.F., Arcalis, E., Robinson, D.G., Depicker, A. and Steinkellner, H. (2011) Expression of Antibody Fragments with a Controlled N-Glycosylation Pattern and Induction of Endoplasmic Reticulum-Derived Vesicles in Seeds of Arabidopsis. *Plant Physiol.* **155**, 2036-2048.

Luca, S. and Mihaescu, T. (2013) History of BCG Vaccine. *Maedica* **8**, 53-58.

Lundqvist, C., Hammarström, M.-L., Athlin, L. and Hammarström, S. (1992) Isolation of functionally active intraepithelial lymphocytes and enterocytes from human small and large intestine. *J. Immunol. Methods* **152**, 253-263.

Lycke, N. (2012) Recent progress in mucosal vaccine development: potential and limitations. *Nat. Rev. Immunol.* **12**, 592-605.

Maillet, A., Congy-Jolivet, N., Le Guellec, S., Vecellio, L., Hamard, S., Courty, Y., Courtois, A., Gauthier, F., Diot, P., Thibault, G., Lemarie, E. and Heuze-Vourc'h, N. (2008) Aerodynamical, immunological and pharmacological properties of the anticancer antibody cetuximab following nebulization. *Pharm Res* **25**, 1318-1326.

Marillonnet, S., Thoeringer, C., Kandzia, R., Klimyuk, V. and Gleba, Y. (2005) Systemic Agrobacterium tumefaciens-mediated transfection of viral replicons for efficient transient expression in plants. *Nat Biotechnol* **23**, 718-723.

Mattu, T.S., Pleass, R.J., Willis, A.C., Kilian, M., Wormald, M.R., Lellouch, A.C., Rudd, P.M., Woof, J.M. and Dwek, R.A. (1998) The glycosylation and structure of human serum IgA1, Fab, and Fc regions and the role of *N*-glycosylation on Fcα receptor interactions. *J. Biol. Chem.* **273**, 2260-2272.

McCafferty, J., Griffiths, A.D., Winter, G. and Chiswell, D.J. (1990) Phage antibodies: filamentous phage displaying antibody variable domains. *Nature* **348**, 552-554.

McConnell, A.D., Zhang, X., Macomber, J.L., Chau, B., Sheffer, J.C., Rahmanian, S., Hare, E., Spasojevic, V., Horlick, R.A., King, D.J. and Bowers, P.M. (2014) A general approach to antibody thermostabilization. *Mabs-Austin* **6**, 1274-1282.

Meissner, H.C. (2016) Viral Bronchiolitis in Children. *N. Engl. J. Med.* **374**, 62-72.

Melkebeek, V., Rasschaert, K., Bellot, P., Tilleman, K., Favoreel, H., Deforce, D., De Geest, B.G., Goddeeris, B.M. and Cox, E. (2012) Targeting aminopeptidase N, a newly identified receptor for F4ac fimbriae, enhances the intestinal mucosal immune response. *Mucosal Immunol.* **5**, 635-645.

Menzel, S., Schwarz, N., Haag, F. and Koch-Nolte, F. (2018) Nanobody-Based Biologics for Modulating Purinergic Signaling in Inflammation and Immunity. *Front Pharmacol* **9**.

Meselson, M. and Yuan, R. (1968) DNA restriction enzyme from E. coli. *Nature* **217**, 1110-1114.

Meurens, F., Summerfield, A., Nauwynck, H., Saif, L. and Gerdts, V. (2012) The pig: a model for human infectious diseases. *Trends Microbiol.* **20**, 50-57.

Miyairi, I. and DeVincenzo, J.P. (2008) Human genetic factors and respiratory syncytial virus disease severity. *Clin Microbiol Rev* **21**, 686-703.

Mohanan, D., Slutter, B., Henriksen-Lacey, M., Jiskoot, W., Bouwstra, J.A., Perrie, Y., Kundig, T.M., Gander, B. and Johansen, P. (2010) Administration routes affect the quality of immune responses: A cross-sectional evaluation of particulate antigen-delivery systems. *J. Control. Release* **147**, 342-349.

Mohapatra, S.S. and Boyapalle, S. (2008) Epidemiologic, experimental, and clinical links between respiratory syncytial virus infection and asthma. *Clin Microbiol Rev* **21**, 495-504.

Monnier, P., Vigouroux, R. and Tassew, N. (2013) In vivo applications of single chain Fv (variable domain)(scFv) fragments. *Antibodies* **2**, 193-208.

Moonens, K., De Kerpel, M., Coddens, A., Cox, E., Pardon, E., Remaut, H. and De Greve, H. (2014) Nanobody mediated inhibition of attachment of F18 fimbriae expressing *Escherichia coli*. *PLoS ONE* **9**, e114691.

Mor, T.S. (2015) Molecular pharming's foot in the FDA's door: Protalix's trailblazing story. *Biotechnol. Lett.* **37**, 2147-2150.

Mora, A.L., Detalle, L., Gallup, J.M., Van Geelen, A., Stohr, T., Duprez, L. and Ackermann, M.R. (2018) Delivery of ALX-0171 by inhalation greatly reduces respiratory syncytial virus disease in newborn lambs. *Mabs-Austin* **10**, 778-795.

Mora, J.R. and von Andrian, U.H. (2009) Role of retinoic acid in the imprinting of gut-homing IgA-secreting cells. In: *Seminars in immunology* pp. 28-35. Elsevier.

Morell, A., Terry, W.D. and Waldmann, T.A. (1970) Metabolic Properties of Igg Subclasses in Man. *J. Clin. Invest.* **49**, 673-&.

Moyle, P.M. and Toth, I. (2013) Modern Subunit Vaccines: Development, Components, and Research Opportunities. *ChemMedChem* **8**, 360-376.

Mufson, M.A., Orvell, C., Rafnar, B. and Norrby, E. (1985) 2 Distinct Subtypes of Human Respiratory Syncytial Virus. *J. Gen. Virol.* **66**, 2111-2124.

Muyldermans, S. (2001) Single domain camel antibodies: current status. *J Biotechnol* **74**, 277-302.

Muyldermans, S. (2013) Nanobodies: natural single-domain antibodies. *Annu. Rev. Biochem.* **82**, 775-797.

Muyldermans, S., Atarhouch, T., Saldanha, J., Barbosa, J.A.R.G. and Hamers, R. (1994) Sequence and Structure of V-H Domain from Naturally-Occurring Camel Heavy-Chain Immunoglobulins Lacking Light-Chains. *Protein Eng.* **7**, 1129-1135.

Nair, H., Nokes, D.J., Gessner, B.D., Dherani, M., Madhi, S.A., Singleton, R.J., O'Brien, K.L., Roca, A., Wright, P.F., Bruce, N., Chandran, A., Theodoratou, E., Sutanto, A., Sedyaningsih, E.R., Ngama, M., Munywoki, P.K., Kartasasmita, C., Simoes, E.A., Rudan, I., Weber, M.W. and Campbell, H. (2010) Global burden of acute lower respiratory infections due to respiratory syncytial virus in young children: a systematic review and meta-analysis. *Lancet* **375**, 1545-1555.

Narasimhan, B., Goodman, J.T. and Vela Ramirez, J.E. (2016) Rational design of targeted next-generation carriers for drug and vaccine delivery. *Annu. Rev. Biomed. Eng.* **18**, 25-49.

Neutra, M.R. and Kozlowski, P.A. (2006) Mucosal vaccines: the promise and the challenge. *Nat Rev Immunol* **6**, 148-158.

Ngwuta, J.O., Chen, M., Modjarrad, K., Joyce, M.G., Kanekiyo, M., Kumar, A., Yassine, H.M., Moin, S.M., Killikelly, A.M., Chuang, G.Y., Druz, A., Georgiev, I.S., Rundlet, E.J., Sastry, M., Stewart-Jones, G.B.E., Yang, Y.P., Zhang, B.S., Nason, M.C., Capella, C., Peeples, M.E., Ledgerwood, J.E., McLellan, J.S., Kwong, P.D. and Graham, B.S. (2015) Prefusion F-specific antibodies determine the magnitude of RSV neutralizing activity in human sera. *Sci. Transl. Med.* **7**.

Niewiesk, S. and Prince, G. (2002) Diversifying animal models: the use of hispid cotton rats (Sigmodon hispidus) in infectious diseases. *Lab Anim-Uk* **36**, 357-372.

Nilson, B.H.K., Lögdberg, L., Kastern, W., Björck, L. and Åkerström, B. (1993) Purification of antibodies using protein-L-binding framework structures in the light-chain variable domain. *J. Immunol. Methods* **164**, 33-40.

Nimmerjahn, F., Bruhns, P., Horiuchi, K. and Ravetch, J.V. (2005) FcgammaRIV: a novel FcR with distinct IgG subclass specificity. *Immunity* **23**, 41-51.

Nimmerjahn, F. and Ravetch, J.V. (2007) Antibodies, Fc receptors and cancer. *Curr. Opin. Immunol.* **19**, 239-245.

Nimmerjahn, F. and Ravetch, J.V. (2008) Fc gamma receptors as regulators of immune responses. *Nat. Rev. Immunol.* **8**, 34-47.

Nimmerjahn, F. and Ravetch, J.V. (2011) FcgammaRs in health and disease. *Curr. Top. Microbiol. Immunol.* **350**, 105-125.

Nokes, D.J., Ngama, M., Bett, A., Abwao, J., Munywoki, P., English, M., Scott, J.A., Cane, P.A. and Medley, G.F. (2009) Incidence and severity of respiratory syncytial virus pneumonia in rural Kenyan children identified through hospital surveillance. *Clin Infect Dis* **49**, 1341-1349.

Null, D., Bimle, C., Weisman, L., Johnson, K., Steichen, J., Singh, S., Wang, E., Asztalos, E., Loeffler, A.M., Azimi, P.H., Lieberman, J.M., O'Donnell, N.E., Cooke, R.J., McCormick, K., Koo, W., Hammami, M., Milner, A.D., Gaon, P., Nachman, S., Tarpey, K.P., Sanchez, P.J., Broyles, R.S., Bratcher, D., Ball, M.V., Duda, F.J., DeCuir, P.M., Pollara, B., Nelson, L.S., Balbus, M., Schultz, M.J., Chipps, B.E., Givner, L.B., O'Shea, M., Everard, M., Pfeffer, K., Page, A.J., Dennehy, P.H., Modlin, J., Rhodes, T., DeVincenzo, N., Nickerson, B., Arrieta, A., Boucher, F.D., Keeney, R.E., Young, T.E., Stevens, J.C., Ariagno, R., Adams, M., Polak, M.J., Lynch, S.K., Gerdes, J.S., Kuba, M., Aouthmany, M., LaMar, K., Chang, G.Y.W., Shelton, M.M., Hadeed, S.K.W., Vasan, U., Hennessy, A., Yogev, R., Welliver, R.C., Tristram, D., Albin, C., Jefferson, T.T., Purdy, G.D., Buckner, C.M., Schlessel, J., Sia, C., Tan, B., Sankaran, K., Morley, C.J., White, D.K., Meissner, H.C., Frantz, I., Desai, S.A., Stanley, C.W., Inwood, R., Solecki, L.E., Wald, E., Smail, K., Fox, R.E., Taciak, V., Park, C.L., Vidyasagar, D., Redding, G., Mayock, D.E., Reuman, P.D., Bifano, E.M., Estrada, B., Mancao, M.Y., Hook, B., McDavid, G., Rowen, J.L., Patel, J.A., Robinson, J., Lee, B., Rodriguez, W., Arrobio, J., Hocker, J.R., McConnell, C., Piedimonte, G., Sosenko, I., Patel, B., Shervinski, S., Stobie, P.E., Perea, K., Chartrand, S.A., Wilson, M.C., de Lemos, R., Ramanathan, R., Barnett, B.A., Luber, S.R., Raszka, W.V., Holsclaw, D.S., Klein, D.L., Law, B.J., Balsan, M.J., Douglass, B.H., O'Sullivan, B.P., Spaulding, R., Van Dyke, R.B., Merza, A., Hendley, J.O., Boyle, R.J., Hughes, P.A., Horgan, M.J., Maynard, R.C., Teufert, K., Majure, M., George, J.A., Kuerschner, D.R., Ghai, V., Thomas, D., MacDonald, N., Kovesi, T., Blayney, M., Mani, C.S., San Joaquin, V.H., Roberts, L., Wiznia, A., Rosenberg, M., Karna, P., Murray, D.L., Lenney, W., Clayton, S., Oelberg, D.G., Reininger, M.M., Eppes, S.C., Childs, J.A., Gruber, W.C., Hazinski, T.R., Steinberg, E.A., Lopez, L.C., Elliott, G.R., Groothuis, J.R., Simoes, E.E.A.F., Hakim, A., Mimouni, F., Rubin, L., Sood, S.K., Sadiq, H.F., Marshall, T.G., Miller, D., Drayton, M.R., O'Neill, S., Chetcuti, P., Trupp, D.L., Heart, J., Cooper, E.R., Brown, E.R., Chetty, A., Rice, T.B., Rupar, D., Cho, C.T., Leff, R.D., Levine, S.D., Kolls, J.K., Hall, M., Smith, S.L., Schwartz, L., Lemen, R.J., Hall, C.B., Long, C.E., Panitch, H., Kolb, S.M., Colombo, J.L., Judy, C.G., Golembe, B.L., Anderson, J.D., McDonald, J., McCormack, D., Ruggerie, D.P., Triplett, C., Odom, M.W., Lopez-Cox, G., Sawyer, M.H., Connor, J.D., Fergie, J.E., Purcell, K., Kantak, A.D., Fihe, D.M., Davies, H.D., Mitchell, L., Subramanian, K.N.S.,

Smith, Y., St John, E.B., Stolz, J.W., Sheils, C., Cox, F., Foshee, W., Diaz, R., Coonce, S., Keyserling, H.L., Padrick, C.B., Lamprecht, C., Livingston, F.R., Langley, J.M., Weller, P., Cropp, G.J., Sola, A., Kumar, M.L., Lapin, C.D., Carlisle, P., Martz, R., Radetsky, M., Midani, S., Rathore, M.H., Riff, E.J., Shay, G.F., Hogvall, E., Russell, D.W., Thomson, A.H., Lawrey, S.M., Hardy, K., Harvey, K., Turner, R., Cox, E.O., Dana, A., Madan, A., Wallace, J., Stevens, D.C., Asmar, B., Selewski, N.A., Kelly, J., Klerr, T., Spruill, S., Conner, E.M., Carlin, D., Top, F.H. and Grp, T.I.-R.S. (1998) Palivizumab, a humanized respiratory syncytial virus monoclonal antibody, reduces hospitalization from respiratory syncytial virus infection in high-risk infants. *Pediatrics* **102**, 531-537.

Nuttall, J., Vine, N., Hadlington, J.L., Drake, P., Frigerio, L. and Ma, J.K.C. (2002) ER-resident chaperone interactions with recombinant antibodies in transgenic plants. *Eur. J. Biochem.* **269**, 6042-6051.

Ober, R.J., Radu, C.G., Ghetie, V. and Ward, E.S. (2001) Differences in promiscuity for antibody-FcRn interactions across species: implications for therapeutic antibodies. *Int. Immunol.* **13**, 1551-1559.

Ogunsemowo, O., Olaleye, D.O. and Odaibo, G.N. (2018) Human Respiratory Syncytial Virus Subtypes A and B Infection Among Children Attending Primary and Secondary Health Care Facilities in Ibadan, Nigeria. *Archives of basic and applied medicine* **6**, 73-78.

Ou, J., Guo, Z., Shi, J., Wang, X., Liu, J., Shi, B., Guo, F., Zhang, C. and Yang, D. (2014) Transgenic rice endosperm as a bioreactor for molecular pharming. *Plant Cell Rep.* **33**, 585-594.

Palaci, J., Virdi, V. and Depicker, A. (2019) Transformation strategies for stable expression of complex hetero-multimeric proteins like secretory immunoglobulin A in plants. *Plant Biotechnol J*.

Pardon, E., Laeremans, T., Triest, S., Rasmussen, S.G.F., Wohlkönig, A., Ruf, A., Muyldermans, S., Hol, W.G.J., Kobilka, B.K. and Steyaert, J. (2014) A general protocol for the generation of Nanobodies for structural biology. *Nat. Protoc.* **9**, 674-693.

Pasetti, M.F., Simon, J.K., Sztein, M.B. and Levine, M.M. (2011) Immunology of gut mucosal vaccines. *Immunol. Rev.* **239**, 125-148.

Patton, J.S., Bukar, J.G. and Eldon, M.A. (2004) Clinical pharmacokinetics and pharmacodynamics of inhaled insulin. *Clin Pharmacokinet* **43**, 781-801.

Paul, M. and Ma, J.K. (2011a) Plant-made pharmaceuticals: leading products and production platforms. *Biotechnol Appl Biochem* **58**, 58-67.

Paul, M., Reljic, R., Klein, K., Drake, P.M.W., van Dolleweerd, C., Pabst, M., Windwarder, M., Arcalis, E., Stoger, E., Altmann, F., Cosgrove, C., Bartolf, A., Baden, S. and Ma, J.K.-C. (2014) Characterization of a plant-produced recombinant human secretory IgA with broad neutralizing activity against HIV. *Mabs-Austin* **6**, 1585-1597.

Peipp, M., Saul, D., Barbin, K., Bruenke, J., Zunino, S.J., Niederweis, M. and Fey, G.H. (2004) Efficient eukaryotic expression of fluorescent scFv fusion proteins directed against CD antigens for FACS applications. *J Immunol Methods* **285**, 265-280.

Perez, J.M.J., Renisio, J.G., Prompers, J.J., van Platerink, C.J., Cambillau, C., Darbon, H. and Frenken, L.G.J. (2001) Thermal unfolding of a llama antibody fragment: A two-state reversible process. *Biochemistry* **40**, 74-83.

Peyvandi, F., Scully, M., Hovinga, J.A.K., Cataland, S., Knobl, P., Wu, H.F., Artoni, A., Westwood, J.P., Taleghani, M.M., Jilma, B., Callewaert, F., Ulrichts, H., Duby, C., Tersago, D. and Investigators, T. (2016) Caplacizumab for Acquired Thrombotic Thrombocytopenic Purpura. *N. Engl. J. Med.* **374**, 511-522.

Philibert, P., Stoessel, A., Wang, W., Sibler, A.P., Bec, N., Larroque, C., Saven, J.G., Courtete, J., Weiss, E. and Martineau, P. (2007) A focused antibody library for selecting scFvs expressed at high levels in the cytoplasm. *BMC Biotechnol.* **7**.

Piron, R., Santens, F., De Paepe, A., Depicker, A. and Callewaert, N. (2015) Using GlycoDelete to produce proteins lacking plant-specific N-glycan modification in seeds. *Nat Biotechnol* **33**, 1135-1137.

Pliaka, V., Kyriakopoulou, Z. and Markoulatos, P. (2012) Risks associated with the use of live-attenuated vaccine poliovirus strains and the strategies for control and eradication of paralytic poliomyelitis. *Expert Rev. Vaccines* **11**, 609-628.

Prince, G.A., Hemming, V.G., Horswood, R.L., Baron, P.A. and Chanock, R.M. (1987) Effectiveness of topically administered neutralizing antibodies in experimental immunotherapy of respiratory syncytial virus infection in cotton rats. *J Virol* **61**, 1851-1854.

Purcell, O., Opdensteinen, P., Chen, W., Lowenhaupt, K., Brown, A., Hermann, M., Cao, J., Tenhaef, N., Kallweit, E. and Kastilan, R. (2017) Production of functional anti-Ebola antibodies in Pichia pastoris. *ACS Synth. Biol.* **6**, 2183-2190.

Pyzik, M., Rath, T., Lencer, W.I., Baker, K. and Blumberg, R.S. (2015) FcRn: The Architect Behind the Immune and Nonimmune Functions of IgG and Albumin. *J. Immunol.* **194**, 4595-4603.

Qiu, X., Wong, G., Audet, J., Bello, A., Fernando, L., Alimonti, J.B., Fausther-Bovendo, H., Wei, H., Aviles, J. and Hiatt, E. (2014) Reversion of advanced Ebola virus disease in nonhuman primates with ZMapp. *Nature* **514**, 47.

Ramsland, P.A., Willoughby, N., Trist, H.M., Farrugia, W., Hogarth, P.M., Fraser, J.D. and Wines, B.D. (2007) Structural basis for evasion of IgA immunity by *Staphylococcus aureus* revealed in the complex of SSL7 with Fc of human IgA1. *Proc. Natl. Acad. Sci. USA* **104**, 15051-15056.

Randolph, G.J., Jakubzick, C. and Qu, C. (2008) Antigen presentation by monocytes and monocyte-derived cells. *Curr. Opin. Immunol.* **20**, 52-60.

Raven, N., Rasche, S., Kuehn, C., Anderlei, T., Klockner, W., Schuster, F., Henquet, M., Bosch, D., Buchs, J., Fischer, R. and Schillberg, S. (2015) Scaled-up manufacturing of recombinant antibodies produced by plant cells in a 200-L orbitally-shaken disposable bioreactor. *Biotechnol Bioeng* **112**, 308-321.

Ravetch, J.V. and Lanier, L.L. (2000) Immune inhibitory receptors. *Science* **290**, 84-89.

Rescigno, M., Urbano, M., Valzasina, B., Francolini, M., Rotta, G., Bonasio, R., Granucci, F., Kraehenbuhl, J.P. and Ricciardi-Castagnoli, P. (2001) Dendritic cells express tight junction proteins and penetrate gut epithelial monolayers to sample bacteria. *Nature Immunology* **2**, 361-367.

Ries, J., Kaplan, C., Platonova, E., Eghlidi, H. and Ewers, H. (2012) A simple, versatile method for GFP-based super-resolution microscopy via nanobodies. *Nat. Methods* **9**, 582-+.

Robinson, C.R. and Sauer, R.T. (1998) Optimizing the stability of single-chain proteins by linker length and composition mutagenesis. *Proc. Natl. Acad. Sci. USA* **95**, 5929-5934.

Roopenian, D.C. and Akilesh, S. (2007) FcRn: the neonatal Fc receptor comes of age. *Nat. Rev. Immunol.* **7**, 715.

Rossey, I., Gilman, M.S.A., Kabeche, S.C., Sedeyn, K., Wrapp, D., Kanekiyo, M., Chen, M., Mas, V., Spitaels, J., Melero, J.A., Graham, B.S., Schepens, B., McLellan, J.S. and Saelens, X. (2017) Potent single-domain antibodies that arrest respiratory syncytial virus fusion protein in its prefusion state. *Nat. Commun.* **8**.

Rossey, I., McLellan, J.S., Saelens, X. and Schepens, B. (2018) Clinical Potential of Prefusion RSV F-specific Antibodies. *Trends Microbiol.* **26**, 209-219.

Rothbauer, U., Zolghadr, K., Muyldermans, S., Schepers, A., Cardoso, M.C. and Leonhardt, H. (2008) A versatile nanotrap for biochemical and functional studies with fluorescent fusion proteins. *Mol. Cell. Proteomics* **7**, 282-289.

Rothbauer, U., Zolghadr, K., Tillib, S., Nowak, D., Schermelleh, L., Gahl, A., Backmann, N., Conrath, K., Muyldermans, S., Cardoso, M.C. and Leonhardt, H. (2006) Targeting and tracing antigens in live cells with fluorescent nanobodies. *Nat. Methods* **3**, 887-889.

Rotman, M., Welling, M.M., van den Boogaard, M.L., Moursel, L.G., van der Graaf, L.M., van Buchem, M.A., van der Maarel, S.M. and van der Weerd, L. (2015) Fusion of hIgG1-Fc to In-111-anti-amyloid single domain antibody fragment VHH-pa2H prolongs blood residential time in APP/PS1 mice but does not increase brain uptake. *Nucl Med Biol* **42**, 695-702.

Ruben, F.L., Froeschle, J.E., Meschievitz, C., Chen, K., George, J., Reeves-Hoché, M.K., Pietrobon, P., Bybel, M., Livingood, W.C. and Woodhouse, L. (2001) Choosing a route of administration for quadrivalent meningococcal polysaccharide vaccine: intramuscular versus subcutaneous. *Clinical infectious diseases* **32**, 170-172.

Rup, B., Alon, S., Amit-Cohen, B.C., Brill Almon, E., Chertkoff, R., Tekoah, Y. and Rudd, P.M. (2017) Immunogenicity of glycans on biotherapeutic drugs produced in plant expression systems-The taliglucerase alfa story. *PLoS ONE* **12**, e0186211.

Russell-Jones, G.J. (2000) Oral vaccine delivery. *J. Control. Release* **65**, 49-54.

Rybicki, E.P. (2010) Plant-made vaccines for humans and animals. *Plant Biotechnol J* **8**, 620-637.

Saerens, D., Frederix, F., Reekmans, G., Conrath, K., Jans, K., Brys, L., Huang, L., Bosmans, E., Maes, G., Borghs, G. and Muyldermans, S. (2005) Engineering camel single-domain antibodies and immobilization chemistry for human prostate-specific antigen sensing. *Anal. Chem.* **77**, 7547-7555.

Sallach, R.E., Conticello, V.P. and Chaikof, E.L. (2009) Expression of a recombinant elastin-like protein in *Pichia pastoris*. *Biotechnol. Prog.* **25**, 1810-1818.

Sanchez-Garcia, L., Martín, L., Mangues, R., Ferrer-Miralles, N., Vázquez, E. and Villaverde, A. (2016) Recombinant pharmaceuticals from microbial cells: a 2015 update. *Microb. Cell Fact.* **15**, 33.

Sarrion-Perdigones, A., Falconi, E.E., Zandalinas, S.I., Juárez, P., Fernández-del-Carmen, A., Granell, A. and Orzaez, D. (2011) GoldenBraid: an iterative cloning system for standardized assembly of reusable genetic modules. *PLoS ONE* **6**, e21622.

Schaefer, J.V., Honegger, A. and Plückthun, A. (2010) Construction of scFv fragments from hybridoma or spleen cells by PCR assembly. In: *Antibody engineering* pp. 21-44. Springer.

Schahs, M., Strasser, R., Stadlmann, J., Kunert, R., Rademacher, T. and Steinkellner, H. (2007) Production of a monoclonal antibody in plants with a humanized N-glycosylation pattern. *Plant Biotechnol J* **5**, 657-663.

Scheltema, N.M., Nibbelke, E.E., Pouw, J., Blanken, M.O., Rovers, M.M., Naaktgeboren, C.A., Mazur, N.I., Wildenbeest, J.G., van der Ent, C.K. and Bont, L.J. (2018) Respiratory syncytial virus prevention and asthma in healthy preterm infants: a randomised controlled trial. *Lancet Resp Med* **6**, 257-264.

Schepens, B., Ibanez, L.I., De Baets, S., Hultberg, A., Bogaert, P., De Bleser, P., Vervalle, F., Verrips, T., Melero, J., Vandevelde, W., Vanlandschoot, P. and Saelens, X. (2011) Nanobodies (R) Specific for Respiratory Syncytial Virus Fusion Protein Protect Against Infection by Inhibition of Fusion. *J. Infect. Dis.* **204**, 1692-1701.

Schepens, B., Sedeyn, K., Vande Ginste, L., De Baets, S., Schotsaert, M., Roose, K., Houspie, L., Van Ranst, M., Gilbert, B., van Rooijen, N., Fiers, W., Piedra, P. and Saelens, X. (2014) Protection and mechanism of action of a novel human respiratory syncytial virus vaccine candidate based on the extracellular domain of small hydrophobic protein. *EMBO Mol. Med.* **6**, 1436-1454.

Schirrmann, T., Al-Halabi, L., Dubel, S. and Hust, M. (2008) Production systems for recombinant antibodies. *Front Biosci* **13**, 4576-4594.

Schjetne, K.W., Fredriksen, A.B. and Bogen, B. (2007) Delivery of antigen to CD40 induces protective immune responses against tumors. *The Journal of Immunology* **178**, 4169-4176.

Schmidt, F.R. (2004) Recombinant expression systems in the pharmaceutical industry. *Appl. Microbiol. Biotechnol.* **65**, 363-372.

Schotte, L., Strauss, M., Thys, B., Halewyck, H., Filman, D.J., Bostina, M., Hogle, J.M. and Rombaut, B. (2014) Mechanism of action and capsid-stabilizing properties of VHHs with an in vitro antipolioviral activity. *J Virol* **88**, 4403-4413.

Shaaltiel, Y. and Tekoah, Y. (2016) Plant specific N-glycans do not have proven adverse effects in humans. *Nat. Biotechnol.* **34**, 706-+.

Shan, D., Press, O.W., Tsu, T.T., Hayden, M.S. and Ledbetter, J.A. (1999) Characterization of scFv-Ig constructs generated from the anti-CD20 mAb 1F5 using linker peptides of varying lengths. *J Immunol* **162**, 6589-6595.

Shen, Z., Yan, H., Zhang, Y., Mernaugh, R.L. and Zeng, X. (2008) Engineering peptide linkers for scFv immunosensors. *Anal Chem* **80**, 1910-1917.

Sheridan, B.S. and Lefrançois, L. (2011) Regional and mucosal memory T cells. *Nature immunology* **12**, 485.

Sheridan, C. (2017) Ablynx's nanobody fragments go places antibodies cannot. *Nat Biotechnol* **35**, 1115-1117.

Shi, T., McAllister, D.A., O'Brien, K.L., Simoes, E.A.F., Madhi, S.A., Gessner, B.D., Polack, F.P., Balsells, E., Acacio, S., Aguayo, C., Alassani, I., Ali, A., Antonio, M., Awasthi, S., Awori, J.O., Azziz-Baumgartner, E., Baggett, H.C., Baillie, V.L., Balmaseda, A., Barahona, A., Basnet, S., Bassat, Q., Basualdo, W., Bigogo, G., Bont, L., Breiman, R.F., Brooks, W.A., Broor, S., Bruce, N., Bruden, D., Buchy, P., Campbell, S., Carosone-Link, P., Chadha, M., Chipeta, J., Chou, M., Clara, W., Cohen, C., de Cuellar, E., Dang, D.A., Dash-yandag, B., Deloria-Knoll, M., Dherani, M., Eap, T., Ebruke, B.E., Echavarria, M., Emediato, C.C.D.L., Fasce, R.A., Feikin, D.R., Feng, L.Z., Gentile, A., Gordon, A., Goswami, D., Goyet, S., Groome, M., Halasa, N., Hirve, S., Homaira, N., Howie, S.R.C., Jara, J., Jroundi, I., Kartasasmita, C.B., Khuri-Bulos, N., Kotloff, K.L., Krishnan, A., Libster, R., Lopez, O., Lucero, M.G., Lucion, F., Lupisan, S.P., Marcone, D.N., McCracken, J.P., Mejia, M., Moisi, J.C., Montgomery, J.M., Moore, D.P., Moraleda, C., Moyes, J., Munywoki, P., Mutyara, K., Nicol, M.P., Nokes, D.J., Nymadawa, P., Oliveira, M.T.D., Oshitani, H., Pandey, N., Paranhos-Baccala, G., Phillips, L.N., Picot, V.S., Rahman, M., Rakoto-Andrianarivelo, M., Rasmussen, Z.A., Rath, B.A., Robinson, A., Romero, C., Russomando, G., Salimi, V., Sawatwong, P., Scheltema, N., Schweiger, B., Scott, J.A.G., Seidenberg, P., Shen, K.L., Singleton, R., Sotomayor, V., Strand, T.A., Sutanto, A., Sylla, M., Tapia, M.D., Thamthitiwat, S., Thomas, E.D., Tokarz, R., Turner, C., Venter, M., Waicharoen, S., Wang, J.W., Watthanaworawit, W., Yoshida, L.M., Yu, H.J., Zar, H.J., Campbell, H., Nair, H. and Network, R.G.E. (2017) Global, regional, and national disease burden estimates of acute lower respiratory infections due to respiratory syncytial virus in young children in 2015: a systematic review and modelling study. *Lancet* **390**, 946-958.

Shields, R.L., Lai, J., Keck, R., O'Connell, L.Y., Hong, K., Meng, Y.G., Weikert, S.H. and Presta, L.G. (2002) Lack of fucose on human IgG1 N-linked oligosaccharide improves binding to human Fcgamma RIII and antibody-dependent cellular toxicity. *J Biol Chem* **277**, 26733-26740.

Shoji, Y., Farrance, C.E., Bautista, J., Bi, H., Musiychuk, K., Horsey, A., Park, H., Jaje, J., Green, B.J. and Shamloul, M. (2012) A plant-based system for rapid production of influenza vaccine antigens. *Influenza and other respiratory viruses* **6**, 204-210.

Shukla, A.A., Wolfe, L.S., Mostafa, S.S. and Norman, C. (2017) Evolving trends in mAb production processes. *Bioeng Transl Med* **2**, 58-69.

Sidwell, R.W. and Barnard, D.L. (2006) Respiratory syncytial virus infections: Recent prospects for control. *Antiviral Res.* **71**, 379-390.

Simoes, E.A., DeVincenzo, J.P., Boeckh, M., Bont, L., Crowe, J.E., Jr., Griffiths, P., Hayden, F.G., Hodinka, R.L., Smyth, R.L., Spencer, K., Thirstrup, S., Walsh, E.E. and Whitley, R.J. (2015) Challenges and opportunities in developing respiratory syncytial virus therapeutics. *J Infect Dis* **211 Suppl 1**, S1-S20.

Singh, S., Kumar, N.K., Dwiwedi, P., Charan, J., Kaur, R., Sidhu, P. and Chugh, V.K. (2018) Monoclonal Antibodies: A Review. *Current clinical pharmacology* **13**, 85-99.

Skea, D.L., Christopoulous, P., Plaut, A.G. and Underdown, B.J. (1988) Studies on the specificity of the IgA-binding lectin, jacalin. *Mol. Immunol.* **25**, 1-6.

Skwarczynski, M., Dougall, A.M., Khoshnejad, M., Chandrudu, S., Pearson, M.S., Loukas, A. and Toth, I. (2012) Peptide-based subunit vaccine against hookworm infection. *PLoS ONE* **7**, e46870.

Sletta, H., Tondervik, A., Hakvag, S., Aune, T.E.V., Nedal, A., Aune, R., Evensen, G., Valla, S., Ellingsen, T.E. and Brautaset, T. (2007) The presence of N-terminal secretion signal sequences leads to strong stimulation of the total expression levels of three tested medically important proteins during high-cell-density cultivations of Escherichia coli. *Appl. Environ. Microbiol.* **73**, 906-912.

Smith, D.K., Seales, S. and Budzik, C. (2017) Respiratory Syncytial Virus Bronchiolitis in Children. *American family physician* **95**, 94-99.

Smith, G., Raghunandan, R., Wu, Y.Y., Liu, Y., Massare, M., Nathan, M., Zhou, B., Lu, H.X., Boddapati, S., Li, J.N., Flyer, D. and Glenn, G. (2012) Respiratory Syncytial Virus Fusion Glycoprotein Expressed in Insect Cells Form Protein Nanoparticles That Induce Protective Immunity in Cotton Rats. *PLoS ONE* **7**.

Smith, S.L. (1996) Ten years of Orthoclone OKT3 (muromonab-CD3): a review. *Journal of transplant coordination : official publication of the North American Transplant Coordinators Organization* **6**, 109-119; quiz 120-101.

Snoeck, V., Van den Broeck, W., De Colvenaer, V., Verdonck, F., Goddeeris, B. and Cox, E. (2008) Transcytosis of F4 fimbriae by villous and dome epithelia in F4-receptor positive pigs supports importance of receptor-dependent endocytosis in oral immunization strategies. *Vet. Immunol. Immunopathol.* **124**, 29-40.

Srivastava, A., Gowda, D.V., Madhunapantula, S.V., Shinde, C.G. and Iyer, M. (2015) Mucosal vaccines: a paradigm shift in the development of mucosal adjuvants and delivery vehicles. *Apmis* **123**, 275-288.

Stamova, S., Feldmann, A., Cartellieri, M., Arndt, C., Koristka, S., Apel, F., Wehner, R., Schmitz, M., Bornhauser, M., von Bonin, M., Ehninger, G., Bartsch, H. and Bachmann, M. (2012) Generation of single-chain bispecific green fluorescent protein fusion antibodies for imaging of antibody-induced T cell synapses. *Anal Biochem* **423**, 261-268.

Stapleton, N.M., Andersen, J.T., Stemerding, A.M., Bjarnarson, S.P., Verheul, R.C., Gerritsen, J., Zhao, Y.X., Kleijer, M., Sandlie, I., de Haas, M., Jonsdottir, I., van der Schoot, C.E. and Vidarsson, G. (2011) Competition for FcRn-mediated transport gives rise to short half-life of human IgG3 and offers therapeutic potential. *Nat. Commun.* **2**.

Steeland, S., Vandenbroucke, R.E. and Libert, C. (2016) Nanobodies as therapeutics: big opportunities for small antibodies. *Drug Discov. Today* **21**, 1076-1113.

Stein, R.T., Bont, L.J., Zar, H., Polack, F.P., Park, C., Claxton, A., Borok, G., Butylkova, Y. and Wegzyn, C. (2017) Respiratory syncytial virus hospitalization and mortality: Systematic review and meta-analysis. *Pediatr Pulmonol* **52**, 556-569.

Stirling, C.M., Charleston, B., Takamatsu, H., Claypool, S., Lencer, W., Blumberg, R.S. and Wileman, T.E. (2005) Characterization of the porcine neonatal Fc receptor--potential use for trans-epithelial protein delivery. *Immunology* **114**, 542-553.

Stoger, E., Fischer, R., Moloney, M. and Ma, J.K.C. (2014) Plant Molecular Pharming for the Treatment of Chronic and Infectious Diseases. *Annual Review of Plant Biology, Vol 65* **65**, 743-+.

Strasser, R., Stadlmann, J., Schahs, M., Stiegler, G., Quendler, H., Mach, L., Glossl, J., Weterings, K., Pabst, M. and Steinkellner, H. (2008) Generation of glyco-engineered Nicotiana benthamiana for the production of monoclonal antibodies with a homogeneous human-like N-glycan structure. *Plant Biotechnol J* **6**, 392-402.

Strohl, W.R. (2009) Optimization of Fc-mediated effector functions of monoclonal antibodies. *Curr. Opin. Biotechnol.* **20**, 685-691.

Strugnell, R.A. and Wijburg, O.L.C. (2010) The role of secretory antibodies in infection immunity. *Nat. Rev. Microbiol.* **8**, 656-667.

Suzuki, T., Ishii-Watabe, A., Tada, M., Kobayashi, T., Kanayasu-Toyoda, T., Kawanishi, T. and Yamaguchi, T. (2010) Importance of Neonatal FcR in Regulating the Serum Half-Life of Therapeutic Proteins

Containing the Fc Domain of Human IgG1: A Comparative Study of the Affinity of Monoclonal Antibodies and Fc-Fusion Proteins to Human Neonatal FcR. *J. Immunol.* **184**, 1968-1976.

Swiech, K., Picanco-Castro, V. and Covas, D.T. (2012) Human cells: New platform for recombinant therapeutic protein production. *Protein Expr. Purif.* **84**, 147-153.

Taleb, S.A., Al Thani, A.A., Al Ansari, K. and Yassine, H.M. (2018) Human respiratory syncytial virus: pathogenesis, immune responses, and current vaccine approaches. *Eur J Clin Microbiol Infect Dis* **37**, 1817-1827.

Tan, L., Coenjaerts, F.E.J., Houspie, L., Viveen, M.C., van Bleek, G.M., Wiertz, E.J.H.J., Martin, D.P. and Lemey, P. (2013) The Comparative Genomics of Human Respiratory Syncytial Virus Subgroups A and B: Genetic Variability and Molecular Evolutionary Dynamics. *J. Virol.* **87**, 8213-8226.

Tay, M.Z., Wiehe, K. and Pollara, J. (2019) Antibody-Dependent Cellular Phagocytosis in Antiviral Immune Responses. *Front. Immunol.* **10**, 332

Teplyakov, A., Obmolova, G., Malia, T.J., Raghunathan, G., Martinez, C., Fransson, J., Edwards, W., Connor, J., Husovsky, M. and Beck, H. (2018) Structural insights into humanization of anti-tissue factor antibody 10H10. In: *Mabs-Austin* pp. 269-277. Taylor & Francis.

Toleikis, L. and Frenzel, A. (2012) Cloning single-chain antibody fragments (ScFv) from hyrbidoma cells. *Methods Mol Biol* **907**, 59-71.

Travella, S., Ross, S.M., Harden, J., Everett, C., Snape, J.W. and Harwood, W.A. (2005) A comparison of transgenic barley lines produced by particle bombardment and Agrobacterium-mediated techniques. *Plant Cell Rep.* **23**, 780-789.

Tschofen, M., Knopp, D., Hood, E. and Stoger, E. (2016) Plant Molecular Farming: Much More than Medicines. *Annu Rev Anal Chem* **9**, 271-294.

Unciti-Broceta, J.D., Arias, J.L., Maceira, J., Soriano, M., Ortiz-Gonzalez, M., Hemandez-Quero, J., Munoz-Torres, M., de Koning, H.P., Magez, S. and Garcia-Salcedo, J.A. (2015) Specific Cell Targeting Therapy Bypasses Drug Resistance Mechanisms in African Trypanosomiasis. *PLoS Pathog.* **11**.

Unnikrishnan, M., Rappuoli, R. and Serruto, D. (2012) Recombinant bacterial vaccines. *Curr. Opin. Immunol.* **24**, 337-342.

Vaghchhipawala, Z., Rojas, C.M., Senthil-Kumar, M. and Mysore, K.S. (2011) Agroinoculation and agroinfiltration: simple tools for complex gene function analyses. In: *Plant Reverse Genetics* pp. 65-76. Springer.

Van Audenhove, I. and Gettemans, J. (2016) Nanobodies as versatile tools to understand, diagnose, visualize and treat cancer. *EBioMedicine* **8**, 40-48.

Van den Hoecke, S., Ehrhardt, K., Kolpe, A., El Bakkouri, K., Deng, L., Grootaert, H., Schoonooghe, S., Smet, A., Bentahir, M., Roose, K., Schotsaert, M., Schepens, B., Callewaert, N., Nimmerjahn, F., Staeheli, P., Hengel, H. and Saelens, X. (2017) Hierarchical and Redundant Roles of Activating FcgammaRs in Protection against Influenza Disease by M2e-Specific IgG1 and IgG2a Antibodies. *J Virol* **91**.

van der Linden, R.H., Frenken, L.G., de Geus, B., Harmsen, M.M., Ruuls, R.C., Stok, W., de Ron, L., Wilson, S., Davis, P. and Verrips, C.T. (1999) Comparison of physical chemical properties of llama VHH antibody fragments and mouse monoclonal antibodies. *Biochim Biophys Acta* **1431**, 37-46.

Van der Weken, H., Cox, E. and Devriendt, B. (2019) Rapid production of a chimeric antibody-antigen fusion protein based on 2A-peptide cleavage and green fluorescent protein expression in CHO cells. In: *Mabs-Austin*. Taylor & Francis.

van Drunen Littel-van den Hurk, S. and Watkiss, E.R. (2012) Pathogenesis of respiratory syncytial virus. *Curr Opin Virol* **2**, 300-305.

Van Heeke, G., Allosery, K., De Brabandere, V., De Smedt, T., Detalle, L. and de Fougerolles, A. (2017) Nanobodies (R)dagger as inhaled biotherapeutics for lung diseases. *Pharmacol Therapeut* **169**, 47-56.

Van Landuyt, L., Lonigro, C., Meuris, L. and Callewaert, N. (2018) Customized protein glycosylation to improve biopharmaceutical function and targeting. *Curr Opin Biotechnol* **60**, 17-28.

Van Roy, M., Ververken, C., Beirnaert, E., Hoefman, S., Kolkman, J., Vierboom, M., Breedveld, E., t Hart, B.A., Poelmans, S., Bontinck, L., Hemeryck, A., Jacobs, S., Baumeister, J. and Ulrichts, H. (2015) The preclinical pharmacology of the high affinity anti-IL-6R Nanobody (R) ALX-0061 supports its clinical development in rheumatoid arthritis. *Arthritis Research & Therapy* **17**.

Vanlandschoot, P., Stortelers, C., Beirnaert, E., Ibanez, L.I., Schepens, B., Depla, E. and Saelens, X. (2011) Nanobodies (R): New ammunition to battle viruses. *Antiviral Res.* **92**, 389-407.

Vartak, A. and Sucheck, S. (2016) Recent advances in subunit vaccine carriers. *Vaccines* **4**, 12.

Vermeer, A.W. and Norde, W. (2000) The thermal stability of immunoglobulin: unfolding and aggregation of a multi-domain protein. *Biophys J* **78**, 394-404.

Vermeer, A.W., Norde, W. and van Amerongen, A. (2000) The unfolding/denaturation of immunogammaglobulin of isotype 2b and its F(ab) and F(c) fragments. *Biophys J* **79**, 2150-2154.

Vezina, L.P., Faye, L., Lerouge, P., D'Aoust, M.A., Marquet-Blouin, E., Burel, C., Lavoie, P.O., Bardor, M. and Gomord, V. (2009) Transient co-expression for fast and high-yield production of antibodies with human-like N-glycans in plants. *Plant Biotechnol J* **7**, 442-455.

Vincke, C., Loris, R., Saerens, D., Martinez-Rodriguez, S., Muyldermans, S. and Conrath, K. (2009) General Strategy to Humanize a Camelid Single-domain Antibody and Identification of a Universal Humanized Nanobody Scaffold. *J. Biol. Chem.* **284**, 3273-3284.

Virdi, V., Coddens, A., De Buck, S., Millet, S., Goddeeris, B.M., Cox, E., De Greve, H. and Depicker, A. (2013) Orally fed seeds producing designer IgAs protect weaned piglets against enterotoxigenic *Escherichia coli* infection. *Proc. Natl. Acad. Sci. USA* **110**, 11809-11814.

Virdi, V., Juarez, P., Boudolf, V. and Depicker, A. (2016) Recombinant IgA production for mucosal passive immunization, advancing beyond the hurdles. *Cell. Mol. Life Sci.* **73**, 535-545.

Virdi, V., Palaci, J., Laukens, B., Ryckaert, S., Cox, E., Vanderbeke, E., Depicker, A. and Callewaert, N. (2019) Yeast-secreted, dried and food-admixed monomeric IgA prevents gastrointestinal infection in a piglet model. *Nat Biotechnol* **37**, 527-530.

Vukusic, K., Sikic, S. and Balen, B. (2016) Recombinant therapeutic proteins produced in plants: towards engineering of human-type O- and N-glycosylation. *Period Biol* **118**, 75-90.

Walsh, E.E., McConnochie, K.M., Long, C.E. and Hall, C.B. (1997) Severity of respiratory syncytial virus infection is related to virus strain. *J. Infect. Dis.* **175**, 814-820.

Walsh, G. and Jefferis, R. (2006) Post-translational modifications in the context of therapeutic proteins. *Nat. Biotechnol.* **24**, 1241-1252.

Wang, J., Wang, X., Shi, L., Qi, F., Zhang, P., Zhang, Y., Zhou, X., Song, Z. and Cai, M. (2017) Methanol-independent protein expression by AOX1 promoter with trans-acting elements engineering and glucose-glycerol-shift induction in Pichia pastoris. *Sci. Rep.* **7**, 41850.

Wang, M., Jiang, S. and Wang, Y. (2016) Recent advances in the production of recombinant subunit vaccines in Pichia pastoris. *Bioengineered* **7**, 155-165.

Wang, P.L., Lo, B.K.C. and Winter, G. (2005) Generating molecular diversity by homologous recombination in Escherichia coli. *Protein Eng Des Sel* **18**, 397-404.

Weinacker, D., Rabert, C., Zepeda, A.B., Figueroa, C.A., Pessoa, A. and Farías, J.G. (2013) Applications of recombinant *Pichia pastoris* in the healthcare industry. *Braz. J. Microbiol.* **44**, 1043-1048.

Wildt, S. and Gerngross, T.U. (2005) The humanization of N-glycosylation pathways in yeast. *Nature reviews. Microbiology* **3**, 119-128.

Wilkinson, R. and Neville, S. (1988) Jacalin: its binding reactivity with immunoglobulin A from various mammalian species. *Vet. Immunol. Immunopathol.* **18**, 195-198.

Wines, B.D., Ramsland, P.A., Trist, H.M., Gardam, S., Brink, R., Fraser, J.D. and Hogarth, P.M. (2011) Interaction of human, rat, and mouse immunoglobulin A (IgA) with staphylococcal superantigen-like 7 (SSL7) decoy protein and leukocyte IgA receptor. *J. Biol. Chem.* **286**, 33118-33124.

Wines, B.D., Willoughby, N., Fraser, J.D. and Hogarth, P.M. (2006) A competitive mechanism for staphylococcal toxin SSL7 inhibiting the leukocyte IgA receptor, FcαRI, is revealed by SSL7 binding at the Cα2/Cα3 interface of IgA. *J. Biol. Chem.* **281**, 1389-1393.

Woodham, A.W., Cheloha, R.W., Ling, J.J., Rashidian, M., Kolifrath, S.C., Mesyngier, M., Duarte, J.N., Bader, J.M., Skeate, J.G., Da Silva, D.M., Kast, W.M. and Ploegh, H.L. (2018) Targeted delivery of antigens to CD11b(+) cells via nanobodies induces strong antigen-specific T cell and anti-tumor responses. *J. Immunol.* **200**.

Wright, M. and Piedimonte, G. (2011) Respiratory syncytial virus prevention and therapy: past, present, and future. *Pediatric pulmonology* **46**, 324-347.

Wu, T.T., Johnson, G. and Kabat, E.A. (1993) Length distribution of CDRH3 in antibodies. *Proteins* **16**, 1-7.

Yang, C., Gao, X. and Gong, R. (2017) Engineering of Fc Fragments with Optimized Physicochemical Properties Implying Improvement of Clinical Potentials for Fc-Based Therapeutics. *Front Immunol* **8**, 1860.

Yao, J., Weng, Y.Q., Dickey, A. and Wang, K.Y. (2015) Plants as Factories for Human Pharmaceuticals: Applications and Challenges. *Int. J. Mol. Sci.* **16**, 28549-28565.

Yu, R., Mai, Y., Zhao, Y., Hou, Y., Liu, Y. and Yang, J. (2018) Targeting strategies of liposomal subunit vaccine delivery systems to improve vaccine efficacy. *Journal of drug targeting*, 1-10.

Yusibov, V., Kushnir, N. and Streatfield, S.J. (2016) Antibody Production in Plants and Green Algae. *Annu Rev Plant Biol* **67**, 669-701.

Zahrl, R.J., Peña, D.A., Mattanovich, D. and Gasser, B. (2017) Systems biotechnology for protein production in Pichia pastoris. *FEMS Yeast Res.* **17**, fox068.

Zeitlin, L., Bohorov, O., Bohorova, N., Hiatt, A., Kim, D.H., Pauly, M.H., Velasco, J., Whaley, K.J., Barnard, D.L., Bates, J.T., Crowe, J.E., Piedra, P.A. and Gilbert, B.E. (2013) Prophylactic and therapeutic testing of Nicotiana-derived RSV-neutralizing human monoclonal antibodies in the cotton rat model. *Mabs-Austin* **5**, 263-269.

Zeitlin, L., Pettitt, J., Scully, C., Bohorova, N., Kim, D., Pauly, M., Hiatt, A., Ngo, L., Steinkellner, H., Whaley, K.J. and Olinger, G.G. (2011) Enhanced potency of a fucose-free monoclonal antibody being developed as an Ebola virus immunoprotectant. *Proc Natl Acad Sci U S A* **108**, 20690-20694.

Zhao, G.Y., He, L., Sun, S.H., Qiu, H.J., Tai, W.B., Chen, J.W., Li, J.F., Chen, Y.H., Guo, Y., Wang, Y.F., Shang, J., Ji, K.Y., Fan, R.W., Du, E.Q., Jiang, S.B., Li, F., Du, L.Y. and Zhou, Y.S. (2018) A Novel Nanobody Targeting Middle East Respiratory Syndrome Coronavirus (MERS-CoV) Receptor-Binding Domain Has Potent Cross-Neutralizing Activity and Protective Efficacy against MERS-CoV. *J. Virol.* **92**.

Zhong, Q., Gu, Z. and Glatz, C.E. (2006) Extraction of recombinant dog gastric lipase from transgenic corn seed. *J. Agric. Food Chem.* **54**, 8086-8092.

Zhu, J. and Hatton, D. (2018) New Mammalian Expression Systems. *Adv Biochem Eng Biot* **165**, 9-50.

ACKNOWLEDGEMENTS

I have been fortunate to work on two cross-functional collaborative projects with different people. The projects have been both challenging and rewarding. Many people have provided me with assistance and support, for which I am grateful.

At the outset, I would like to express my sincere gratitude to my promoter Prof. Ann Depicker, for her supervision, patience and motivation which has enriched me as an aspiring scientist and as a person in so many ways. She shared her experience, knowledge and wisdom to the highest standards. With her inspiration and support, I gained a deepened appreciation for the topic and was able to fine-tune my research. I could not have imagined having a better mentor for my PhD study. It has been my pleasure to become a part of "Ann-bodies".

Also, I am very grateful to my co-promoters who provided me with an opportunity to learn a different aspect of my PhD research. Dr. Bert Schepens is a true professional in every sense of the word. With his insightful scientific opinions, I have gained new perspectives and confidence in my research project. I would like to extend special thanks to Prof. Xavier Saelens. His continuous optimism and guidance have been essential for this work. I would like to thank everyone from the group of Prof. Saelens for their kindness and help, especially Dr. Iebe Rossey for assisting with the qBase analysis.

I owe eternal gratitude to Prof. Eric Cox, who provided me with an opportunity to learn from the scientific discussions in GOA meetings and also gave access to the laboratory and research facilities at the Faculty of Veterinary Medicine (Ghent University). My sincere thanks also goes to Dr. Bert Devriendt, Hans Van Der Weken, and Raquel Sanz Garcia for being so nice and helpful throughout.

I am in indebted to all of my colleagues for making the lab such a pleasant environment to work in, especially Dr. Vikram Virdi, Dr. Paloma Juarez and Jonah Nolf for their invaluable help and advice. Thanks, Jonah, for storing my never-ending clones. Enormous thanks to Dr. Jorge Palaci, and Ashuwini Tharad, for all the support, smiles and most importantly the friendship; Dr. Veronique Boudolf for all the help, especially with the administration. I am sincerely thankful to

CURRICULUM VITAE

Personal Information

Name and Surname:	Shruti Bakshi
Place and date of birth:	Shivpuri (India), May 20th, 1990
Current address:	Rooigemlaan 296, 9000 Ghent, Belgium
Phone number:	+32 (0) 485241574
Email:	shruti.bakshi205@gmail.com
LinkedIn:	www.linkedin.com/in/shruti-bakshi-b8a47825

Education

Ph.D. (Biochemistry and Biotechnology): VIB-UGent, Belgium	2015 – 2019
M.Sc. (Biotechnology): Pune University, India	2010 – 2012
B.Sc. (Biotechnology): Devi Ahilya University, India	2007 – 2010

Professional experience

Ph.D.   June 2015 – August 2019

Title of the thesis: "Engineering single domain antibodies into antivirals and vaccine delivery vehicles to combat infectious diseases".

Ghent University – Department of Plant Biotechnology and Bioinformatics
VIB – Center for Plant Systems Biology

Research Fellow   July 2012 – April 2015

Title of the project – "Development of ELISA-based diagnostic assay for Chikungunya Virus mediated sickness".

University of Delhi South Campus – Department of Biochemistry, New Delhi, India

Master thesis   Jan 2012 – June 2012

Title of the thesis – "Comprehensive serum proteome analysis for Biomarker discovery for breast cancer".

National Centre for Cell Science, Pune, India

Competences and additional courses

Scientific expertise

- Molecular biology – molecular cloning (GoldenBraid, Gibson assembly), DNA/RNA extraction, cDNA synthesis, PCR, qPCR, phage display, protein expression in yeast (*Pichia pastoris*), plant (transient expression systems- *Nicotiana benthamiana*) and bacteria (*Escherichia coli*).
- Biochemistry – protein purification on AKTA by affinity, ion exchange and size exclusion chromatography, protein characterization - SDS-PAGE, western blotting, ELISA.
- Immunology – cell culture, immunohistochemistry, binding assay, endocytosis assay, hybridoma technology, microneutralization assay, basics of flow cytometry, handling ad manipulation of mouse as RSV disease model.

Computer skills

- GraphPad Prism, Unicorn for protein purification, DNA analysis software (CLC, Vector NTI, MacVector), Bioinformatics tools such as BLAST, ClustalW.
- Microsoft office, programming languages (C and C++)

Additional training

- Laboratory animal science to obtain FELASA C certificate, Ghent University, Merelbeke
- Basic statistics training, VIB, Leuven
- Effective writing session, VIB, Ghent
- BioXP DNA printer workshop from SGI-DNA, VIB, Ghent
- MST/Prometheus workshop from NanoTemper, VIB, Ghent

Oral and Poster presentations

Oral
- Engineering chimeric antibodies aimed for passive mucosal immunization against HRSV (The 2nd conference of the International Society for Plant Molecular Farming (ISPMF), Ghent (Belgium)- May 2016).

Poster
- Evaluating effector function of VHH-Fc fusions for developing therapeutics (EMBO workshop, Antibodies and complement: Effector functions, therapies and technologies, Girona (Spain)- June 2018)
- Evaluating VHH-Fc fusions as therapeutics (3rd Conference of the International Society of Plant Molecular Farming, Helsinki (Finland)- June 2018)
- Both the VHH and Fc influence the integrity of a VHH-Fc fusion (Plant-based Vaccines, Antibodies and Biologics, Albufeira (Portugal)- June 2017).

- Evaluating VHH-Fc fusions as Therapeutics (2nd Next-Generation Antibodies and Protein Analysis, Ghent (Belgium)- October 2017).
- Engineering chimeric antibodies aimed for passive mucosal immunization against HRSV (2nd International Symposium on Alternatives to Antibiotics (ATA)- Challenges and Solutions in Animal Production, Paris (France)- December 2016).

Scientific publication

- Bakshi et al., 2019. A two-amino acid mutation in murine IgA enables downstream processing and purification on staphylococcal superantigen- like protein 7. Journal of Biotechnology. **294**, 26-29.

Awards/Fellowships

- Travel grant to attend 3rd conference of the International Society for Plant Molecular Farming (ISPMF), Helsinki (Finland)- June 2018
- Ph.D. studentship for 4 years, Ghent University (Belgium).
- CSIR-NET-JRF award (Junior Research Fellowship funded by Council of Scientific & Industrial Research, Government of India) to pursue Ph.D. research (5-years fellowship); secured All India Rank 49 in National Eligibility Test (NET).
- DBT-JRF award (Junior Research Fellowship funded by Department of Biotechnology, Government of India) to pursue Ph.D. research (5-years fellowship); secured all India Rank 79.
- Qualified for Graduate Aptitude Test in Engineering (GATE) with 98.6 percentile to pursue Ph.D. research at Indian Institute of Technology (IIT), Government of India (5-years fellowship); secured all India Rank 193.
- Received 2-years scholarship for master's degree by Department of Biotechnology (DBT), Government of India (Combined Biotechnology Entrance Examination (CBEE) conducted by Jawaharlal Nehru University (JNU); secured All India Rank 40.

Volunteering experience

- Prepared content for the newsletter of the 3rd ISPMF conference 2018, Helsinki, Finland
- Participated in Biotech day, 200-years of Ghent university.

Languages

| English - | Full-professional proficiency | Hindi   - | Native or bilingual proficiency |
| Dutch   - | Elementary Proficiency | Marathi - | Native or bilingual proficiency |